SMOKE CONTROL BASED ON A SOLAR ASSISTED NATURAL VENTILATION SYSTEM IN AN ATRIUM BUILDING

アトリウム型ソーラーチムニーの自然換気システムによる煙制御に関する研究

March 2004

Wenting Ding

Graduate School of Science and Engineering
Waseda University

TABLE OF CONTENTS

ACKNOWLEDGEMENTS

The present thesis is the results of the research works conducted at Hasemi Laboratory, Department of Architecture, Waseda University, in the past three years.

Up to the completion of this thesis, I would like to express my sincere gratitude to my supervisor, Professor Y. Hasemi, Department of Architecture, Waseda University, who offered me the chance to carry out this research and gave me quite a lot of valuable advices and encouragements during the research process which kept me from getting astray when I met difficulties. His kindly instructions influenced my attitude to both research and life.

I would like to thank Professor T. Ojima and Professor T. Tanabe, Department of Architecture, Waseda University, and Visiting Professor Y, Nakajima, Research Institute of Science and Engineering, Waseda University, for their careful reviewing and constructive advices on this thesis.

I thank Mr. T. Yamada, National Research Institute of Fire and Disaster, for his cooperation and constructive advices on conducting the model experiments, which consist a quite important part of this research.

I would like to thank Associate Professor Weijun Gao of Kitakyushu University, who introduced me to my present supervisor and gave me great help and many advices on my research work and my life in Japan.

I am grateful to Mr. Y. Minegishi, Mr. S. Nishimoto, Mr. S. Tanaka and Mr. Y. Egawa at Hasemi Laboratory of Waseda University, for their help and discussions to carry out all the experiments and to finish this research.

I would like to thank all the members at Hasemi Laboratory of Waseda University, especially Mr. N. Yasui, Mr. S. Moriyama, Mr. S. Tsuchiya, Ms. Y. Furukawa, Mr. M. Nakamura who is now at Taisei Corporation, Mr. D. Kamikawa, and Mr. D. Nam for their kindness and warm-hearted help in my study.

This research was carried out with the support of the JSPS Science Promotion Fund No.13450241--Control of Stack Effect as a Basic of Fire-safety Green Buildings, which is gratefully acknowledged.

I am much obliged to Jinnai Scholarship Foundation for giving me constant financial support to let me concentrate on my study and finish this thesis smoothly in 3 years.

I am grateful to Dr. Lei Xu, Research Institute of Science and Engineering, Waseda University, who gave me full support in the whole research process, especially in the aspect of CFD study.

I would like to thank Professor Cunyang Fan and Professor Weiding Long of Tongji University, for their constant support and valuable advices on my study.

Last but not least, I am indebted to my parents who constantly support my study and my life.

March 2004

Wenting Ding

NOMENCLATURE

a	= fire growth coefficient, kW/s^2
A_{in}	= area of the inlet , m^2
A_{out}	= area of the outlet, m^2
C_n	= interpolation constant for the smoke layer interface
C_p	= specific heat at constant pressure, J/kg·K
C_w	= dimensionless pressure coefficient
D	= diameter, m
Fr	= Froude number
g	= acceleration due to gravity, m/s^2
Gr	= Grashof number
h_c	= convective heat transfer coefficient, $W/m^2 \cdot K$
H	= height, m
k	= entrainment constant or molecular conductivity, W/m·K
k_t	= conductivity due to turbulent transport, W/m·K
K	= overall heat transfer coefficient, $W/m^2 \cdot K$
L	= length scale, m
m	= mass flow rate, kg/s
n	= wind exponent
P	= pressure, Pa
Pr	= Prandtl number
Q	= heat release rate, kW
R	= the universal gas constant
S	= wall surface area for convection, m^2
t	= time, s
t_g	= growth time of fire, s
T	= temperature, K
T_b	= temperature near the bottom of the compartment, K
T_{max}	= maximum temperature, K

T_n = temperature at the interface height, K

T_0 = ambient air temperature, K

U = characteristic velocity, m/s

v = velocity, m/s

V = ventilation rate, m^3/h, or volume, m^3

x = coordinates

z = height, m

z_0 = reference height, m

Z_f = height of the fire source, m

Greek Symbols

α = discharge coefficient

β = thermal expansion coefficient

ε = dissipation of turbulent kinetic energy

ΔH_c = effective heat of combustion, kJ/kg

κ = turbulent kinetic energy

Δp = pressure difference, Pa

Δt = burning time, s

ΔT = temperature difference, K

ρ = density, kg/m^3

ρ_0 = ambient air density, kg/m^3

σ = Stefan-Boltsman constant, 5.67×10^{-8} $W/m2 \cdot K^4$

μ = viscosity

μ_t = turbulent viscosity

μ_{eff} = effective viscosity

Γ = diffusion coefficient

Subscripts

a	= atrium
bot	= bottom of the atrium
c	= chimney
eff	= effective
F	= full-scale
i	= i term
in	= inlet
j	= j term
M	= model
out	= outlet
s	= smoke
top	= top of the chimney
t	= turbulent
w	= wall

CHAPTER 1

INTRODUCTION

CHAPTER 1
INTRODUCTION

1.1 BACKGROUND OF THIS RESEARCH

In recent years, with people paying more attention to energy conservation and indoor air quality, natural ventilated modern buildings are being designed and constructed increasingly, among which the planning of utilizing atria or vertical shafts to promote stack ventilation is not scarce. To improve the natural ventilation effectiveness, the boundary of atrium/vertical shaft and adjacent spaces usually is completely open; this runs contrary to the traditional ways of designing fire safety buildings with horizontal compartmentation and vertical separation. Smoke can travel from atrium/shaft to adjacent spaces and rooms that would be unaffected in the absence of an atrium. Although there have been no small such buildings built or being built, for none of them the feature of natural ventilation has been taken into account when considering the smoke control methods. In fact it is common to design the smoke control system completely separated from the consideration of the natural ventilation system.

Here two examples of buildings with natural ventilation planning are presented as following. Their fire safety planning will be introduced.

(1) Yamanouchi Lotus Garden

The design brief of this building called for a passive design, minimizing energy consumption at the same time as providing a comfortable internal environment all year round. These objectives are achieved by maximizing the daylight throughout the building via the atrium and utilizing natural ventilation via the stack effect in the atrium. The air in the atrium is warmed up by solar radiation and natural ventilation is promoted due to stack effect. The fresh air is drawn in from the ventilation windows of each floor, passes through the occupant space, and then is exhausted from the openings on top of the atrium.

The fire safety of the building depends greatly on the shutters, which are installed on both sides of the atrium. Because the number of the shutters is quite great, besides high initial cost, it is doubtable that all shutters can work properly in an event of a fire since they are only used in an emergency.

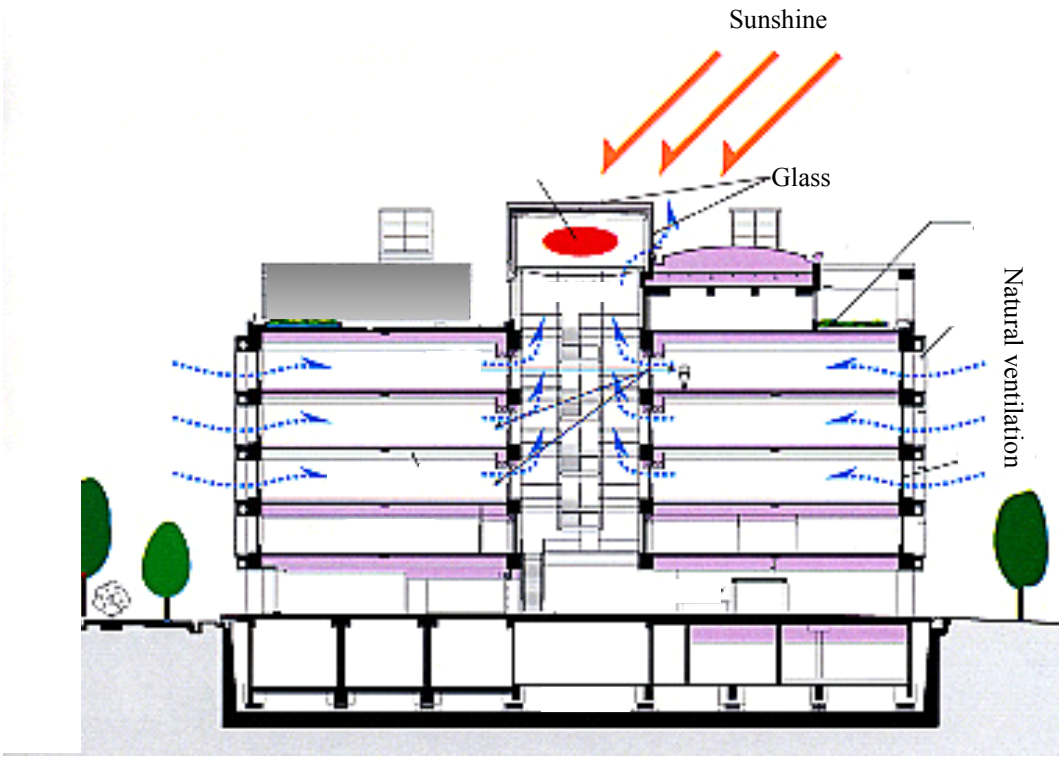

Fig. 1-1 Yamanouchi Lotus Garden

(2) School Building of the Kitakyushu University

The objectives of the designers are to create a low energy building and at the same time provide a comfortable internal environment all year round. The techniques used to fulfill these objectives include use of daylight and use of natural ventilation. Solar chimneys are designed on top of the building to promote stack effect and therefore to encourage natural ventilation.

Just as shown in the figure, the shaft connects all the openings distributed at each floor, through which air flows from the occupant rooms/corridors to the shaft and then is exhausted from the outlets of the solar chimney. In an event of a fire, smoke also flows from the fire room to the shaft, and it is quite possible for the smoke to travel from the shaft to other floors. Since the building is a school building, smoke control is not strictly required. The fire safety performance of the building is not clear.

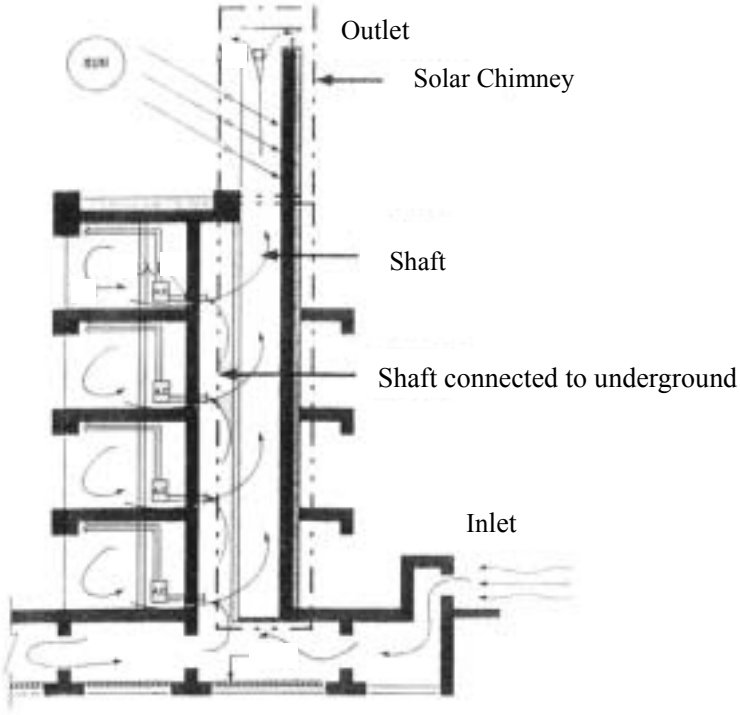

Fig. 1-2 School Building of the Kitakyushu University

1.2 OBJECTIVE OF THIS RESEARCH

Just as mentioned above, stack effect plays an important role on promoting natural ventilation. However when considering the smoke control of the spaces including vertical shafts, stack effect is always thought to be the factor of helping smoke spread and therefore enlarging the fire damage. In fact considering the mechanism of natural ventilation and smoke movement, it is clear that they own the same nature--both are driven by stack effect and have the same purpose of exhausting unnecessary gas (air or smoke) from a building.

Basing on above considerations, in this research, for buildings with natural ventilation promoted by stack effect occurring in atria/vertical shafts, the possibility of utilizing the same stack effect to realize smoke control is discussed.

1.2.1 Accordance with the design policy

In conditional fire safety planning, when occupant space or escape route are open to the atria/shafts, it is usual to separate the occupant space or escape route from the atria/shafts by shutters and extract smoke using mechanical or natural smoke exhaust system. To promote

natural ventilation, the building space tends to be defenseless to smoke infiltration. Therefore the fire safety of the building depends greatly on the mechanical or other additional equipments. For most of the existing buildings, complex systems and large quantities of shutters are installed to secure the fire safety.

However, considering the primitive of natural ventilation, it tries to avoid the usage of mechanical equipments. But for solving the problem of smoke control, mechanical exhaust system brings about complex engineering problems. The policy of the smoke control conflicts to that of the natural ventilation. The purpose of this research is to make the best of stack effect to realize both natural ventilation and smoke control without depending on excessive mechanical equipments. The technical possibility of the concept will be examined and discussed.

1.2.2 Pursuing a reasonable design

As mentioned above, to prevent the propagation of smoke from the fire origin to other spaces through the atria/vertical shafts, mechanical exhaust equipments and shutters are always employed in many buildings. In fact such equipments are usually accompanied with following problems.

- ◆Effectiveness/Uncertainty of their operability
- ◆High initial and maintenance cost
- ◆Restriction on the space design

Against above problems, the significance of this research can be stated as below:

Regarding to the effectiveness of the equipments, it is difficult to ensure that all shutters work properly, if only one of those shutters fails to close, evacuation behavior may be delayed or fail. Furthermore usually fire equipments are only used in case of emergency, their effectiveness is difficult to ensure. As to the mechanical exhaust system, besides great exhaust rate is required, the effectiveness of mechanical exhaust system in a low airtight space is doubtable. In this research, because the operation and maintenance of the target system, which works as natural ventilation system, is conducted almost at all times, so high reliability of the system in an emergency can be expected.

Since the target system is used as both natural ventilation system and smoke control system, it is thought the equipment cost can be considerably cut down. In addition, space reduced due to conserved equipment gives more freedom to space design.

CHAPTER 2

PROPOSITION OF THE PROTOTYPE BUILDING

CHAPTER 2
PROPOSITION OF THE PROTOTYPE BUILDING

Just as mentioned in Chapter 1, the purpose of this research is to discuss the possibility of realizing smoke control based on the natural ventilation system. In this chapter, a prototype building is proposed, which is thought to be advantageous to natural ventilation and smoke control. The design objective is established.

2.1 BASIC CONCEPT EMPLOYED IN THIS RESEARCH

2.1.1 Stack effect in buildings

Stack effect in buildings is the same as that occurring in a chimney. When the inside air temperature of a building is higher or lower than that of the outside, because of the temperature difference, the air inside the building is either more or less dense than the air outside. If there is an opening high in the building and another one low in the building, a natural flow will be caused. If the air in the building is warmer than the outside, this warmer air will flow out from the top opening, and then the building space will be replaced with cooler air from outside. If the air inside is cooler than that of the outside, the cooler air will be drawn out from the low opening, and then the building space will be replaced with warmer air from outside. Usually the greater the temperature difference is, the greater the stack effect will be.

2.1.2 Solar chimney

Just as mentioned before, stack effect happens due to the temperature difference between outside and inside. To increase the stack effect in buildings, a solar chimney with a glazing wall and three thermal storage walls is employed in this research. Solar radiation passes through the glazing wall and is absorbed by the thermal storage walls. Then the high temperature thermal storage walls give heat to the air inside the solar chimney through convective heat transfer. Heated air goes out from the high opening and the fresh air is drawn in from the low opening.

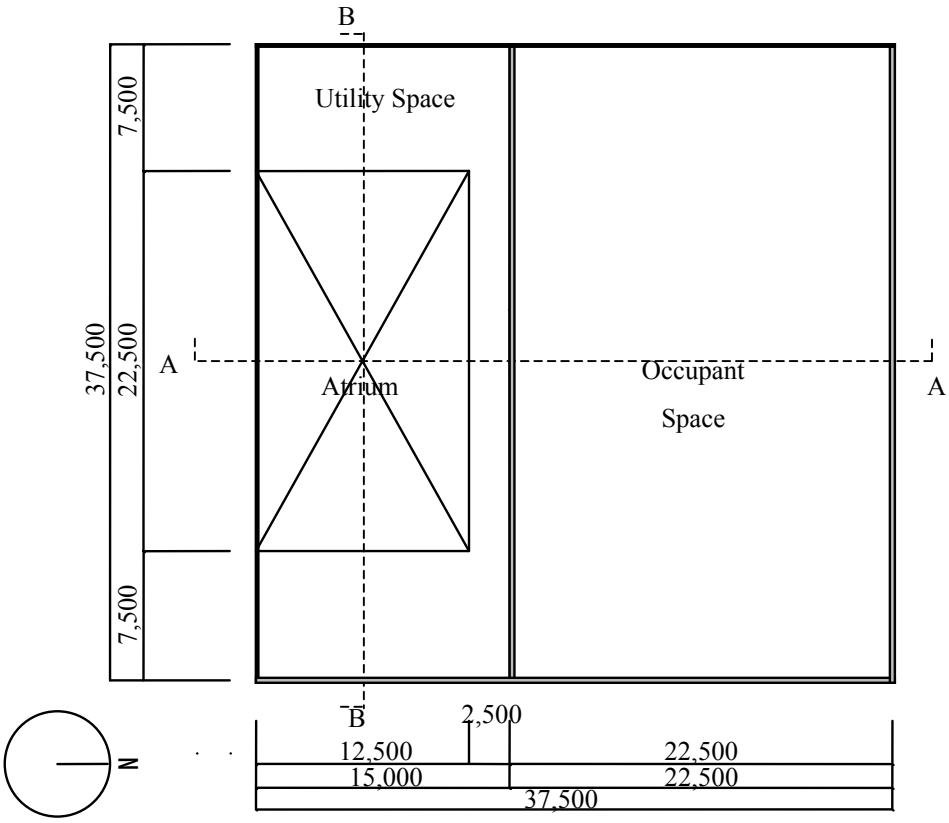

Fig. 2-1 Plan of the prototype building (Units: mm)

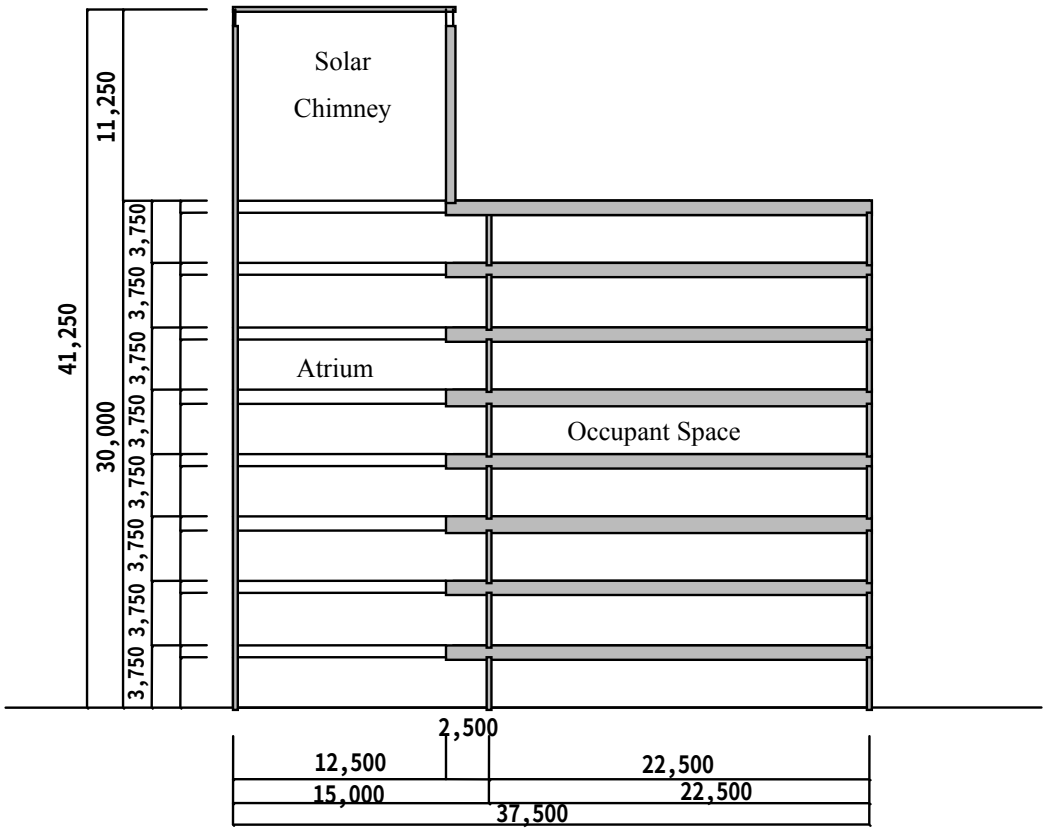

Fig. 2-2 A-A Section of the prototype building (Units: mm)

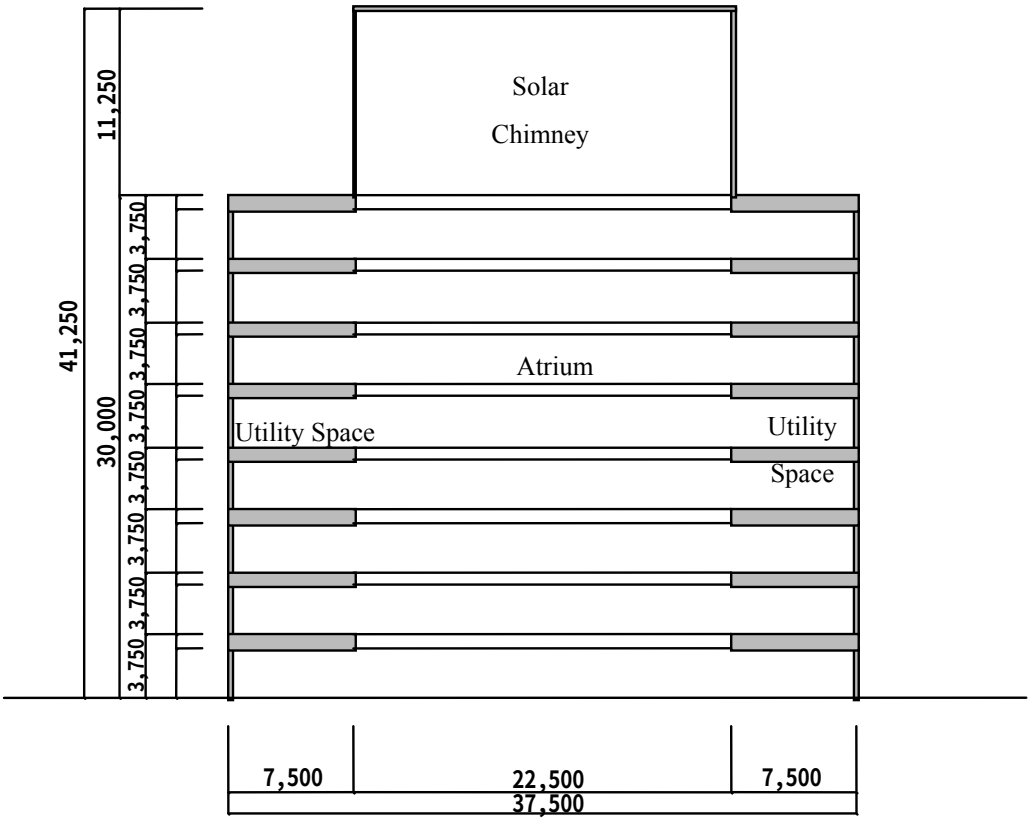

Fig. 2-3 B-B Section of the prototype building (Units: mm)

2.2 OUTLINE OF THE PROTOTYPE BUILDING

To discuss the technical possibility of the design objective, a prototype building is proposed, which is thought to be advantageous to both natural ventilation and smoke control.

2.2.1 Architectural outline

It is supposed to be a very common, medium scale 8-storey office building with a standard floor area of about 850 m^2. The utility space and the atrium are thought to be in the south direction of the building with an area of about 280 m^2 respectively. To promote stack effect for natural ventilation, on top of the atrium, a 3-storey high solar chimney is built. Escape staircases and safety zones are located on both sides of the atrium. Their detail distributions will be discussed later.

2.2.2 Natural ventilation in the prototype building

The roof and the south-facing wall of the chimney are made of glass, which allows solar radiation to pass through. The thermal storage wall absorbs solar radiation and warms up air inside the chimney. By stack effect the outside air flows into the atrium from the inlets (for simplicity of the discussion, inlets are considered to concentrate at the lower part), passes through the utility space/atrium and finally is discharged from the outlets. Temperature rise of air mainly occurs in the chimney and thus the neutral pressure plane almost automatically stays within the chimney (Fig. 2-4). Effective ventilation can be expected.

2.2.3 Smoke control in the prototype building

Because the utility space is open to the atrium, when a fire breaks out in the atrium, the utility space is defenseless to the propagation of smoke. Since 1980s, with the expanding need for atrium architecture, performance-oriented fire safety design method tends to be an appealing research subject. The favorite smoke control design method is to use the upper space of the atrium to reserve smoke and at the same time exhaust smoke through the openings on top of the atrium.

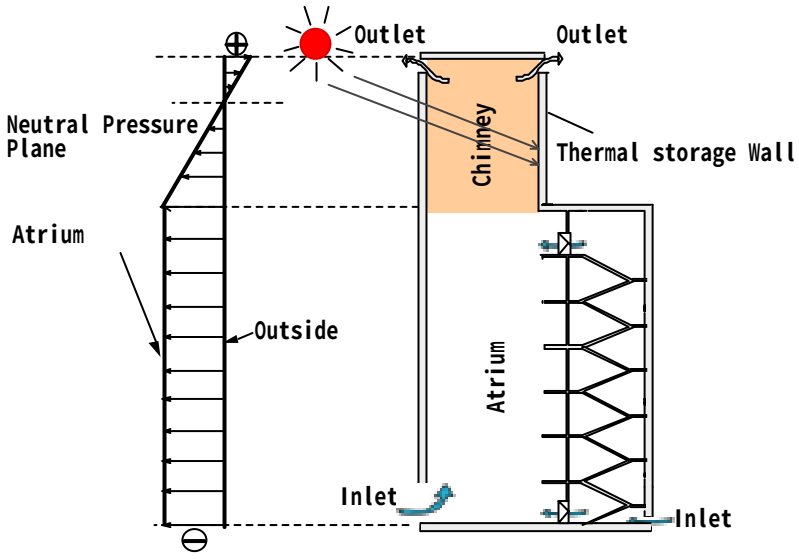

Fig. 2-4 Concept of natural ventilation (⊕: Positive to outside; ⊖: Negative to outside)
(Left: pressure difference distribution between the atrium/chimney and outside)

In an event of a fire occurring in the atrium or in any office room, smoke leaks into the atrium space. It is always reserved in the upper space and descends to the lower space with the increasing of the smoke volume. Usually the fire space can be considered as two layers, the high temperature smoke layer and the low temperature fresh air layer. In case of natural ventilation, temperature rise concentrates in the chimney. While in case of smoke control, temperature rise occurs in the whole smoke layer. The outlets can be used for smoke exhaustion and from the inlets fresh air is drawn in. Pressure difference distribution forms as shown in Fig. 2-5. Here considering the escape route from the occupant space is connoted in the utility space, that is to say the corridors or the staircases are connected with the utility space, the necessary conditions for the fire safety will be discussed.

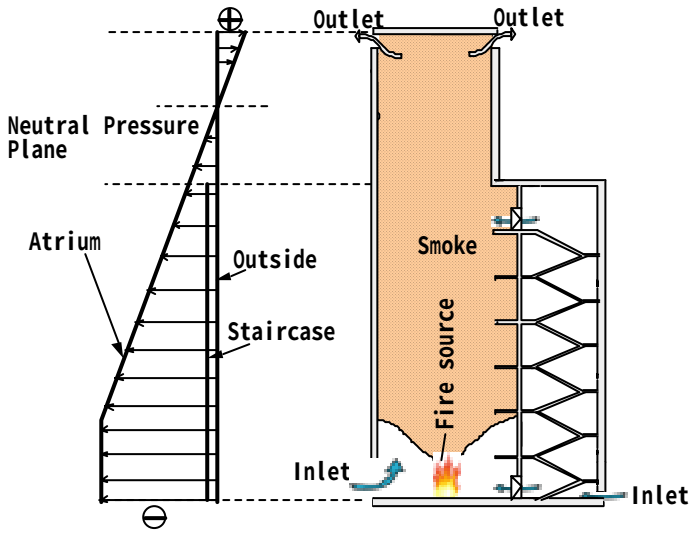

Fig. 2-5 Concept of smoke control (⊕: Positive to outside; ⊖: Negative to outside)
(Left: pressure difference distribution between the atrium/chimney and outside)

2.2.3.1 The possibility of safety escape if the escape routes/staircases are completely open to the atrium

If there is no escape corridor separated from the atrium and the escape staircases are completely open to the atrium, to ensure the safety of all the persons in the building, their evacuation behavior should be finished before the smoke descends to the height of the

occupant space. Supposing the fire origin is at the base of the atrium, to keep the smoke layer stay above the occupant space, the smoke that needs to be exhausted should be:

$$M(z) = kQ^{\frac{1}{3}} z^{\frac{5}{3}} \tag{2-1}$$

where

Q is heat release rate of the fire source, kW;

k is entrainment constant, 0.076;

M is mass flow rate of smoke production, kg/s;

z is height from top of the fuel surface to bottom of the smoke layer, m;

Assuming the heat release rate is 3,000 kW and 3-storey high space (12 m), the mass flow rate of smoke exhaust is about 60 kg/s. it is a quite great quantity for passive smoke exhaust. Furthermore, the equation shows that the necessary mass flow rate of smoke exhaust is extremely sensitive to the height of the space. For the prototype building, it is very difficult to make the smoke stay inside the solar chimney. Of course, if the evacuation can finish before the smoke layer descends to the occupant space, there is no danger for the escapers to expose to the smoke. For a steady fire, the allowable time for escape can be calculated as:

$$t = \frac{3A(H^{2/3} - z^{2/3})}{2k(QH^2 z^2)^{1/3}} \tag{2-2}$$

where

t is allowable time for escape, s;

A is floor area of the space, m^2;

H is height of the space, m;

z is height of the smoke layer, m;

k is entrainment constant, 0.076;

Q is heat release rate of the fire source, kW.

Assuming H is 40 m and z is 12 m, the allowable time for escape is about 0.15A. As long as the floor area of the space is not extremely large, it is difficult to make the escape time

shorter than above value.

From above discussion, it is clear that when the escape route/staircases are completely open to the atrium, it is extremely difficult to secure the fire safety of the building.

2.2.3.2 Smoke prevention by pressure difference when the main escape route is separated from the atrium

Actually from the consideration of architectural function, the necessity for above planning is very small. To secure the fire safety more easily, the planning, in which the escape staircase and safety zone are separated from the atrium, is considered.

During the escape process, when the smoke layer descends to the floor where escape is being carried out, in case the door of the safety zone/staircase facing the atrium/utility space should be open temporarily, as long as the pressure of the staircase and the safety zone is lower than that of the atrium/utility space at the same height, smoke spreading into the escape route can be prevented. Therefore the fire safety is in fact decided by the floor escape. Here if the neutral pressure plane of the smoke layer is higher than the occupant space, escape of all the floors can be protected.

For the natural ventilation, temperature rise normally happens only in the solar chimney; while for the smoke control, the high temperature smoke layer descends to below the solar chimney (Fig. 2-5). To keep the neutral pressure plane stay inside the solar chimney, according to the mass flow balance of the inlet and outlet, the following equation should be satisfied:

$$A_{out}(\rho_s H_c)^{1/2} \geq A_{in}(\rho_0 H_a)^{1/2} \qquad (2\text{-}3)$$

where

A_{out} is area of the outlet, m^2;

A_{in} is area of the inlet , m^2;

ρ_s is density of the smoke, kg/m^3;

ρ_0 is density of the ambient air, kg/m^3;

H_c is height of the chimney, m;

H_a is height of the atrium, m.

From Eq. (2-3), area ratio of the outlet to inlet should meet the following relationship:

$$\frac{A_{out}}{A_{in}} \geq \left(\frac{\rho_0 H_a}{\rho_s H_c} \right)^{1/2} \tag{2-4}$$

Supposing the smoke temperature rise is about 100 K and H_a/H_c is about 3, A_{out}/A_{in} should be not less than 2 to keep the neutral pressure plane stay inside the solar chimney. Such area ratio condition is also normal to natural ventilation. The detail condition will be discussed through model experiments and numerical calculations in following chapters.

2.3 CONVENTIONAL RESEARCHES

2.3.1 Conventional researches about solar chimney

In this research, solar chimney is employed to enhance the driving force of natural ventilation. As to solar chimney itself, many researches have been carried out.

The use of solar chimney as ventilation devices can be found in some historical buildings, such as the so-called “Scirocco room” in Italy, which dated back to at least the 16th century, where the solar chimneys were used in conjunction with underground corridors and water features to provide ventilation and cooling (Cristofalo SD et al, 1989). Due to the general availability of electric power in the early 20th century and the expansion of air-conditioning in the 1930s, ventilation devices driven by natural forces such as solar energy and wind force became obsolete (Janssen JE, 1999). As a consequence, in contrast to the dramatic developments in mechanical ventilation systems, research and developments of solar chimney is relatively limited up to 1980s.

During the last two decades, increasing awareness of greenhouse gas emissions and the need for effective, efficient and ecologically sound building ventilation have led to renewed interest in solar chimneys. In recent years, a number of experimental, numerical and theoretical investigations have contributed to the current understanding of solar chimneys.

Bouchair et al. (1988) and Bouchair (1994) reported investigations on a full-scale experimental solar chimney with both front and back walls maintained at the same uniform temperature by heating elements. It was shown that properly designed solar chimneys can be used for daytime ventilation as well as night cooling in hot climates by driving cooler

outdoor air into buildings using the thermal energy stored during the daytime. By inducing air movement across the room, thermal comfort in buildings can be achieved by using solar chimneys.

Kumar et al. (1998) studied indoor air quality in a prototype house with a solar chimney system, and showed that passive outdoor air ventilation is effective in reducing indoor air contaminants. By comparing the performance of a conventional brick solar chimney and a solar chimney with the sun-facing wall replaced by glazing, Afonso and Oliveira (2003) showed that the glazed solar chimney drew about 10-20% more air through the chimney.

Z.D. Chen et al. (2003) and Toshio Yamanaka et al. (2002) studied the performance of solar chimney through model experiments. The influence of the inclination angle, the gap to height ratio and the wall heat flux etc on the performance of the solar chimney is discussed. Similar research was also conducted by SungWoo Cho et al. (2000).

2.3.2 Conventional researches about smoke control in atrium buildings

Social and technical changes have led to changes in building environments which incorporate new building forms and the use of innovative construction techniques and new synthetic materials. The buildings adopting these changes often have included within their design large spaces or voids, often integrated with many of the stories. These large spaces have been described as malls, atria, arcades and light wells. The generic term for the building type tends to be ‘atrium’ and, by their very nature, atrium buildings often run contrary to the traditional building regulations’ approach in terms of horizontal compartmentation and vertical separation.

Recently experience of fires in atrium buildings in the USA has shown the problem of hot and toxic gases travel internally through the atrium, spread throughout the building and affect escape routes. Thus there appears to be a need for a properly designed smoke control system in atrium buildings.

The ideal option would be to prevent any smoke from a room fire entering the atrium at all. An easily understood way of achieving this is to ensure that the boundary between the room and the atrium is both imperforate and fire resisting, and that the atrium base has only a very restricted use. This option has frequently been used, but is widely regarded as being architecturally restrictive. Consequently it is usually not favored by designers. The concept

has been labeled the ‘Sterile tube’ (Saxon R., 1983).

Greater architectural freedom becomes possible if the atrium façade need not be sealed, but can be allowed to be leaky, even if the upper atrium is filled with smoke. If such leakage paths do not have tight seals, smoke from the atrium may enter many adjacent spaces. Hence smoke must be prevented from passing in appreciable quantities through these small leakage openings. One way of achieving this may be by depressurizing the atrium. Hansell G. O. and Morgan H. P. (1990) had introduced the method in detail.

George V. H. et al. (1999) presented the numerical study of the effectiveness of atrium smoke exhaust systems. It presents numerical predictions obtained using a computational fluid dynamics (CFD) model and compares the numerical results with the experimental data obtained from the tests. Results are also presented for a real-scale atrium and are compared to the results of the scaled-down models. Ray Sinclair (2001) presents a list of factors for architects and mechanical engineers to consider early in the design of atrium smoke management systems. CFD computer simulations are recommended as an alternative method of proving the capacity and performance of proposed smoke management systems. Examples of real design projects presented demonstrate the effective use of CFD results.

The conventional researches have presented relatively mature techniques and methods for the design of solar chimney ventilation systems and the smoke control for atrium buildings. But there is almost no research integrating smoke control with natural ventilation.

2.4 METHODS FOR EXAMINING THE PERFORMANCE OF THE PROTOTYPE BUILDING

Qualitative and quantitative analysis are carried out in the present study to inspect the natural ventilation and smoke control performance of the prototype building. Firstly reduced scale model experiments are carried out to examine the natural ventilation and smoke control performance of the prototype building. The results of experiments then are used to evaluate the appropriation of the CFD modeling. Then the detail natural ventilation and smoke control performance of the prototype building will be inspected by CFD. Finally the procedure for designing a building with passive ventilation and smoke control function will be presented based on the discussion of the prototype building.

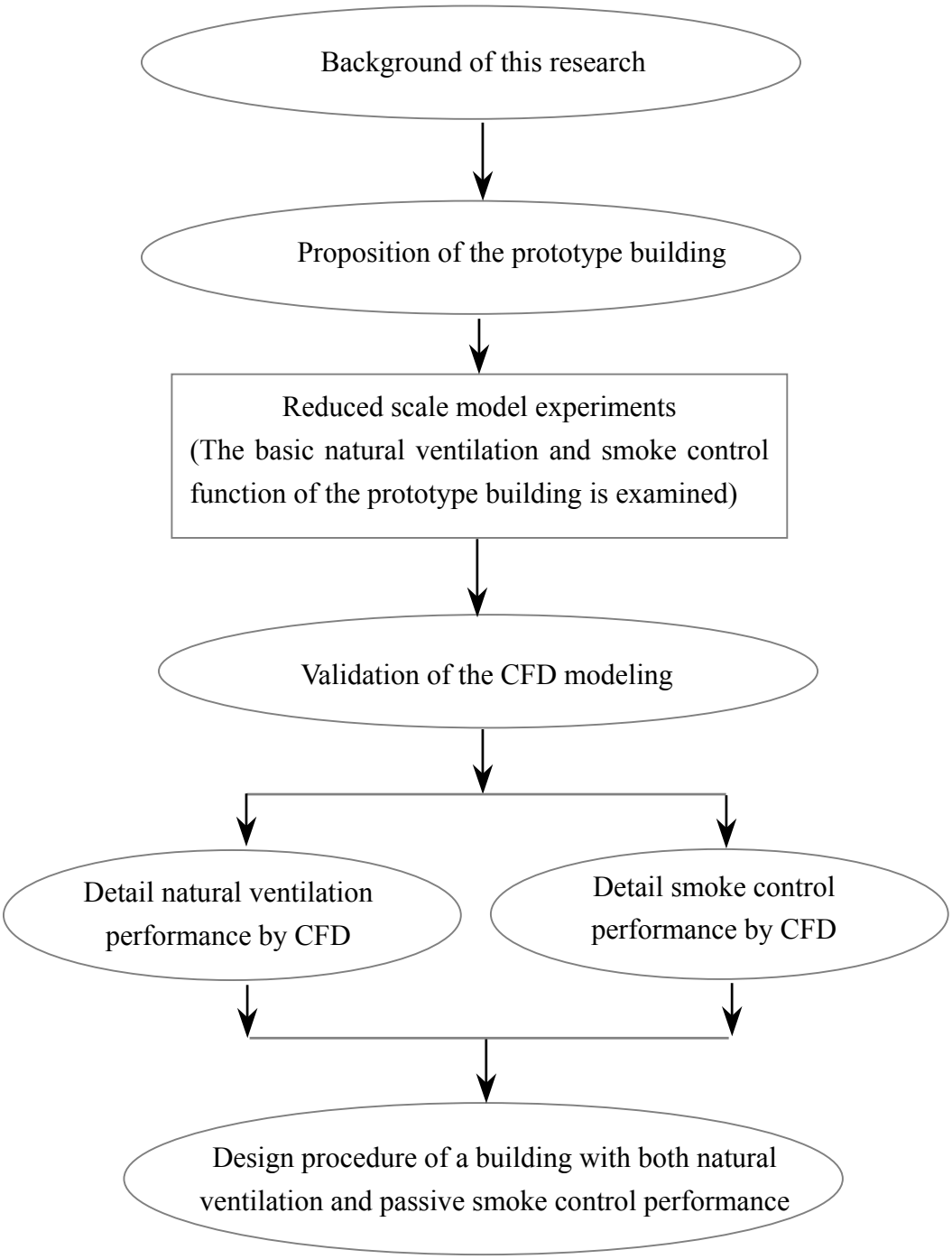

Fig. 2-6 Flow of this research

CHAPTER 3

MODEL EXPERIMENTS

CHAPTER 3
MODEL EXPERIMENTS

To assess the natural ventilation and smoke control performance of the prototype building, reduced scale model experiments are carried out. The experimental model is introduced and several series experiments with different opening and temperature conditions are conducted. The experimental results are presented and analyzed.

3.1 OUTLINE OF THE EXPERIMENTAL MODEL AND TESTING INSTRUMENTS

3.1.1 Outline of the experimental model

Fig. 3-1 is the picture of the experimental model. Fig. 3-2 and Fig.3-3 show the detail of the experimental model.

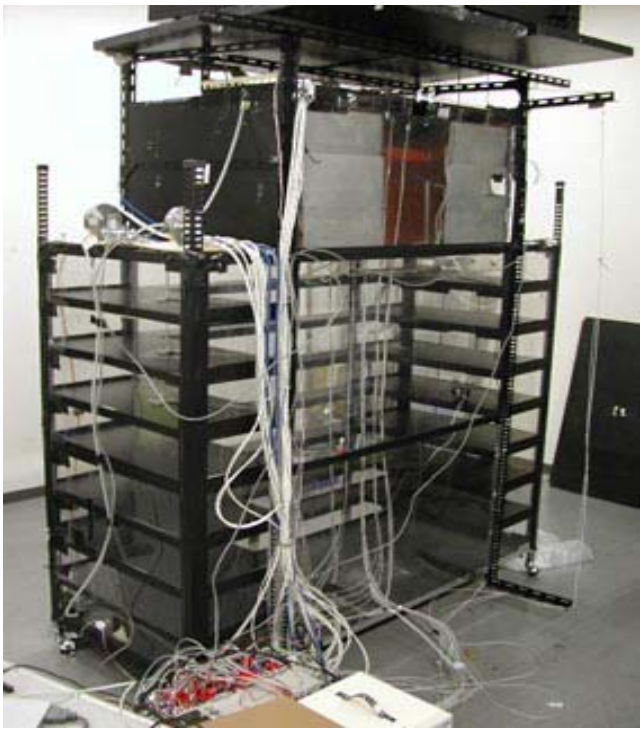

Fig. 3-1 Picture of the experimental model

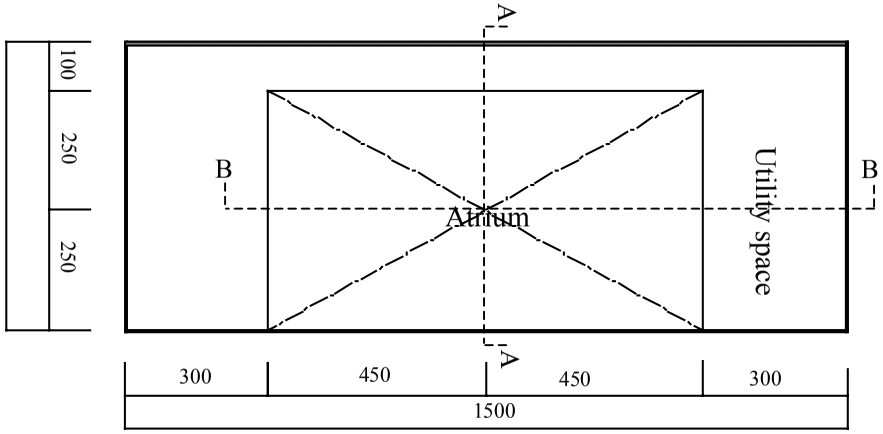

Fig. 3-3 Plan of the experimental model (Units: mm)

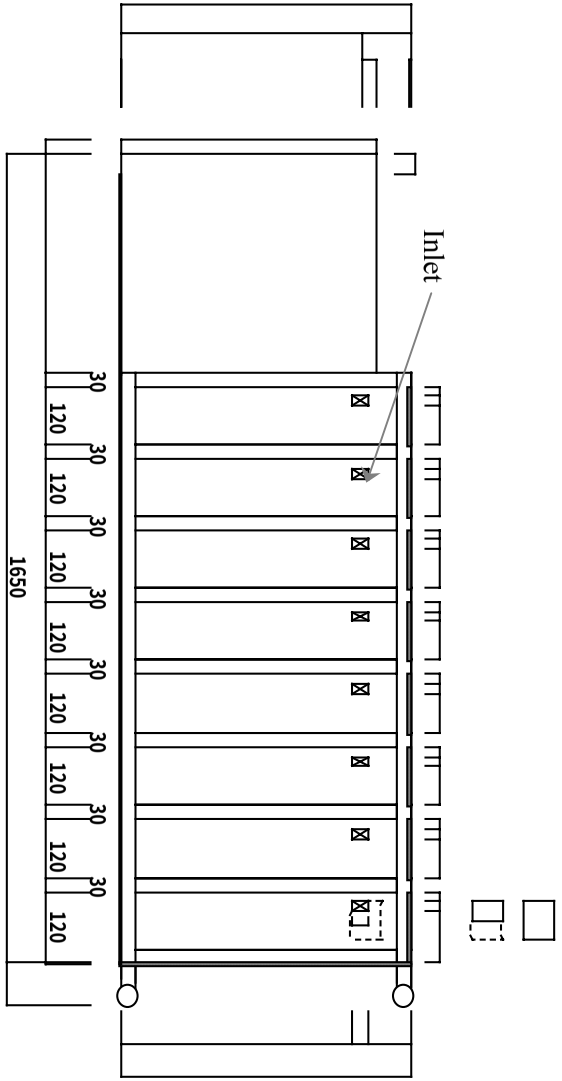

Fig. 3-2 Elevation of the experimental model (Units: mm)

◆Scale: 1/25 of the full-scale building

Considering the dimension of the laboratory, the manual operability of constructing the model and the effectiveness of the similarity laws, a 1/25 scale model is produced. All the phenomena pertaining to natural ventilation and smoke movement are thought of as able to be reproduced under the scale. To simplify the discussion and for the easy operation of the model experiments, only the atrium and the utility space are reproduced.

◆Components and specification:

Materials:

Walls of the atrium and the utility space

To observe the inside situation clearly during the experiments, the perimeter walls of the atrium and the utility space are made of 1mm thick transparent acrylic sheets.

Walls of the chimney

Interior surface: panel heater (silicon rubber sheet with 1mm thick aluminum panel on the back surface, through which electric current passes thus to generate heat)

Exterior surface: 30 mm thick polystyrene panels

To reproduce the temperature rise due to solar radiation absorption, panel heaters are used as the interior surfaces of the walls. 30 mm thick polystyrene boards are attached outside the panel heaters to reduce heat loss.

Structure

Framework: Angle steel

Floors/ceilings: 15mm thick wood panels

Notes:

1. The inlets are produced on both sides of the atrium and uniformly distributed at each floor. All the inlets are created adjustably to conduct different area conditions.
2. The outlets are also created on both sides and on the top of the chimney sidewalls. The width of the outlets is set as 4 cm and the length is made adjustable to create different area conditions.
3. When selecting the materials for the experimental model, thermal performance similarity between the model materials and the real building materials has not been considered. As a compromise to observe the phenomenon occurring inside the experimental model, heat loss from the experimental model is considered to be slightly greater than the real building.

3.1.2 Distribution of the measured points

Due to temperature rise of the panel heaters, temperature and pressure distribution inside the model begin to vary and natural airflow occurs. To assess the natural ventilation quantitatively, temperature distribution, pressure difference distribution and velocities those pertaining to the effectiveness of the natural ventilation system are measured and recorded. Along the centerline of the atrium/chimney, temperatures are measured every 15 cm in the atrium and every 5 cm in the solar chimney. Pressure differences between the atrium/chimney and the outside are measured at the base of the atrium, the border of the atrium and the chimney, the half height of the chimney and the top of the chimney. For the smoke control, the point at the half height of the chimney is moved to the half height of the atrium, because it is estimated that the smoke would descend to the atrium. At the same time velocities of the inlets and the outlets are measured. The distribution of the measured points is shown in Fig. 3-4.

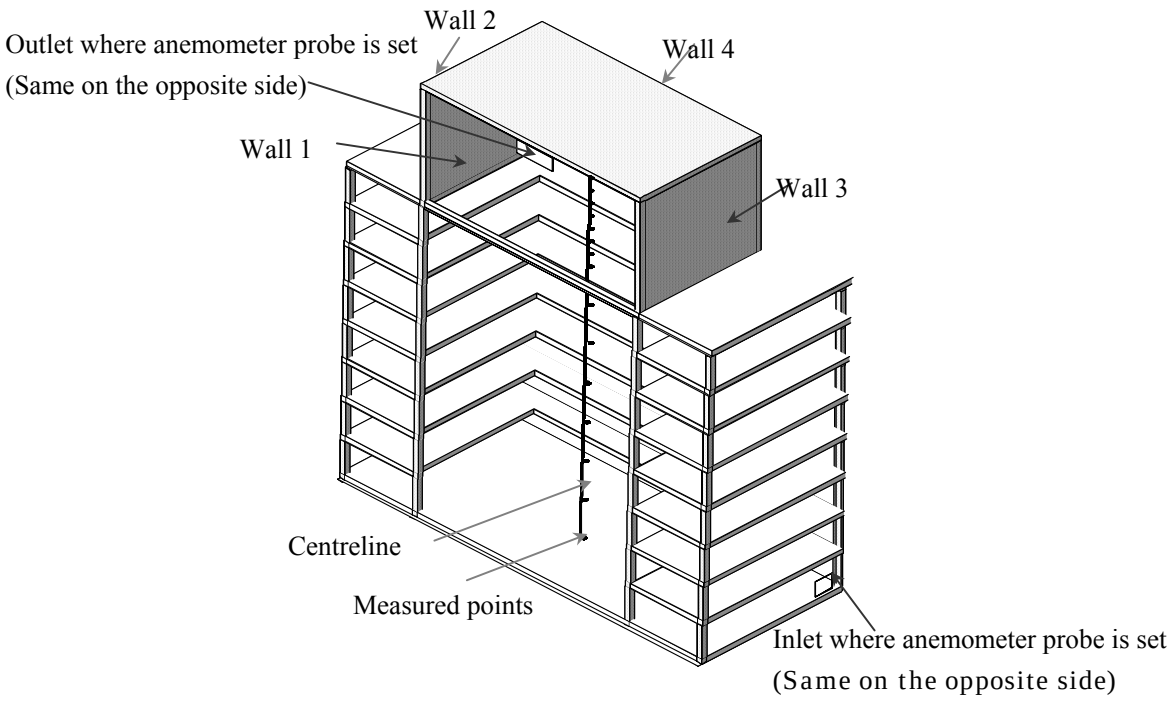

Fig. 3-4 Distribution of the measured points

3.2 OUTLINE OF THE EXPERIMENTAL INSTRUMENTS

◆Panel heaters

Silicon rubber heater

Temperature controller

On the surface of the panel heater, temperature sensor is set, through which the temperature of the panel heater can be controlled as wanted value by adjusting the electric current passing it.

Fig. 3-5a Temperature controller

Fig. 3-5b Panel heater

◆Testing instruments

Temperature: K-type thermocouples (diameter: 0.4 mm)

Along the centerline, K-type thermocouples are distributed every 15 cm in the atrium and every 5 cm in the solar chimney.

Velocity: Thermal anemometer

Air velocities of the inlets and outlets are measured using a 4-channel thermal anemometer. As to the thermal anemometer, a filum is subjected to a constant electronic current and the temperature of the filum depends upon the convective cooling of air flowing past it. The electric current through the filum is adjusted corresponding to the airflow.

Pressure difference:

Pressure differences between outside and the atrium/chimney are measured using electric pressure transducers. The pressure transducers are of diaphragm type.

All instruments are connected with a data collector to record the data every one second.

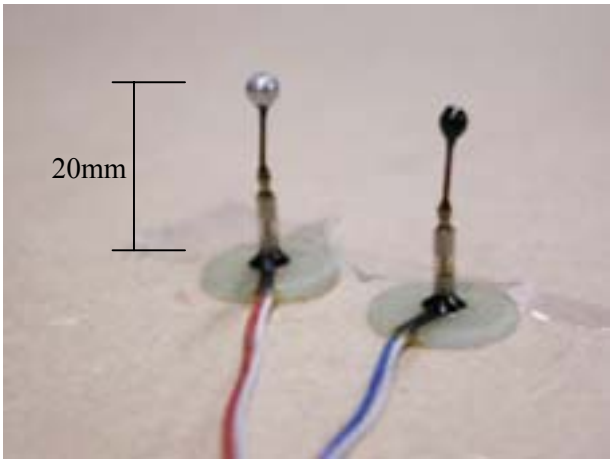

Fig. 3-6a Probe of the thermal anemometer

Fig. 3-6b The main part of the thermal anemometer

Fig. 3-7a Demodulator for analog output of pressure

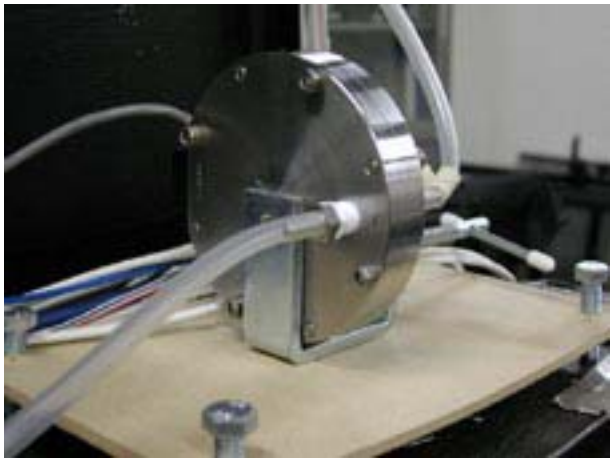

Fig. 3-7b The pressure transducer

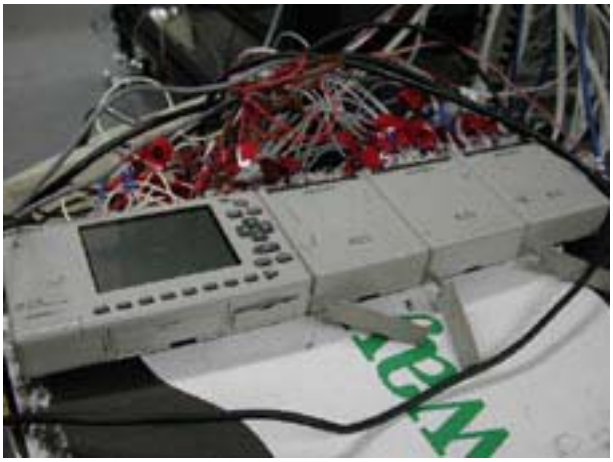

Fig. 3-8 The data collector

Table 3-1 Testing instruments

Measured items	Instruments	Range and Accuracy	Type
Temperature	Thermocouple		K-type
Velocity	Anemometer	Range 0.1m/s～10.0m/s Accuracy ±0.1m/s	Hot-wire GeY-40DA
Pressure difference	Electronic pressure transducer	Range ±2.2mmH_2O Accuracy ±0.05Pa	Diaphragm DP103

Photography device

Digital camera, video camera, CCD camera

3.3 EXPERIMENTS ON THE NATURAL VENTILATION PERFORMANCE

3.3.1 Procedures of the experiments

To simulate the high temperature wall due to absorption of solar radiation, the panel heaters are put into operation. Then with the temperature rising of the panel heaters, the air temperature in the chimney began to rise. Accompanying the variation of temperature, pressure and velocity begin to vary also. After several minutes, the values of temperature, pressure and velocities of outlet and inlet become almost constant, which means the flow has become stable. To assess the flow in detail, the following procedures are taken:

1. In the preliminary experiments, the flow at the inlet and outlet are photographed by following methods:

   Photography at the inlet

   Near the inlet, incense sticks are lit to generate smoke, which makes the flow at the inlet visible. Then the visible flow is photographed by video cameral. During the process of the photography, a laser beam is used.

   Photography at the outlet

   Smoke generation stick is used to generate smoke in the space of atrium/chimney. Accompanying the flow inside the atrium/chimney, the smoke flows out from the outlet. Just as at the inlet, the visible flow of the smoke is photographed.

2. After several minutes when the flow almost becomes stable, temperature distribution, velocities at the inlet and outlet, pressure difference distribution are measured and recorded. The distribution of the measured points is shown in Fig. 3-4.

3. Based on the temperature distribution along the centerline in the atrium/chimney, pressure difference distribution is calculated according to following methods.

   The temperature between measured points k and k+1 is supposed to be the average of the two points. Assuming the pressure difference at the base of the atrium as Δp_{bot} (Pa), and the pressure difference at the top of the chimney as Δp_{top} (Pa), we can get:

$$\Delta p_{top} - \Delta p_{bot} = -\sum_{k=1}^{18}\left(\frac{\rho_k + \rho_{k+1}}{2} - \rho_0\right) g \Delta z_k \qquad (3\text{-}8)$$

   where

Δz_k is vertical distance between point k+1 and point k, m;

ρ_0 is density of ambient air, kg/m^3;

ρ_k is air density at point k, kg/m^3. It can be approximately calculated as:

$$\rho = \frac{353}{T_k} \tag{3-9}$$

According to the Bernoulli's law, the velocity of the opening at the base of the atrium v_{bot} (m/s) and at the top of the chimney v_{top} (m/s) can be expressed as:

$$v_{bot} = \alpha \sqrt{\frac{2 \mid \Delta p_{bot} \mid}{\rho_{bot}}} \tag{3-10}$$

$$v_{top} = \alpha \sqrt{\frac{2 \mid \Delta p_{top} \mid}{\rho_{top}}} \tag{3-11}$$

where α is discharge coefficient, dimensionless.

And the mass flow rate M (kg/m^3) is:

$$M = vA\rho \tag{3-12}$$

where

v is velocity, m/s.

A is opening area, m^2.

Considering the conservation of mass flow rate, we can get:

$$\frac{\left|\Delta p_{top}\right|}{\left|\Delta p_{bot}\right|} = \frac{{A_{in}}^2 \rho_{bot}}{{A_{out}}^2 \rho_{top}} \tag{3-13}$$

where

A_{in} is area of inlet, m^2;

A_{out} is area of outlet, m^2.

According to Eq. (3-8) and Eq. (3-13), Δp_{top} and Δp_{bot} can be obtained from measured temperature distribution. And pressure difference at other testing points can be calculated as:

$$\Delta p_l = \Delta p_{bot} - \sum_{k=1}^{l} \left(\frac{\rho_k + \rho_{k+1}}{2} - \rho_0 \right) g \Delta z_k \qquad (3\text{-}14)$$

3.3.2 Experimental conditions

In the experiments, the area ratio of outlet to inlet and the temperature of the thermal storage wall are considered as important parameters that will affect the effectiveness of natural ventilation. The combination of different area ratio and different wall temperature (5 series in total) are set as experimental conditions. The considerations for the wall temperature and openings are as following:

◆Wall temperature

The interior surfaces' temperatures of the chimney can be set by controlling the temperatures of the panel heaters. In the experiments, the north-facing wall is considered as the main thermal storage wall, whose temperature is supposed to be higher than others. Thus the temperature of the north-facing wall is set by controlling the panel heater, while the temperatures of the other walls of the chimney are left as they are. Although the temperatures of the other walls are not set, due to the radiation from the north-facing wall, the temperatures of the other walls also rise. Their temperatures are measured by thermocouples.

◆Openings

Outlets: The outlets are set at the both sides of the chimney. For the easy operations of the experiments, the widths of the outlets are kept as constant as 4 cm and the lengths are changed to create different area conditions.

Inlets: The inlets are set at the both sides of the atrium. Two conditions are examined in the experiments. One is that all the inlets are supposed to concentrate at the lower part of the atrium. The other is that the inlets are uniformly distributed at each floor.

Table 3-2 Experimental conditions

Opening areas ( ) is the full-scale area		Temperature rise of the north-facing wall					
Outlets	Inlets	+15℃		+20℃		+25℃	
			No.		No.		No.
48 cm^2 (3 m^2)	96 cm^2 (6 m^2)			○	nv1－0.5		
96 cm^2 (6 m^2)	96 cm^2 (6 m^2)	○	nv4(1)－15	○	nv1－1 nv2－1 nv4(1)－20	○	nv4(1)－25
192 cm^2 (12 m^2)	96 cm^2 (6 m^2)			○	nv1－2		
288 cm^2 (18 m^2)	96 cm^2 (6 m^2)	○	nv4(3)－15	○	nv1－3 nv4(2)－20	○	nv4(3)－25
384 cm^2 (24 m^2)	96 cm^2 (6 m^2)			○	nv1－4		
480 cm^2 (30 m^2)	96 cm^2 (6 m^2)			○	nv1－5		
48 cm^2 (3 m^2)	48 cm^2 (3 m^2)			○	nv2－0.5		
192 cm^2 (12 m^2)	192 cm^2 (12 m^2)			○	nv2－2		
288 cm^2 (18 m^2)	288 cm^2 (18 m^2)			○	nv2－3		
48 cm^2 (3 m^2)	12 cm^2 at each floor (0.75 m^2)			○	nv3－0.5		
96 cm^2 (6 m^2)	12 cm^2 at each floor (0.75 m^2)	○	nv5(1)－15	○	nv3－1 nv5(1)－20	○	nv5(1)－25
192 cm^2 (12 m^2)	12 cm^2 at each floor (0.75 m^2)			○	nv3－2		
288 cm^2 (18 m^2)	12 cm^2 at each floor (0.75 m^2)	○	nv5(3)－15	○	nv3－3 nv5(2)－20	○	nv5(3)－25

◆Preliminary experiment

At first the flow is examined by visualization when the temperature of the north-facing wall is set as 20 ˚C higher than the ambient temperature.

Table 3-3 Conditions for preliminary experiment

No.	Temperature rise of Wall 4	Outlets (full-scale)	Inlets (full-scale)
nv0-1	+20 °C	4cm×12cm×2=96 cm^2 (6 m^2)	2cm×3cm×2×8 floors＝96 cm^2 (6 m^2)

◆Conditions for series nv 1

The total areas of the inlets are set as around 1/45 of the floor area of the atrium. The outlet area is changed to make the area ratio of outlets to inlets as 0.5,1,2,3,4,5 respectively. The temperature of the north-facing wall is set as 20 °C higher than the ambient temperature.

Table 3-4 Experimental conditions for series nv1

No.	Temperature rise of Wall 4	Outlets (full-scale)	Inlets (full-scale)
nv1-0.5	+20 °C	4cm×6cm×2=48 cm^2 (3 m^2)	8cm×6cm×2＝96 cm^2 (6 m^2)
nv1-1		4cm×12cm×2=96 cm^2 (6 m^2)	
nv1-2		4cm×24cm×2=192 cm^2 (12 m^2)	
nv1-3		4cm×36cm×2=288 cm^2 (18 m^2)	
nv1-4		4cm×48cm×2=384 cm^2 (24 m^2)	
nv1-5		4cm×60cm×2=480 cm^2 (30 m^2)	

◆Conditions for series nv2

The areas of the outlets and inlets are set as the same as 3,6,12,18 ㎡ respectively. The temperature of the north-facing wall is set as 20 °C higher than the ambient temperature.

Table 3-5 Experimental conditions for series nv2

No.	Temperature rise of Wall 4	Outlets (full-scale)	Inlets (full-scale)
nv2-0.5	+20 °C	4cm×6cm×2=48 cm^2 (3 m^2)	4cm×6cm×2=48 cm^2 (3 m^2)
nv2-1		4cm×12cm×2=96 cm^2 (6 m^2)	8cm×6cm×2=96 cm^2 (6 m^2)
nv2-2		4cm×24cm×2=192 cm^2 (12 m^2)	8cm×6cm×2×2 floors=192 cm^2 (12 m^2)
nv2-3		4cm×36cm×2=288 cm^2 (18 m^2)	8cm×6cm×2×3 floors=288 cm^2 (18 m^2)

◆Conditions for series nv3

Comparing with the conditions for series nv1, the inlets are set uniformly distributed at each floor. The temperature of the north-facing wall is set as 20 °C higher than the ambient temperature.

Table 3-6 Experimental conditions for series nv3

No.	Temperature rise of Wall 4	Outlets (full-scale)	Inlets (full-scale)
nv3-0.5	+20 °C	4cm×6cm×2=48 cm^2 (3 m^2)	2cm×3cm×2×8 floors=96 cm^2 (6 m^2)
nv3-1		4cm×12cm×2=96 cm^2 (6 m^2)	
nv3-2		4cm×24cm×2=192 cm^2 (12 m^2)	
nv3-3		4cm×36cm×2=288 cm^2 (18 m^2)	

◆Conditions for series nv4

Keeping the area of outlets and inlets as constant and the north-facing wall temperature is changed to create different temperature conditions.

Table 3-7 Experimental conditions for series nv4

No.	Wall temperature rise	Outlets (full-scale)	Inlets (full-scale)
nv4(1)-15	+15℃	4cm×12cm×2=96 cm^2 (6 m^2)	8cm×6cm×2=96 cm^2 (6 m^2)
nv4(1)-20	+20℃		
nv4(1)-25	+25℃		
nv4(3)-15	+15℃	4cm×36cm×2=288 cm^2 (18 m^2)	
nv4(3)-20	+20℃		
nv4(3)-25	+15℃		

◆Conditions for series nv5

Comparing with the conditions for series nv4, the inlets are set uniformly distributed at each floor.

Table 3-8 Experimental conditions for series nv5

No.	Wall temperature rise	Outlets (full-scale)	Inlets (full-scale)
nv5(1)-15	+15℃	4cm×12cm×2=96 cm^2 (6 m^2)	2cm×3cm×2×8 floors＝96 cm^2 (6 m^2)
nv5(1)-20	+20℃		
nv5(1)-25	+25℃		
nv5(3)-15	+15℃	4cm×36cm×2=288 cm^2 (18 m^2)	
nv5(3)-20	+20℃		
nv5(3)-25	+25℃		

◆Visualization experiments

These experiments are conducted to confirm the natural airflow in the experimental model. The temperature of the north-facing wall (wall 4) is set as 20 °C higher than the ambient temperature. To grasp the position of the neutral pressure plane, partitions are set at the boundary of the atrium and the utility space from 6F to 8F. Moreover, small openings are set on the partitions to observe the smoke movement between the atrium and the utility space. As to the experimental methods, after the airflow inside the experimental model becomes stable, smoke generation stick put at the base of the atrium is ignited. Since there is almost no heat released from the smoke generation stick itself, the observed movement of the smoke can be thought of as reflecting the natural airflow throughout the atrium/chimney space.

Table 3-9 Experimental conditions for series nvs

<table>
<tr><th rowspan="2">No.</th><th rowspan="2">Temperature rise of wall 4</th><th colspan="2">Opening area</th></tr>
<tr><th>Outlets (full-scale)</th><th>Inlets (full-scale)</th></tr>
<tr><td>nvs(1)-0.5</td><td rowspan="4">+20 °C</td><td>4cm×6cm×2=96 cm^2
(3 m^2)</td><td rowspan="2">6cm×8cm×2=96 cm^2
(6 m^2)</td></tr>
<tr><td>nvs(1)-3</td><td>4cm×36cm×2=288 cm^2
(18 m^2)</td></tr>
<tr><td>nvs(8)-0.5</td><td>4cm×6cm×2=96 cm^2
(3 m^2)</td><td rowspan="2">2cm×3cm×2×8 floors=96 cm^2
(6 m^2)</td></tr>
<tr><td>nvs(8)-3</td><td>4cm×36cm×2=288 cm^2
(18 m^2)</td></tr>
</table>

3.3.3 Experimental results

The measured values of temperature distribution, pressure difference distribution, the ambient temperature, and the wall surface temperatures during the experiments are shown as following.

3.3.3.1 Results of the preliminary experiment

The panel heater is put into operation and then the air temperature inside the chimney channel begins to rise. Due to the stack effect, the air inside the atrium/chimney flows out

from the outlets and the outside air flows into the atrium from the inlets, just as shown in the following pictures.

Fig. 3-9a Airflow at the outlet

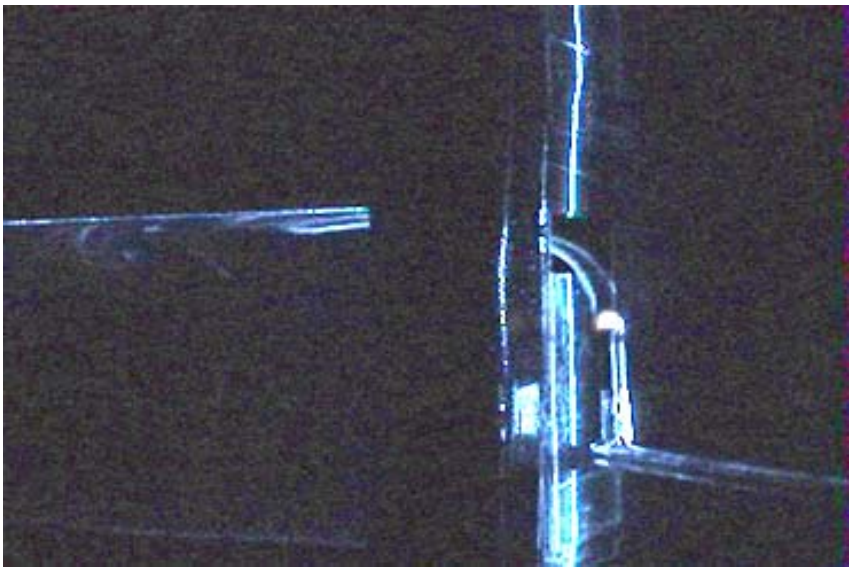

Fig. 3-9b Airflow at the inlet

3.3.3.2 Experimental results of series nv1~nv5

◆Surface temperatures of the solar chimney walls

During the experiments, although only the main thermal storage wall is given a constant temperature, the surface temperatures of other walls also rise due to the radiation heat exchange between each wall. The measured surface temperature of each wall is as following. Wall 5 is the ceiling of the chimney.

Table 3-10 Tested surfaces' temperatures in series nv1

No.	Ambient temperature [℃]	Surface temperature[℃] (Temperature rise [℃])				
		1	2	3	4	5
nv1-0.5	24.26	28.03 (3.77)	27.66 (3.4)	28.27 (4.01)	42.12 (17.85)	29.01 (4.75)
nv1-1	25.45	28.82 (3.37)	28.49 (3.04)	29.08 (3.63)	43.15 (17.7)	31.04 (5.59)
nv1-2	25.49	29.10 (3.61)	28.86 (3.37)	29.35 (3.86)	43.04 (17.55)	31.11 (5.62)
nv1-3	25.46	28.86 (3.4)	28.66 (3.2)	29.20 (3.74)	43.99 (18.53)	31.00 (5.54)
nv1-4	25.43	28.76 (3.33)	28.50 (3.07)	29.06 (3.63)	43.98 (18.55)	30.88 (5.45)
nv1-5	25.49	28.72 (3.23)	28.46 (2.97)	29.02 (3.53)	44.00 (18.51)	31.01 (5.52)

Table 3-11 Tested surfaces' temperatures in series nv2

No.	Ambient temperature [℃]	Surface temperature [℃] (Temperature rise [℃])				
		1	2	3	4	5
nv2-0.5	25.47	28.98 (3.51)	28.60 (3.13)	29.24 (3.77)	43.21 (17.74)	30.94 (5.47)
nv2-1	25.45	28.82 (3.37)	28.49 (3.04)	29.08 (3.63)	43.15 (17.7)	31.04 (5.59)
nv2-2	25.44	28.16 (2.72)	27.95 (2.51)	28.45 (3.01)	43.07 (17.63)	30.32 (4.88)
nv2-3	25.46	28.20 (2.74)	28.04 (2.58)	28.56 (3.1)	43.04 (17.58)	30.39 (4.93)

Table 3-12 Tested surfaces' temperatures in series nv3

No.	Ambient temperature [℃]	Surface temperature [℃] (Temperature rise [℃])				
		1	2	3	4	5
nv3-0.5	24.24	27.93 (3.69)	27.50 (3.26)	28.08 (3.84)	42.09 (17.85)	28.98 (4.74)
nv3-1	26.96	30.71 (3.75)	30.30 (3.34)	30.86 (3.9)	44.52 (17.56)	32.63 (5.67)
nv3-2	26.85	30.30 (3.45)	29.99 (3.14)	30.48 (3.63)	45.58 (18.73)	32.26 (5.41)
nv3-3	25.61	28.53 (2.92)	28.30 (2.69)	28.85 (3.24)	43.20 (17.59)	30.80 (5.19)

Table 3-13 Tested surfaces' temperatures in series nv4

No.	Ambient temperature [℃]	Surface temperature [℃] (Temperature rise [℃])				
		1	2	3	4	5
nv4(1)-15	26.69	29.47 (2.78)	29.20 (2.51)	29.68 (2.99)	41.13 (14.44)	31.55 (4.86)
nv4(1)-20	25.45	28.82 (3.37)	28.49 (3.04)	29.08 (3.63)	43.15 (17.7)	31.04 (5.59)
nv4(1)-25	25.48	29.94 (4.46)	29.61 (4.13)	30.24 (4.76)	47.68 (22.2)	32.07 (6.59)
nv4(3)-15	26.57	28.74 (2.17)	28.30 (1.73)	28.76 (2.19)	39.90 (13.33)	30.33 (3.76)
nv4(3)-20	25.46	28.86 (3.4)	28.66 (3.2)	29.20 (3.74)	43.99 (18.53)	31.00 (5.54)
nv4(3)-25	27.32	32.04 (4.72)	31.56 (4.24)	32.15 (4.83)	50.18 (22.86)	34.42 (7.1)

Table 3-14 Tested surfaces' temperatures in series nv5

No.	Ambient temperature [℃]	Surface temperature [℃] (Temperature rise [℃])				
		1	2	3	4	5
nv5(1)-15	26.72	29.66 (2.94)	29.43 (2.71)	29.88 (3.16)	40.65 (13.93)	31.81 (5.09)
nv5(1)-20	26.96	30.71 (3.75)	30.30 (3.34)	30.86 (3.9)	44.52 (17.56)	32.63 (5.67)
nv5(1)-25	26.90	31.97 (5.07)	31.49 (4.59)	32.14 (5.24)	49.52 (22.62)	33.98 (7.08)
nv5(3)-15	25.59	28.53 (2.94)	28.31 (2.72)	28.83 (3.24)	38.58 (12.99)	30.67 (5.08)
nv5(3)-20	25.61	28.53 (2.92)	28.30 (2.69)	28.85 (3.24)	43.20 (17.59)	30.80 (5.19)
nv5(3)-25	25.57	29.89 (4.32)	29.54 (3.97)	30.17 (4.6)	47.60 (22.03)	31.88 (6.31)

◆ Temperature rise distribution in the atrium/chimney, pressure difference distribution, velocities of the outlets and inlets and calculated pressure difference according to the measured temperature distribution are shown in following pages.

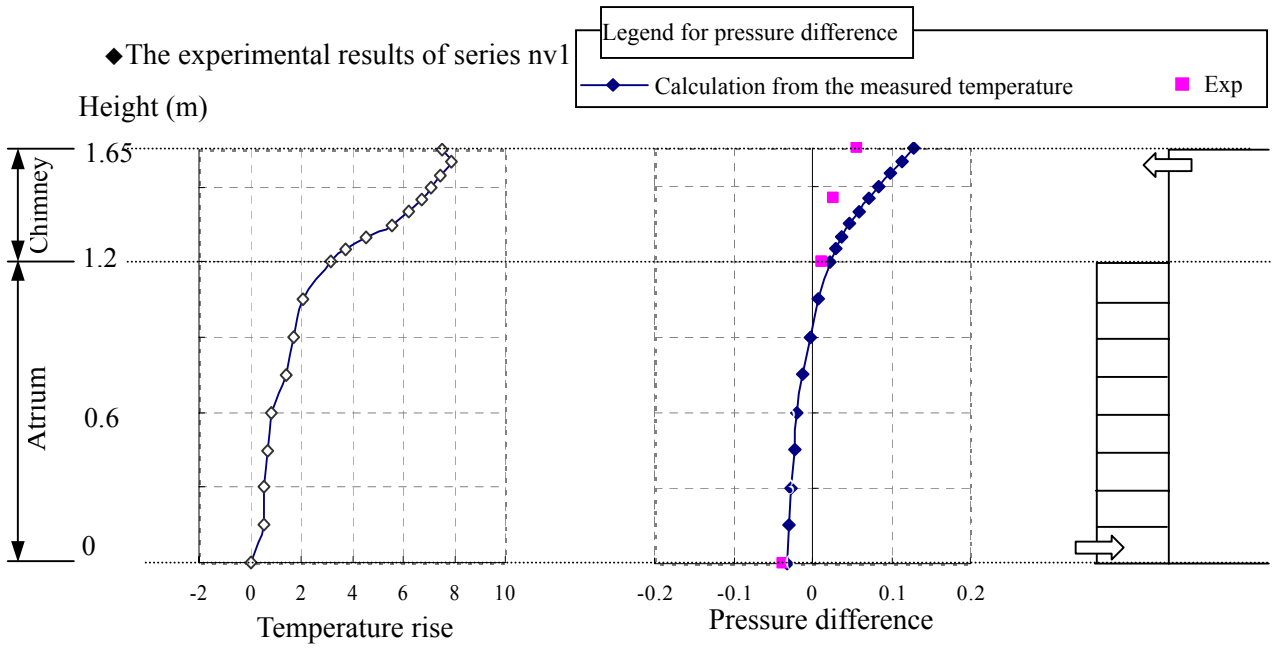

Fig. 3-10a Temperature rise and pressure difference of nv1-0.5

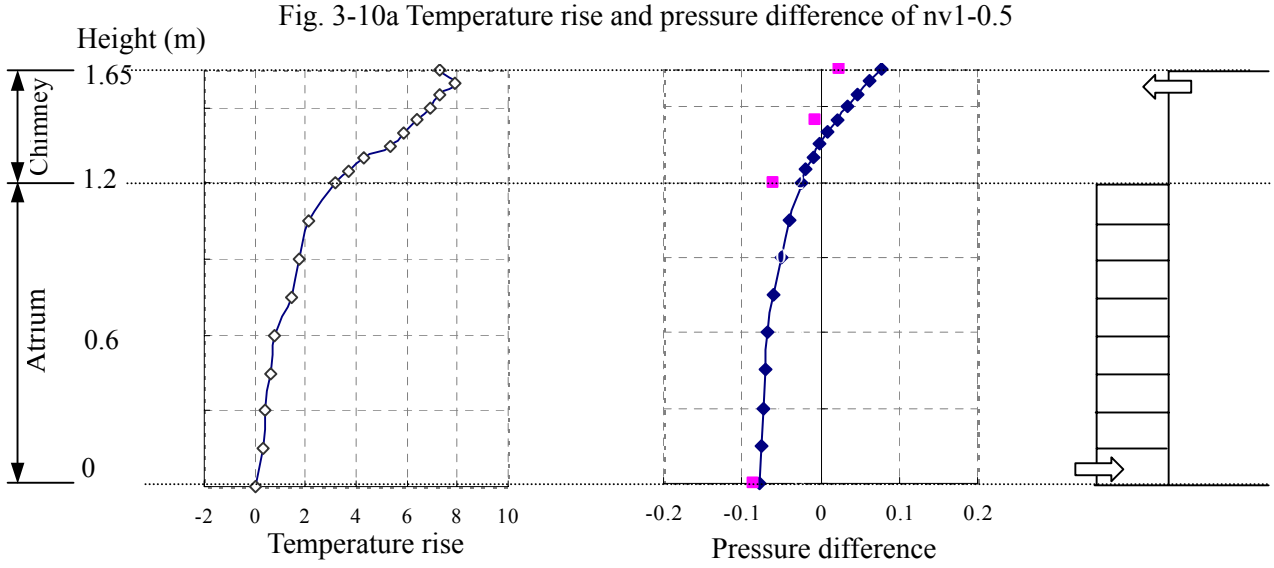

Fig. 3-10b Temperature rise and pressure difference of nv1-1

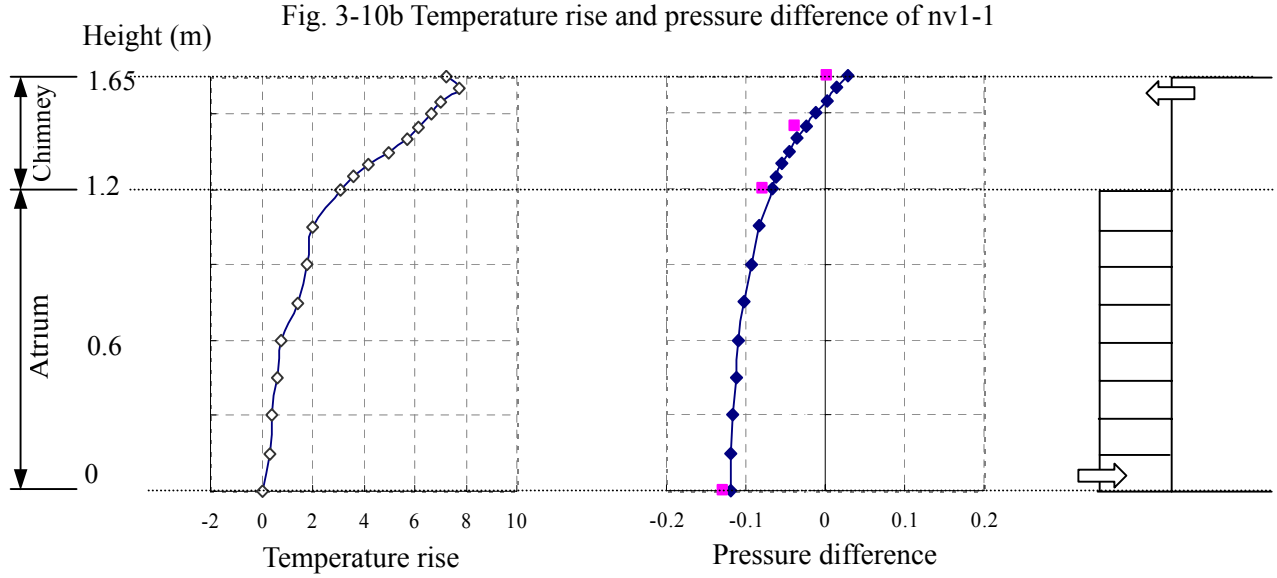

Fig. 3-10c Temperature rise and pressure difference of nv1-2

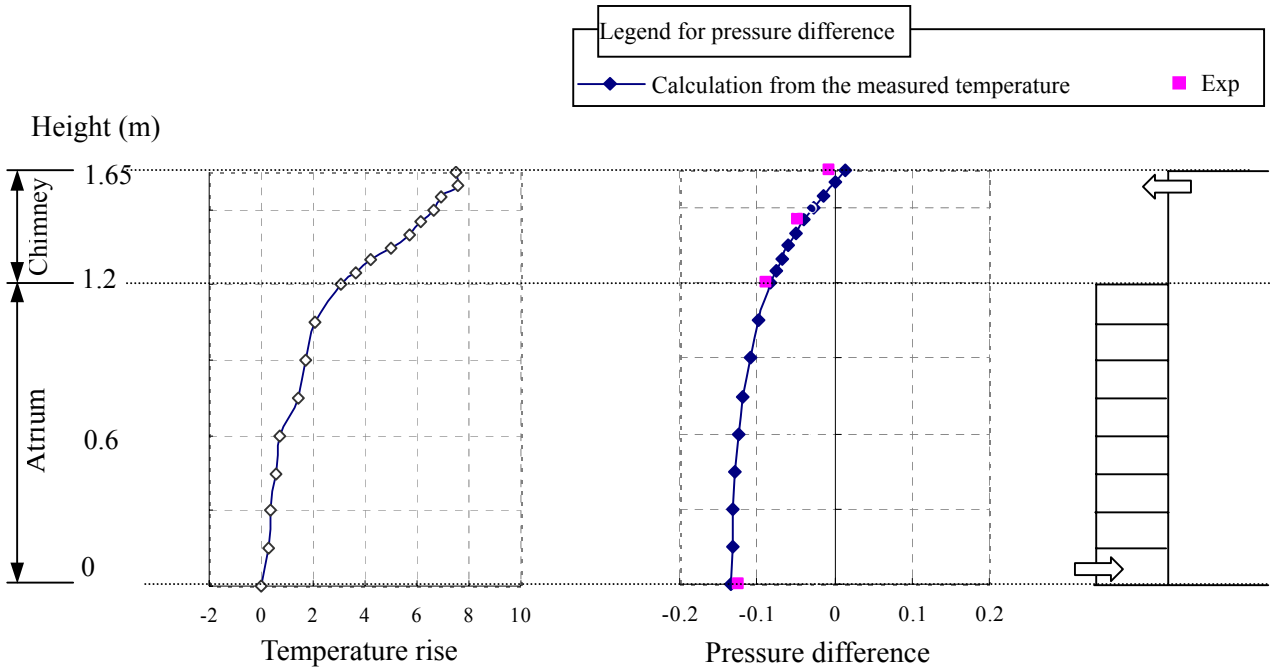

Fig. 3-10d Temperature rise and pressure difference of nv1-3

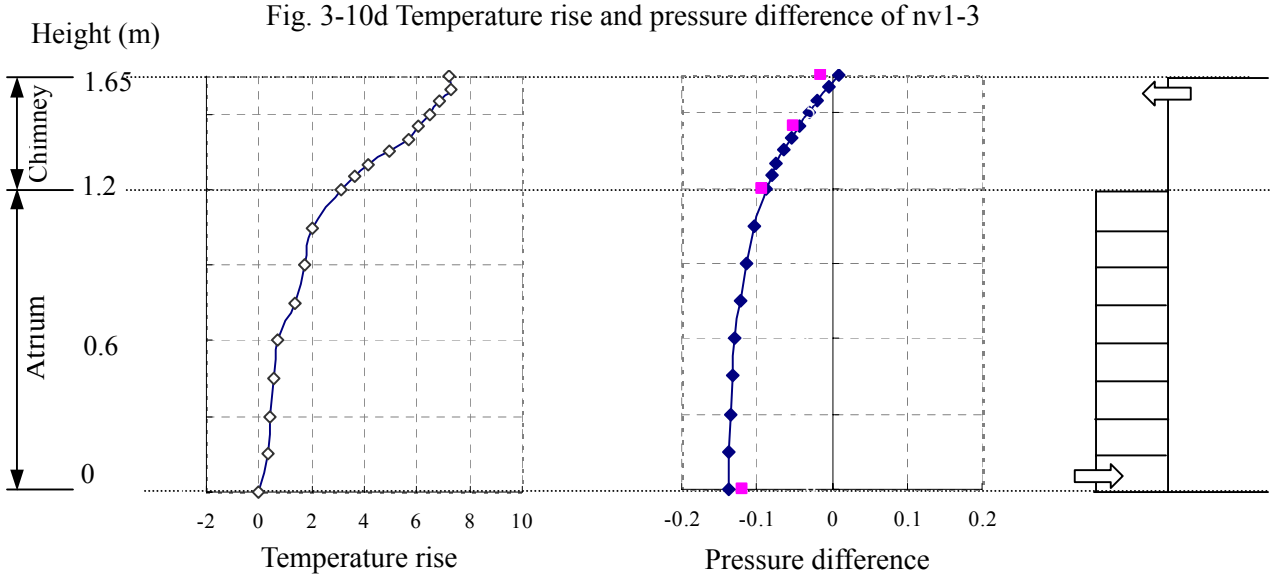

Fig. 3-10e Temperature rise and pressure difference of nv1-4

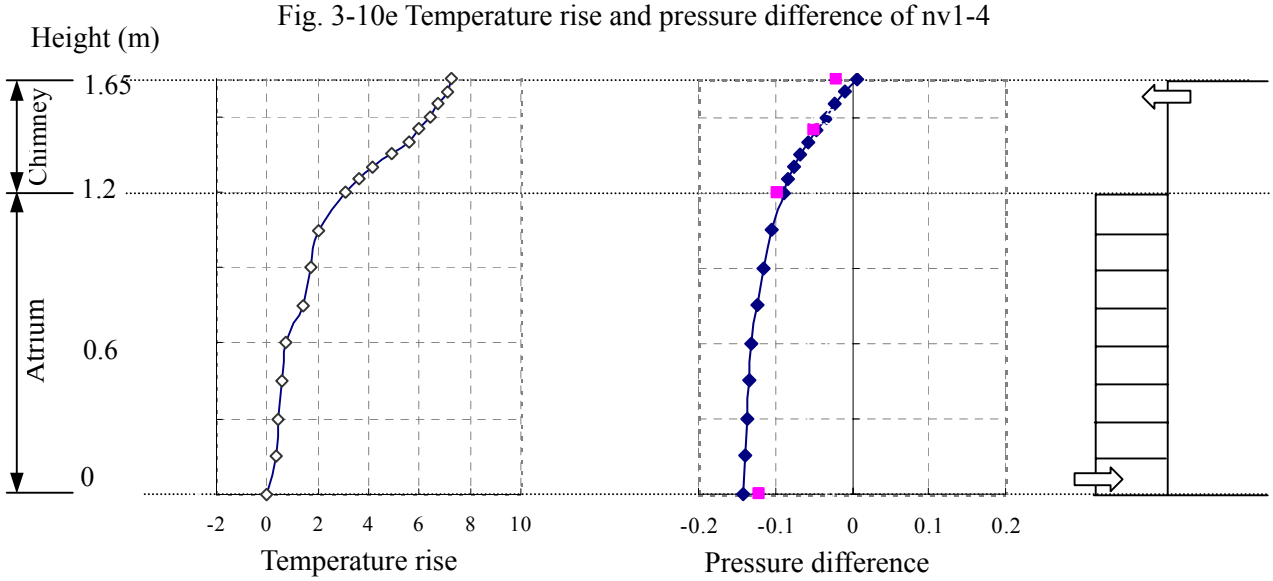

Fig. 3-10f Temperature rise and pressure difference of nv1-5

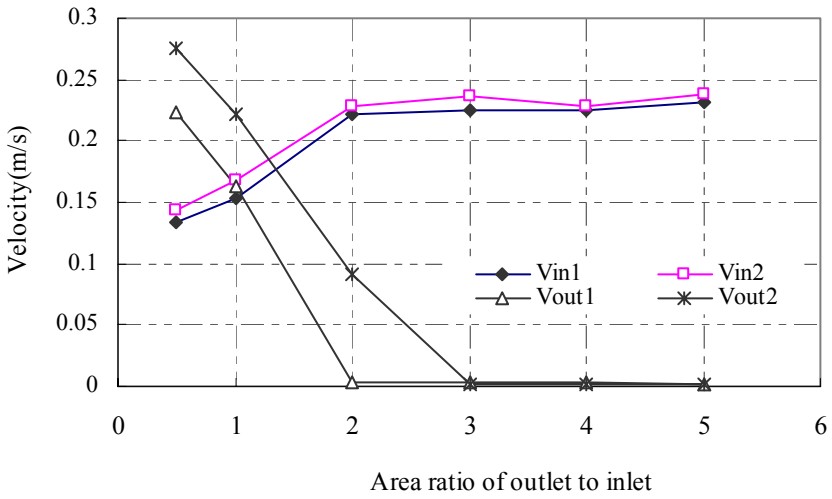

Fig. 3-10g Velocities of outlets and inlets

Note:

When the outlet area becomes over 2 times of the inlet area, the outlet velocity is too small to be recorded.

◆The experimental results of series nv2

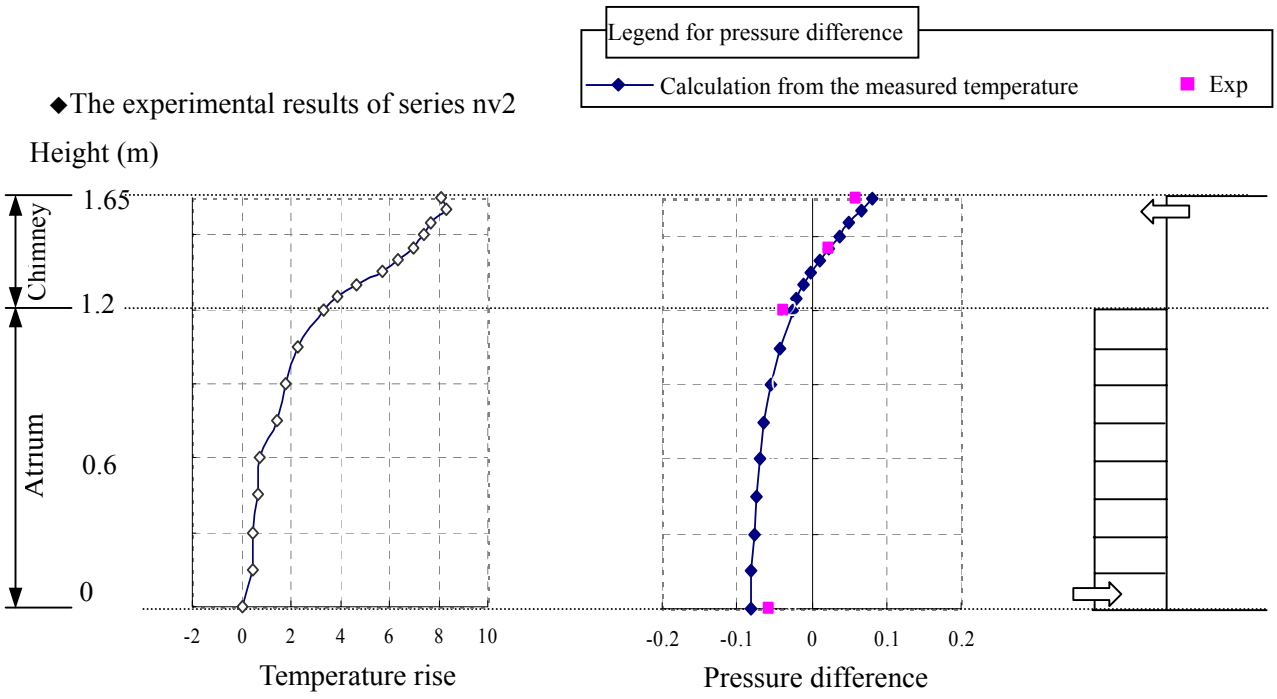

Fig. 3-11a Temperature rise and pressure difference of nv2-0.5

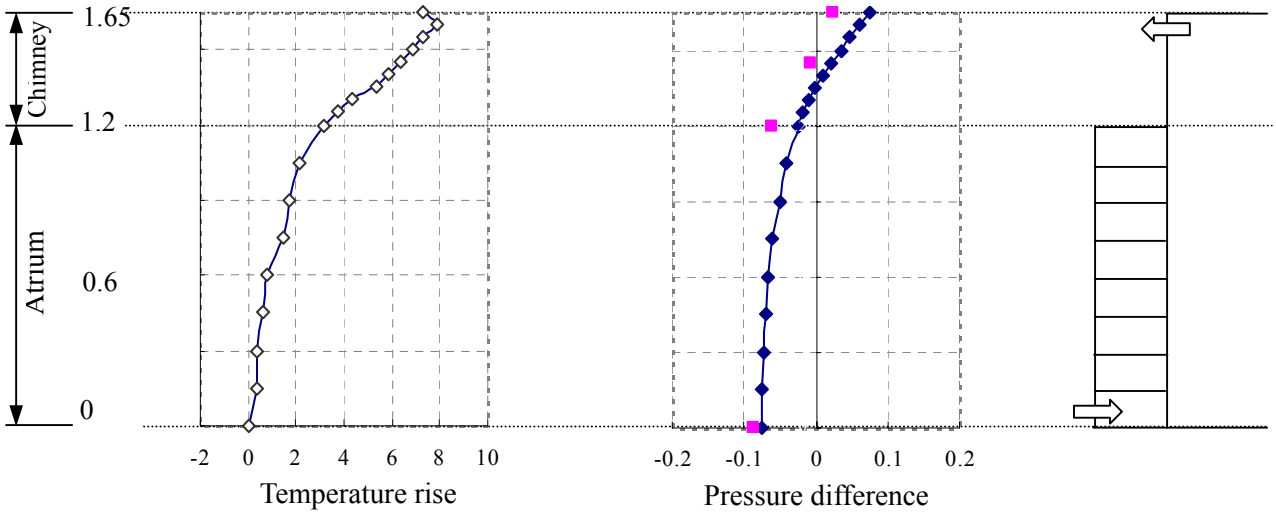

Fig. 3-11b Temperature rise and pressure difference of nv2-1

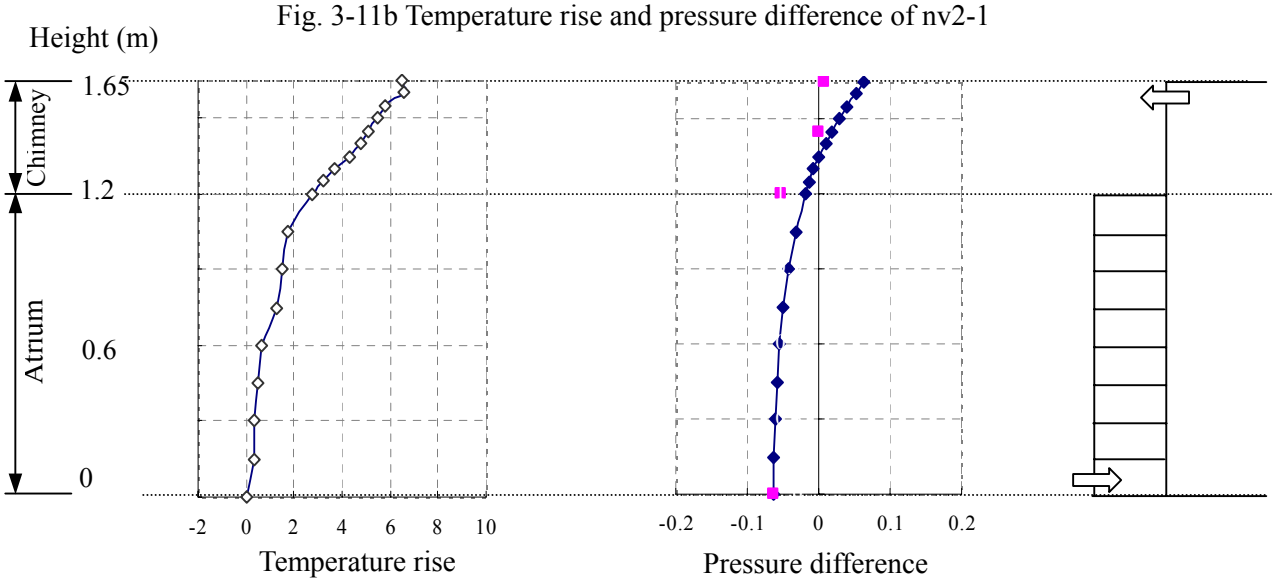

Fig. 3-11c Temperature rise and pressure difference of nv2-2

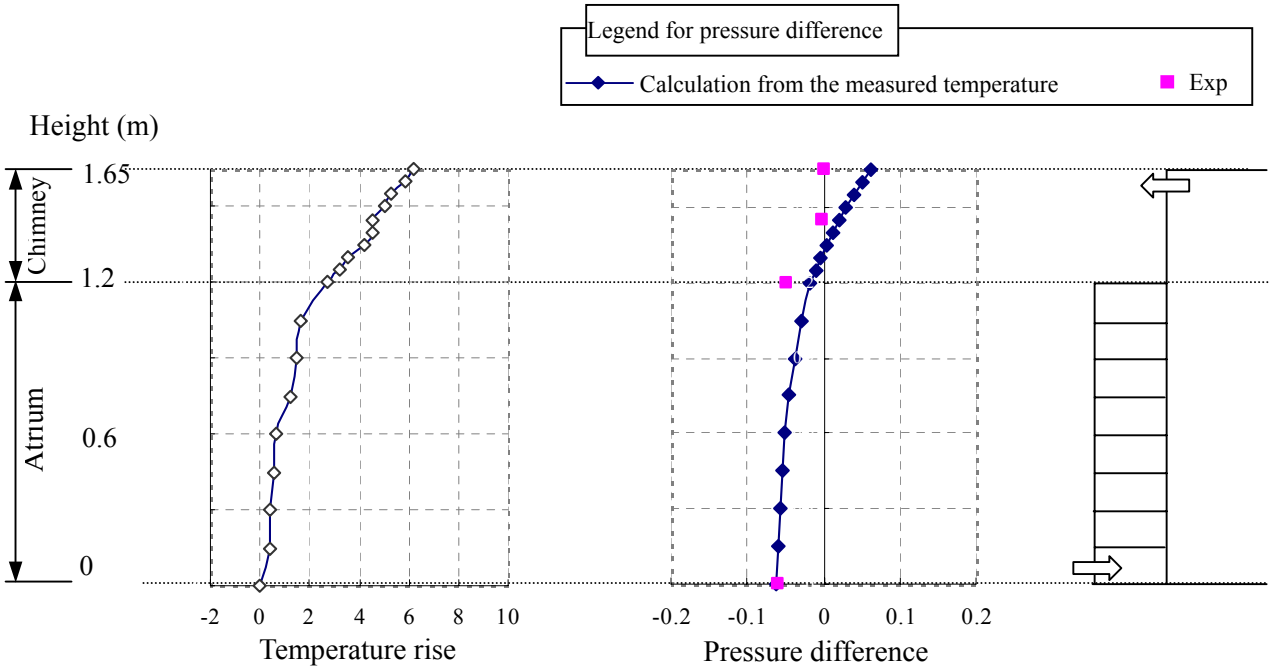

Fig. 3-11d Temperature rise and pressure difference of nv2-3

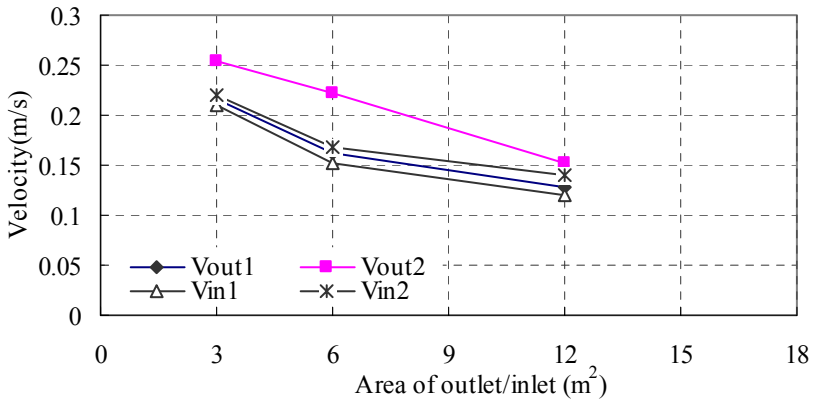

Fig. 3-11e Velocities of outlets and inlets

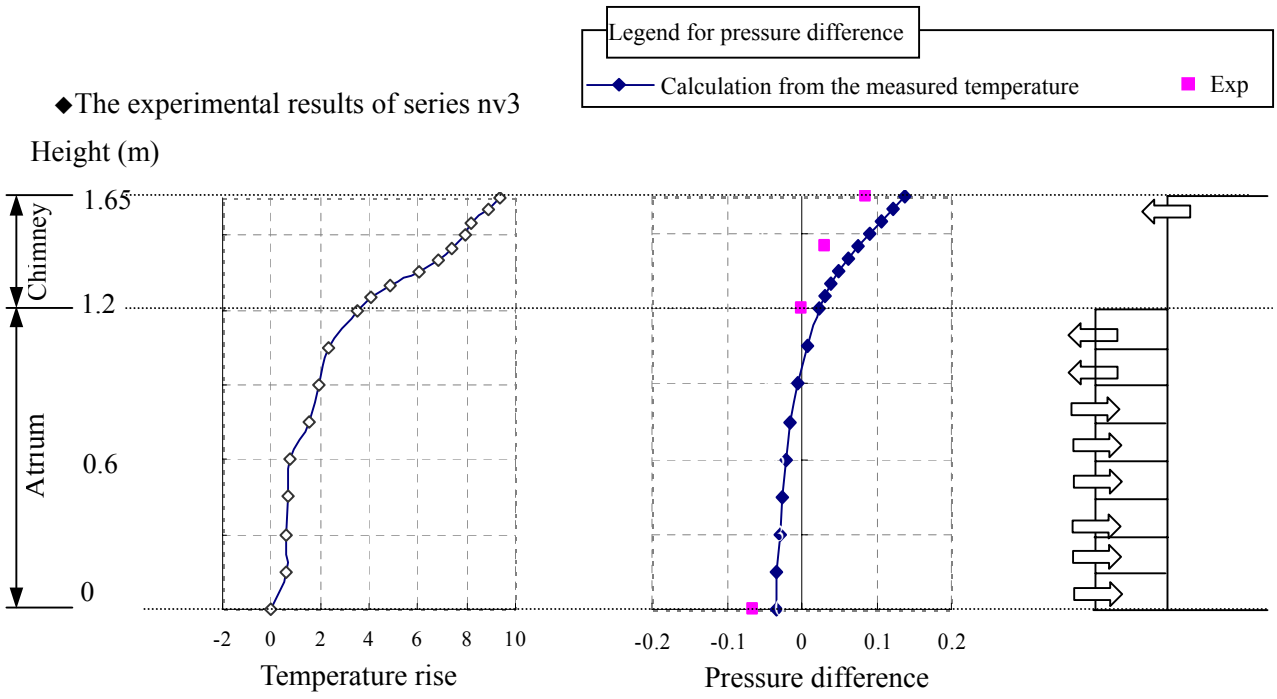

Fig. 3-12a Temperature rise and pressure difference of nv3-0.5

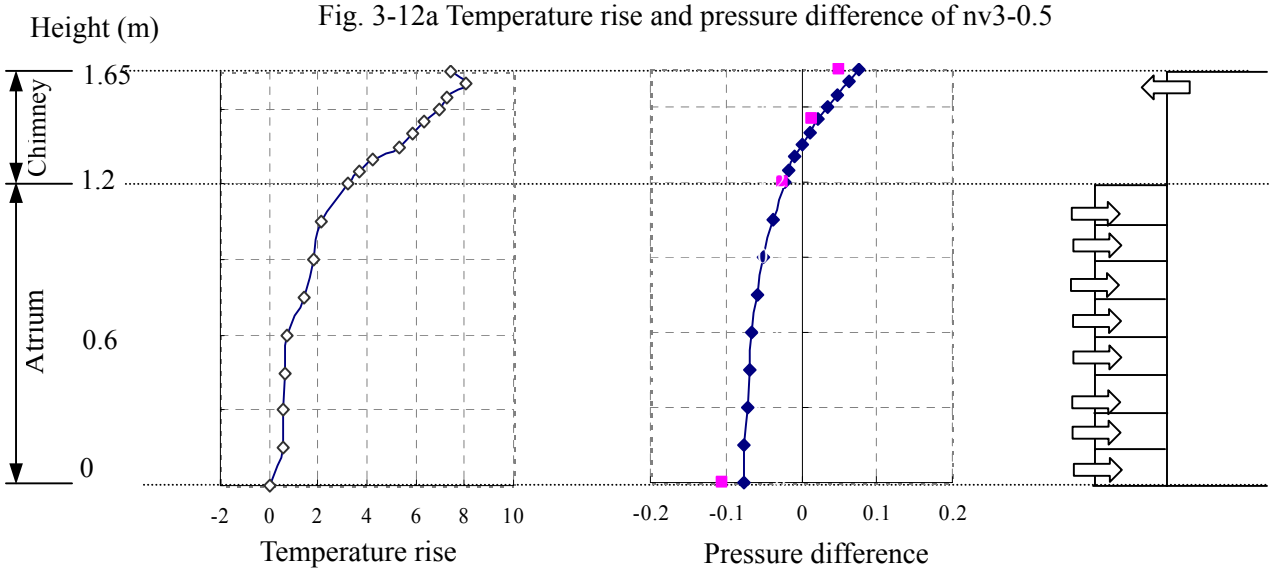

Fig. 3-12b Temperature rise and pressure difference of nv3-1

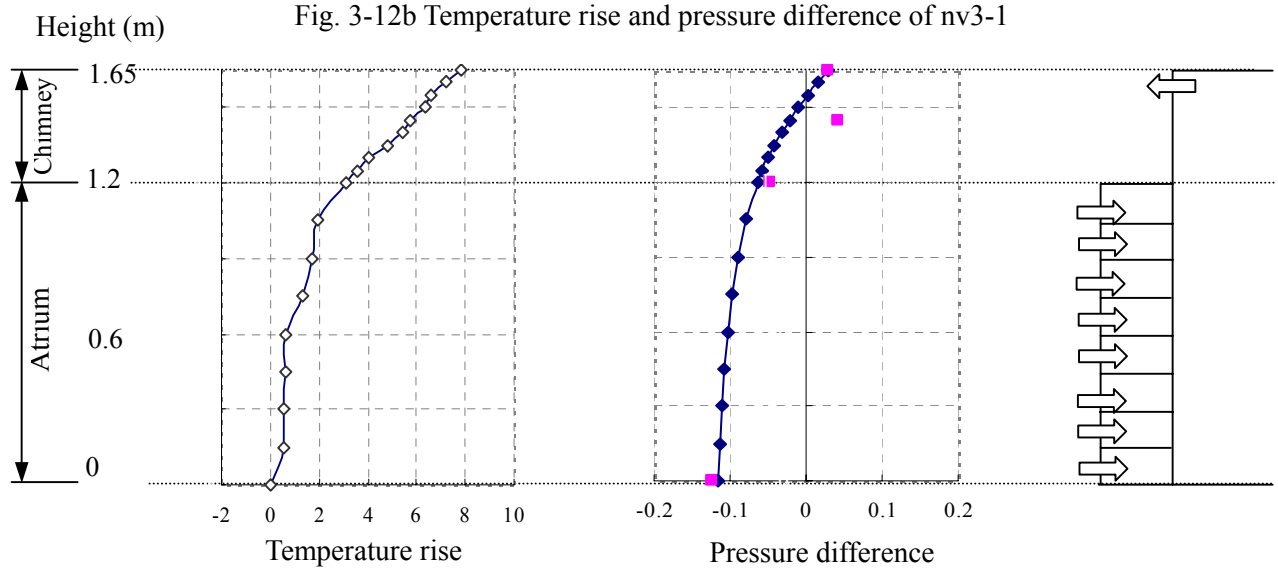

Fig. 3-12c Temperature rise and pressure difference of nv3-2

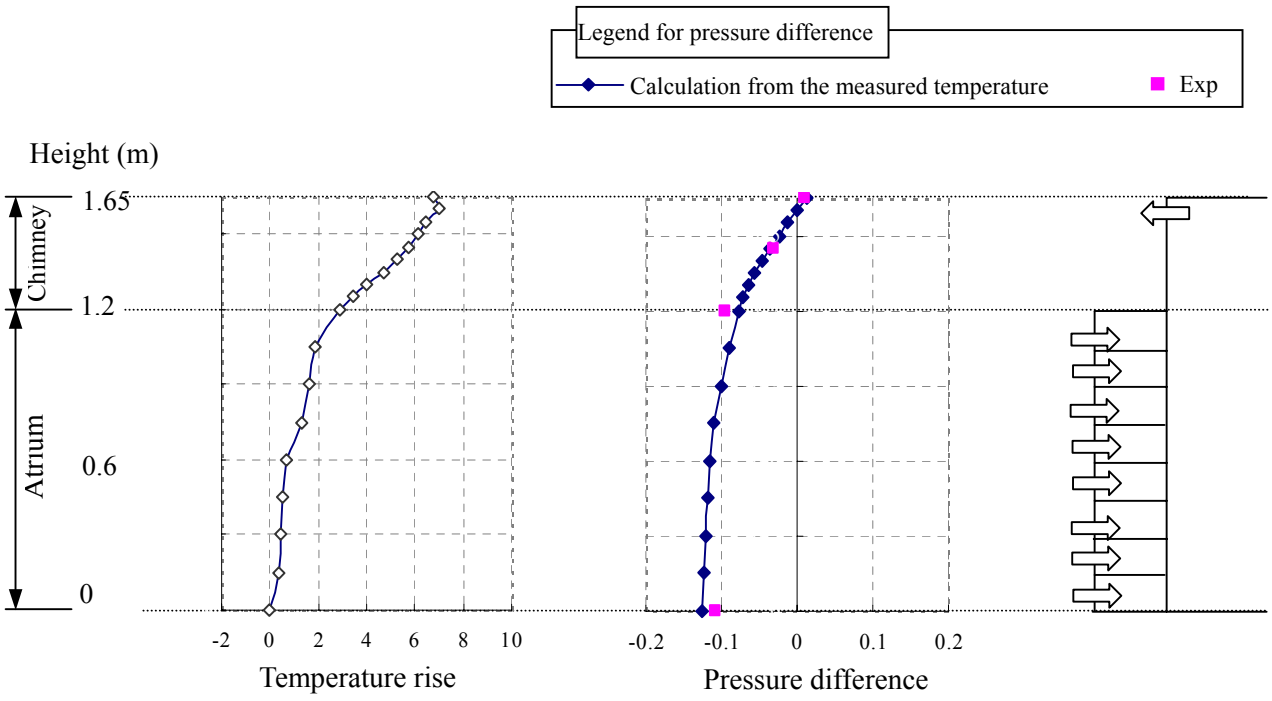

Fig. 3-12d Temperature rise and pressure difference of nv3-3

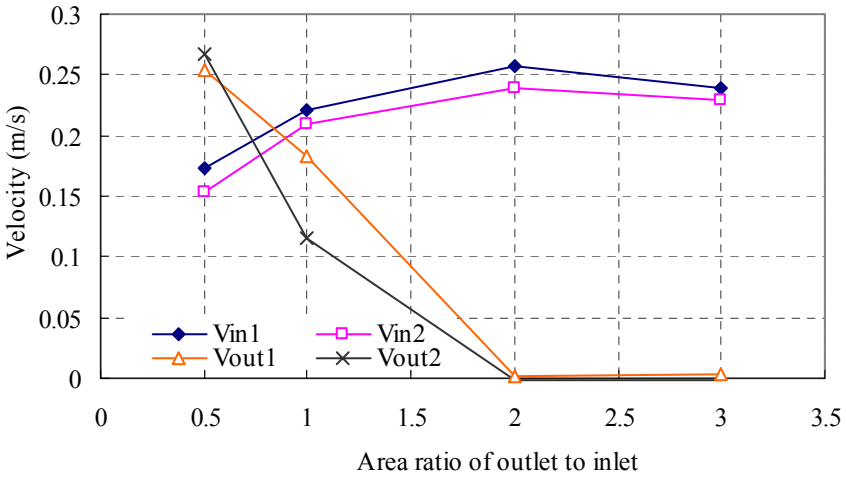

Fig. 3-12e Velocities of outlets and inlets (1F)

Note:

Although the inlets are uniformly distributed at each floor, only the inlets of 1F are recorded.

◆The experimental results of series nv4

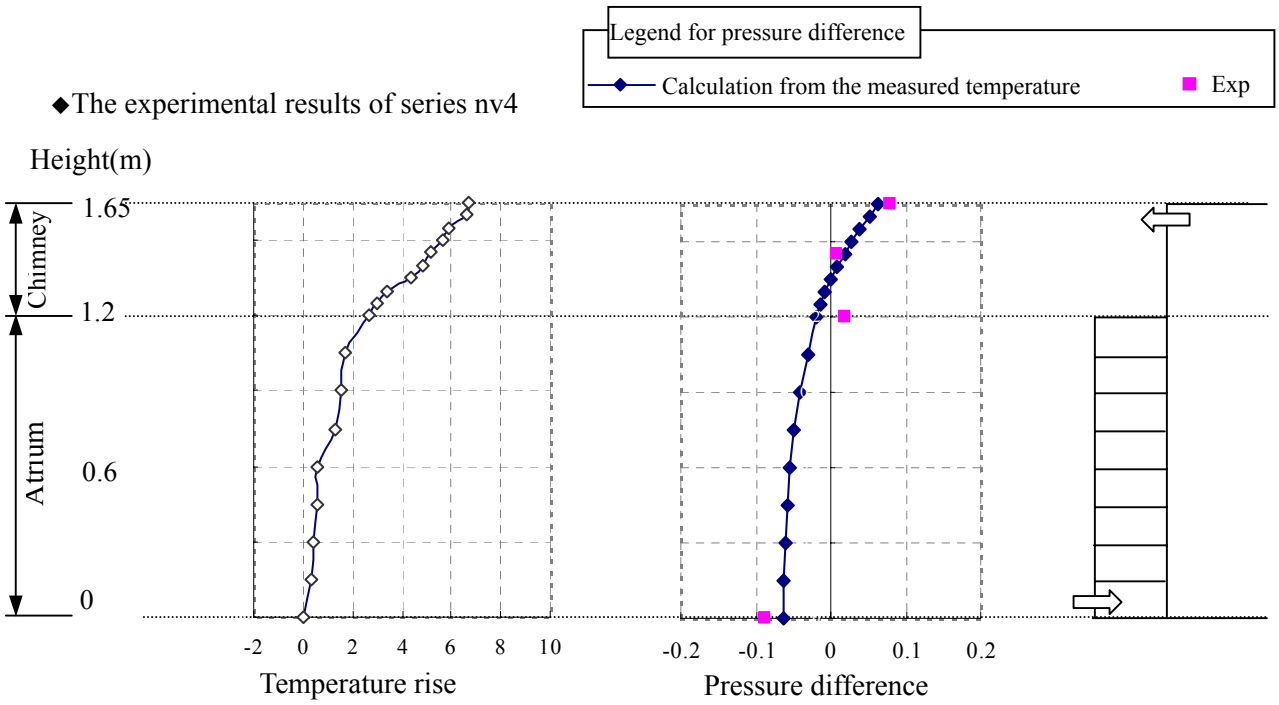

Fig. 3-13a Temperature rise and pressure difference of nv4(1)-15

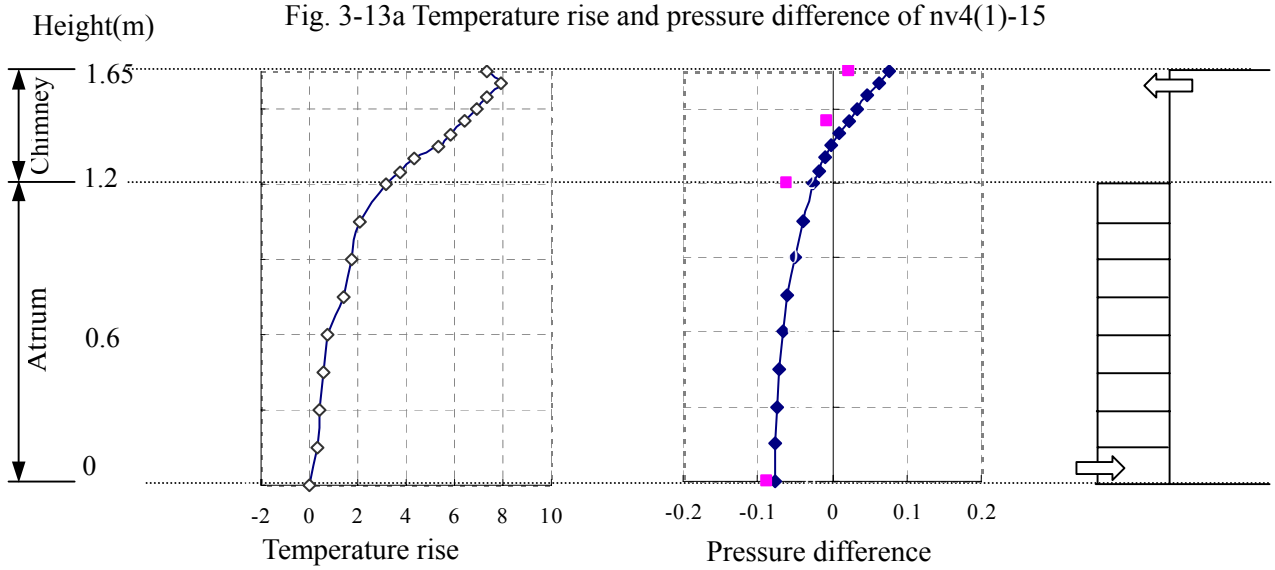

Fig. 3-13b Temperature rise and pressure difference of nv4(1)-20

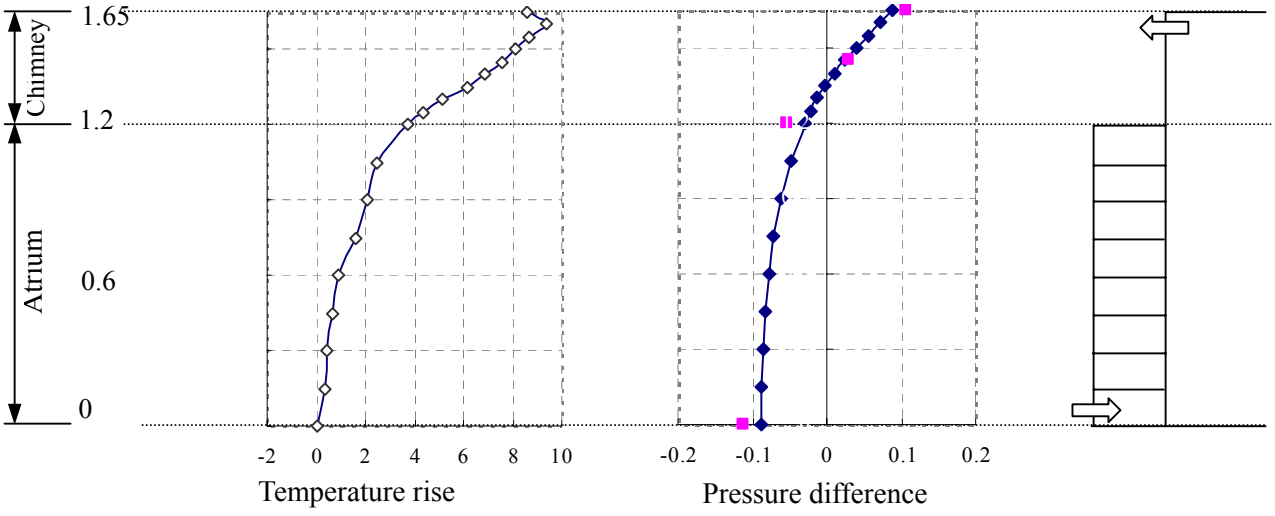

Fig. 3-13c Temperature rise and pressure difference of nv4(1)-25

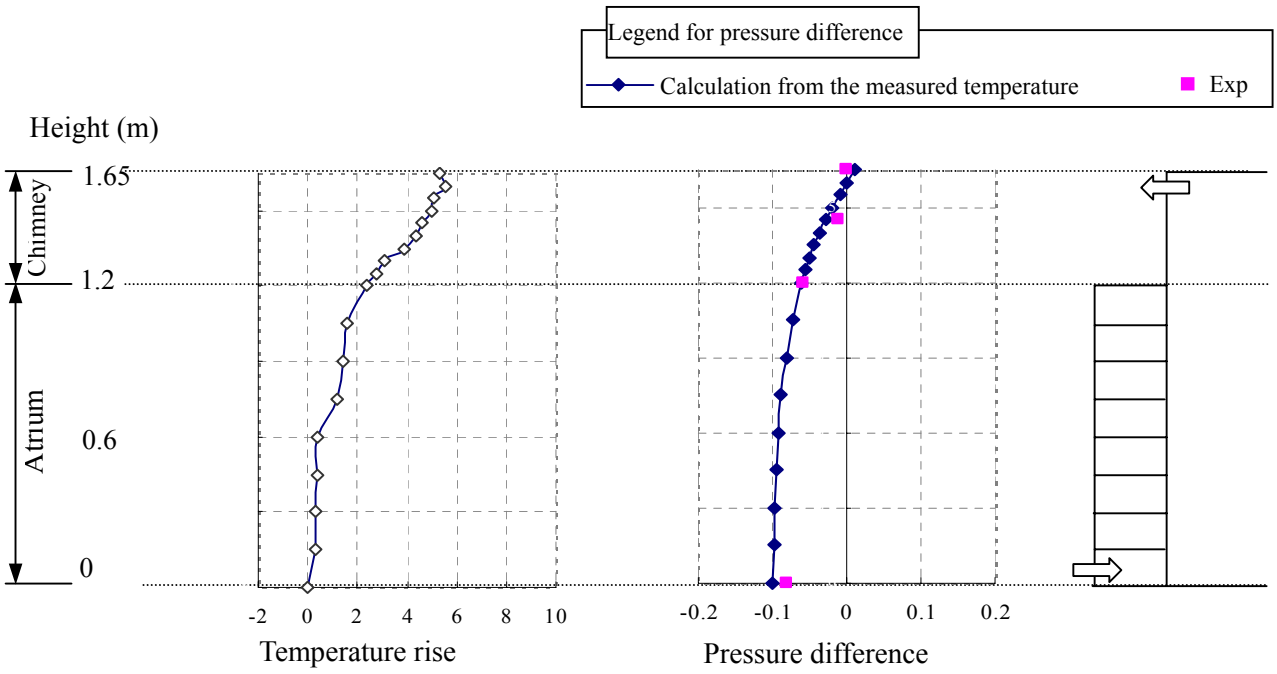

Fig. 3-13d Temperature rise and pressure difference of nv4(3)-15

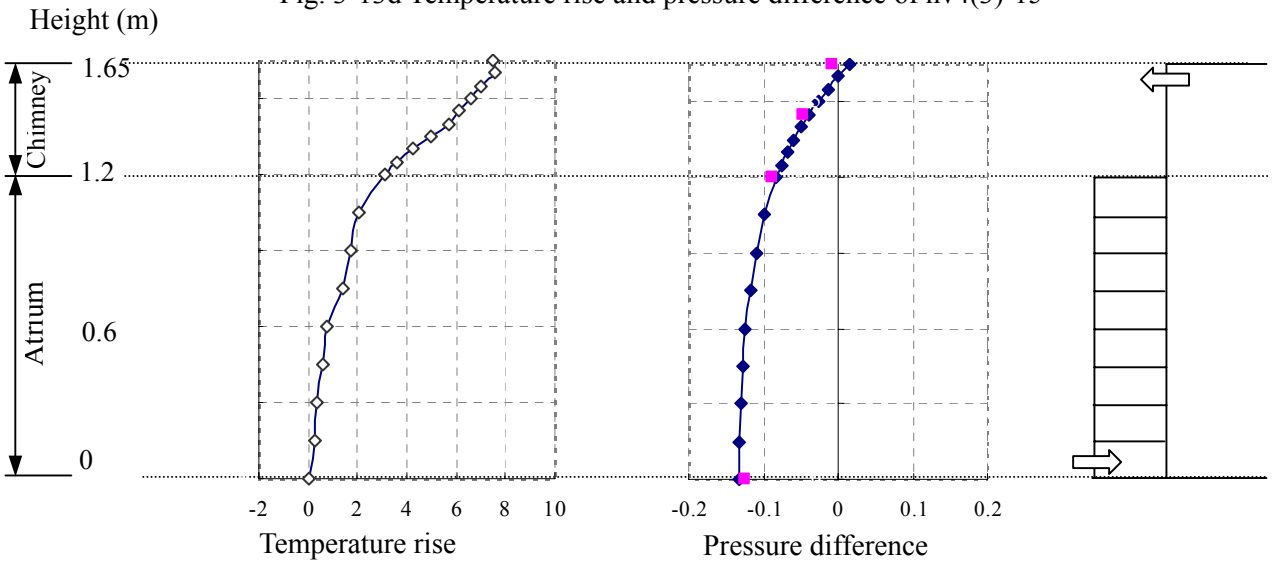

Fig. 3-13e Temperature rise and pressure difference of nv4(3)-20

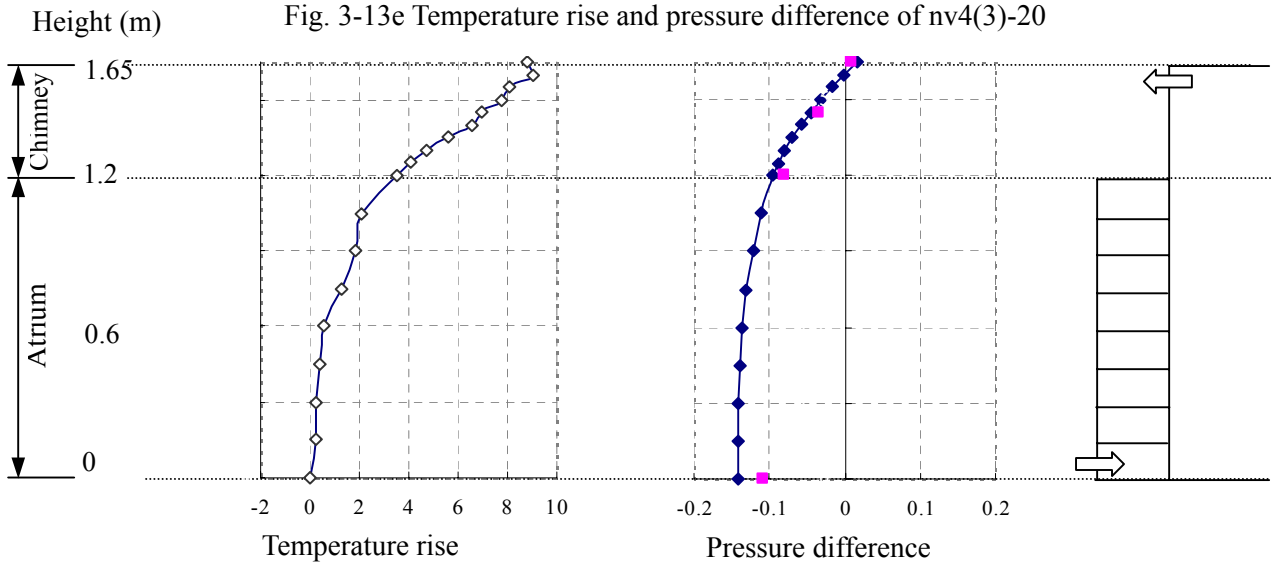

Fig. 3-13f Temperature rise and pressure difference of nv4(3)-25

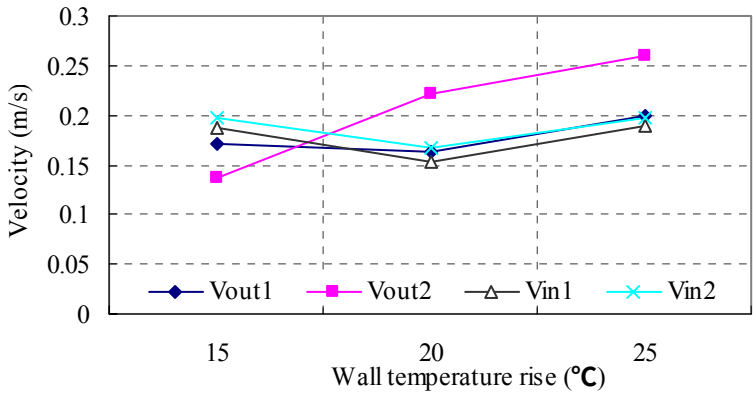

Fig. 3-13g Velocities of outlets and inlets (Outlet 96 cm^2/Inlet 96 cm^2)

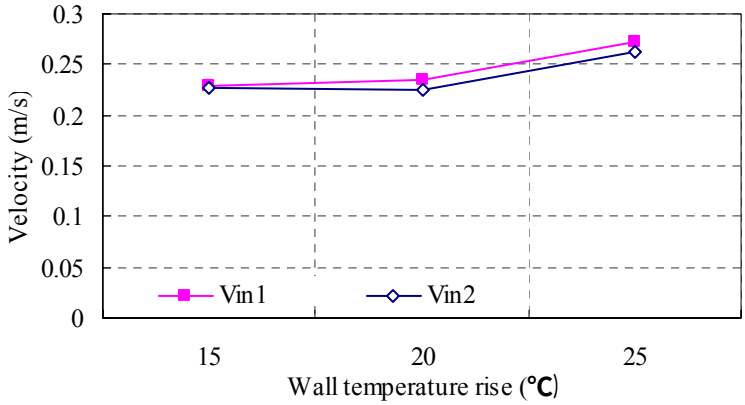

Fig. 3-13h Velocities of inlets (Outlet 288 cm^2/Inlet 96 cm^2)

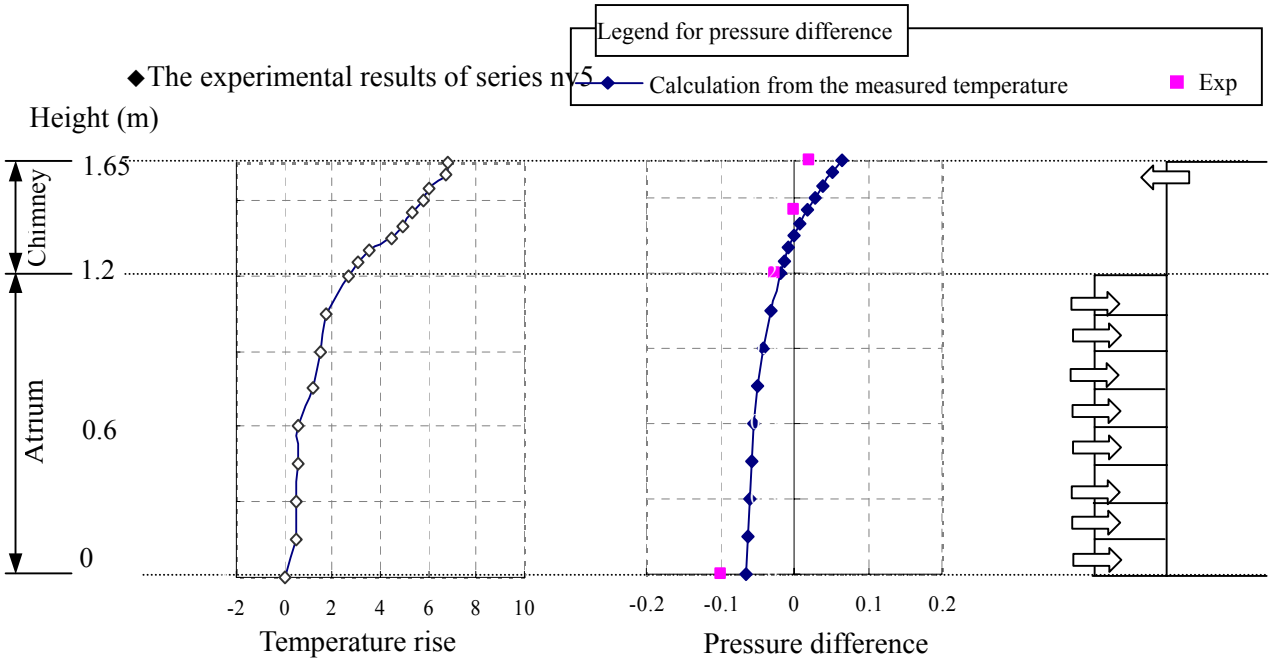

Fig. 3-14a Temperature rise and pressure difference of nv5(1)-15

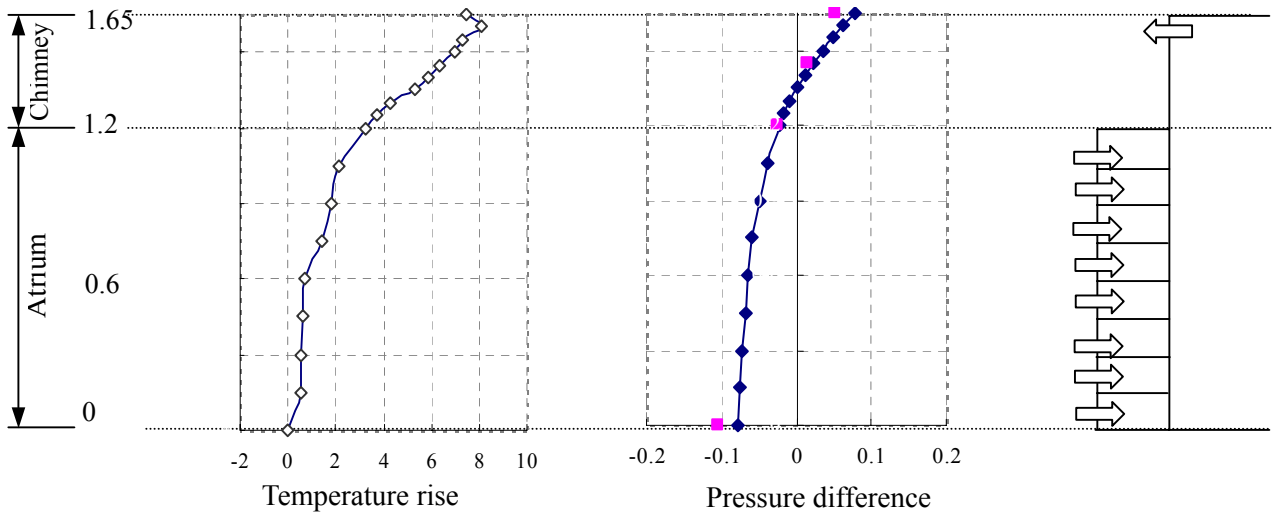

Fig. 3-14b Temperature rise and pressure difference of nv5(1)-20

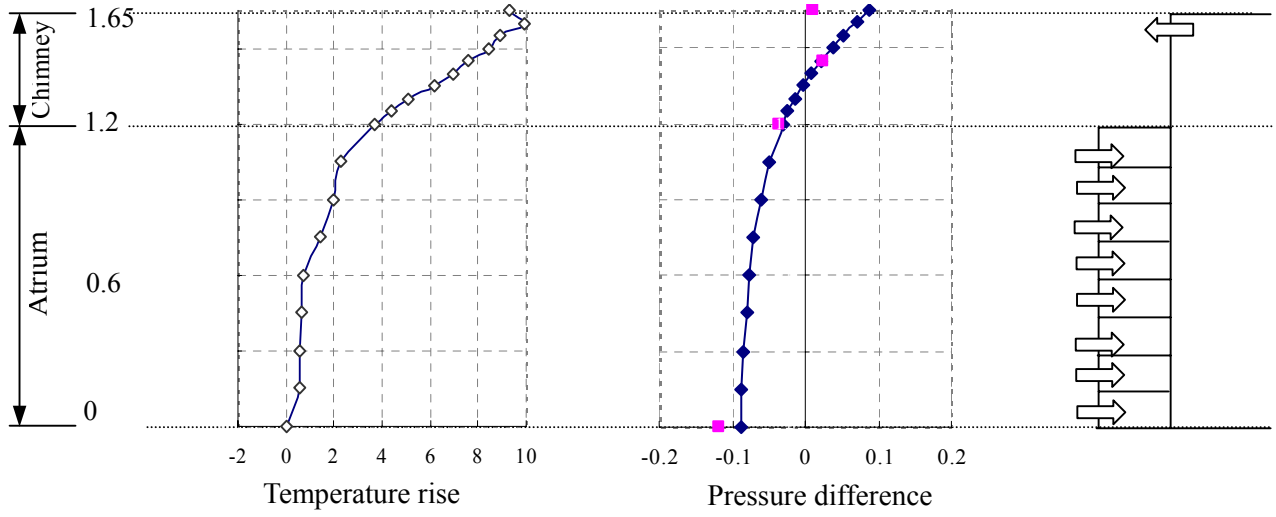

Fig. 3-14c Temperature rise and pressure difference of nv5(1)-25

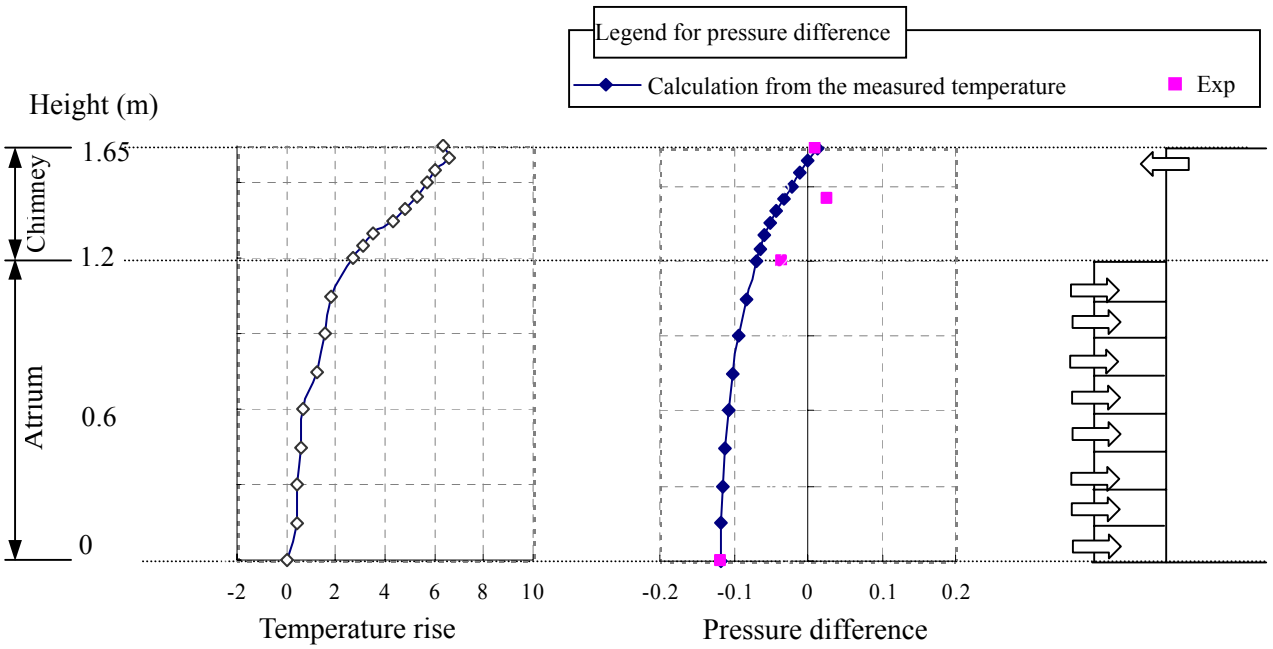

Fig. 3-14d Temperature rise and pressure difference of nv5(3)-15

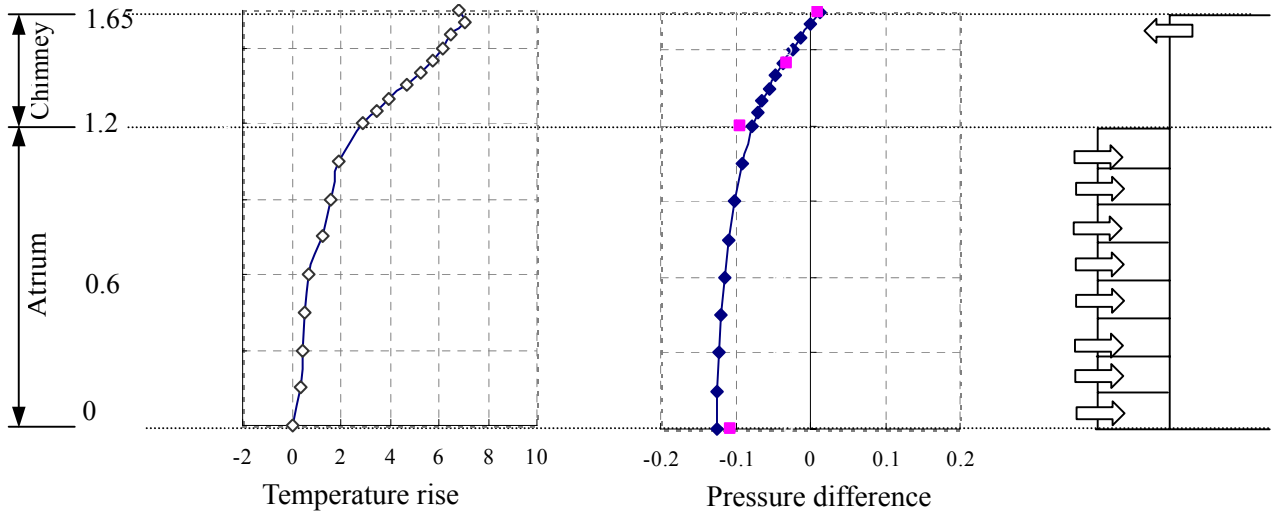

Fig. 3-14e Temperature rise and pressure difference of nv5(3)-20

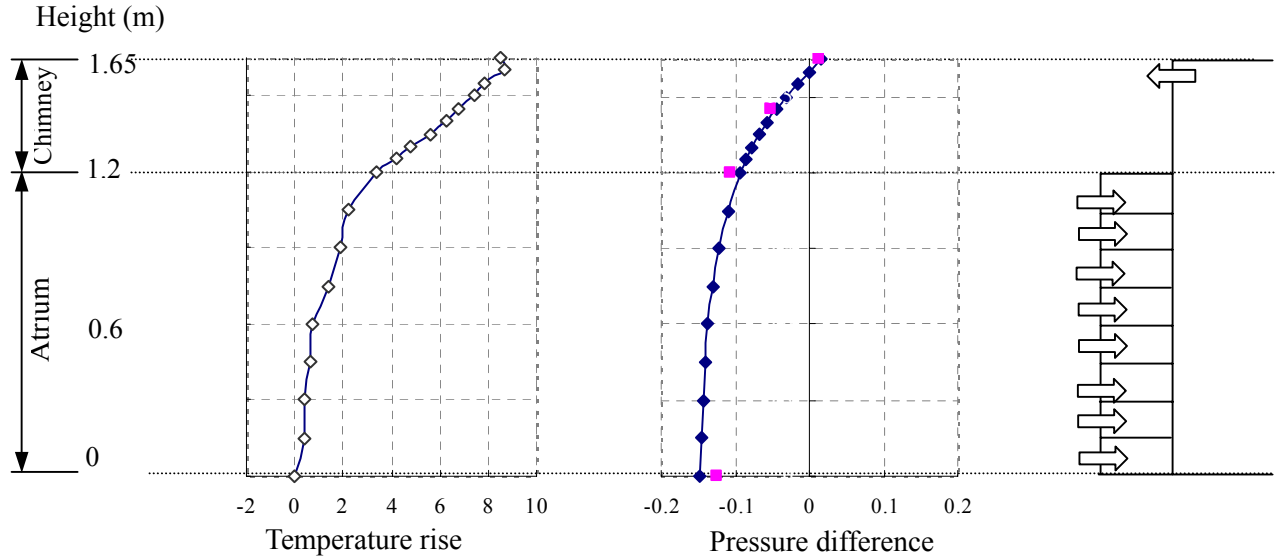

Fig. 3-14f Temperature rise and pressure difference of nv5(3)-25

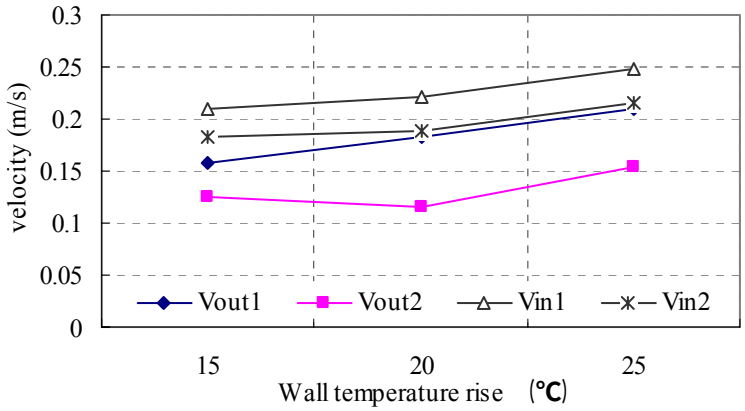

Fig. 3-14g Velocities of outlets and inlets (Outlet 96 cm^2/Inlet 12×8 floors = 96 cm^2)

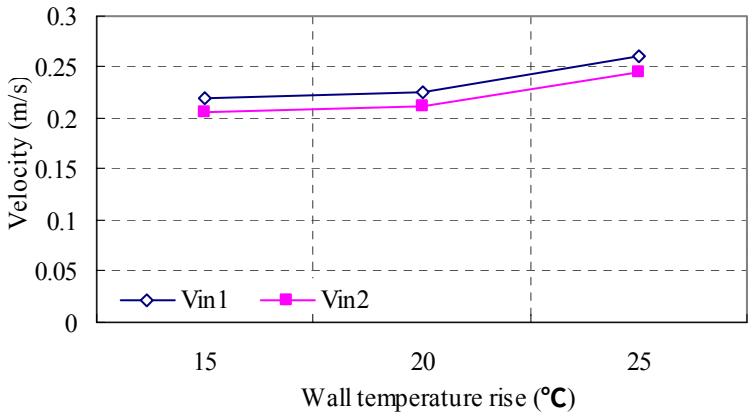

Fig. 3-14h Velocities of inlets (Outlet 288 cm^2/Inlet 12×8 floors = 96 cm^2)

3.3.3.3 Experimental results of series nvs

The experimental results of series nvs(1)-0.5

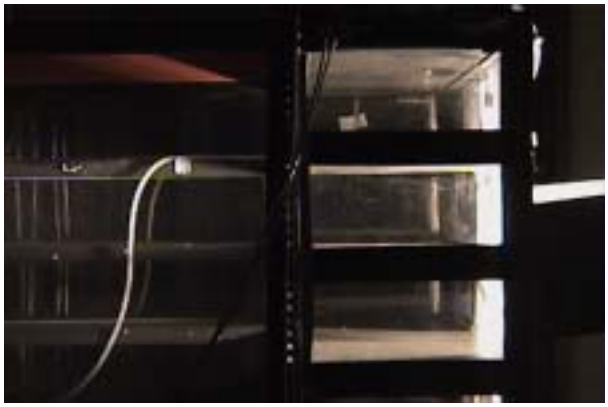

Ignition

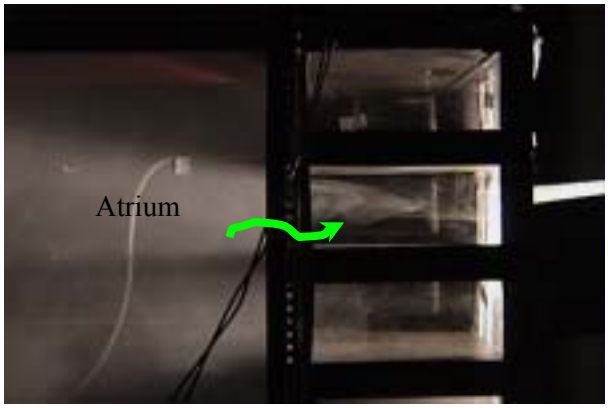

40s after ignition

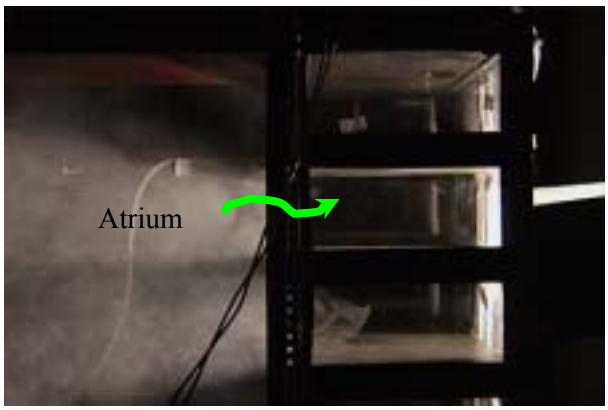

10s after ignition

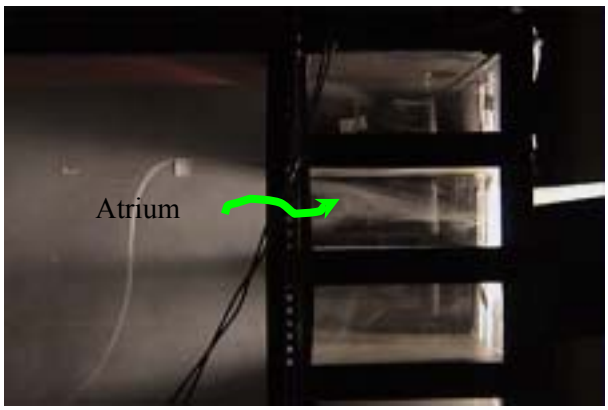

50s after ignition

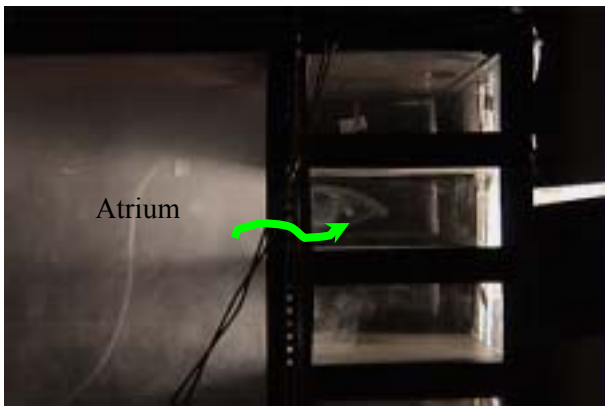

20s after ignition

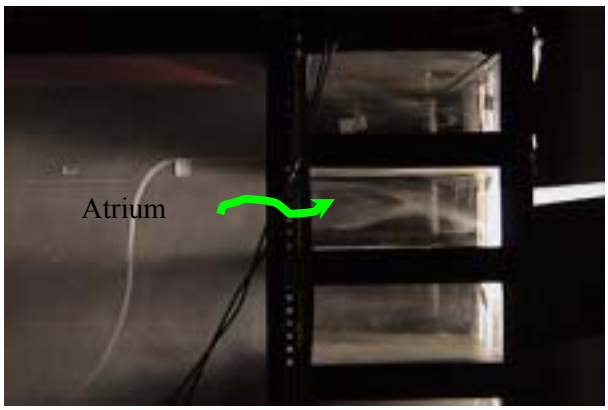

60s after ignition

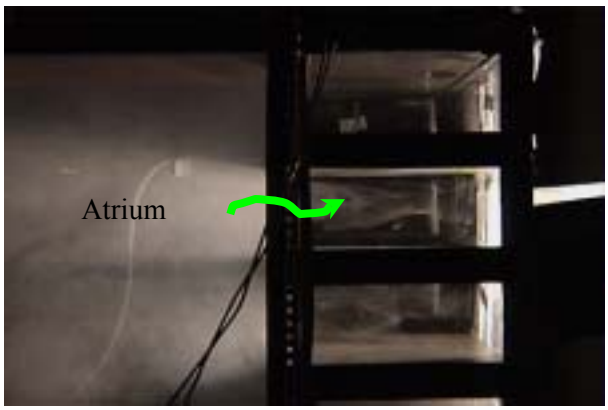

30s after ignition

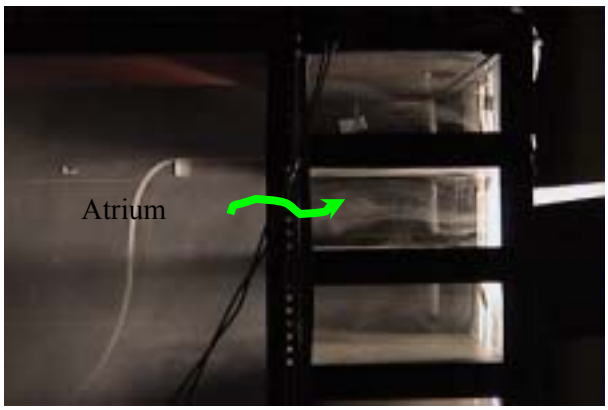

70s after ignition

Fig. 3-15 Smoke spread process of series nvs(1)-0.5

Visualization experiments of natural airflow Wall 4: +20 °C Outlets: 3 m^2; Inlets: 6 m^2

The experimental results of series nvs(8)-0.5

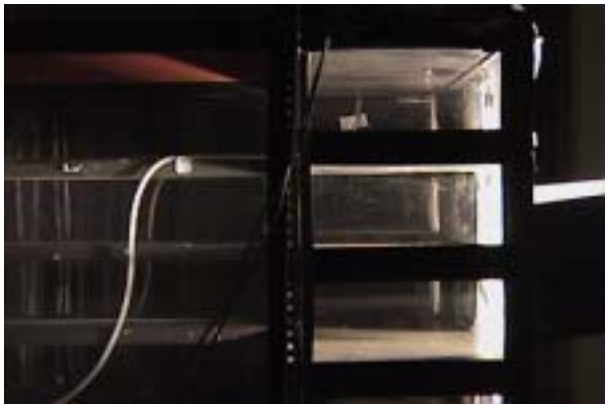
Ignition

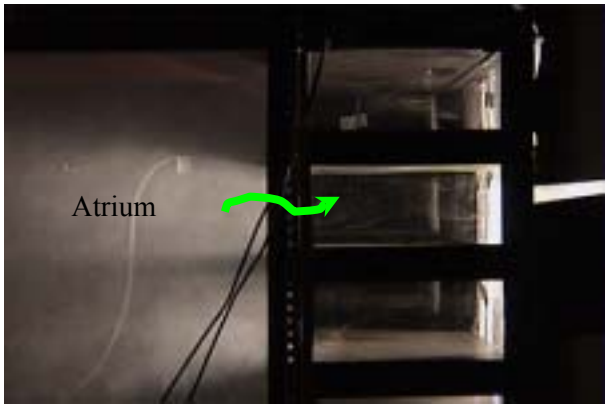

40s after ignition

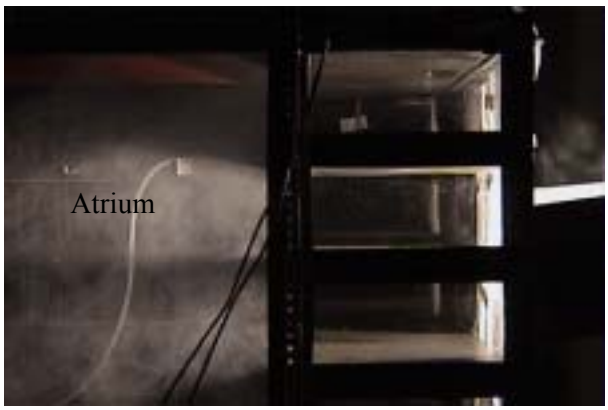

10s after ignition

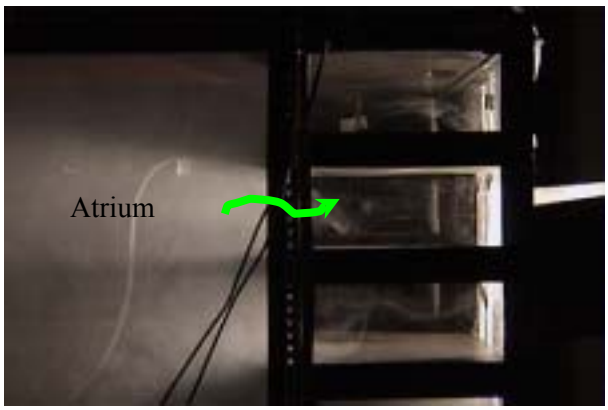

50s after ignition

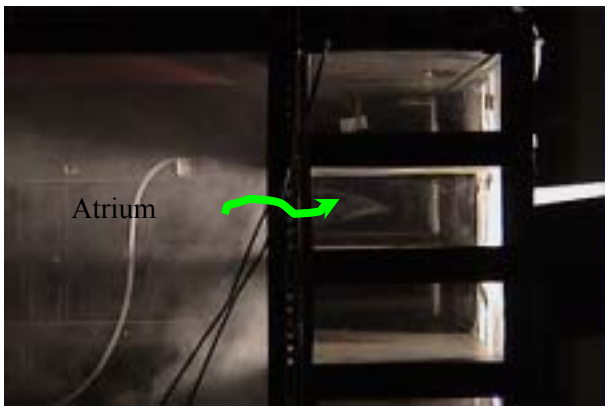

20s after ignition

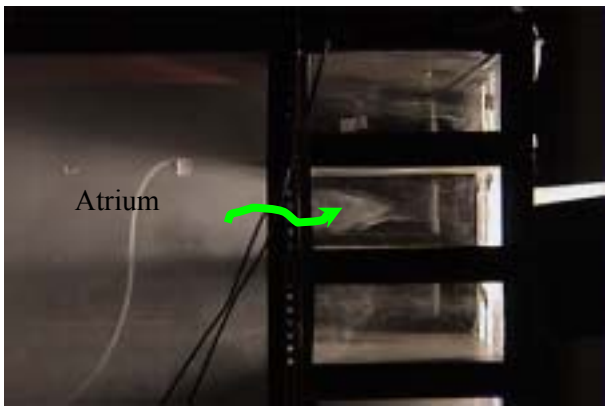

60s after ignition

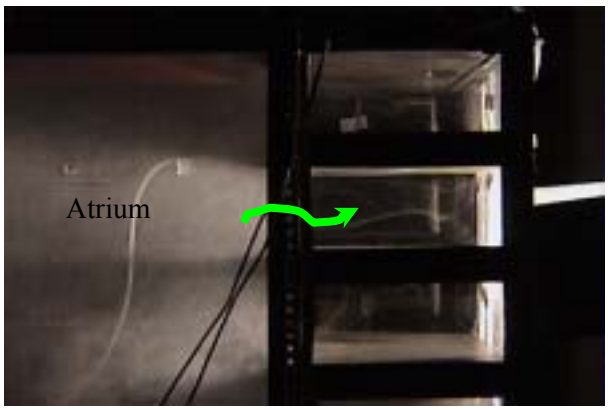

30s after ignition

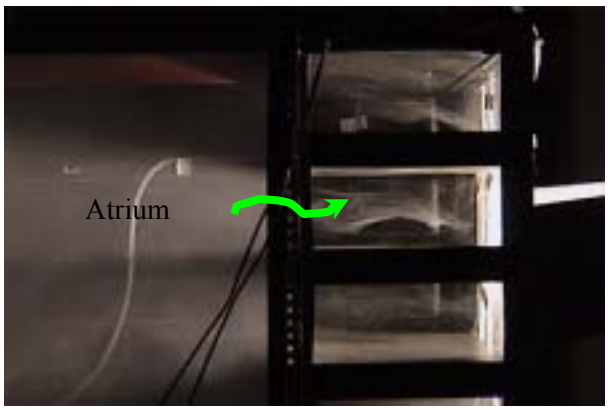

70s after ignition

Fig. 3-16 Smoke spread process of series nvs(8)-0.5

Visualization experiments of natural airflow
Wall 4: +20 °C
Outlets: 3 m^2; Inlets: 0.75 m^2 at each floor

The experimental results of series nvs(1)-3

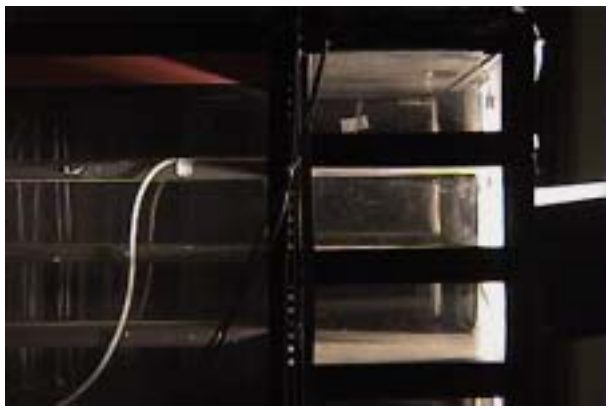
Ignition

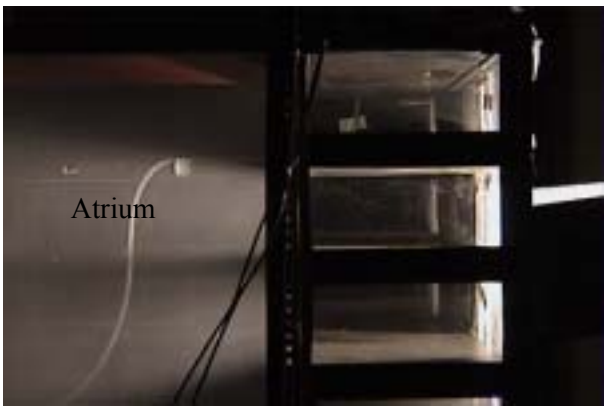

40s after ignition

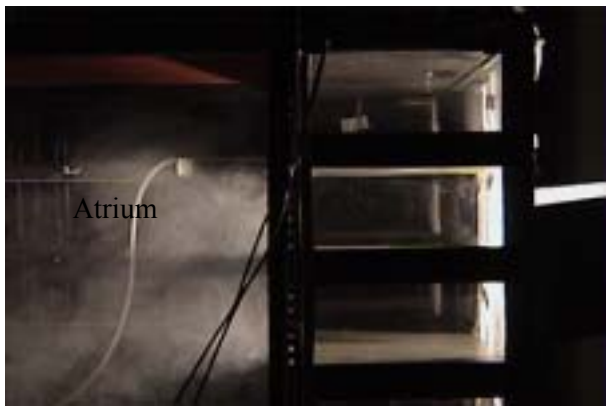

10s after ignition

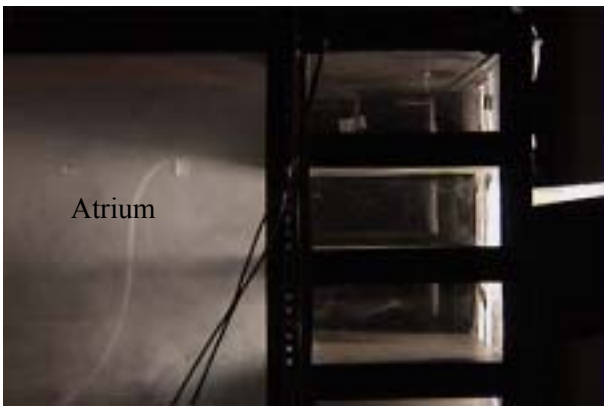

50s after ignition

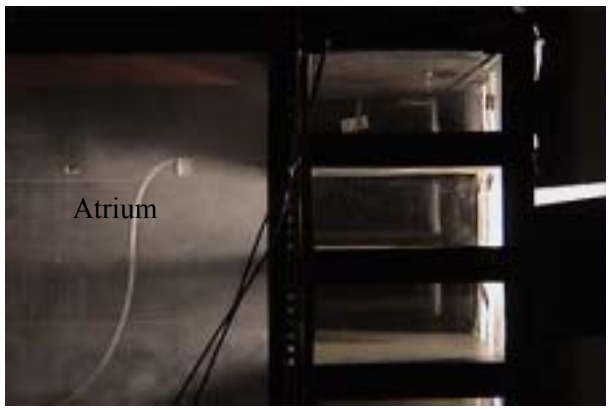

20s after ignition

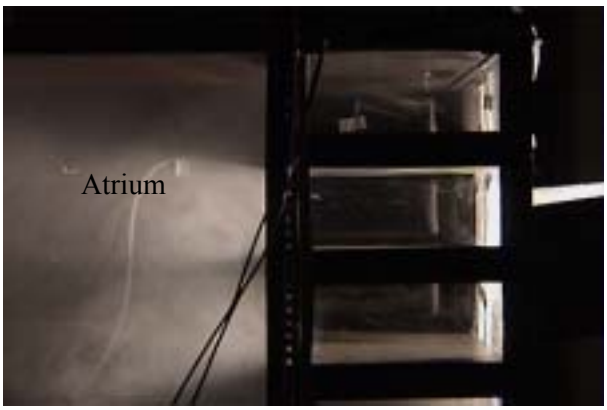

60s after ignition

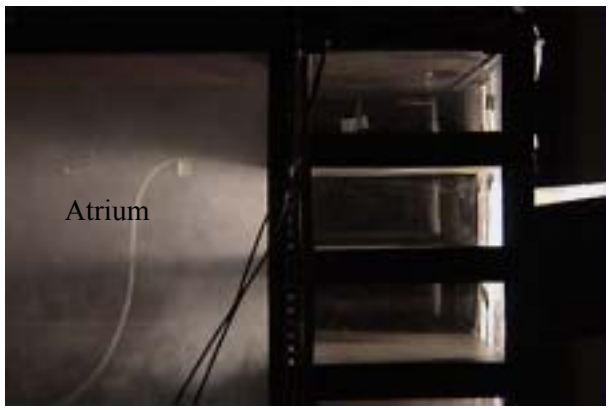

30s after ignition

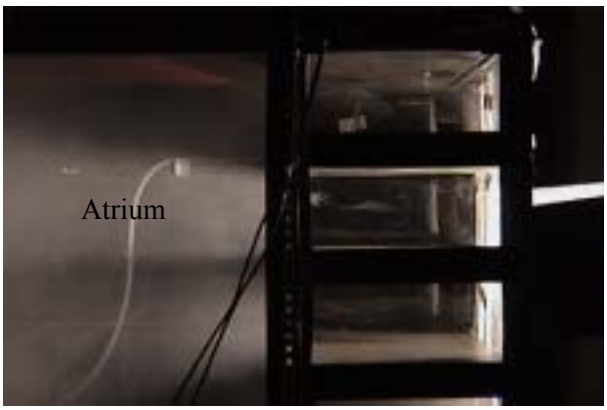

70s after ignition

Fig. 3-17 Smoke spread process of series nvs(1)-3

Visualization experiments of natural airflow
Wall 4: +20 °C
Outlets: 18 m^2; Inlets: 6 m^2

The experimental results of series nvs(8)-3

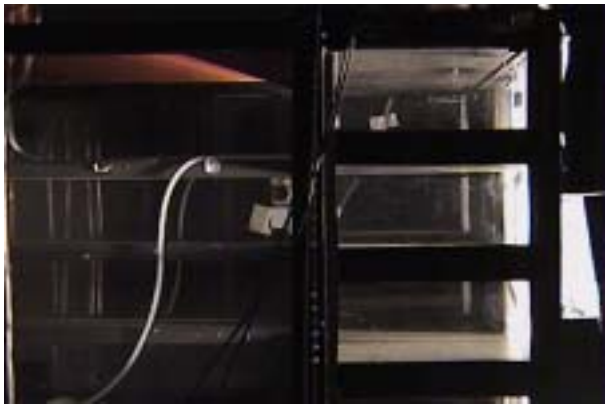
Ignition

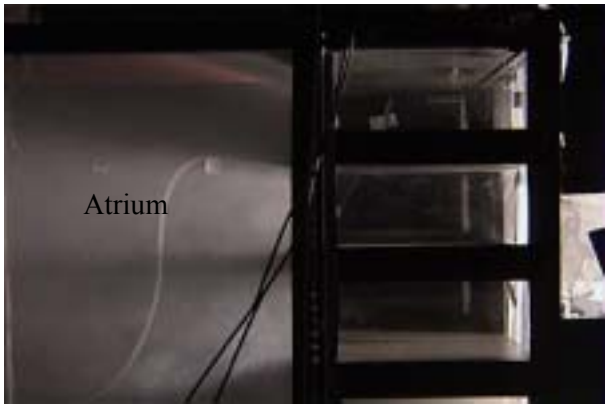

40s after ignition

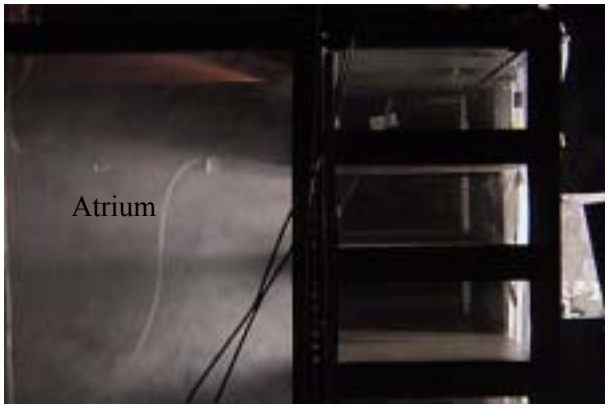

10s after ignition

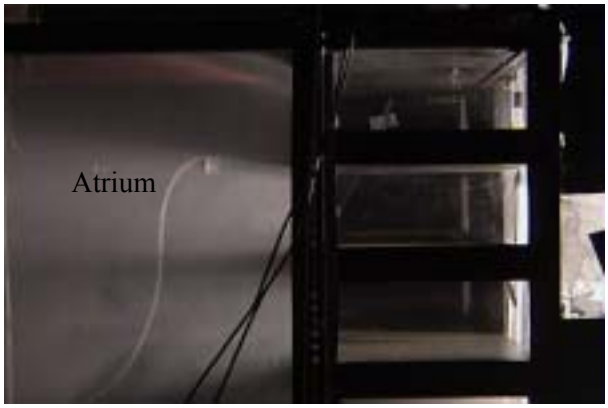

50s after ignition

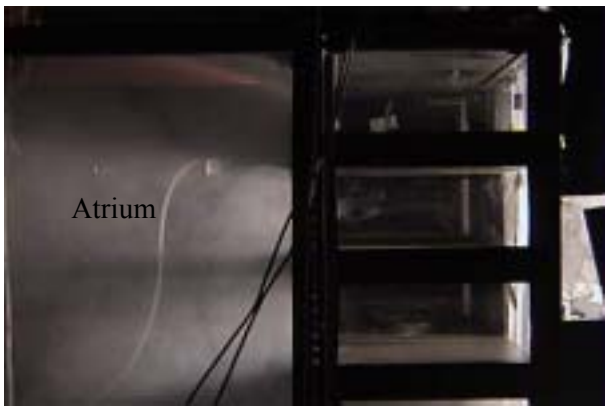

20s after ignition

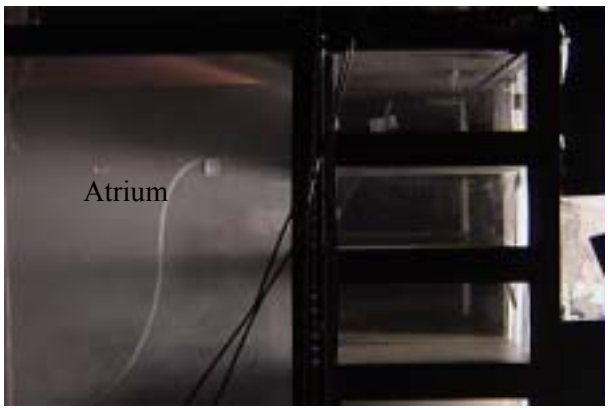

60s after ignition

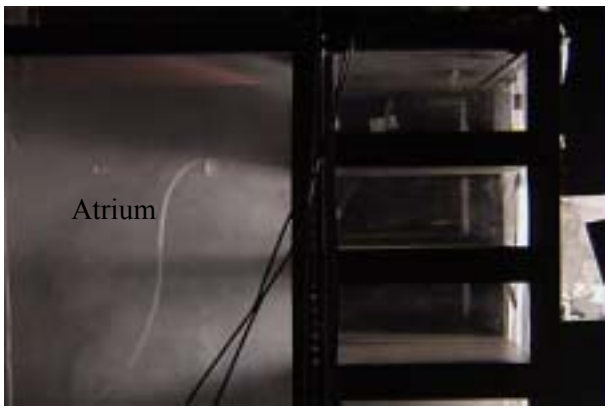

30s after ignition

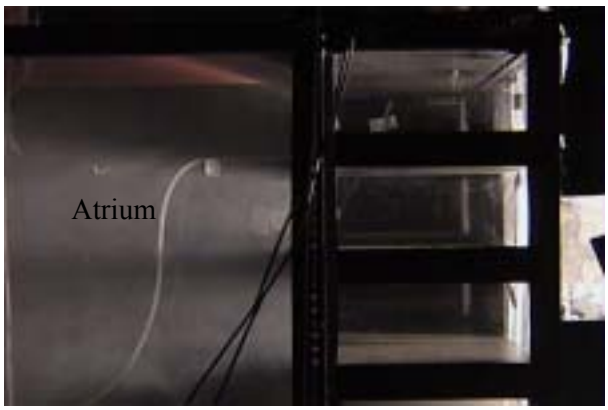

70s after ignition

Fig3-18 Smoke spread process of series nvs(8)-3

Visualization experiments of natural airflow
Wall 4: +20 °C
Outlets: 18 m^2; Inlets: 0.75 m^2 at each floor

3.3.4 Analysis of the experimental results

Through the reduced scale model experiments, with the temperature rise of the walls of the solar chimney, natural ventilation flow due to the stack effect is confirmed. The warmed up air in the atrium/chimney flows out from the upper openings and the fresh air flows in from the lower openings, which means effective natural ventilation can be expected in the prototype building.

◆Surface temperature

In the experiments, although only one of the chimney walls is heated, the temperatures of the other walls also rise due to the radiation heat transfer with the high temperature wall.

◆Results of series nv1 and nv3

Experiments of series nv1 and nv3 are carried out almost with the same conditions except that for series nv1 inlets are concentrated at the lower part; while for series nv3 inlets are uniformly distributed at each floor. The same inclination can be found in the temperature rise distribution. With the increasing of outlet area, temperature rise from the base of the atrium to the top of the chimney slightly decreases. The total temperature rise is about 6~10℃.

Regarding the pressure difference distribution, as shown in the figures, although pressure difference at only 4 points have been measured, they are almost near the distribution line calculated from the measured temperature. For both series nv1 and nv3, the neutral pressure plane normally stays inside the chimney for all cases excluding the case in which the outlet area is only half of the inlet area. In fact the height of the neutral pressure plane is mainly decided by the area ratio of outlet to inlet. From the results it can be inferred that it is desirable to keep the area ratio of the outlet to inlet not less than 1. Consequently the neutral pressure plane can stay inside the chimney and effective natural ventilation can be expected.

Since velocity can not be recorded if the value is less than 0.1 m/s due to the accuracy of the testing instrument, for both series nv1 and nv3, when the outlet area is over 2 times of the inlet area, the velocity of the outlet are not be recorded. The inlet velocity shows that when the area ratio is over 2, the inlet velocity hardly rises with the increasing of the outlet area, which indicates the area ratio of 2~3 will be preferred to obtain effective natural ventilation rate.

◆Results of nv2

During the experiments of series nv2, the outlet area is set as the same as the area of the inlet. Just as mentioned above, the neutral pressure plane is mainly decided by the area ratio of outlet to inlet, for the 4 cases of series nv2, the neutral pressure plane almost forms at the same height. Of course, the increasing of the outlet area makes some decrease of the temperature rise. For all cases, velocities of the outlets and inlets decrease with the increase of area.

◆Results of series nv4 and nv5

For series nv4, the inlets are concentrated at the first floor while for series nv5, the inlets are uniformly distributed at each floor. The results show no great difference between these two series. With increasing of the wall temperature, temperature rise of the air from the base of the atrium to the top of the chimney rises while the neutral pressure plane changes little with the temperature rise. Velocities of the outlets and inlets rise with the increasing of the wall temperature.

◆Results of series nvs

For all cases, the smoke stagnation phenomena at some height are observed (Fig. 3-19). This is considered as reflecting the phenomenon of the low temperature air gradually fused into the high temperature air.

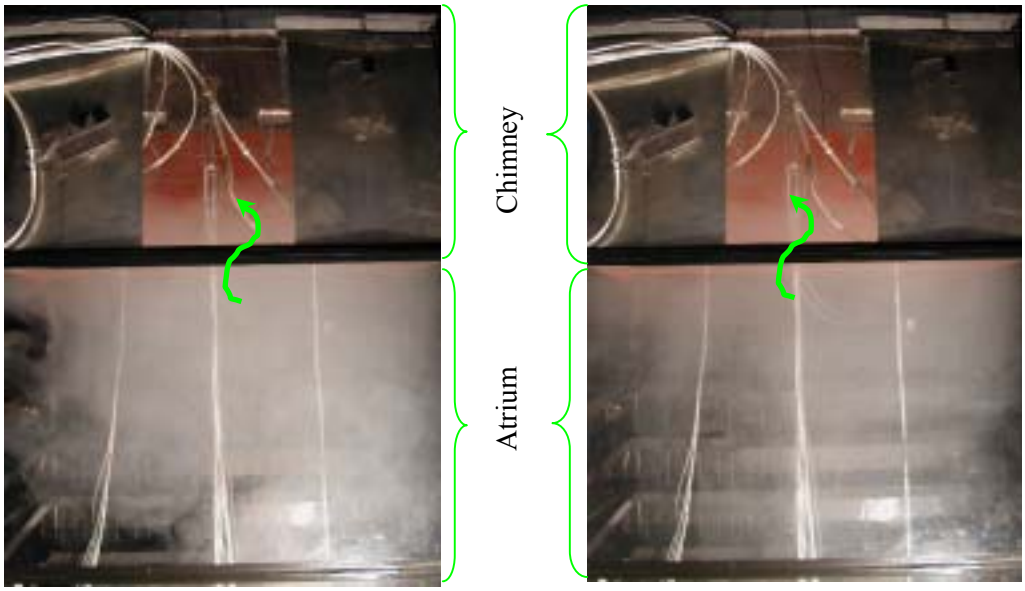

Fig. 3-19 Smoke stagnation phenomena in experiments with only smoke generation stick

Furthermore, when the outlet area is half of the inlet area, smoke is observed to infiltrate into the separated space through the small openings. When the outlet area becomes 3 times of the inlet area, there is almost no smoke observed in the separated space. These phenomena are just agreeable to the results of series nv1 and nv3. Smoke infiltration into the separated space means the neutral pressure plane is below the chimney and with the increase of the outlet area, it rises into the chimney and smoke infiltration is prevented. There is no great difference observed due to the different distribution of the inlets.

From above experiments, the general characteristics of airflow concerning natural ventilation have been grasped.

3.4 EXPERIMENTS ON THE SMOKE CONTROL PERFORMANCE

3.4.1 Design fires

The design fire has a major impact on the atrium smoke management system. The fire size is expressed in terms of heat release rate. Fire growth is the change of the heat release rate and is sometimes expressed as a growth constant that identifies the time required for the fire to attain a particular rate of heat release. Designs may be based on either steady or unsteady fires.

It is the nature of fires to be unsteady, but the steady fire is a useful idealization. Steady fires have a constant heat release rate. In many applications, use of a steady design fire leads to straightforward and conservative design.

Morgan (1979) suggests a typical rate of heat release per unit floor area for mercantile occupancies of 500 kW/m^2. Fang and Breese (1980) determined about the same rate of heat release for residential occupancies. Morgan and Hansell (1987) and Law (1982) suggest a heat release per unit floor area for office buildings of 225 kW/m^2.

In many atria, the fuel loading is severely restricted with the intent of restricting fire size. Such atria are characterized by interior finishes of metal, brick, stone, or gypsum board and are furnished with objects made of similar materials plus plants. Even for such a fuel-restricted atrium, there are many combustible objects that are in the atrium for short periods. Packing materials, Christmas decorations, displays, construction materials, and furniture being moved into another part of the building are a few examples of transient fuels.

Transient fuels must not be overlooked when selecting a design fire. The approach suggested by Klote and Milke (1992) to incorporate transient fuels in a design fire is to consider the fire occurring over 9.3 m^2 of floor space. This would result in a design fire of 2,100 kW for restricted fuel atria. If a fire occurred over 9.3 m^2 of floor area with combustibles, a design fire of 4,600 kW would result. For this paper, discussion of a steady design fire will be focused on 2,000 kW.

3.4.2 The experimental fire source

For the reduced scale model experiments, fire size is determined according to the real design fire based on the Froude modeling, which preserves the Froude number. It is a measure of the relative importance of inertia force and buoyancy in the system, and is conveniently expressed as

$$Fr = \frac{U^2}{gl} \tag{3-15}$$

where

U is velocity of the gases, m/s;

g is acceleration due to gravity, m/s^2;

l is a characteristic dimension, m;

Indeed, a 'dimensionless heat release rate' (Q*), introduced in the 1970s by Zukoski (1975) and others, is the square root of a Froude number expressed in terms of the heat release rate of a fire. It is used to classify fire types and correlate aspects of fire behavior. It is given by:

$$Q^* = \frac{Q}{\rho_0 C_p T_0 \sqrt{gl} \cdot l^2} \tag{3-16}$$

where

ρ_0 is ambient air density, kg/m^3;

C_p is specific heat of air, kJ/kg·K.

T_0 is ambient air temperature, K.

Considering the same ambient environment, the following relations can be obtained:

$$T_M = T_F \tag{3-17}$$

$$\frac{U_M}{U_F} = \left(\frac{l_M}{l_F}\right)^{\frac{1}{2}} \tag{3-18}$$

$$\frac{Q_M}{Q_F} = (\frac{l_M}{l_F})^{\frac{5}{2}} \tag{3-19}$$

where M indicates model and F indicates full-scale.

Froude modeling does not preserve the Reynolds number, but appropriate selection of the size of the scale model can ensure that this does not have an adverse effect on the applicability of the modeling. In full-scale applications, the flow in malls, atria, shops, balconies, and corridors is fully developed turbulent flow. The basic characteristic of fully developed turbulent flow is the same over a wide range of Reynolds number. The flow at a specific location in the scale model can have a very different Reynolds number from that at the corresponding location in the full-scale facility, but this does not impact the validity of the Froude modeling provided the flow in the model is fully developed turbulent flow.

When considering the free convection, the Grashof number is always used, which is the ratio of the buoyancy to viscous force.

$$Gr = \frac{g\beta\Delta T l^3}{\nu^2} \tag{3-20}$$

g is acceleration due to gravity, m/s^2;
β is thermal expansion coefficient, 1/K;
ΔT is temperature rise, K;
l is characteristic length, m;
ν is viscosity, m^2/s.

Actually it is almost impossible to preserve the Grashof number in the reduced scale model and the full-scale building. However it is found that even for the free convection, as long as the turbulent intensity of the flow is over some value of the Grashof number, the basic characteristic of the flow becomes independent on the Grashof number. For the natural ventilated space, most of the flow region can be regarded as such state (Shuzo Murakami et al. 1987). Therefore substituting the turbulent viscosity (It is proportional to the product of the local velocity and length.) for the Grashof number,

$$\nu_t \propto Ul \tag{3-21}$$

$$(Gr)_t \propto \frac{g\beta\Delta Tl}{U^2} \tag{3-22}$$

Considering TM =TF, the turbulent Grashof number actually becomes in accordance with the Froude number.

$$\frac{U_M}{U_F} = (\frac{l_M}{l_F})^{\frac{1}{2}} \tag{3-23}$$

Basically the similarity laws mentioned above can be used to establish relations between the scaled-down model and the full-scale prototype.

Just as mentioned above, considering the dimension of the laboratory and the effectiveness of the similarity law, the scale criterion of the experimental model is decided to be 1/25. Therefore, for a design fire of 2,000 kW in the full-scale prototype building, the fire size for the experimental model should be

$$Q_M = \left(\frac{l_M}{l_F}\right)^{5/2} Q_F = (\frac{1}{25})^{\frac{5}{2}} \times 2000000 = 640 \ \text{W} \tag{3-24}$$

In the preliminary experiments, ethanol is used as the liquid fuel. Several laboratory dishes with different diameters are selected to reproduce the fire. As the results, the laboratory dish with 4.5 cm diameter is chosen.

3.4.3 The outline of the experimental model

The experimental model is almost the same as that used for natural ventilation experiments. Partitions are set at the boundary of the atrium and the utility space from 6F to 8F (Fig. 3-20). Moreover, small openings are set on the partitions to observe the smoke movement between the atrium and the utility space (Fig. 3-21). Thermocouples are placed in the separated space to confirm the invasion of the smoke.

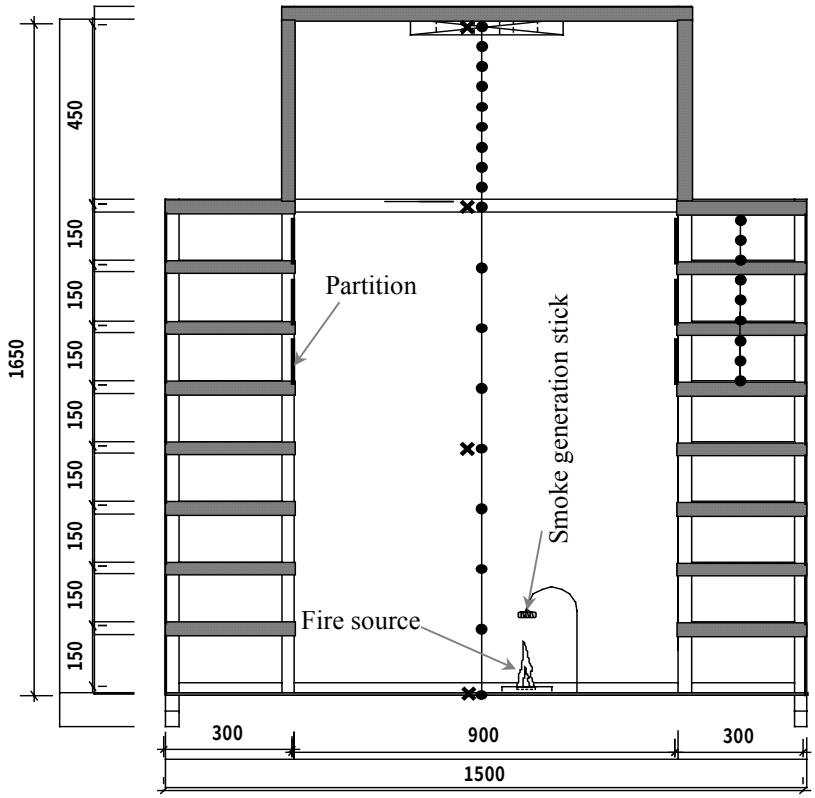

Fig. 3-20 Outline of the experimental model for smoke control experiments

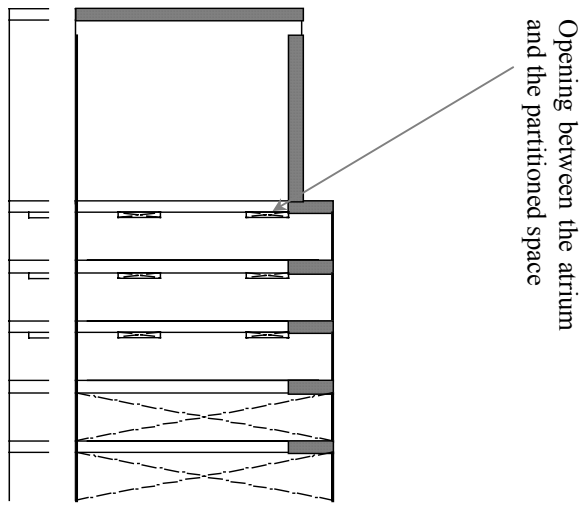

Fig. 3-21 Section of the partition

3.4.4 Conditions for the smoke control experiments

Experiments are conducted with two kinds of fire sources. One is only ethanol to measure the temperature and pressure difference distribution; and the other is ethanol with smoke generation stick to confirm the smoke movement. In all the experiments, considering the smoke temperature is higher than that of the solar chimney wall, the panel heaters are not used.

3.4.4.1 Experiments with only ethanol

The purpose of the following experiments is to measure the temperature and pressure difference distribution during the ethanol is burning. The opening conditions are set just as that of the conditions for natural ventilation experiments.

Ethanol put in the laboratory dish with 4.5 cm diameter is used as the fire source for the experiments. The dish is put on the base of the atrium with 10 cm far away from the centerline where temperature and pressure difference are measured. For each case, 20 ml ethanol is burned. The heat release rate of the fire source is calculated using following equation:

$$q = \frac{\rho V \Delta H_c}{\Delta t} \tag{3-25}$$

where

q is time-averaged heat release rate, kW;

ρ is density of ethanol (0.791×10^3 kg/m^3);

V is volume of burned ethanol (20×10^{-6} m^3);

ΔH_c is effective heat of combustion of ethanol (26.8×10^3 kJ/kg);

t is burning time, s.

◆Series ef1

The total area of the inlets is set as about 1/45 of the floor area of the atrium, while the outlet area is changed to make the area ratio of the outlets to inlets as 0.5, 1, 2, 3, 4, 5 respectively.

Table 3-15 Experimental conditions for series ef1

No.	Opening Area	
	Outlets (full-scale)	Inlets (full-scale)
ef1-0.5	4cm×6cm×2 = 48 cm^2 (3 m^2)	8cm×6cm×2 = 96 cm^2 (6 m^2)
ef1-1	4cm×12cm×2 = 96 cm^2 (6 m^2)	
ef1-2	4cm×24cm×2 = 192 cm^2 (12 m^2)	
ef1-3	4cm×36cm×2 = 288 cm^2 (18 m^2)	
ef1-4	4cm×48m×2 = 384 cm^2 (24 m^2)	
ef1-5	4cm×60cm×2 = 480 cm^2 (30 m^2)	

◆Series ef2

The outlet area is set as the same as that of the inlet area.

Table 3-16 Experimental conditions for series ef2

No.	Opening Area	
	Outlets (full-scale)	Inlets (full-scale)
ef2-0.5	4cm×6cm×2 = 48 cm^2 (3 m^2)	4cm×6cm×2 = 48 cm^2 (3 m^2)
ef2-1	4cm×12cm×2 = 96 cm^2 (6 m^2)	8cm×6cm×2 = 96 cm^2 (6 m^2)
ef2-2	4cm×24cm×2 = 192 cm^2 (12 m^2)	8cm×6cm×2×2 floors = 192 cm^2 (12 m^2)
ef2-3	4cm×36cm×2 = 288 cm^2 (18 m^2)	8cm×6cm×2×3 floors = 288 cm^2 (18 m^2)

◆Series ef3

The inlets are uniformly distributed at each floor and the total inlet area is kept as 1/45 of the floor area of the atrium. The outlet area is changed to adjust the area ratio of the outlets to inlets.

Table 3-17 Experimental conditions for series ef3

No.	Opening Area	
	Outlets (full-scale)	Inlets (full-scale)
ef3-0.5	4cm×6cm×2 = 48 cm^2 (3 m^2)	2cm×3cm×2×8 floors＝96 cm^2 (6 m^2)
ef3-1	4cm×12cm×2=96 cm^2 (6 m^2)	
ef3-2	4cm×24cm×2=192 cm^2 (12 m^2)	
ef3-3	4cm×36cm×2=288 cm^2 (18 m^2)	

3.4.4.2 Experiments with ethanol and smoke generation stick

Ethanol put in the laboratory dish is used as the fire source. At the same time smoke generation stick is put above the flame, thus smoke rises and spreads with the hot plume. The movement of the smoke is photographed using video camera.

Table 3-18 Experimental conditions for series esf

No.	Opening area	
	Outlets (full-scale)	Inlets (full-scale)
esf-0.5	4cm×6cm×2 = 48 cm^2 (3 m^2)	2cm×3cm×2×8 floors = 96 cm^2 (6 m^2)
esf-1	4cm×12cm×2 = 96 cm^2 (6 m^2)	
esf-3	4cm×36cm×2 = 288 cm^2 (18 m^2)	

3.4.5 Experimental results

3.4.5.1 Results of the experiments with only ethanol

For all cases, after the ignition, in the first several minutes, the temperature in the atrium/chimney rises with the time, while about 4~5 minutes later, the temperature distribution in the atrium/chimney just varies a little (Fig. 3-22~Fig. 3-24), which means the burning of the ethanol in the atrium reaches a stable state. The results of temperature rise and pressure difference distribution shown in Fig. 3-25~Fig. 3-27 are the averaged value after the burning becomes stable. At this time, temperature rise in the chimney space is almost the same. It can be inferred that the chimney space is filled with uniformly mixed hot plume.

Since pressure differences have only been measured at four points, the pressure difference distribution line calculated from the measured temperature distribution is used to compare with the measured value. The calculation method is just as that used in natural ventilation.

The temperature between measured points k and k+1 is supposed to be the average of the two points. Assuming the pressure difference at the base of the atrium as Δp_{bot} (Pa), and the pressure difference at the top of the chimney as Δp_{top} (Pa), we can get:

$$\Delta p_{top} - \Delta p_{bot} = -\sum_{k=1}^{18}\left(\frac{\rho_k + \rho_{k+1}}{2} - \rho_0\right) g \Delta z_k \tag{3-26}$$

where

Δz_k is vertical distance between point k+1 and point k, m;

ρ_0 is density of ambient air, kg/m^3;

ρ_k is air density at point k, kg/m^3. It can be approximately calculated as:

$$\rho = \frac{353}{T_k} \tag{3-27}$$

According to the Bernoulli's law, the velocity of the opening at the base of the atrium v_{bot} (m/s) and at the top of the chimney v_{top} (m/s) can be expressed as:

$$v_{bot} = \alpha \sqrt{\frac{2 \mid \Delta p_{bot} \mid}{\rho_{bot}}} \tag{3-28}$$

$$v_{top} = \alpha \sqrt{\frac{2 \mid \Delta p_{top} \mid}{\rho_{top}}} \tag{3-29}$$

where

α is discharge coefficient, dimensionless.

And the mass flow rate M (kg/m^3) is:

$$M = vA\rho \tag{3-30}$$

where

v is velocity, m/s.

A is opening area, m^2.

Considering the conservation of mass flow rate, we can get:

$$\frac{\left|\Delta p_{top}\right|}{\left|\Delta p_{bot}\right|} = \frac{{A_{in}}^2 \rho_{bot}}{{A_{out}}^2 \rho_{top}} \tag{3-31}$$

where

A_{in} is area of inlet, m^2;

A_{out} is area of outlet, m^2.

According to Eq. (3-25) and Eq. (3-30), Δp_{top} and Δp_{bot} can be obtained from measured temperature distribution. And pressure difference at other testing points can be calculated as:

$$\Delta p_l = \Delta p_{bot} - \sum_{k=1}^{l} \left(\frac{\rho_k + \rho_{k+1}}{2} - \rho_0 \right) g \Delta z_k \tag{3-32}$$

■Temperature variation of series ef1

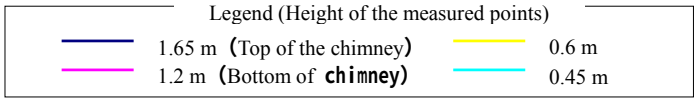

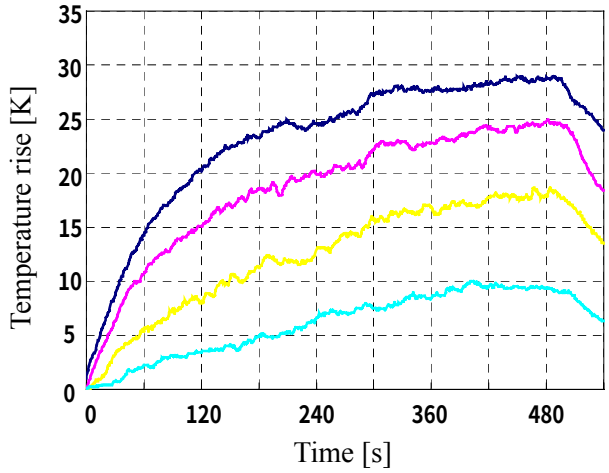

Fig. 3-22a Temperature rise of series ef1-0.5 [Outlet 3m^2/Inlet 6 m^2]

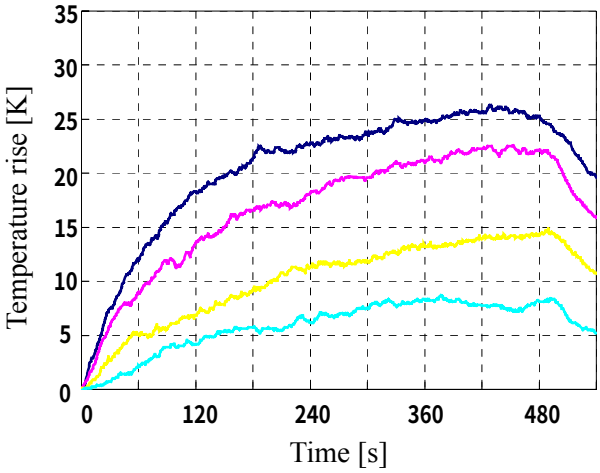

Fig. 3-22b Temperature rise of series ef1-1 [Outlet 6 m^2/Inlet 6 m^2]

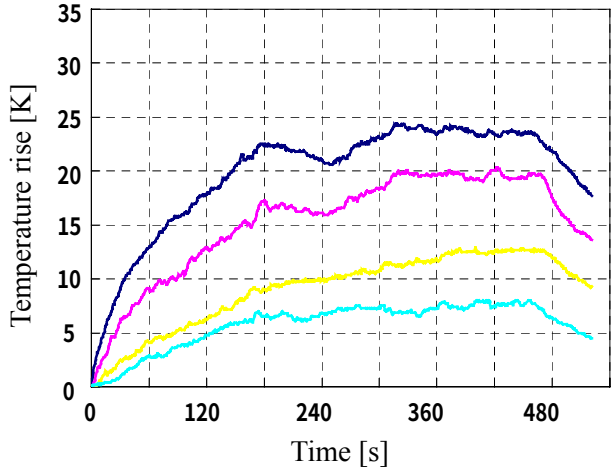

Fig. 3-22c Temperature rise of series ef1-2 [Outlet 12 m^2/Inlet 6 m^2]

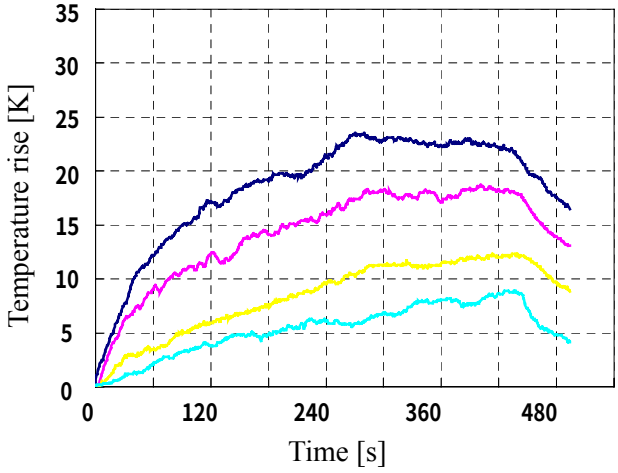

Fig. 3-22d Temperature rise of series ef1-3 [Outlet 18 m^2/Inlet 6 m^2]

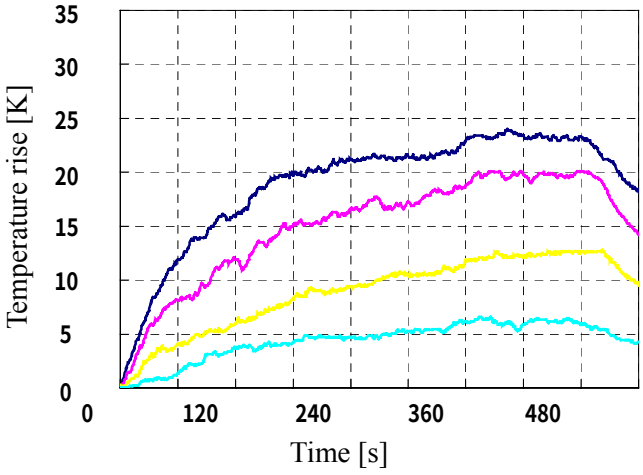

Fig. 3-22e Temperature rise of series ef1-4 [Outlet 24 m^2/Inlet 6 m^2]

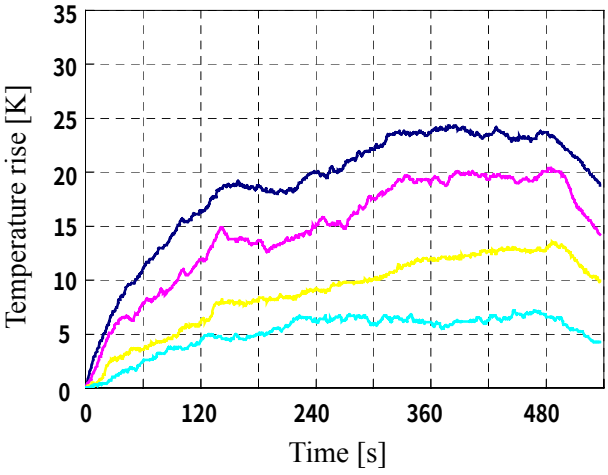

Fig. 3-22f Temperature rise of series ef1-5 [Outlet 30 m^2/Inlet 6 m^2]

■Temperature variation of series ef2

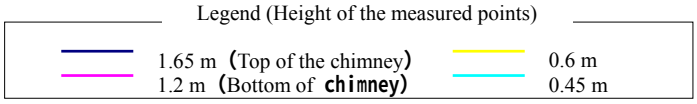

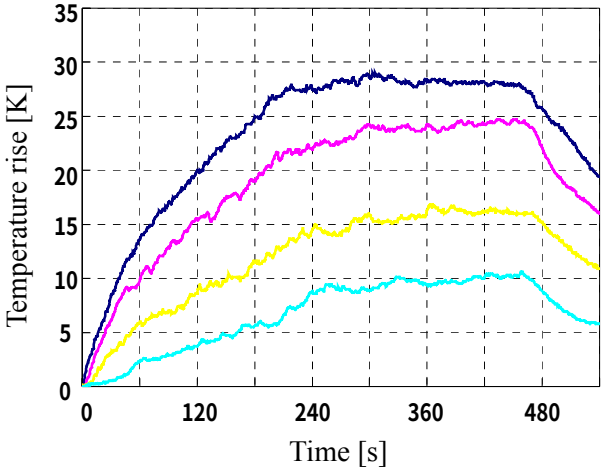

Fig. 3-23a Temperature rise of series ef2-0.5
[Outlet 3 m^2/Inlet 3 m^2]

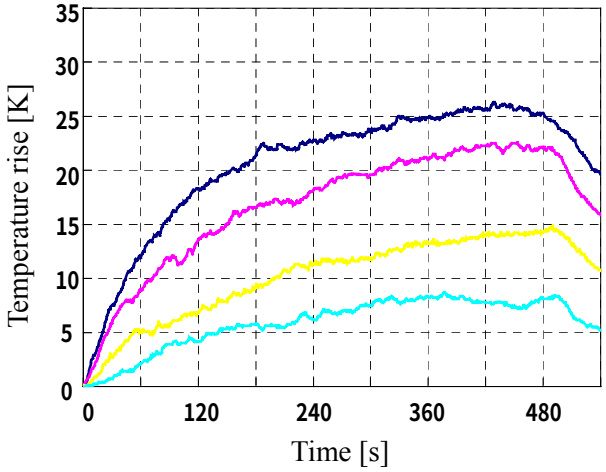

Fig. 3-23b Temperature rise of series ef1-1
[Outlet 6 m^2/Inlet 6 m^2]

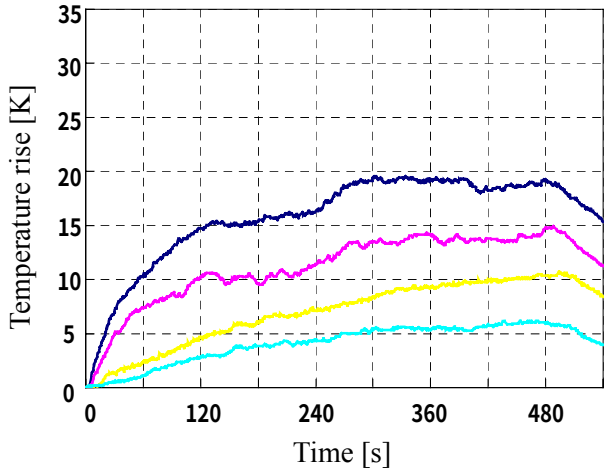

Fig. 3-23c Temperature rise of series ef2-2
[Outlet 12 m^2/Inlet 12 m^2]

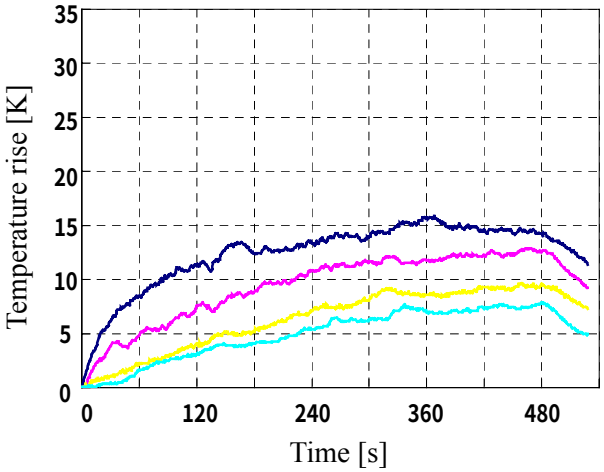

Fig. 3-23d Temperature rise of series ef2-3
[Outlet 18 m^2/Inlet 18 m^2]

■Temperature variation of series ef3

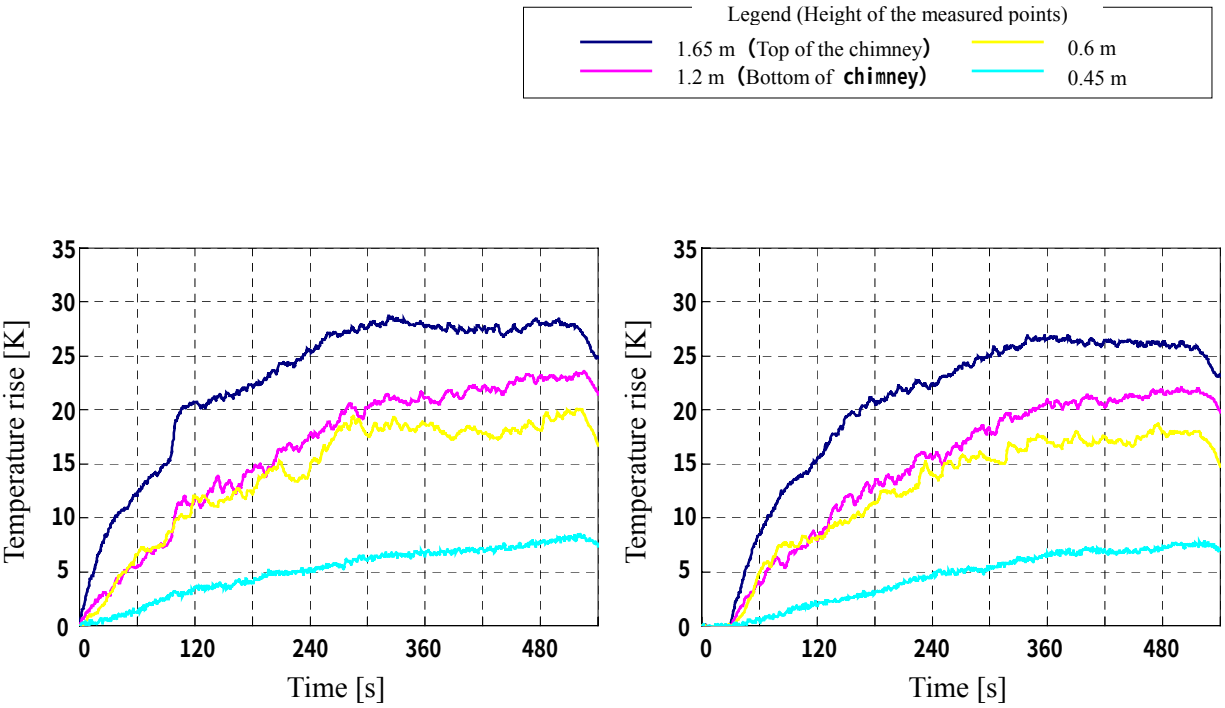

Fig. 3-24a Temperature rise of series ef3-0.5

[Outlet 3 m^2/Inlet 0.75×8 floors = 6 m^2]

Fig. 3-24b Temperature rise of series ef3-1

[Outlet 6 m^2/Inlet 0.75×8 floors = 6 m^2]

Fig. 3-24c Temperature rise of series ef3-2

[Outlet 12 m^2/Inlet 0.75×8 floors = 6 m^2]

Fig. 3-24d Temperature rise of series ef3-3

[Outlet 18 m^2/Inlet 0.75×8 floors = 6 m^2]

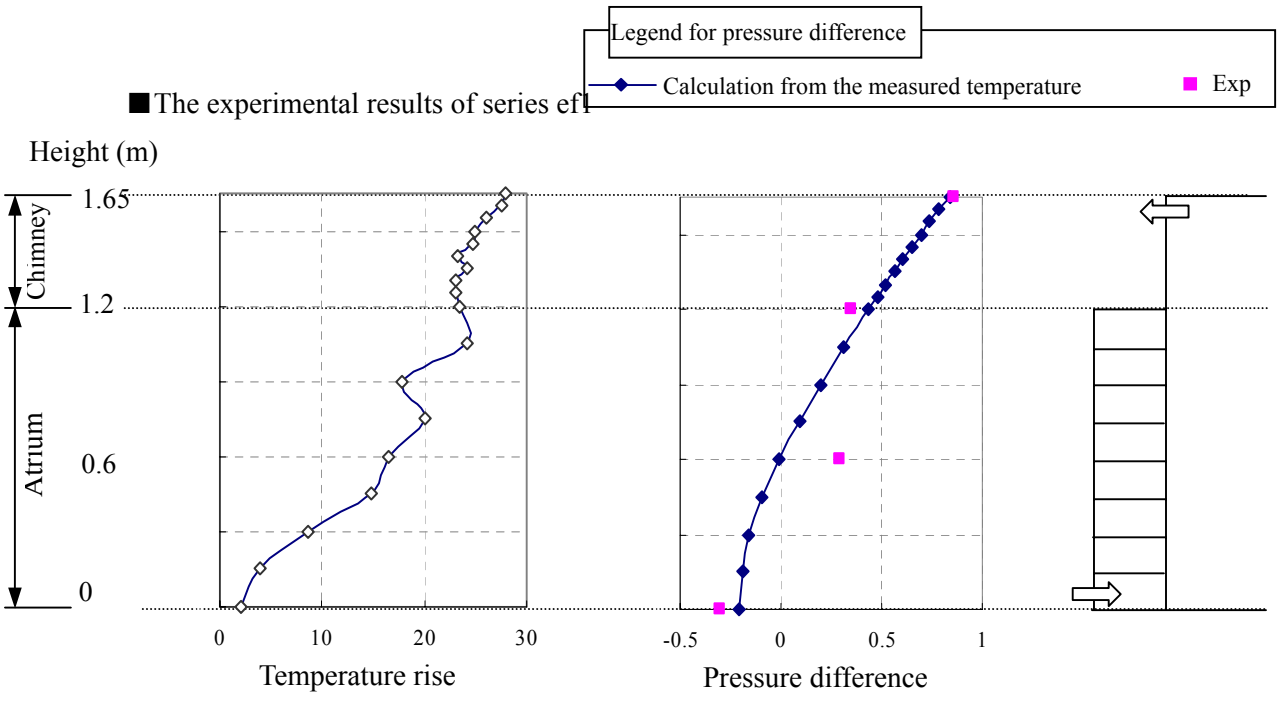

Fig. 3-25a Temperature rise and pressure difference of ef1-0.5

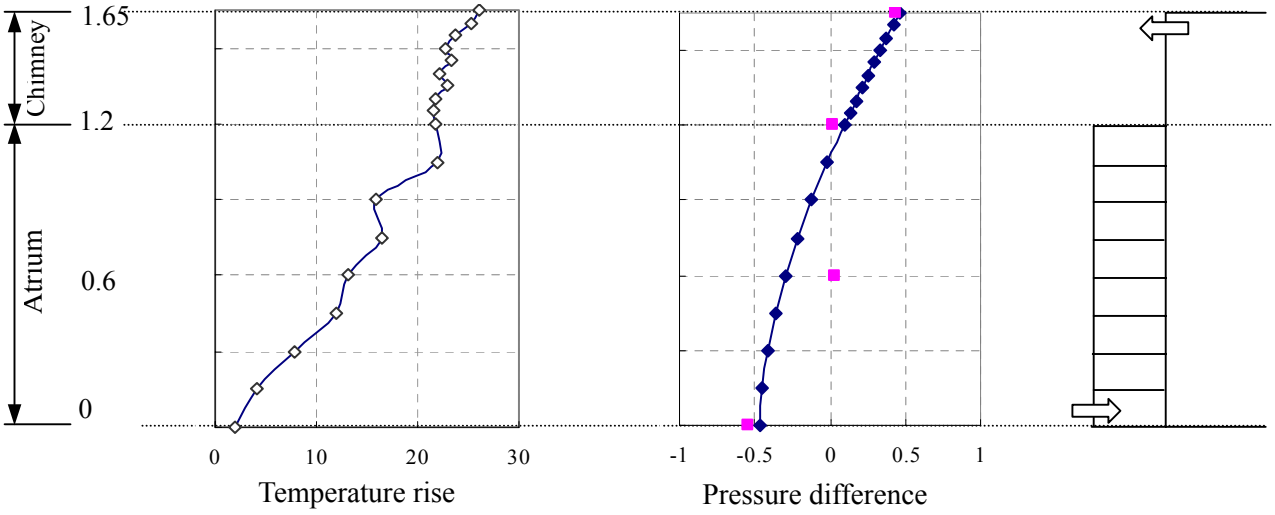

Fig. 3-25b Temperature rise and pressure difference of ef1-1

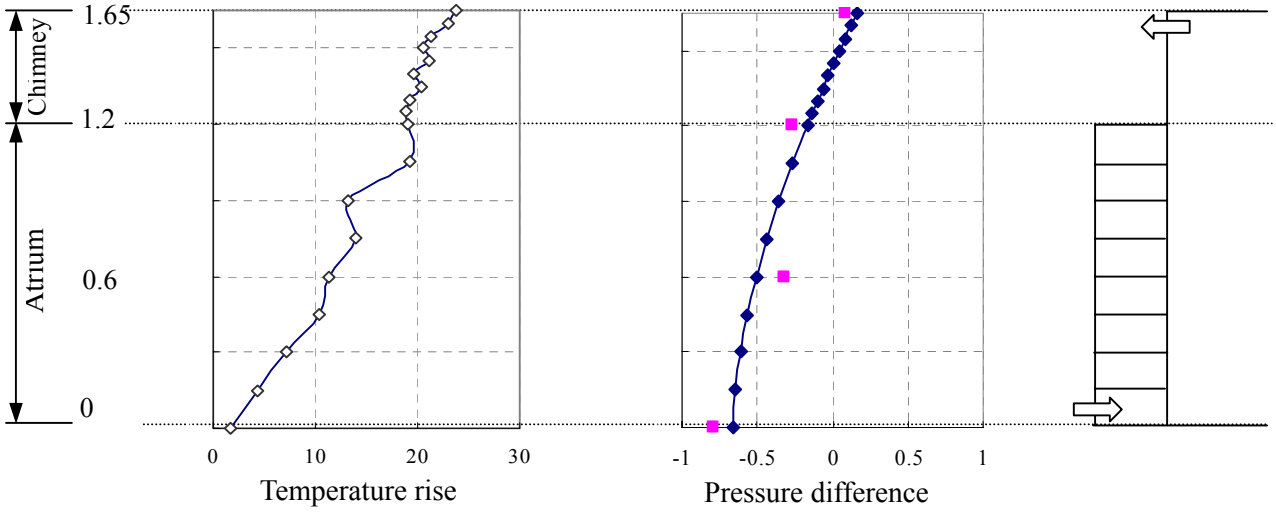

Fig. 3-25c Temperature rise and pressure difference of ef1-2

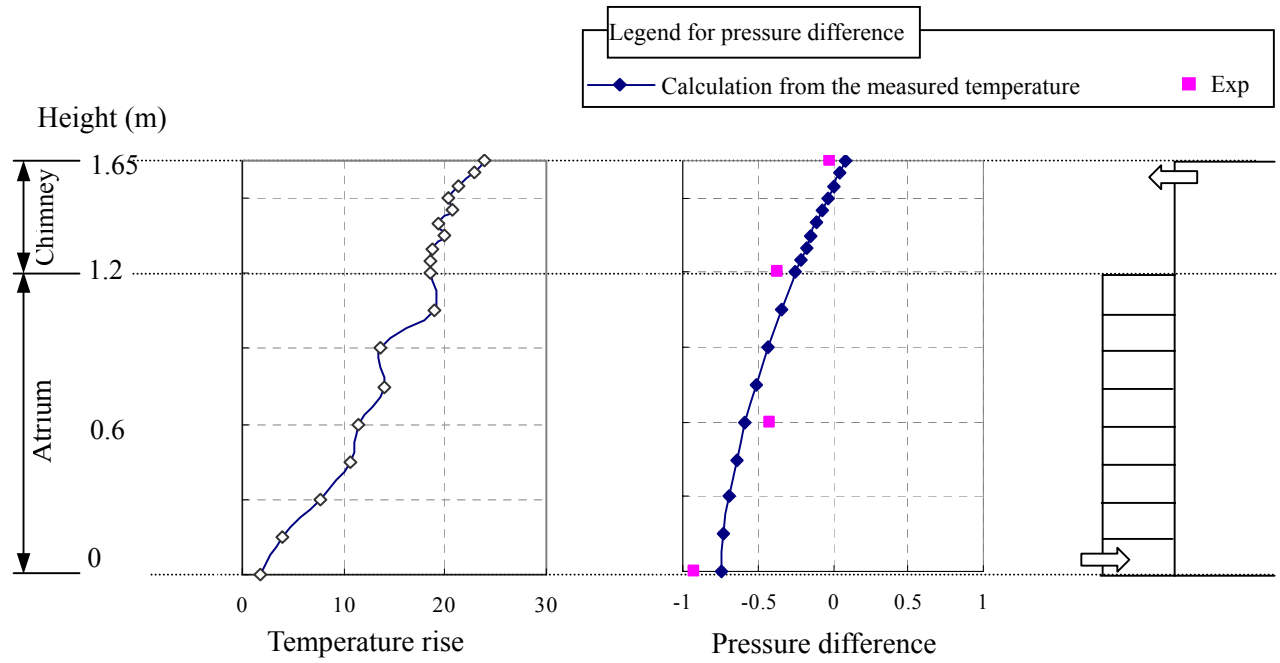

Fig. 3-25d Temperature rise and pressure difference of ef1-3

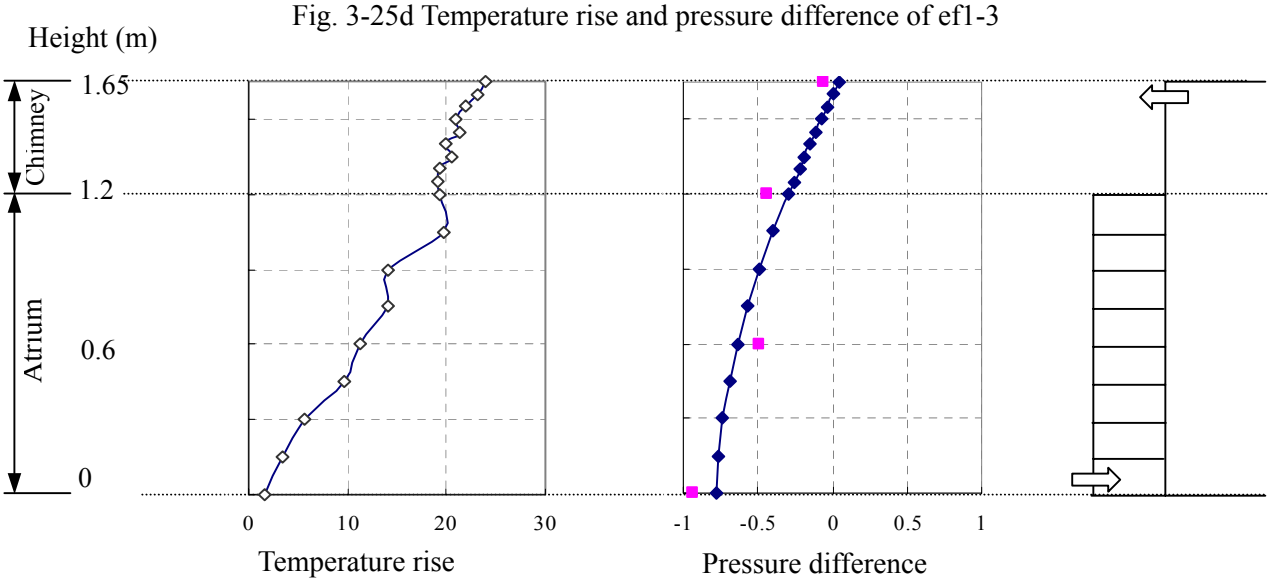

Fig. 3-25e Temperature rise and pressure difference of ef1-4

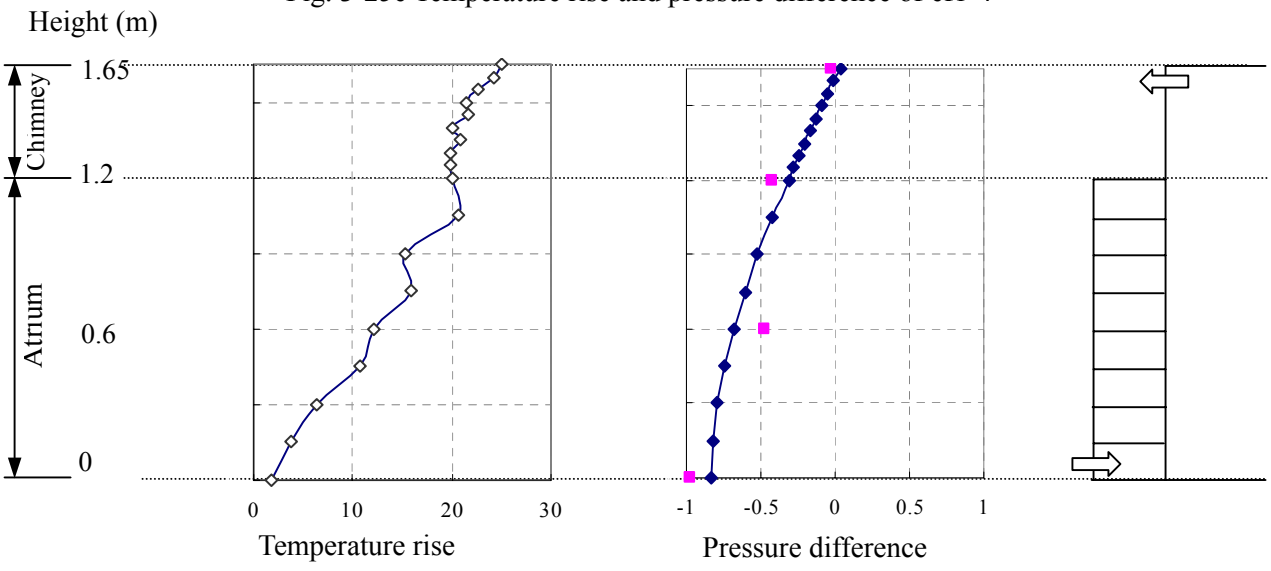

Fig. 3-25f Temperature rise and pressure difference of ef1-5

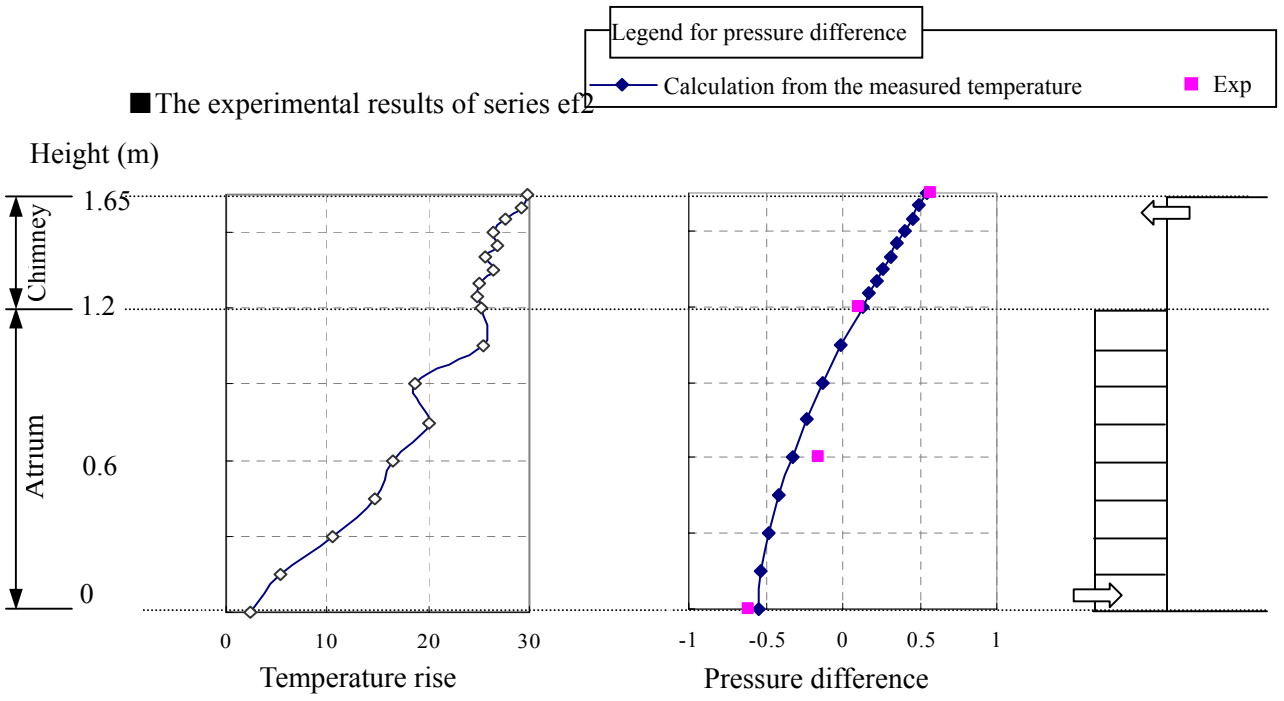

Fig. 3-26a Temperature rise and pressure difference of ef2-0.5

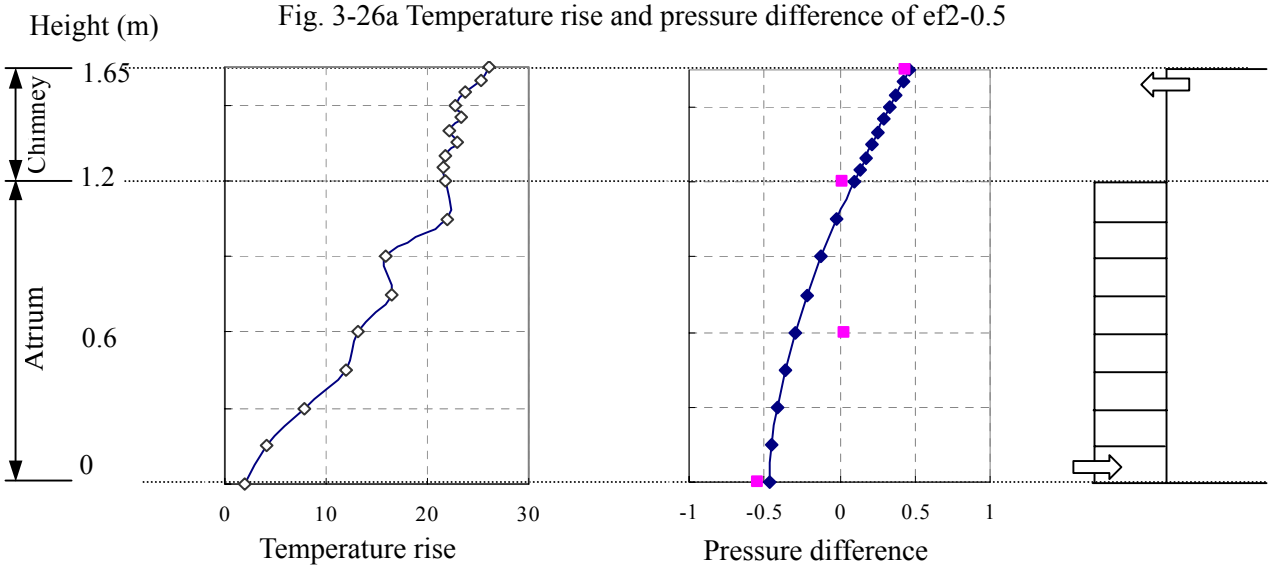

Fig. 3-26b Temperature rise and pressure difference of ef2-1

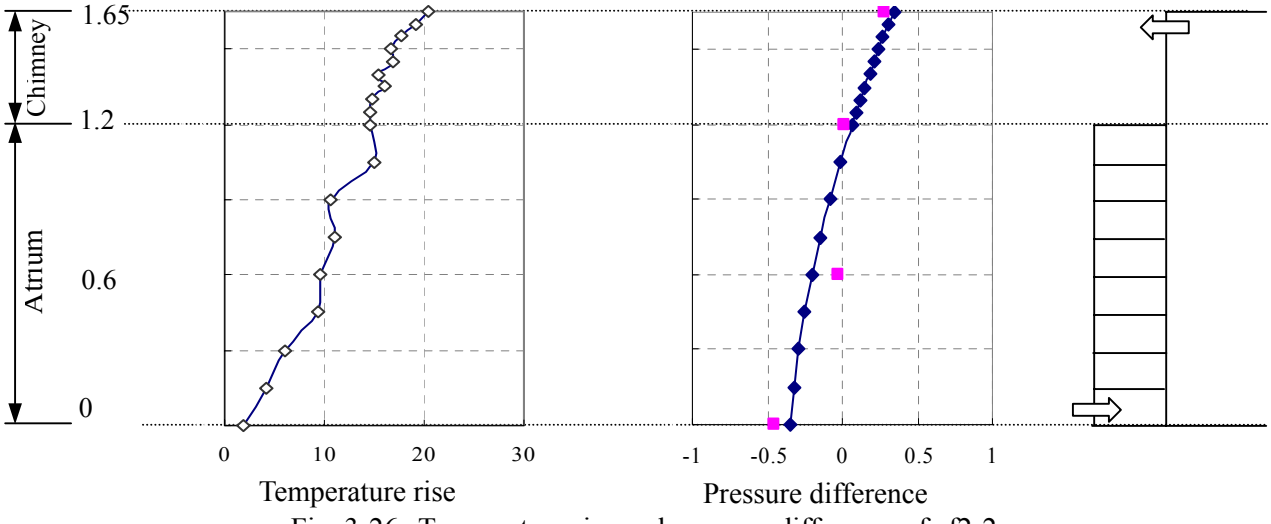

Fig. 3-26c Temperature rise and pressure difference of ef2-2

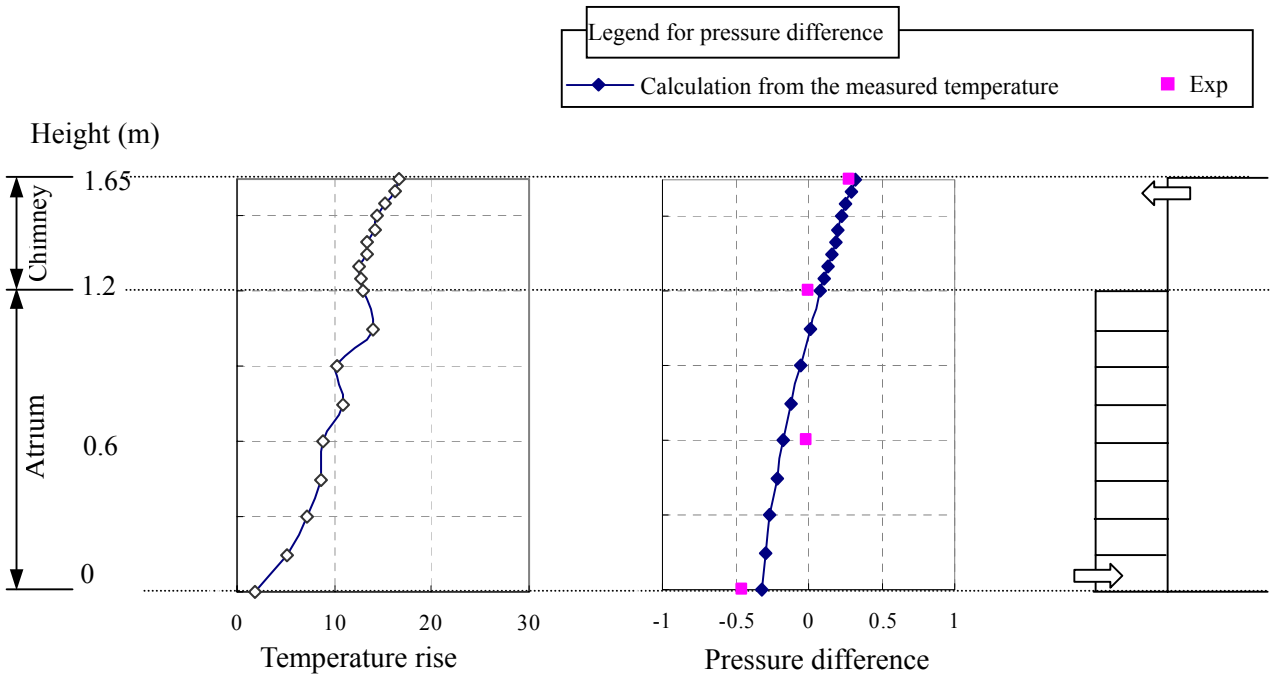

Fig. 3-26d Temperature rise and pressure difference of ef2-3

■The experimental results of series ef3

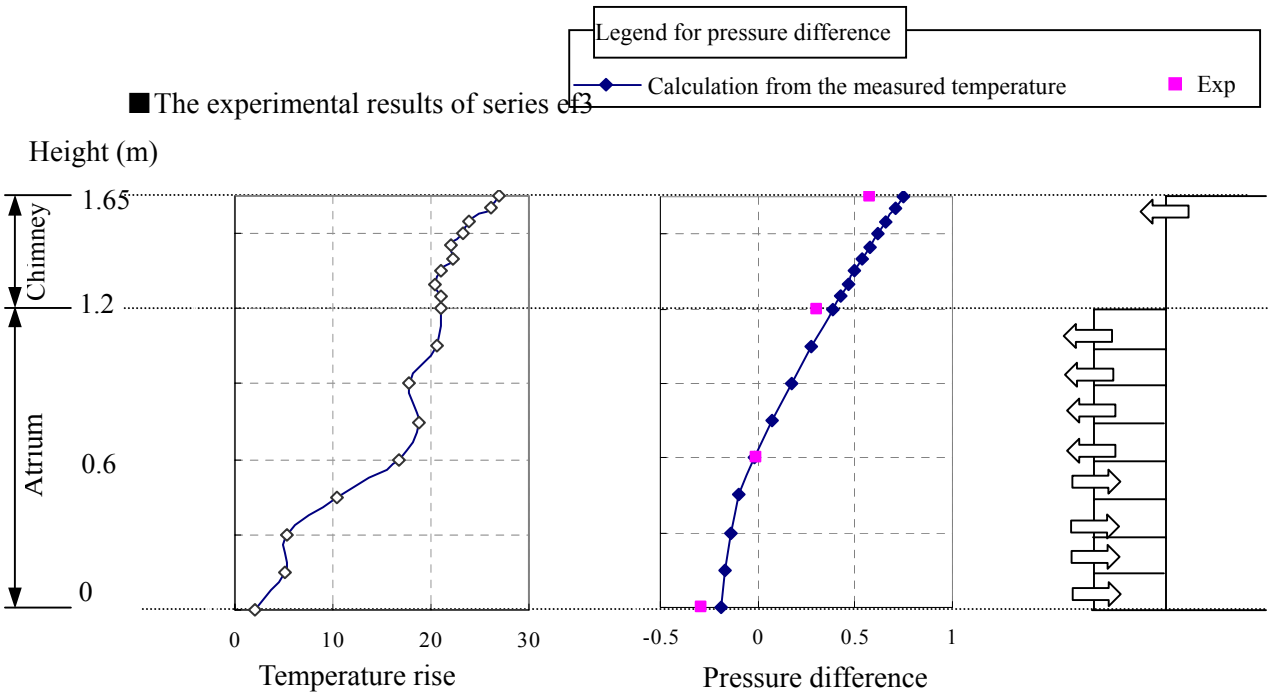

Fig. 3-27a Temperature rise and pressure difference of ef3-0.5

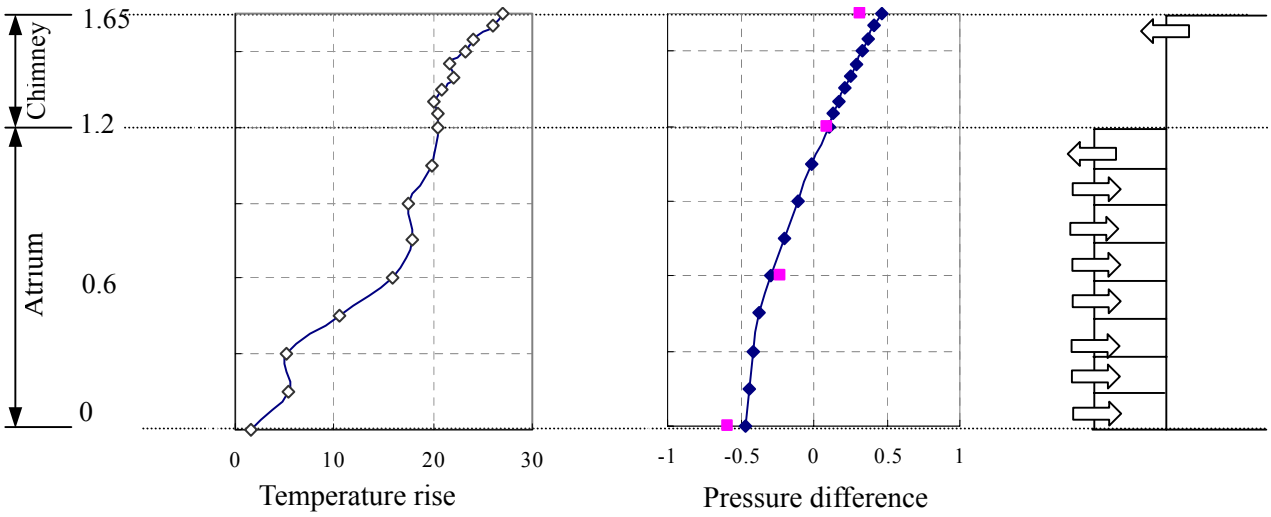

Fig. 3-27b Temperature rise and pressure difference of ef3-1

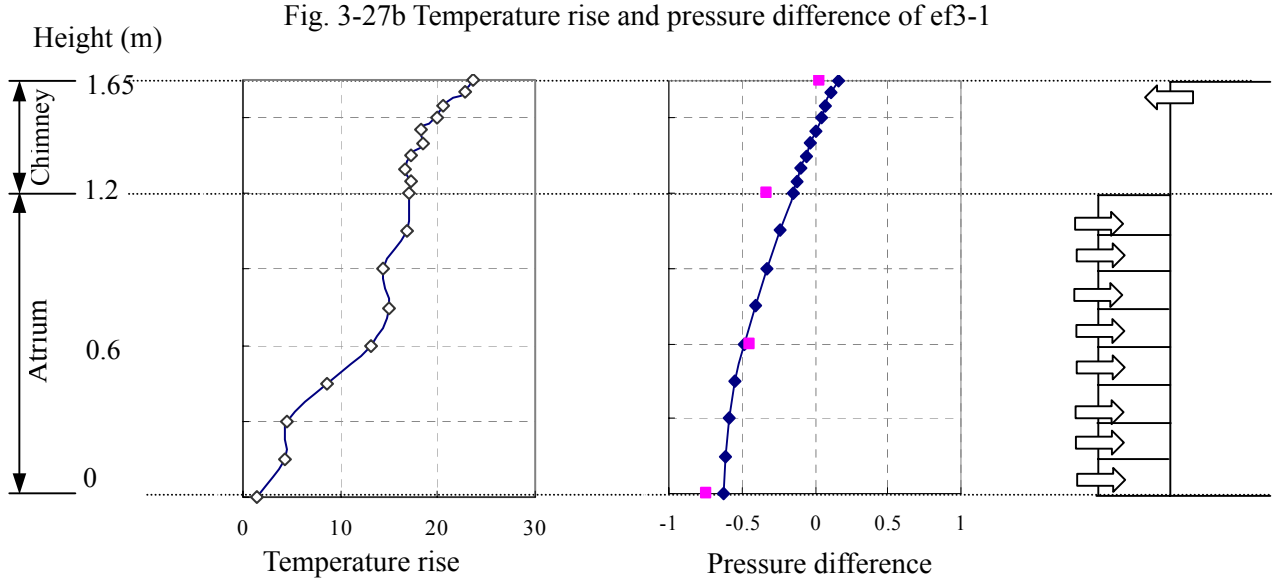

Fig. 3-27c Temperature rise and pressure difference of ef3-2

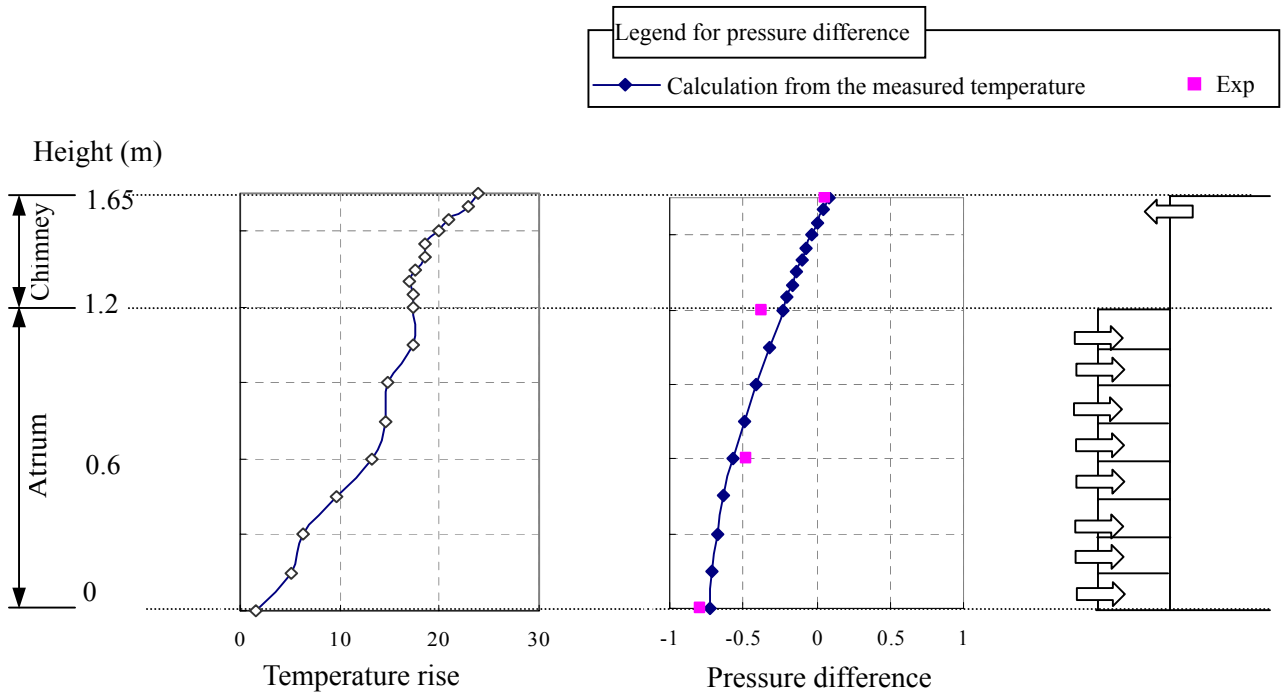

Fig. 3-27d Temperature rise and pressure difference of ef3-3

3.4.5.2 Results of the experiments with ethanol and smoke generation stick

The experimental results of series esf-0.5

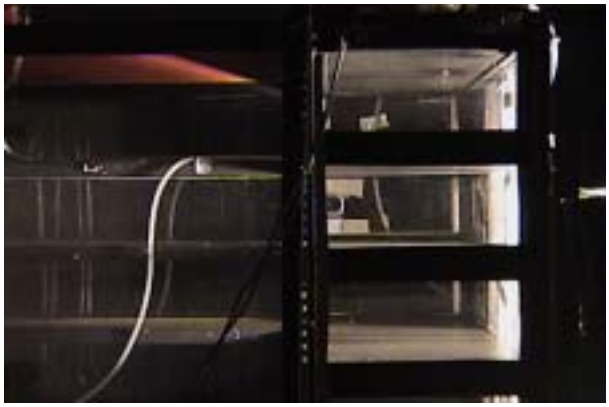

Ignition

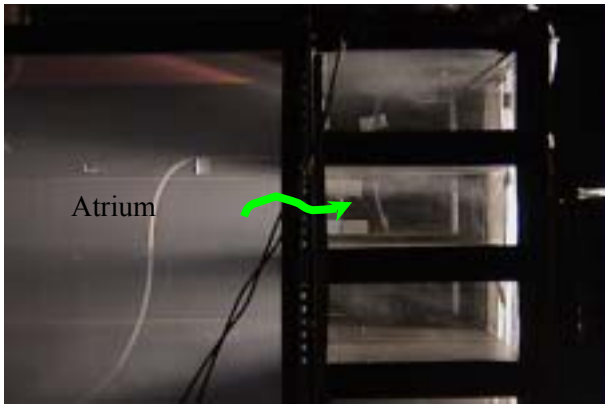

40s after ignition

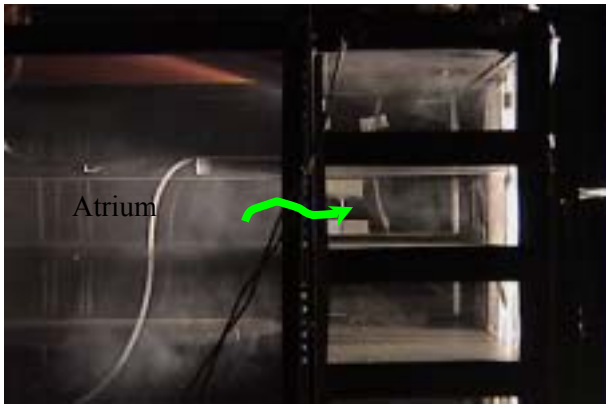

10s after ignition

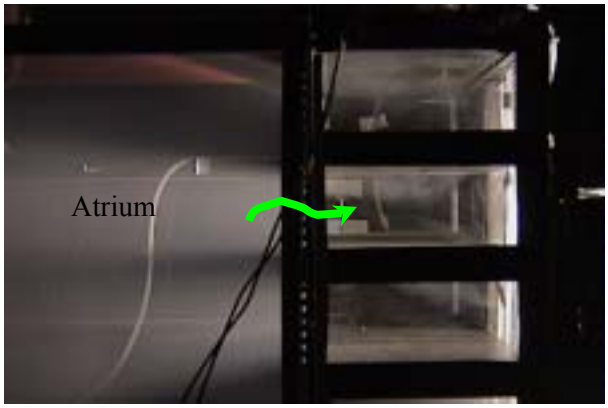

50s after ignition

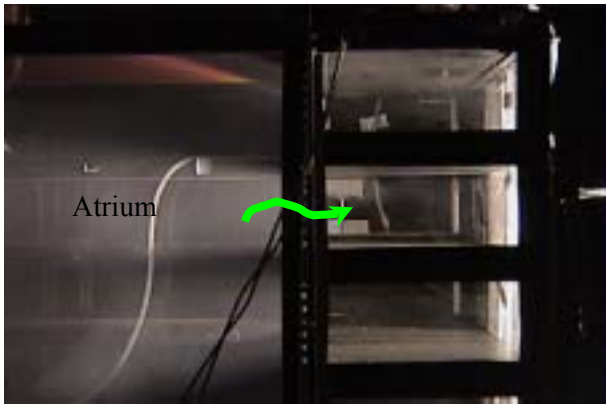

20s after ignition

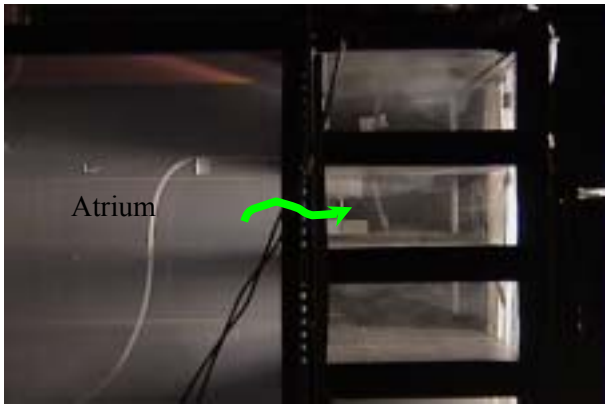

60s after ignition

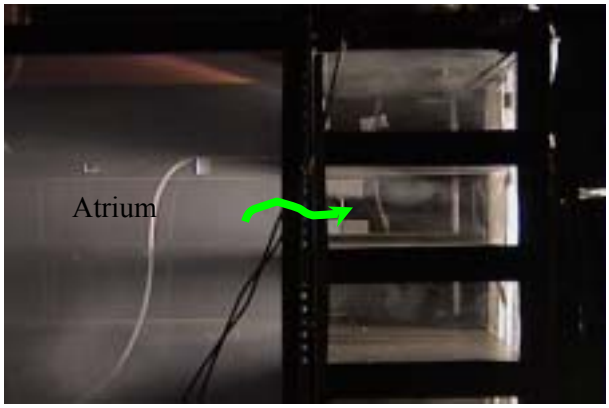

30s after ignition

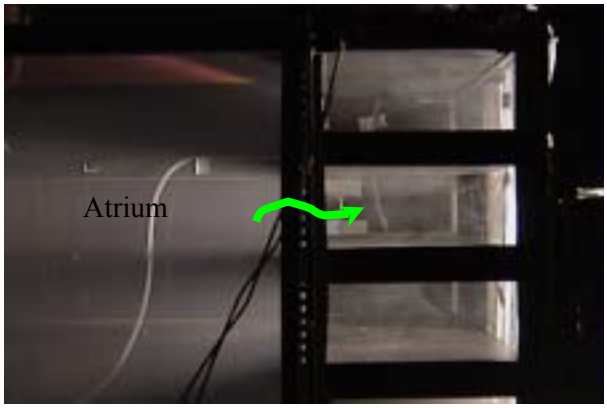

70s after ignition

Fig. 3-28 Smoke spread process of series esf-0.5

Fire source: ethanol + smoke generation stick
Outlets: 3 m^2; Inlets: 0.75 m^2 at each floor

The experimental results of series esf-1

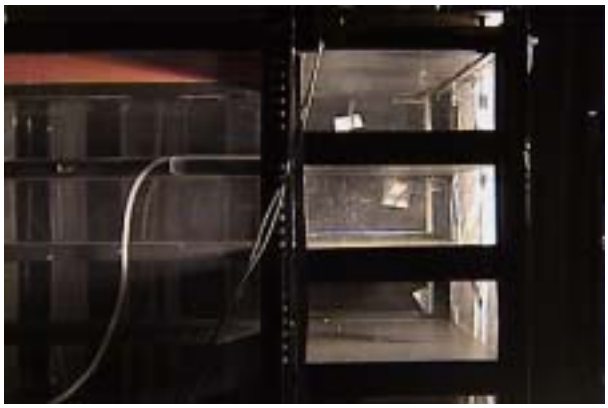

Ignition

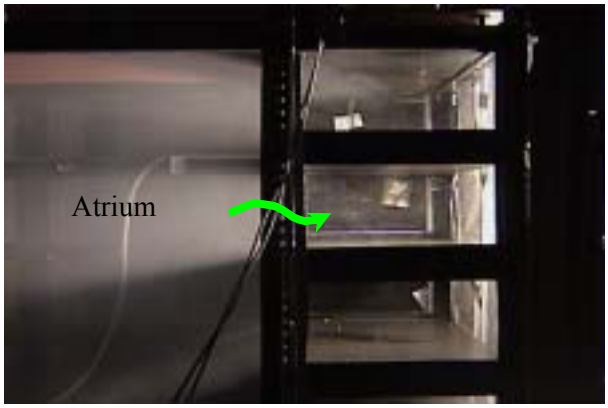

40s after ignition

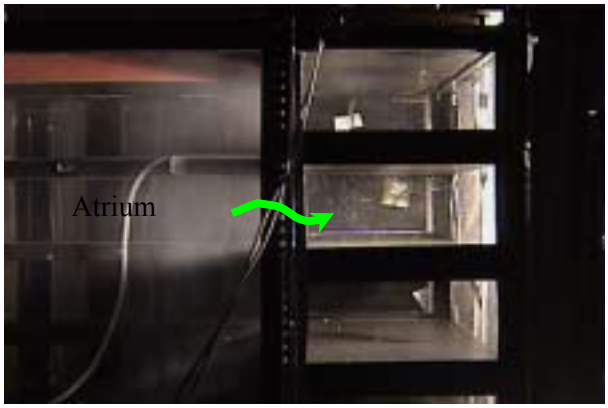

10s after ignition

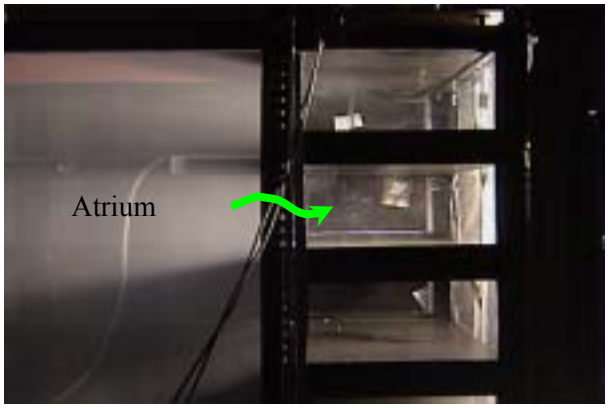

50s after ignition

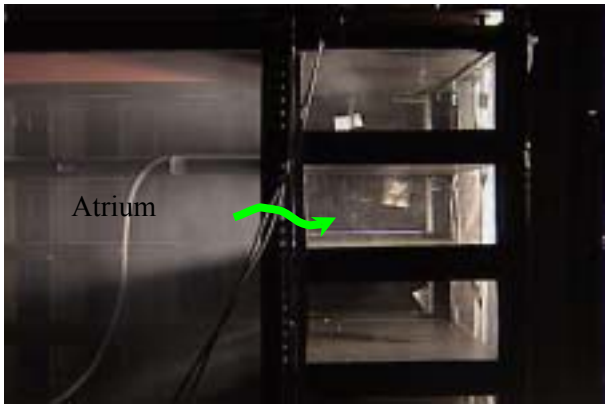

20s after ignition

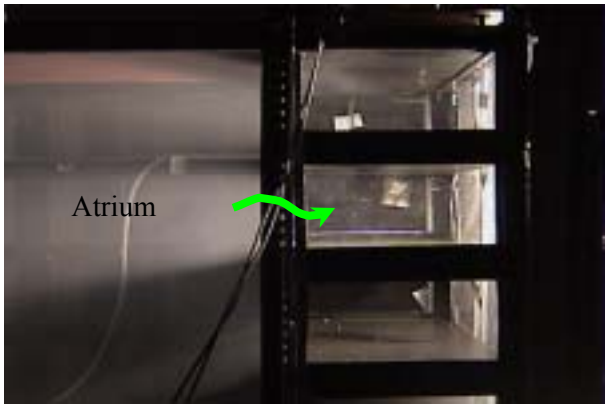

60s after ignition

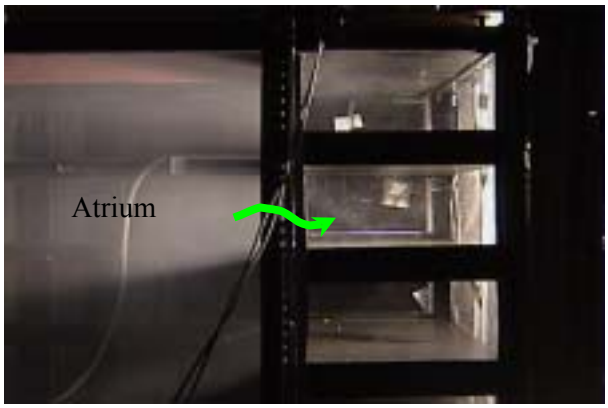

30s after ignition

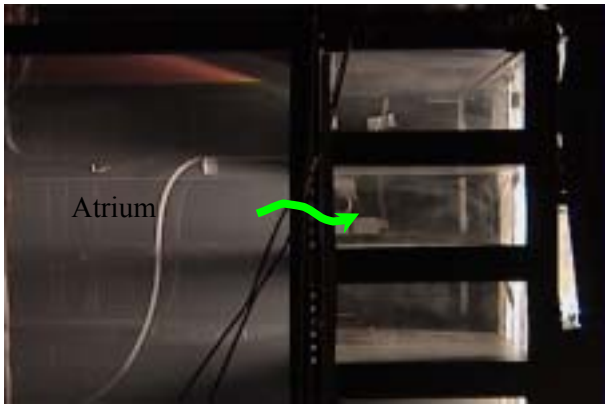

70s after ignition

Fig. 3-29 Smoke spread process of series esf-1

Fire source: ethanol + smoke generation stick

Outlets: 6 m^2; Inlets: 0.75 m^2 at each floor

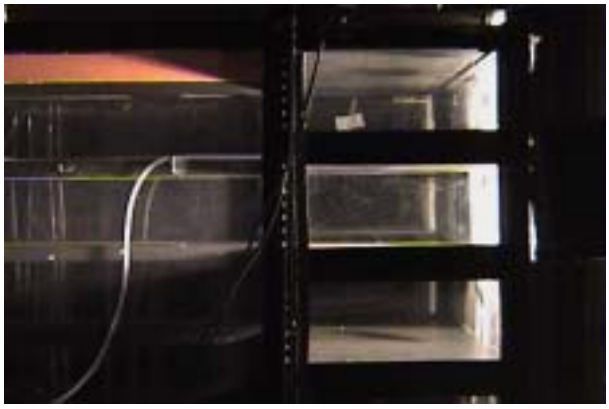

Ignition

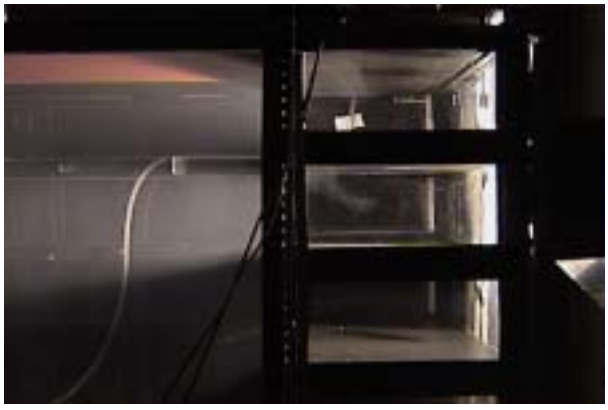

40s after ignition

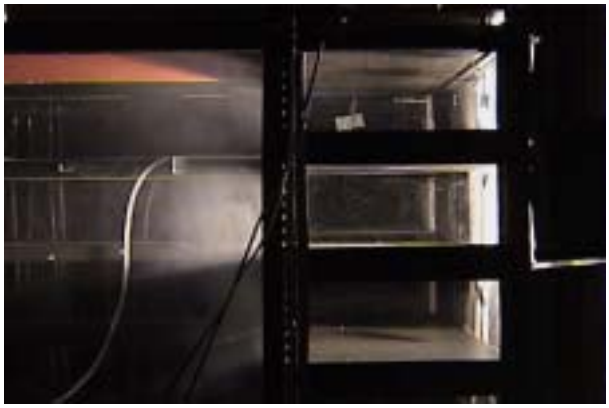

10s after ignition

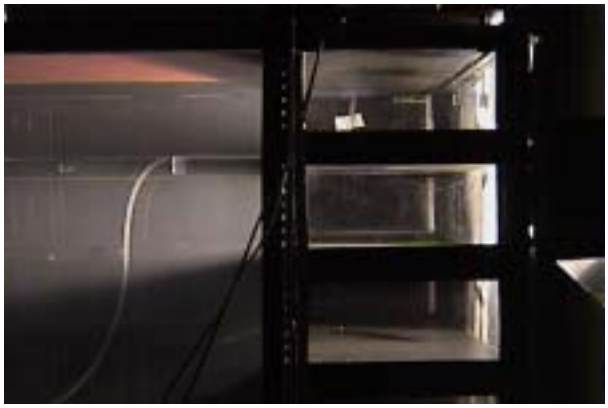

50s after ignition

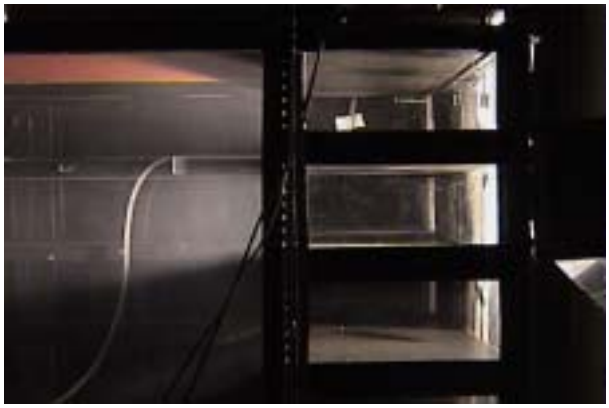

20s after ignition

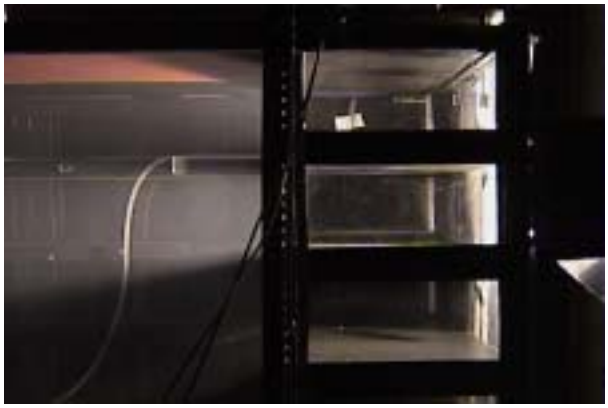

60s after ignition

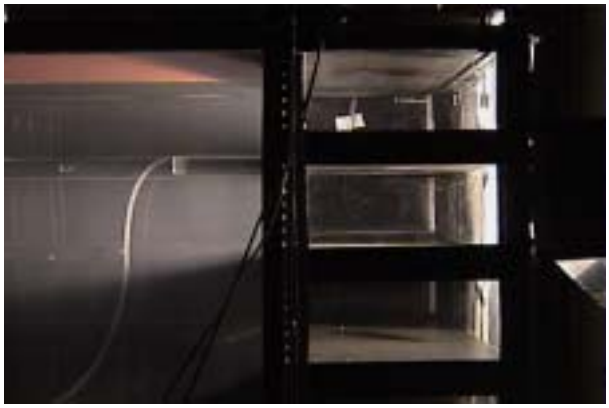

30s after ignition

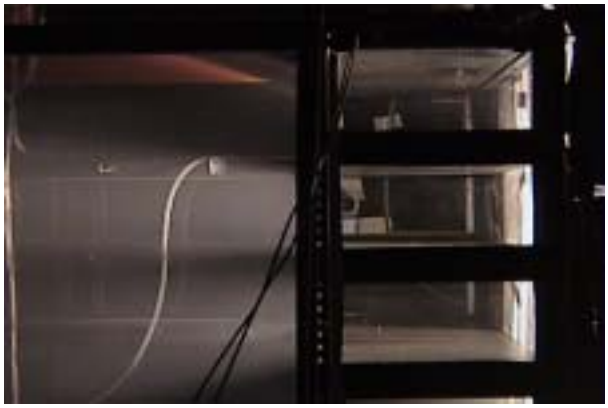

70s after ignition

Fig. 3-30 Smoke spread process of series esf-3

Fire source: ethanol + smoke generation stick

Outlets: 18 m^2; Inlets: 0.75 m^2 at each floor

3.4.6 Analysis of the experimental results

3.4.6.1 Results of the experiments with only ethanol

For series ef1 and ef3, the experiments are carried out under almost the same conditions except the distribution of the inlets. In series ef1 the inlets are concentrated at the first floor, and in series ef3 the inlets are uniformly distributed at each floor. The total area of the inlets is the same. The results of ef1 and ef3 show almost the same inclination, although the distribution of the inlets is different. In all cases, since the fire source is placed at the base of the atrium, temperature rise in the atrium is significant. The total temperature rise in the atrium/chimney decreases with the increase of the outlet area. According to the pressure difference, the height of the neutral pressure plane can be inferred. Although the neutral pressure plane is mainly decided by the area ratio of outlet to inlet, the fluid temperature also will influence the height of the neutral pressure plane in some degree. Comparing with the case of natural ventilation, temperature rise in the atrium/chimney is higher; therefore with the same area conditions, in case of the smoke control, the neutral pressure plane descends a little. When the area ratio of the outlet to inlet is 0.5, the neutral pressure plane is at about half height of the atrium. The neutral pressure plane goes up with increasing of the outlet area. From the experimental results, to keep the neutral pressure plane stay inside the chimney, the area ratio of the outlet to inlet should be greater than 2.

For series ef2, the inlet area is equal to the outlet area. With increasing of the area of outlet/inlet, the total temperature rise in the atrium/chimney decreases. For all cases, the neutral pressure plane forms in the upper part of the atrium.

3.4.6.2 Results of the experiments with ethanol and smoke generation stick

Through the experiments of series ef1~ef3, according to the temperature and pressure difference distribution, the position of the neutral pressure plane is grasped. In the experiments of series esf, smoke generation stick is used to confirm the neutral pressure plane by observing the movement of the smoke. From the results, when the outlet area is only half of the inlet area, the neutral pressure plane is inferred to be at the half height of the atrium. The pictures of the smoke movement show that smoke spreads into the separated space obviously, which matched with the results of the experiments with only ethanol. When the outlet area is three times of the inlet area, the neutral pressure plane is near the top of the

chimney. The pictures of the smoke movement show that although there are openings at the boundary of the atrium and the utility space, because the neutral pressure plane is higher than the occupant space, smoke does not invade into the separated space.

Through above experiments, the smoke movement inside the chimney/atrium is grasped. The influence of the area ratio of the outlet to inlet is discussed. Furthermore, the smoke spread situation has been confirmed by visualization.

In the smoke control experiments, the velocities of the outlets and inlets cannot be recorded due to the temperature limitation of the anemometer. But from the pressure difference distribution, the variation of the velocities can be inferred. In the experiments of series ef1, the inlet velocity increases with the expanding of the outlet area. But when the outlet area becomes more than 2 times of the inlet area, the inlet velocity almost has no obvious change. The outlet velocity reduces with the increasing of the outlet area.

3.5. SUMMARY

In this chapter, the reduced scale model and the experimental methods are introduced. Experiments on natural ventilation performance and smoke control performance are carried out respectively. The results of the experiments are presented and analyzed.

Through the experiments on the natural ventilation performance, it is confirmed that effective natural ventilation can be realized by temperature rise of the chimney walls. In addition, the influence of the opening area and wall temperature rise on the ventilation effectiveness is discussed. Since temperature rise normally happens inside the chimney, as long as the area ratio of the outlet to inlet is greater than 1, effective natural ventilation can be expected.

Through the experiments on the smoke control performance, it is confirmed that smoke spread is quite related with the height of the neutral pressure plane. By observation of the smoke movement, when the area ratio of the outlet to inlet is greater than 2, the neutral plane forms above the occupant space, and although there are openings at the boundary of the atrium and the utility space, smoke does not spread into the partitioned space. Smoke interception by pressure difference is confirmed.

It is verified that natural ventilation can be realized in the prototype building and smoke

control is possible based on the natural ventilation system through the reduced scale model experiments. The detail performance of the prototype building will be discussed in following chapters.

CHAPTER 4

VALIDITY OF CFD METHOD BY COMPARING WITH THE EXPERIMENTAL RESULTS

CHAPTER 4
VALIDITY OF CFD METHOD BY COMPARING WITH EXPERIMENTAL RESULTS

In this chapter, CFD method used in this research is introduced.

Through the reduced scale model experiments, the natural ventilation and smoke control performance of the prototype building have been confirmed in some degree. Based on the results of the model experiments, the validity of the CFD method will be discussed. Then the CFD method will be used to predict the detail performance of the prototype building.

4.1 INTRODUCTION

In the field of fluid dynamics, computational methods have been developed rapidly in recent years as a result of improvements in computer hardware. The engineering applications of computational fluid dynamics (CFD) have also advanced with the development of various turbulence models. In this research the flow of the air inside the building and the chimney is considered to be turbulence flow and two kinds of turbulence models are employed. For the natural ventilation prediction, the flow is considered to be a low level of turbulence and the indoor zero-equation model (Qingyan Chen 1998, Nielsen 1998) is used. For the smoke control prediction, the flow is considered to be a high level of turbulence and the standard κ-ε model is used.

4.2 SIMULATION FOR NATURAL VENTILATION

4.2.1 Numerical modeling

A zero-equation model is a turbulence model where the eddy viscosity μ_t is given as a constant number or given from an analytical equation without involvement of transport equations. During the calculations the Buossinesq approximation is adopted for thermal buoyancy. The approximation takes air density as constant and considers the buoyancy influence on air movement by the difference between the local air density and the pressure

gradient. With an eddy-viscosity model, the airflow is described by the following time-averaged Navier-Stokes equations for the conservation of mass, momentum, and energy.

4.2.1.1 Governing equations

◆The mass conservation equation

$$\frac{\partial u_i}{\partial x_i} = 0 \tag{4-1}$$

where

u_i is the mean velocity component in x_i direction;

x_i is coordinate (for i = 1, 2, 3, x_i corresponds to three perpendicular axes).

◆The momentum conservation equation

$$\frac{\partial(\rho u_i)}{\partial t} + \frac{\partial(\rho u_i u_j)}{\partial x_j} = -\frac{\partial P}{\partial x_i} + \frac{\partial}{\partial x_j}\left[\mu_{eff}\left(\frac{\partial u_i}{\partial x_j} + \frac{\partial u_j}{\partial x_i}\right)\right] + \rho_0 \beta (T_0 - T) g_i \tag{4-2}$$

where

ρ is the air density;

u_j is the velocity component in x_j direction;

P is the static pressure;

μ_{eff} is the effective viscosity;

β is the thermal expansion coefficient of air, 1/T;

T_0 is the reference temperature;

T is temperature;

g_i is the gravity acceleration in i direction.

The last term on the right side of the equation reflects the buoyancy term.

The turbulent influences are lumped into the effective viscosity as the sum of the turbulent viscosity, μ_t, and the laminar viscosity, μ:

$$\mu_{eff} = \mu_t + \mu \tag{4-3}$$

The turbulent viscosity μ_t in the indoor zero-equation model is expressed as:

$$\mu_t = 0.03874 \rho V l \tag{4-4}$$

where

V is the local velocity magnitude;

ρ is the fluid density;

l is defined as the distance from the nearest wall;

0.03874 is an empirical constant.

◆The energy conservation equation

To determine the temperature distribution and the buoyancy term in Eq. (4-2), the equation for energy conservation must be solved.

$$\frac{\partial(\rho T)}{\partial t} + \frac{\partial(\rho u_j T)}{\partial x_j} = \frac{\partial}{\partial x_j}\left(\Gamma_{T,eff} \frac{\partial T}{\partial x_j}\right) + \frac{q}{c_P} \tag{4-5}$$

where

$\Gamma_{T,\,eff}$ is the effective turbulent diffusion coefficient for T;

q is the heat source;

c_p is the specific heat.

Here the effective diffusive coefficient for temperature in Eq. (4-5) is estimated by:

$$\Gamma_{T,eff} = \frac{\mu_{eff}}{\mathrm{Pr}_{eff}} \tag{4-6}$$

where Pr_{eff} is the effective Prandtl number, and here is taken as 0.9.

The heat transfer at the boundary surfaces is determined by computing a convective heat transfer coefficient:

$$h = \frac{\mu_{eff} c_P}{\mathrm{Pr}_{eff} \Delta x_j} \tag{4-7}$$

Where Δx_j is the grid space adjacent to the wall.

4.2.1.2 Calculating process

The equations for conservation of mass, momentum, and energy are solved in time-dependent form. Although the natural ventilation phenomenon is a steady-state problem, activating time dependence is sometimes useful when attempting to solve steady-state problems that tend towards instability (e.g., natural convection problems). It is possible in many cases to reach a steady-state solution by integrating the time-dependent equations.

The calculating time is set as 1800 seconds and the time step increment is set as 1 Second. The number of iterations to be performed per time step is set as 30 times.

4.2.2 Simulation of the reduced scale model

4.2.2.1 Computational grid

To compare with the experimental results, the reduced scale model is generated. The computational domain is basically divided into a grid of 0.03m×0.03m×0.03m control volumes. Additional grid points are embedded near the walls and around the inlets and outlets to enable better resolution in these areas. The total number of the meshes is about 75,000 for the model of which the inlet is concentrated at the first floor, and 95,000 for the model of which the inlets are uniformly distributed at each floor. The outline of the model is shown in Fig 4-1.

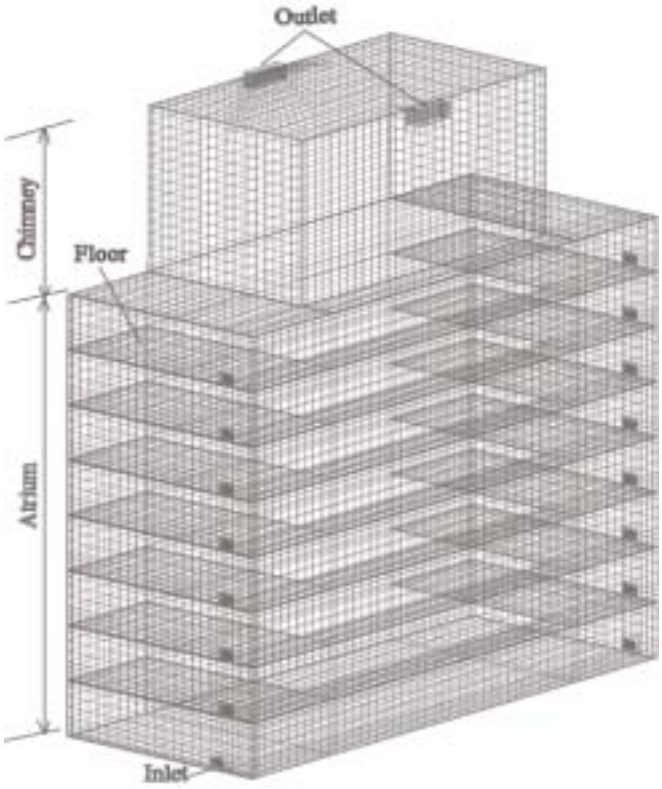

Fig. 4-1 Simulation model for natural ventilation

4.2.2.2 Boundary conditions

To simulate the experiments, the following boundary conditions are used:

(1) Walls: In the simulation of natural ventilation, the interior surfaces' temperatures of the chimney are set as the same as that of the experiments. All the other surfaces are set as adiabatic. Thus heat loss of the experimental model is thought to be a little greater, but for natural ventilation, since temperature rise occurs almost only in the chimney, it is thought that the assumption will not cause great difference on temperature distribution and so on.

(2) Openings: Inlets and outlets are set as pressure boundaries that allow flow in and out of the domain. The pressure is set as the same as ambient.

Although many cases have been conducted through the reduced scale model experiments,

in simulation of the reduced scale model, the following conditions are discussed.

Table 4-1 Conditions for series cnv1

Area ratio (Outlet/Inlet)	Temperature rise of Wall 4	Outlets		Inlets (1F)	
		Reduced Scale	Full-Scale	Reduced Scale	Full-Scale
1	+20℃	4cm×12cm×2	6 m^2	6cm×8cm×2	6 m^2
2		4cm×24cm×2	12 m^2	6cm×8cm×2	6 m^2
3		4cm×36cm×2	18 m^2	6cm×8cm×2	6 m^2

Table 4-2 Conditions for series cnv2

Area ratio (Outlet/Inlet)	Temperature rise of Wall 4	Outlets		Inlets (8Fs)	
		Reduced Scale	Full-Scale	Reduced Scale	Full-Scale
1	+20°C	4cm×12cm×2	6 m^2	2cm×3cm×8×2	6 m^2
2		4cm×24cm×2	12 m^2	2cm×3cm×8×2	6 m^2
3		4cm×36cm×2	18 m^2	2cm×3cm×8×2	6 m^2

Table 4-3 Conditions for series cnv3

Temperature rise of Wall 4	Area ratio (Outlet/Inlet)	Outlets		Inlets (1F)	
		Reduced Scale	Full-Scale	Reduced Scale	Full-Scale
+15 °C	1	4cm×12cm×2	6 m^2	6cm×8cm×2	6 m^2
+20 °C					
+25 °C					

4.2.2.3 Comparison of the results of experiments and CFD

Just as mentioned above, transient calculations are carried out in the simulation. Fig. 4-2 shows the temperature variation of two points on the centerline at the height of 1.4 m (about half height of the chimney) and 1.6 m (near the top of the chimney) respectively. It can be seen that about 600 s later the calculation reaches steady state. The results after reaching steady state are used to conduct discussions.

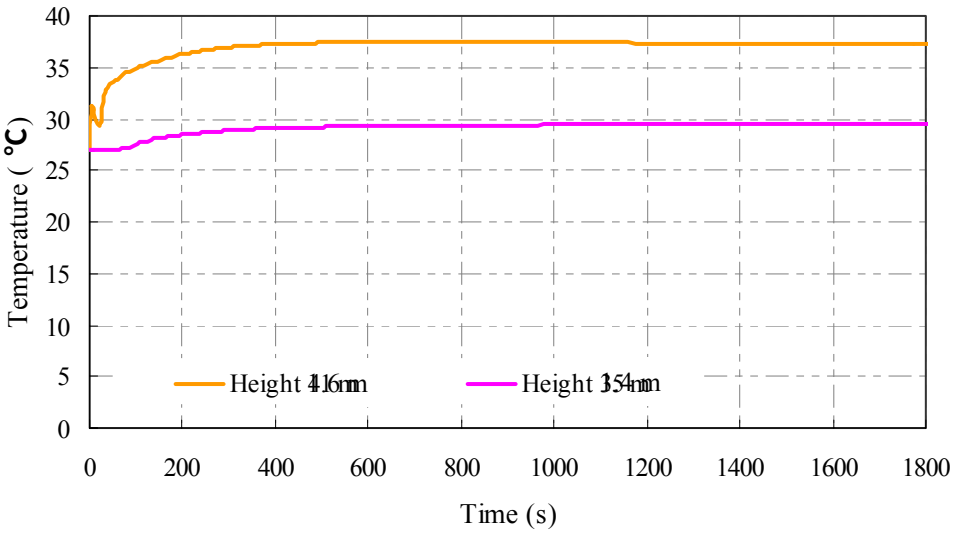

Fig. 4-2 Temperature variation with time during the calculation

The results of model experiments and CFD calculation of each series are shown in following pages.

■ Results of series cnv1

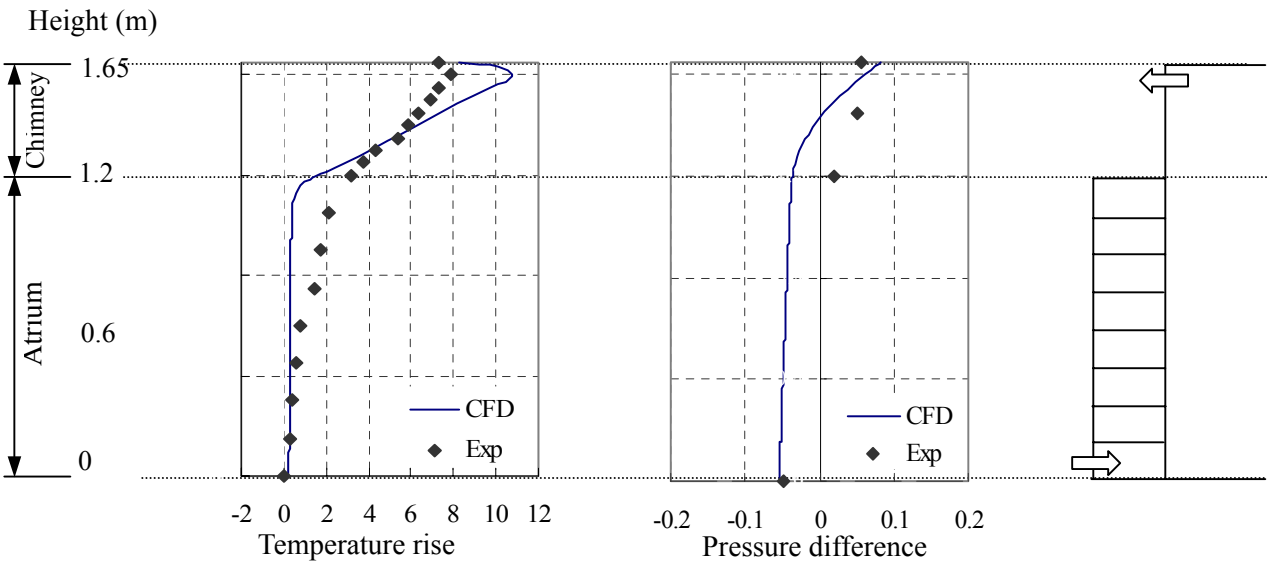

Fig. 4-3a Temperature rise and pressure difference distributions of series cnv1-1

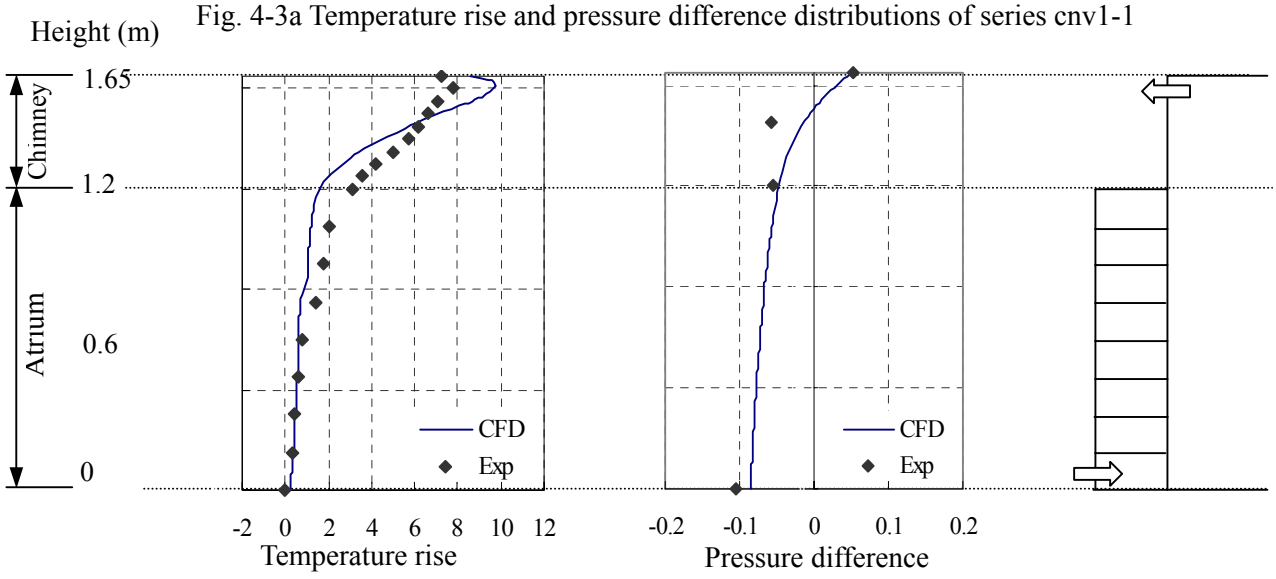

Fig. 4-3b Temperature rise and pressure difference distributions of series cnv1-2

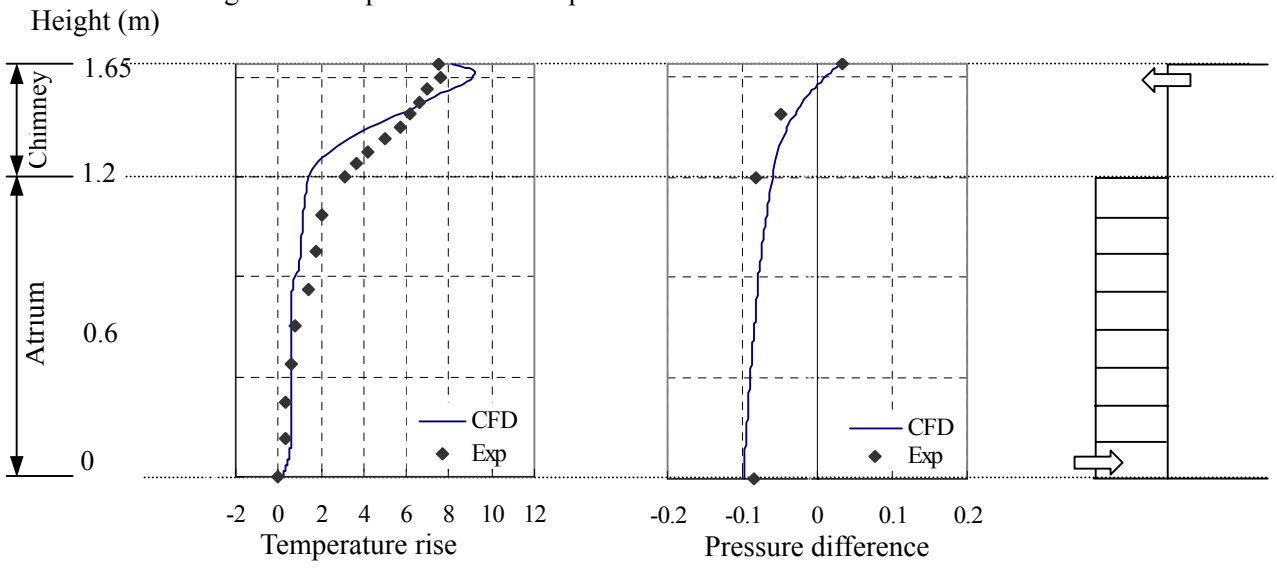

Fig. 4-3c Temperature rise and pressure difference distributions of series cnv1-3

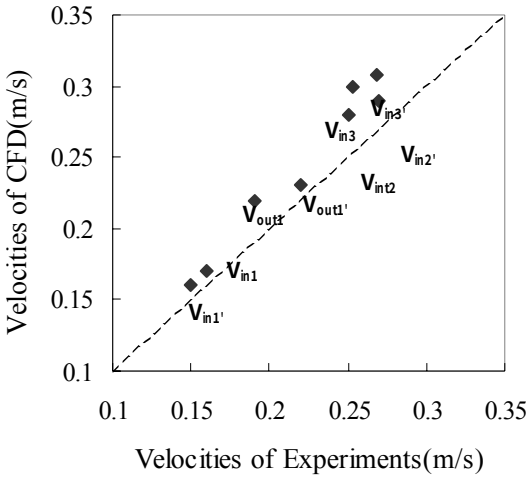

Fig. 4-3d Velocities of series cnv1

■ Results of series cnv2

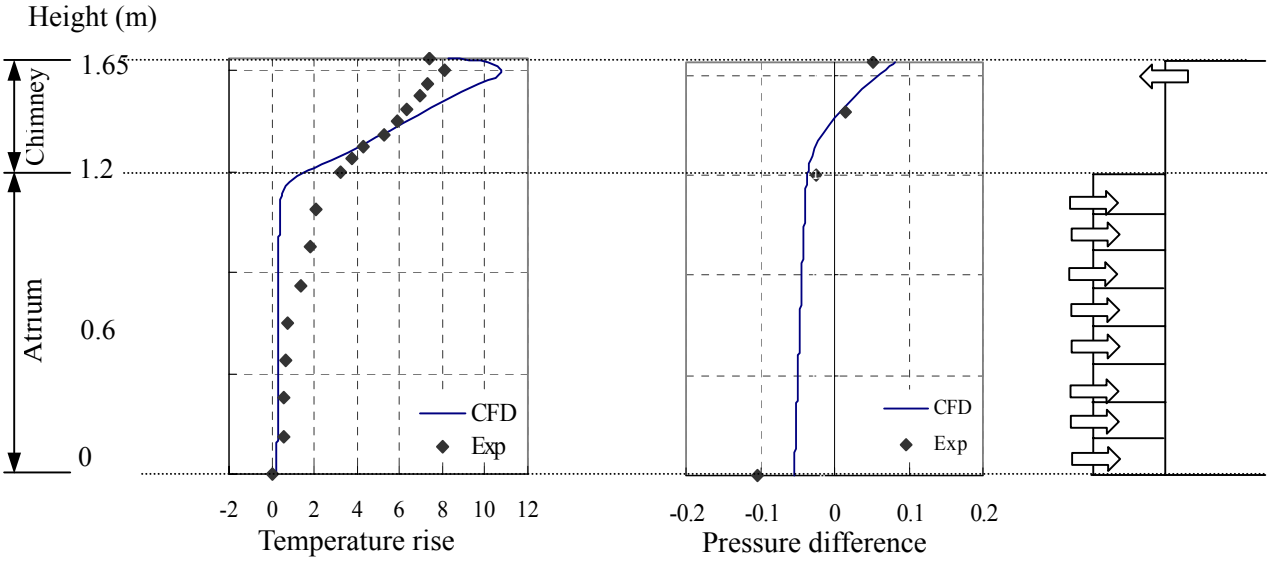

Fig. 4-4a Temperature rise and pressure difference distributions of series cnv2-1

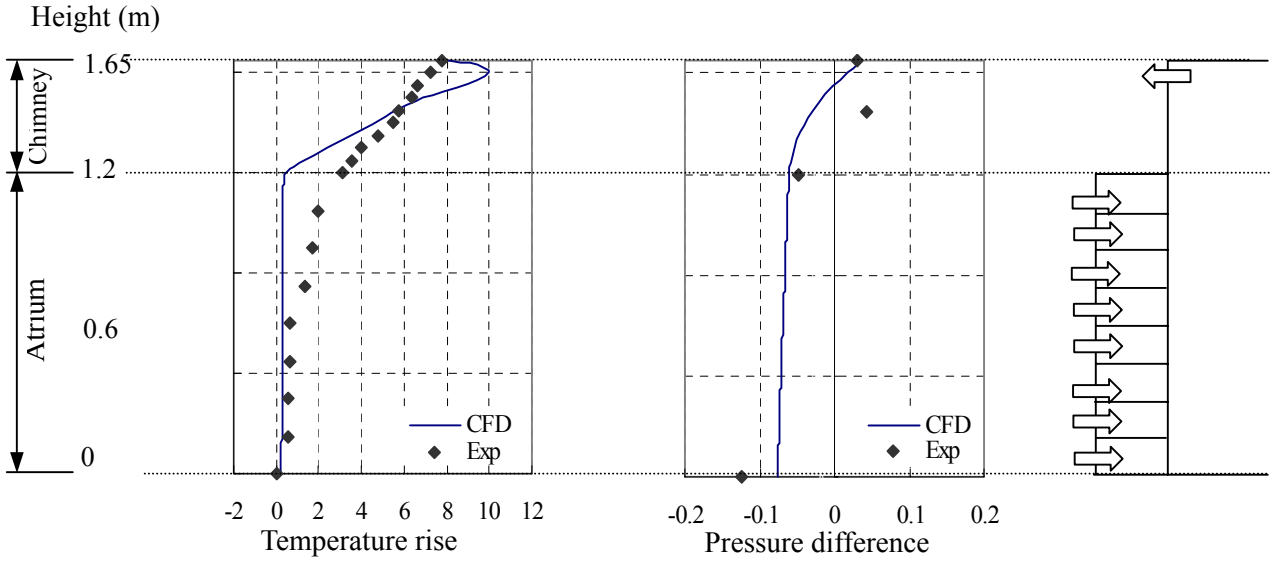

Fig. 4-4b Temperature rise and pressure difference distributions of series cnv2-2

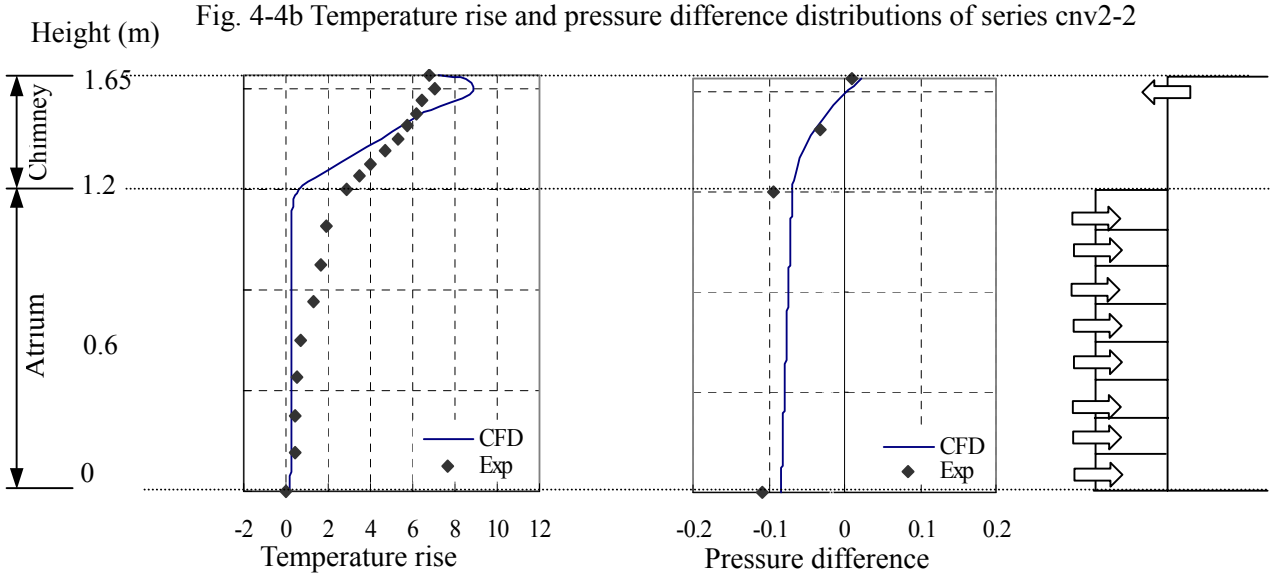

Fig. 4-4c Temperature rise and pressure difference distributions of series cnv2-3

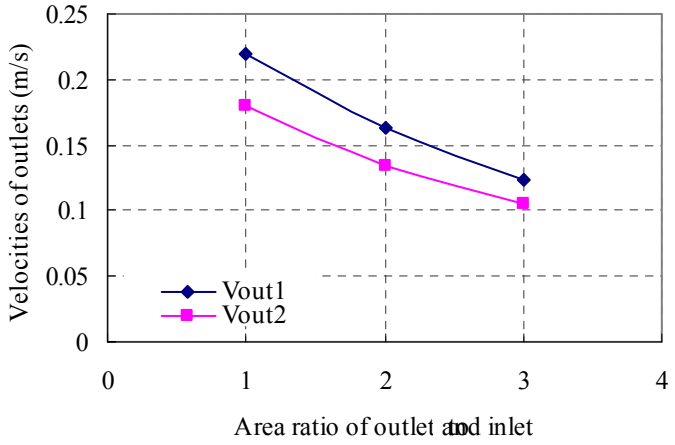

Fig. 4-4d Outlet velocities of cnv2 (CFD)

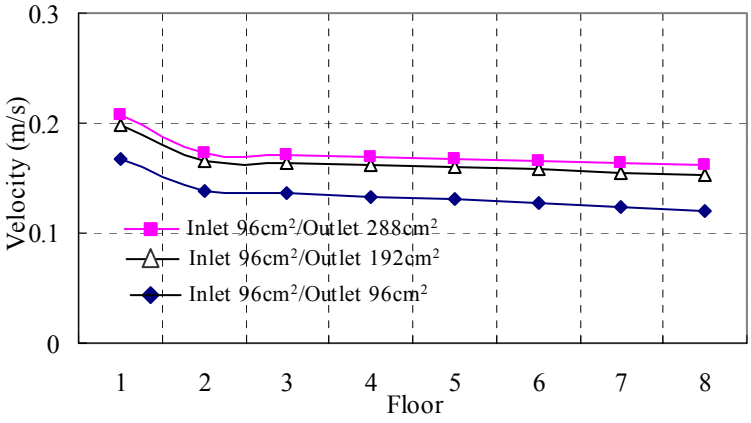

Fig. 4-4e Inlet velocities of cnv2 (CFD)

■ Results of series cnv3

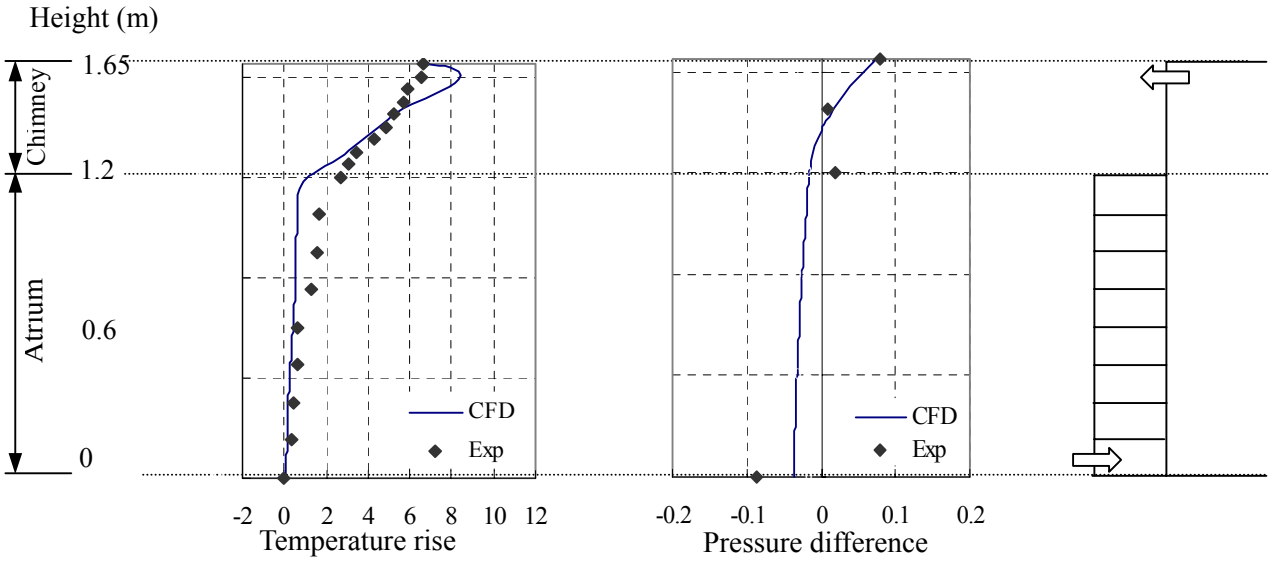

Fig. 4-5a Temperature rise and pressure difference distributions of series cnv3-15

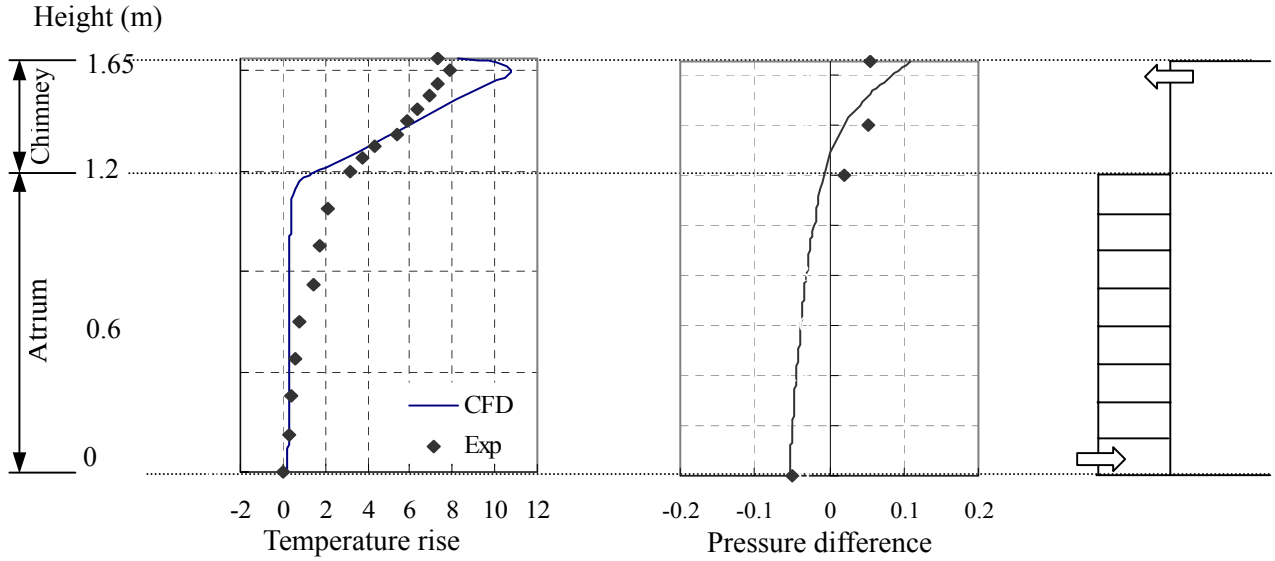

Fig. 4-5b Temperature rise and pressure difference distributions of series cnv3-20

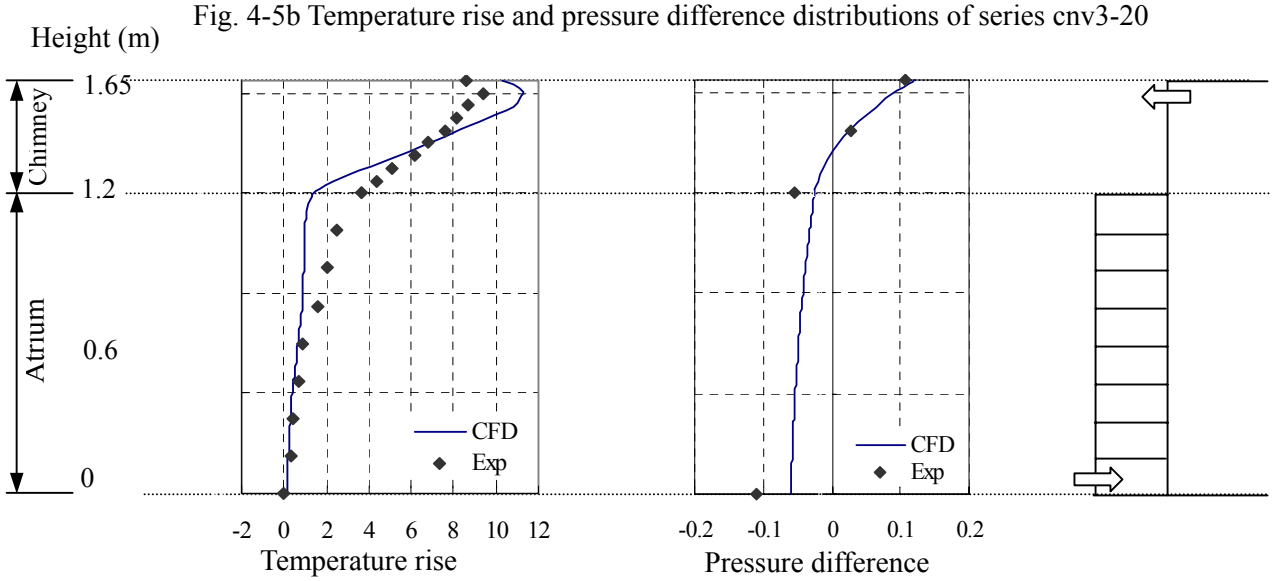

Fig. 4-5c Temperature rise and pressure difference distributions of series cnv3-25

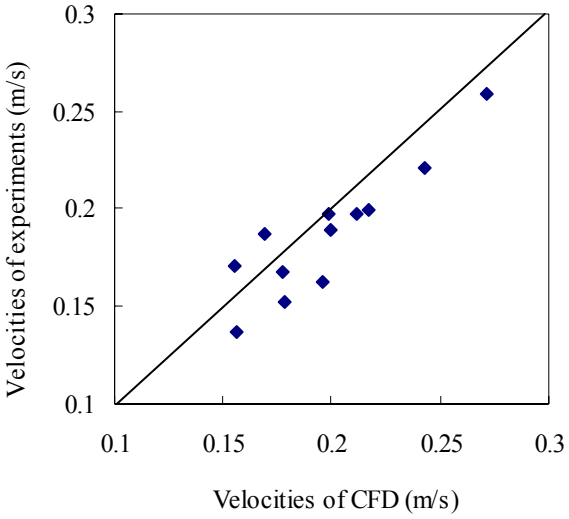

Fig. 4-5d Velocities of outlets and inlets

◆Analysis of the results of series cnv1

(1) Temperature rise and pressure difference

The total temperature rise from the base of the atrium to the top of the chimney resulted from the numerical predictions is a little greater than that of the experiments. The reason is considered to be that heat loss from the experimental model is greater than that of the calculations, in which the walls are set to be as adiabatic. Near the top of the chimney, the air temperature tends to descend a little. This occurs both in the experiments and numerical calculations. Because the 4 cm wide outlets are set on both sides of the chimney, the temperature near the top of the chimney is thought of as affected by the openings.

The pressure differences of the four points measured in the experiments distributes around the pressure difference distribution line calculated by CFD. Although there are some differences between the results of the experiments and CFD, they are thought to be in the tolerance range due to the accuracy problem of the pressure testing instruments.

(2) Velocities of outlets and inlets

Fig. 4-3d shows the velocities of CFD and experiments. The velocities of the outlets are not recorded when the area ratio of the outlet to inlet is greater than 2. The results obtained from the experiments are a little smaller than those of the CFD. The reason is considered as the existing of leakage. For the experimental model, leakage exists in some degree due to the

manual operation; while for the CFD model, leakage is not considered.

◆Analysis of the results of series cnv2

(1) Temperature rise and pressure difference

The total characteristic of the temperature rise and pressure difference distribution is just as that of the results of series cnv1. The results of the CFD match with the experimental results in some degree. Comparing with series cnv1, temperature rise around the border of the atrium and the chimney is almost near zero. In the results of experiments, there is no significant difference between series cnv1 and cnv2, while the results of CFD reveal some difference. Since in the experiments of series cnv2 the inlets are distributed uniformly at each floor, temperature of all the atrium should be near the ambient air due to the airflow from the inlets at each floor. The results of the CFD reflect the influence of the inlets faithfully.

The pressure difference distribution of series cnv2 is also a little different with that of series cnv1. The pressure difference gradient (in the atrium) of series cnv1 is a little greater than that of series cnv2. This is in accordance with the different distribution of inlets. The pressure difference at the top of the chimney is almost the same.

(2) Velocities of outlets and inlets

Fig. 4-4d and Fig. 4-4e show the velocities of the CFD results. The velocities of the outlets decrease with the increasing of the outlet area, while the velocities of the inlets increase correspondingly. The velocity of the first floor is the greatest and the higher the inlet is located, the smaller the velocity is. Therefore when people design such a ventilation system, the ventilation balance of each floor should be considered.

◆Analysis of the results of series cnv3

(1) Temperature rise and pressure difference

The same characteristic is shown as those of series cnv1 and cnv2. With the increasing of the wall temperature, temperature rise and pressure difference from the base of the atrium to the top of the chimney increase correspondingly.

(2) Velocities of outlets and inlets

Fig. 4-5d shows the velocities of CFD and experiments. The results of CFD are slightly greater than those of the experiments.

4.2.3 Natural ventilation performance of the full-scale model

From the comparison of model experiments and CFD predictions, it can be inferred that the CFD results of the reduced scale model match in some degree with the experimental results, which means the CFD technique used in the simulation is valid to reproduce the air flow phenomena occurring with natural ventilation. Therefore the same CFD technique is used to discuss the ventilation effectiveness of the prototype building in a full-scale model.

4.2.3.1 Conditions for the full-scale model

The indoor zero-equation model is used. The computational domain is basically divided into a grid of 0.75m×0.75m×0.75m control volumes. Additional grid points are embedded near the walls and around the inlets and outlets to enable better resolution in these areas. Three different opening conditions (Table 4-4) are discussed and boundary conditions are set as expressed in Table 4-5.

Table 4-4 Conditions for the full-scale model (Natural ventilation)

Area ratio (Outlet/Inlet)	Temperature of Wall 4	Outlets	Inlets
1	+20℃	6 m^2	6 m^2
2		12 m^2	6 m^2
3		18 m^2	6 m^2

Table 4-5 Boundary conditions for the full-scale model (Natural ventilation)

Wall 4 of the chimney	All the other walls	Openings
320 K*	Adiabatic	Pressure

*: The ambient temperature is set as 300 K and the temperature of wall 4 is considered as 20 K higher than the ambient temperature.

4.2.3.2 Results

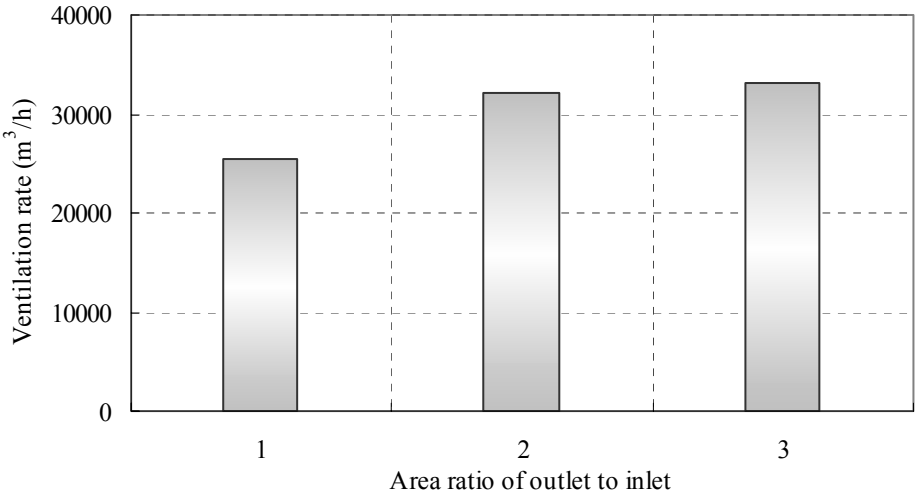

Fig. 4-6 Ventilation rate with area ratio of outlet to inlet

Fig. 4-6 shows the ventilation rate of the full-scale model with different area ratio of outlet to inlet. When the outlet area becomes more than 2 times of the inlet area, the ventilation rate varies hardly. In above cases, the inlet area is set as 1/45 of the floor area of the atrium. Of course, increasing the inlet area may lead to more ventilation rate.

Considering the air change rate of the utility space, when the outlet area is 2 times of the inlet area, the air change rate of the utility space reaches around 2 times per hour. Good indoor environment can be expected in the utility space. At the same time, the position of the neutral pressure plane is shown in Fig. 4-7. Just as the results of the model experiments, for all cases the neutral pressure plane stays inside the chimney. Effective ventilation can be obtained.

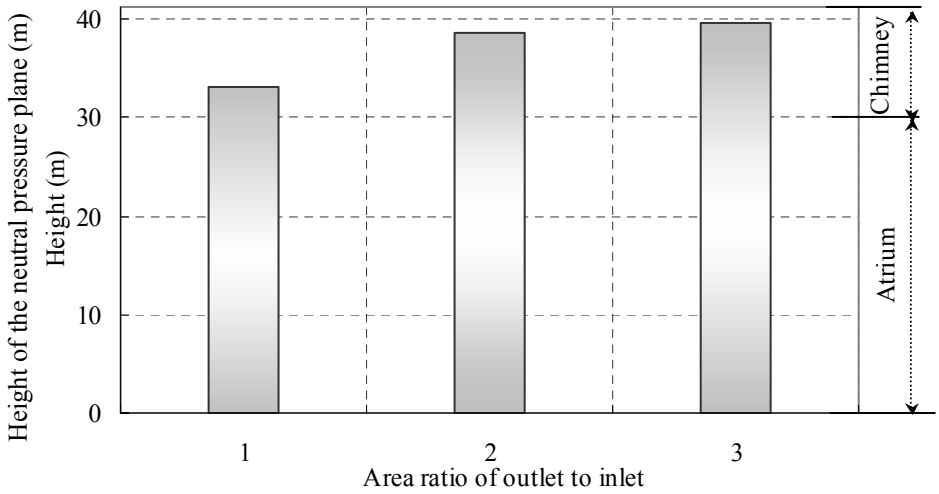

Fig. 4-7 Variation of the neutral pressure plane

4.3 SIMULATION FOR SMOKE CONTROL

4.3.1 Numerical modeling

In the simulation for smoke control, the standard κ-ε model is used which is based on both a transport equation for turbulent kinetic energy κ and a transport equation for the dissipation of turbulent kinetic energy ε. In the simulation of natural ventilation, since the total temperature rise of the air is not so great, density variation caused by temperature rise is expressed using Buossinesq approximation. While in the simulation of smoke control, since there is a fire source existing and temperature rise in the space is thought to be great, density is considered with the assumption of being governed by temperature (pressure is set as ambient pressure).

4.3.1.1 Governing equations

◆The mass conservation equation

$$\frac{\partial \rho}{\partial t} + \frac{\partial}{\partial x_i}(\rho u_i) = 0 \tag{4-8}$$

◆The momentum conservation equation

$$\frac{\partial(\rho u_i)}{\partial t}+\frac{\partial(\rho u_i u_j)}{\partial x_j}=-\frac{\partial P}{\partial x_i}+\frac{\partial}{\partial x_j}\left[\mu_{eff}\left(\frac{\partial u_i}{\partial x_j}+\frac{\partial u_j}{\partial x_i}\right)\right]+(\rho-\rho_0)g_i \tag{4-9}$$

$$\mu_{eff}=\mu+\mu_t \tag{4-10}$$

$$\mu_t=\rho C_\mu\frac{\kappa^2}{\varepsilon} \tag{4-11}$$

where C_μ is a constant; κ and ε are given in Eq. (4-13) and (4-14).

◆The energy conservation equation

$$\frac{\partial}{\partial t}(\rho T)+\frac{\partial}{\partial x_i}(\rho u_i T)=\frac{\partial}{\partial x_i}(k+k_t)\frac{\partial T}{\partial x_i}+\frac{q}{c_P} \tag{4-12}$$

where

k is the molecular conductivity;

k_t is the conductivity due to turbulent transport ($k_t = c_P\mu_t/Pr_t$);

q is the heat source.

$$\rho\frac{D\kappa}{Dt}=\frac{\partial}{\partial x_i}\left[\left(\mu+\frac{\mu_t}{\sigma_k}\right)\frac{\partial\kappa}{\partial x_i}\right]+G_\kappa+G_b-\rho\varepsilon \tag{4-13}$$

$$\rho\frac{D\varepsilon}{Dt}=\frac{\partial}{\partial x_i}\left[\left(\mu+\frac{\mu_t}{\sigma_\varepsilon}\right)\frac{\partial\varepsilon}{\partial x_i}\right]+C_{1\varepsilon}\frac{\varepsilon}{\kappa}\left(G_\kappa+C_{3\varepsilon}G_b\right)-C_{2\varepsilon}\rho\frac{\varepsilon^2}{\kappa} \tag{4-14}$$

where $C_{1\varepsilon} = 1.44$; $C_{2\varepsilon} = 1.92$; $C_{3\varepsilon} = 1$; $C_\mu = 0.09$; $\sigma_k = 1.0$; and $\sigma_\varepsilon = 1.3$.

In case of a fire, the density variation of air is quite great and should be considered. In this research the density is computed as:

$$\rho=\frac{P_{OP}}{\frac{R}{M}T} \tag{4-15}$$

where

R is the universal gas constant;

M is the molecular weight of air;

P_{OP} is defined as ambient pressure.

In the simulation, the turbulent quantities are specified in terms of turbulence intensity I and turbulence length scale l. The turbulent kinetic energy κ is obtained by:

$$\kappa = \frac{3}{2}(u_{avg} I)^2 \qquad (4\text{-}16)$$

where u_{avg} is the mean flow velocity.

And the turbulent dissipation rate ε can be estimated as:

$$\varepsilon = C_{\mu}^{3/4} \frac{\kappa^{3/2}}{l} \qquad (4\text{-}17)$$

where C_{μ} is an empirical constant specified in the turbulence model (approximately 0.09).

4.3.1.2 Calculating process

In the simulation of smoke control, although the fire source is set as a steady fire, accompanying the heat released from the fire source, smoke temperature, fresh air supply velocity and smoke extract velocity vary with time. Therefore transient calculation is used in the simulation. The equations for conservation of mass, momentum, and energy are solved in time-dependent form.

The calculating time is set as 1800 seconds and the time step increment is set as 1 Second. The number of iterations to be performed per time step is set as 30 times.

4.3.2. Simulation of the reduced scale model

4.3.2.1 Computational grid

To compare with the experimental results, the reduced scale model is reproduced. The computational domain is basically divided into a grid of 0.03m×0.03m×0.03m control volumes. Additional grid points are embedded near the walls, around the inlets and outlets, and around the heat source to enable better resolution in these areas. The total number of the meshes is about 85,000 for the model, of which the inlets are concentrated at the first floor, and 110,000 for the model, of which the inlets are uniformly distributed at each floor. The outline of the model is shown in Fig .4-8.

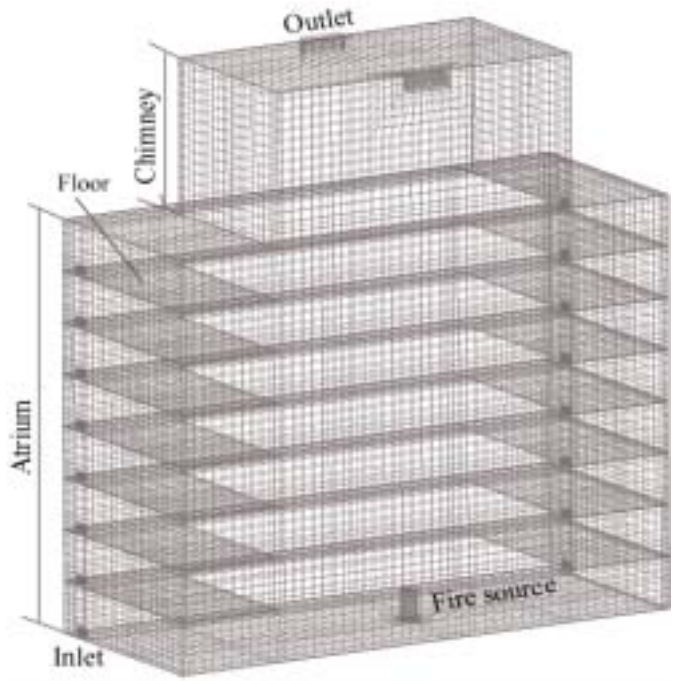

Fig. 4-8 Simulation model for smoke control

4.3.2.2 Boundary conditions

To simulate the experiments, the following boundary conditions are used:

(1) Walls

All the walls are set as adiabatic. Thus heat loss of the experimental model is considered as slightly greater than that of the experimental model.

(2) Openings

Inlets and outlets are set as pressure boundaries that allow flow in and out of the domain. The pressure is set as the same as ambient.

(3) Heat source

Klote and Milke (1992) recommend design fires of approximately 2,000 kW and 5,000 kW for atria with restricted fuel and atria with combustibles, respectively. In this paper we select 2,000 kW to conduct the experiments. Froude number is used to decide the heat release rate of the fire source in model experiments, which is proportional to Q^2/D^5. Because the scaling criterion is 1/25, heat release rate of the fire source in model experiments is expected to be about 640 W. Ethanol put in a dish with 4.5 cm diameter is used as the fire source of the model experiments. According to the results, time-averaged heat release rate of the ethanol is about 700 W. Correspondently heat release rate in the full-scale model is set as 2187.5 kW. A cylinder volumetric heat source is used to simulate the fire source, whose diameter is set to be $0.045 \times 25 = 0.5625$ m; and height is decided by (McCaffrey B.J. 1979):

$$Z_f = 0.08Q^{2/5} \tag{4-18}$$

where Q is heat release rate of the fire source, kW.

(4) Opening conditions

The following opening conditions are carried out for the reduced scale model.

Table 4-6 Conditions for series csf1

Area ratio (Outlet/Inlet)	Outlets		Inlets (1F)	
	Reduced Scale	Full-Scale	Reduced Scale	Full-Scale
1	4cm×12cm×2	6 m^2	6cm×8cm×2	6 m^2
2	4cm×24cm×2	12 m^2	6cm×8cm×2	6 m^2
3	4cm×36cm×2	18 m^2	6cm×8cm×2	6 m^2

Table 4-7 Conditions for series csf2

Area ratio (Outlet/Inlet)	Outlets		Inlets (8Fs)	
	Reduced Scale	Full-Scale	Reduced Scale	Full-Scale
1	4cm×12cm×2	6 m^2	2cm×3cm×8×2	6 m^2
2	4cm×24cm×2	12 m^2	2cm×3cm×8×2	6 m^2
3	4cm×36cm×2	18 m^2	2cm×3cm×8×2	6 m^2

4.3.2.3 Comparison of the results of experiments and CFD

Results of CFD and experiments are shown in following pages.

■ Results of series csf1

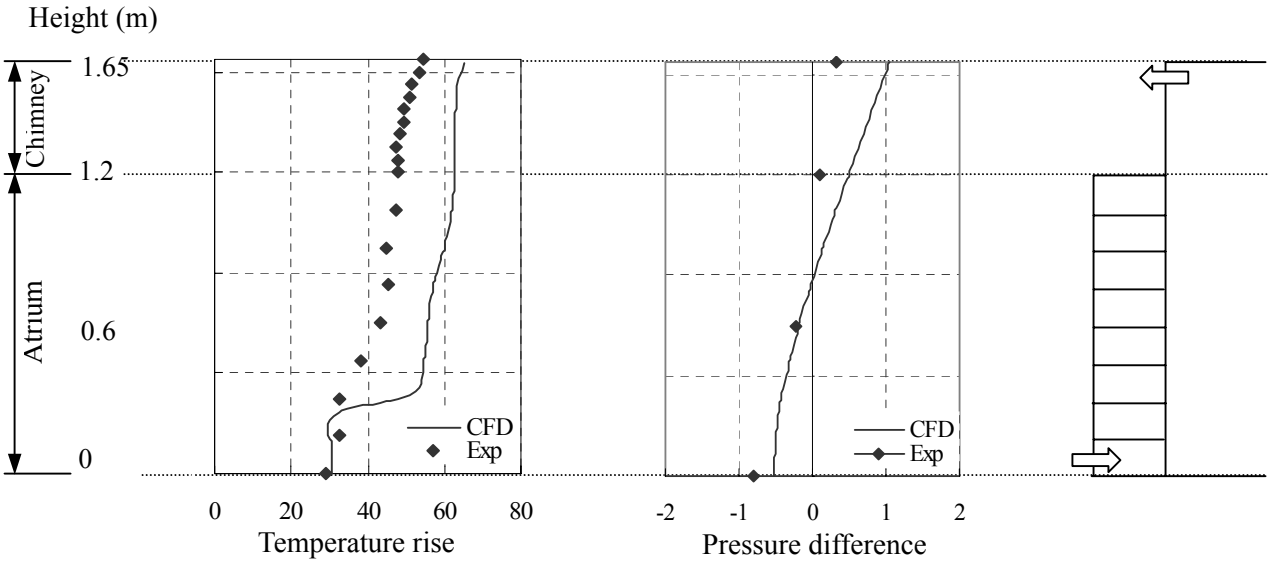

Fig. 4-9b Temperature rise and pressure difference distributions of series csf1-1

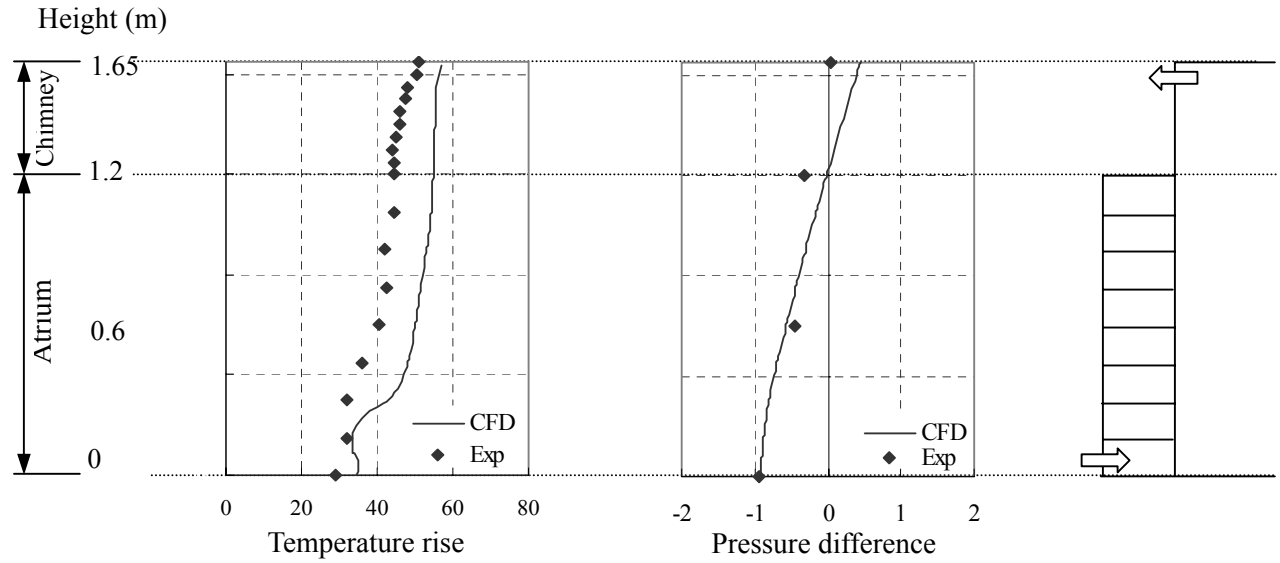

Fig. 4-9b Temperature rise and pressure difference distributions of series csf1-2

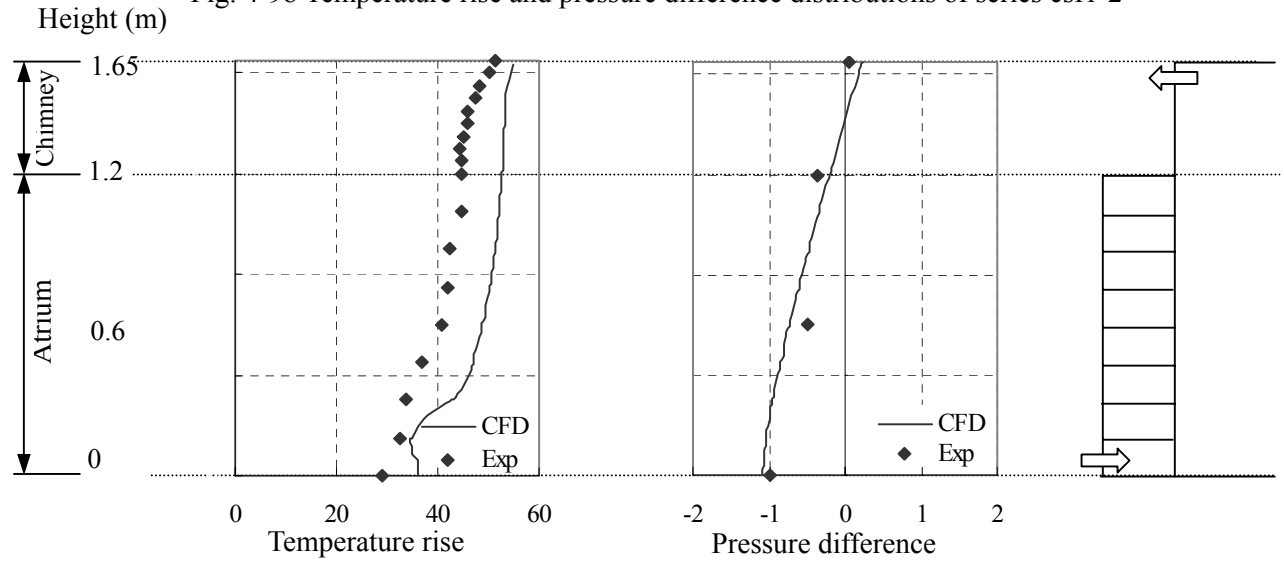

Fig. 4-9c Temperature rise and pressure difference distributions of series csf1-3

■ Results of series csf2

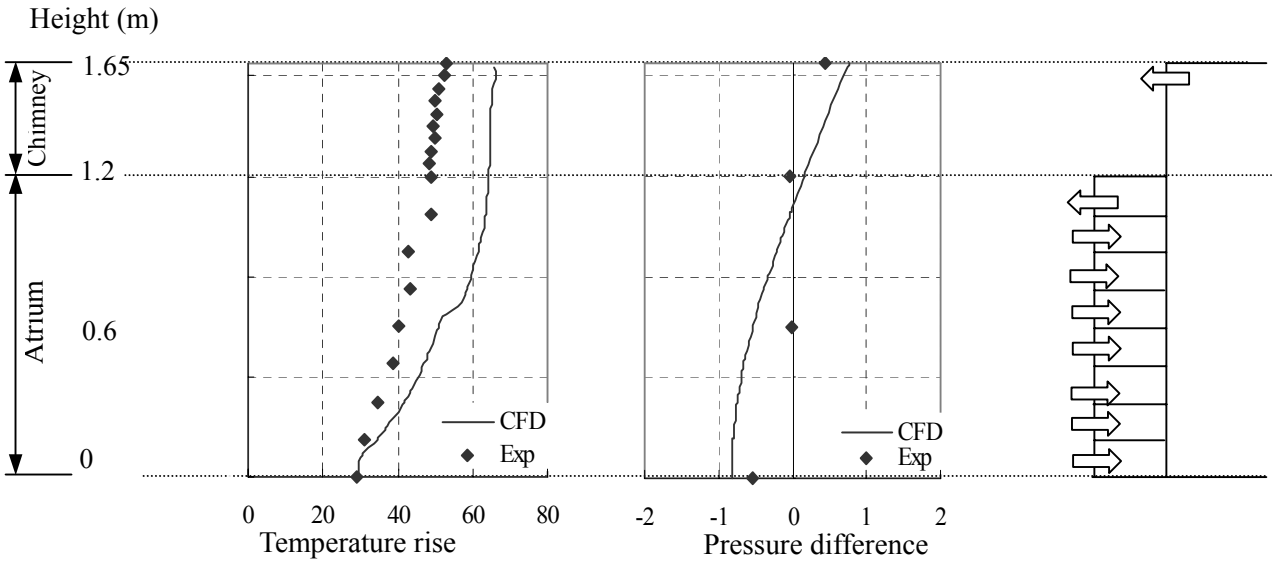

Fig. 4-10a Temperature rise and pressure difference distributions of series csf2-1

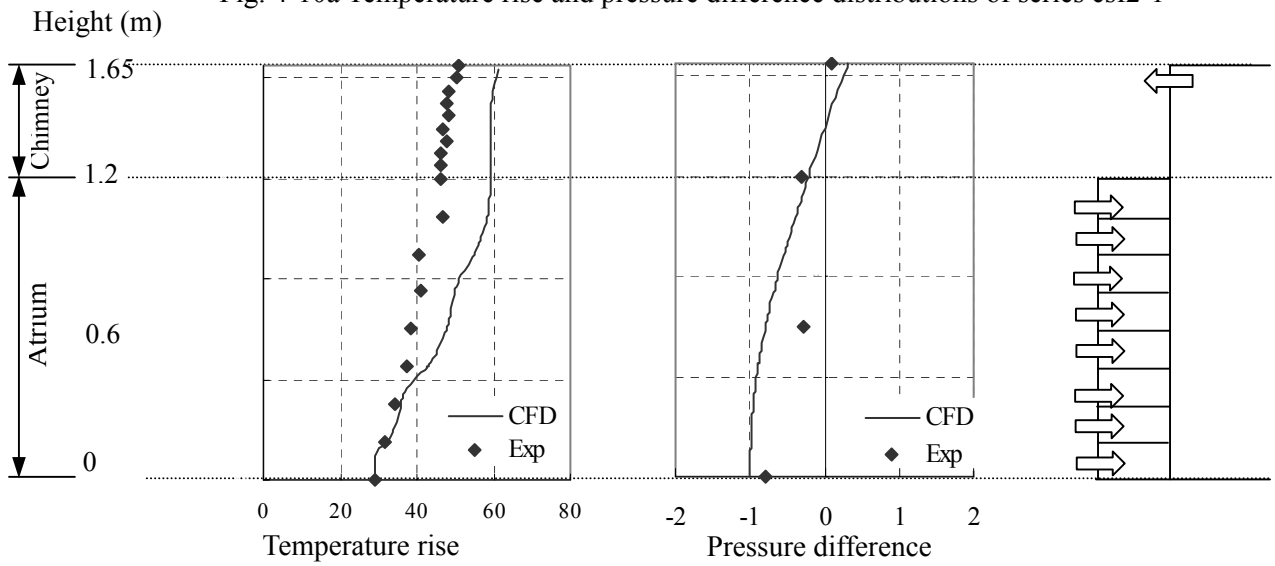

Fig. 4-10b Temperature rise and pressure difference distributions of series csf2-2

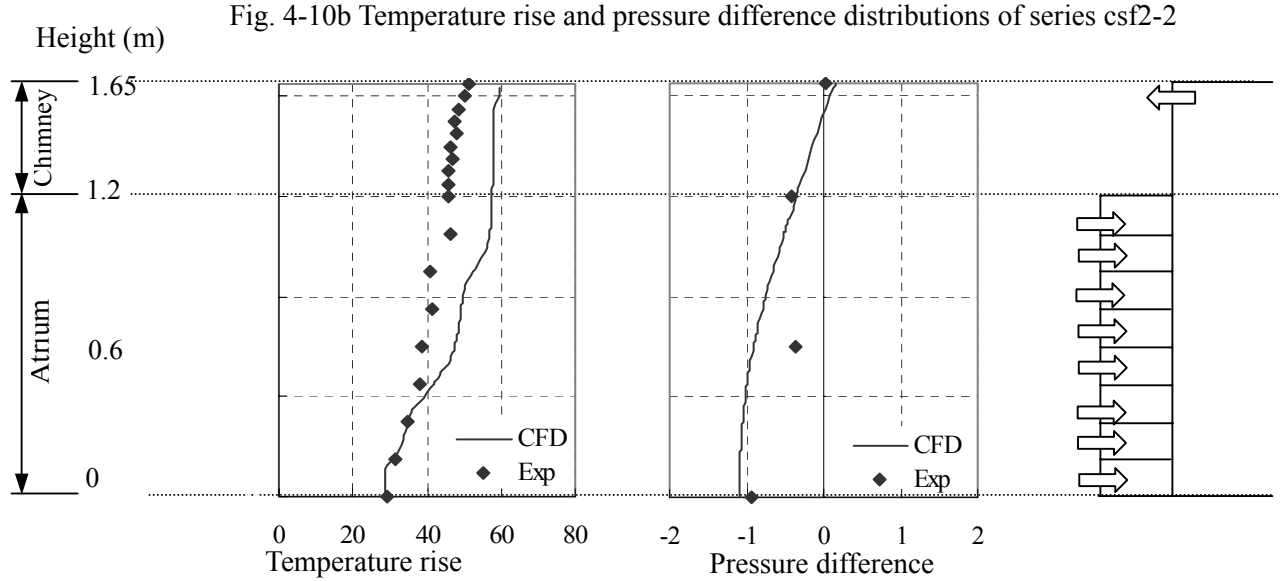

Fig. 4-10c Temperature rise and pressure difference distributions of series csf2-3

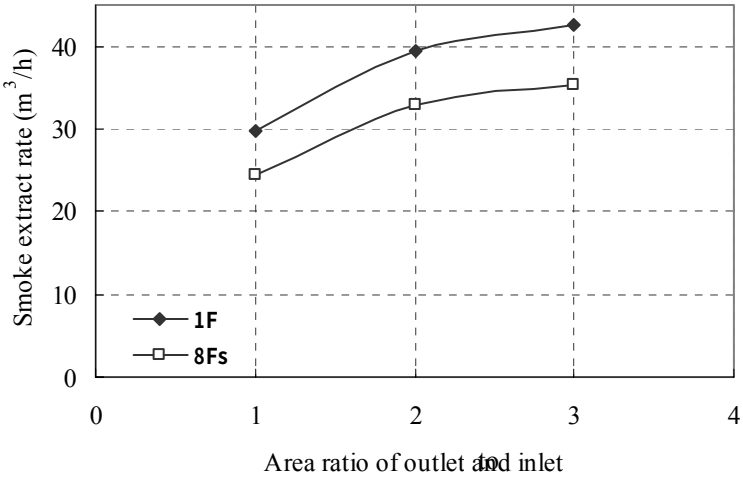

Fig. 4-11 Smoke extract rate of series csf1 and csf2

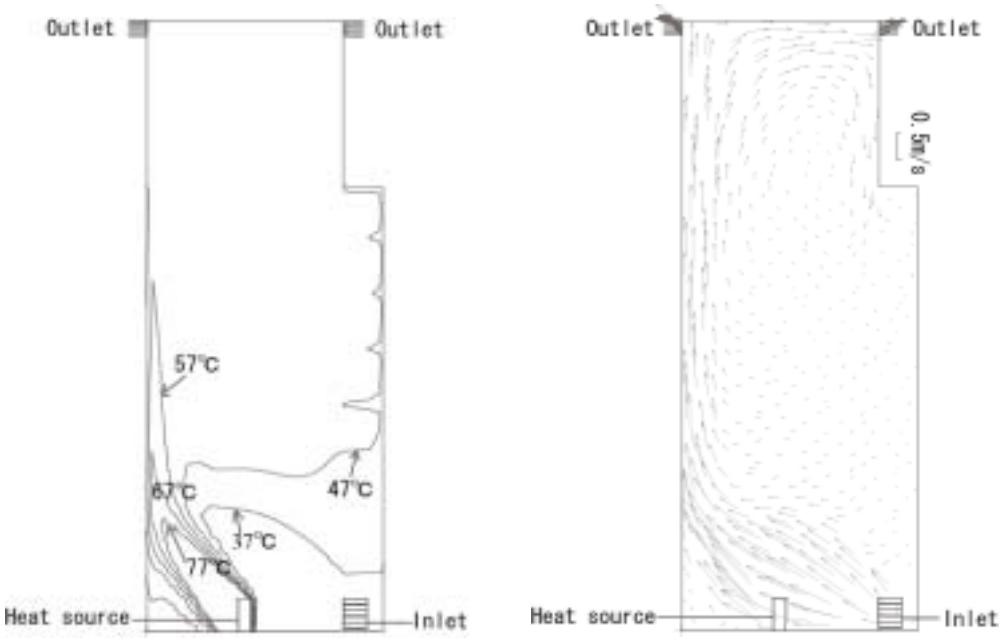

Fig. 4-12 Section of temperature distribution and velocity vector

4.3.2.4 Analysis of the results

(1) Temperature distribution

Although the experimental results of series csf1 and csf2 show almost no difference, the CFD results of series csf1 is a little different with the results of series csf2. For series csf1, the upper layer smoke with almost uniform temperature distribution descends to near the base of the atrium. While for series csf2, since the inlets are distributed at each floor, temperature distribution from 1F to 8F shows a continuous variation. Furthermore, the total temperature rise of series csf2 is a little higher than that of series csf1. For both series csf1 and csf2, the results of CFD predictions are slightly higher than those of the experiments. This can be explained by the heat loss of the experimental model. For the CFD model, all walls are set as adiabatic while for the experimental model, due to the operation and observation of the experiments, heat loss from the experimental model is inevitable.

(2) Pressure difference distribution

The pressure differences of the measured 4 points are dispersed near the pressure difference distribution line calculated by CFD. The CFD results match with the experimental results in some degree. For both series csf1 and csf2, the outlet area is set as the same and from the results, it is clear that pressure difference at the top of the chimney of series csf2 is slightly smaller than that of series csf1, which also means that the outlet velocity of series csf2 is smaller than that of series csf1. The gradient of the pressure difference in the atrium part of series csf1 is greater than that of series csf2, which leads the high position of the neutral pressure plane in series csf2. The results show that although the neutral pressure plane is mainly decided by the total area ratio of the outlet to inlet, the distribution of the openings also slightly influences the neutral pressure plane.

(3) Smoke extract rate

Fig. 4-11 shows the smoke extract rate of series csf1 and csf2. The two series reveals the same inclination. With the increasing of the outlet area, the smoke extract rate increases correspondently. The smoke extract rate of series csf1 is greater than that of series csf2, which leads the higher temperature rise in series csf2.

Fig 4-12 shows the section of temperature distribution and velocity vector crossing the

heat source. It is known from the section of velocity vector that weak airflow circulation occurs in the upper part of the atrium/chimney. For this reason temperature distribution in the upper part of the atrium tends to be distributed uniformly.

4.3.3 Smoke control performance of the full-scale model

4.3.3.1 Conditions for the full-scale model

Considering the operability of the model experiments, the CFD results are thought to match with the experimental results well. It is thought the CFD technique used in the simulation is valid to reproduce the phenomena accompanying a fire occurring at the base of the atrium. Therefore the same CFD technique is used to predict the smoke spread situation in the prototype building in a full-scale model.

The κ-ε turbulence model is adopted in the simulation. The computational domain is basically divided into a grid of 0.75m×0.75m×0.75m control volumes. Additional grid points are embedded near the walls and around the inlets and outlets, and around the heat source to enable better resolution in these areas. All walls are set as adiabatic. Three different opening conditions are discussed.

Table 4-8 Boundary conditions for the full-scale model (Smoke control)

Area ratio (Outlet/Inlet)	Outlets	Inlets
1	6 m^2	6 m^2
2	12 m^2	6 m^2
3	18 m^2	6 m^2

4.3.3.2 Results and analysis

(1) Hot layer interface

It is always difficult to define the hot layer interface. Here the procedure described in Cooper et al.(1982) and Peacock and Baubrauas(1991) is used. It is assumed that the interface is at the height where the temperature, T_n, is given by:

$$T_n=C_n(T_{max}-T_b)+ T_b \tag{4-19}$$

where

T_{max} is the maximum temperature;

T_b is temperature near the bottom of the compartment;

C_n is interpolation constant typically in the range of 0.15 to 0.2. Here we use 0.2 to define the interface height.

Fig. 4-13 shows the height and temperature of the hot layer with different area ratio. From the results we can see with the increasing of the outlet area, the thickness of the hot layer goes down and the temperature also decreases. In designing a smoke management system in an atrium, it is usually required that the smoke management system maintain an interface height of at least 1.8 m above the floor during the time needed for evacuation. The simulation predictions are the results after reaching steady conditions. From the point of the height of the hot layer, all cases meet the requirements. While considering the pressure difference distribution (Fig. 4-14), when the area ratio of the outlet to inlet is 1, the neutral pressure plane of the smoke layer is below the chimney and smoke will evade the evacuation route without extra smoke management. When the area ratio of the outlet to inlet becomes greater than 2, the neutral pressure plane goes up to inside the chimney. Just as mentioned before, it is necessary to keep the neutral pressure plane stay inside the chimney.

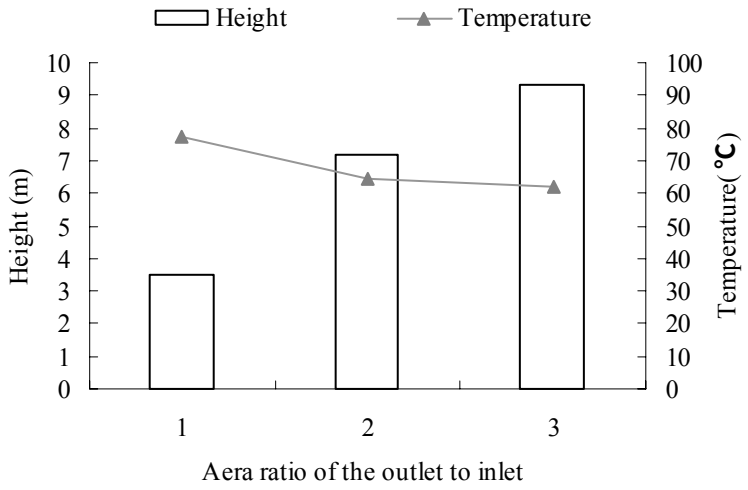

Fig. 4-13 Smoke layer temperature and height with different area ratio

(2) Pressure difference

Fig. 4-14 is the pressure difference distribution with different area ratio of outlet to inlet. It shows the area ratio has great effect on the position of the neutral pressure plane. When the inlet area is 6 m^2 and the outlet area is 12 m^2, the neutral pressure plane is at the border of the atrium and the chimney. When the outlet area extends to 18 m^2, the neutral pressure plane goes up to be inside the chimney. From the point of the requirement of smoke control, the area ratio of the outlet to inlet is expected to be over 2.

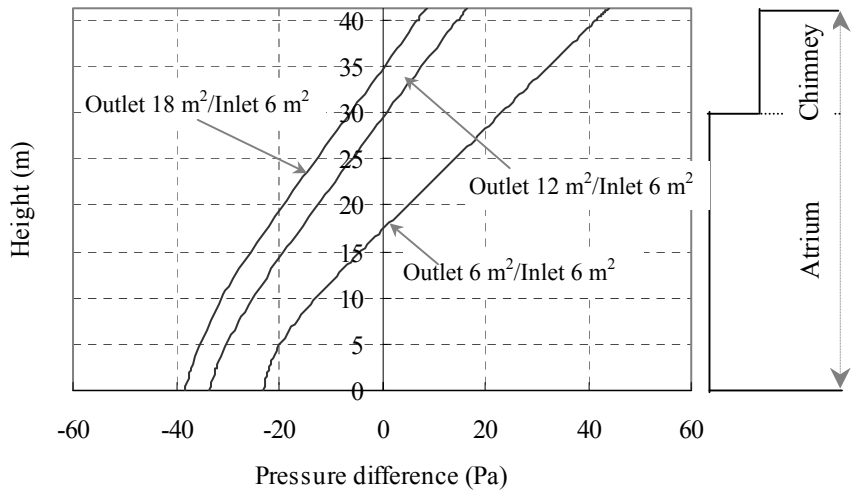

Fig. 4-14 Pressure difference distribution with different area ratio

(3) Smoke extract rate

Fig.4-15 shows the smoke extract rate with different area ratio. Smoke extract rate rises with the increasing of the outlet area. It leads to the reduction of hot layer temperature and thickness, just as shown in Fig.4-13. According to NFPA code, it recommends the ventilation of exhaust times need about 4-6 times per hour. It can be seen that all the three cases meet the requirement, while from the view of pressure difference, only when the area ratio of the outlet to inlet is greater than 2, smoke prevention can be expected.

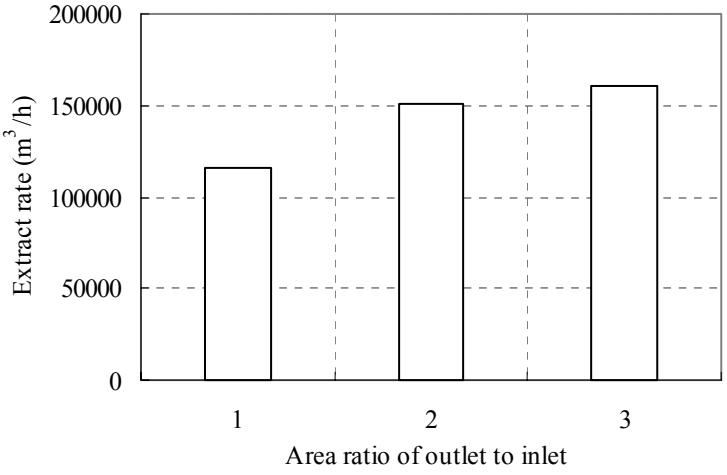

Fig. 4-15 Smoke extract rate with different area ratio

4.4 SUMMARY

According to the results of reduced scale model experiments, the natural ventilation performance of the prototype building is confirmed. At the same time when a fire breaks out at the base of the atrium, the natural ventilation system is verified to be functional as a smoke control system.

The experimental results are used to prove the validity of the CFD method. Through the comparison of the results of CFD and experiments, the CFD method is thought of as effective in reproducing the airflow phenomena of natural ventilation and the phenomena accompanying with a fire.

Then the CFD method is used to predict the natural ventilation and smoke performance of

the full-scale prototype building. As the results, when the area ratio of outlet to inlet is greater than 2, preferable natural ventilation rate for the utility space can be obtained and at the same time, when a fire happens, the neutral pressure plane stays above the occupant space, smoke infiltration into the safety zone/staircase can be prevented.

CHAPTER 5

DETAIL PERFORMANCE OF THE NATURAL VENTILATION SYSTEM

CHAPTER 5
DETAIL PERFORMANCE OF THE NATURAL VENTILATION SYSTEM

As reported in Chapter 4, the compatibility of natural ventilation and smoke control in the prototype building has been verified. And the validity of the CFD technique has also been confirmed. In this paper, the same CFD technique is used to predict the detail performance of the natural ventilation system. Parameters that will affect the natural ventilation performance of the prototype building are considered to include mainly height of the solar chimney, area ratio of the outlet to inlet, and the outside climate conditions.

5.1 NUMERICAL MODELING

Just as described in Chapter 4, the indoor zero-equation model is used to predict the detail performance of the natural ventilation system. The computational domain is basically divided into a grid of 0.75m×0.75m×0.75m control volumes. Additional grid points are embedded near the walls and around the inlets and outlets to enable better resolution in these areas. As to the boundary conditions, the typical meteorological climate data of Tokyo is used. Suppose the absorbability of the glass is 0.1 and the transmissivity of the glass is 0.8, the emissivity of all walls is 0.9, the absorbed solar radiation of each wall of the solar chimney is given as their boundary conditions. All other walls are set as adiabatic. Outlets and inlets are set as pressure boundary conditions

5.2 CLIMATE CONDITIONS OF TOKYO

5.2.1 Outside air temperature and humidity

Fig. 5-1 shows the outside air temperature and humidity of Tokyo according to the typical meteorological year data. Assuming the climate conditions suitable for natural ventilation as 17℃<Temperature<28℃ and 40%<RH<70%, the period during which natural ventilation

can be expectable accounts for about 16% of the whole year.

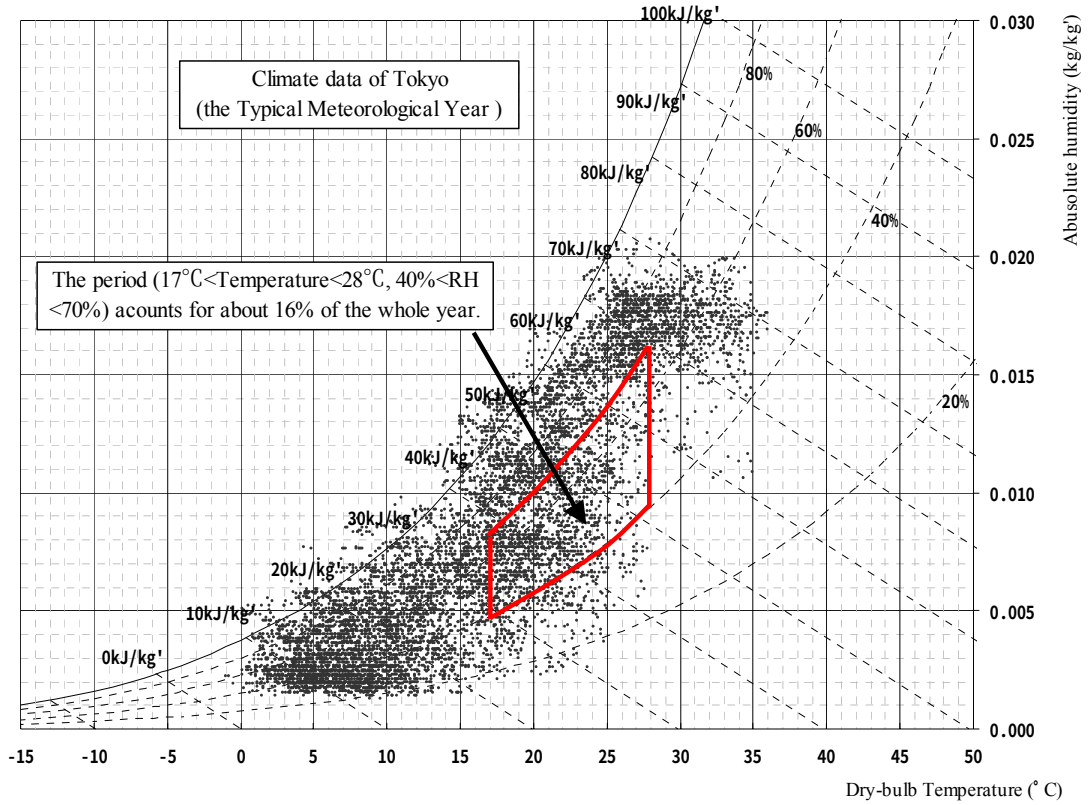

Fig. 5-1 Outside air temperature and humidity of Tokyo

5.2.2 Solar radiation

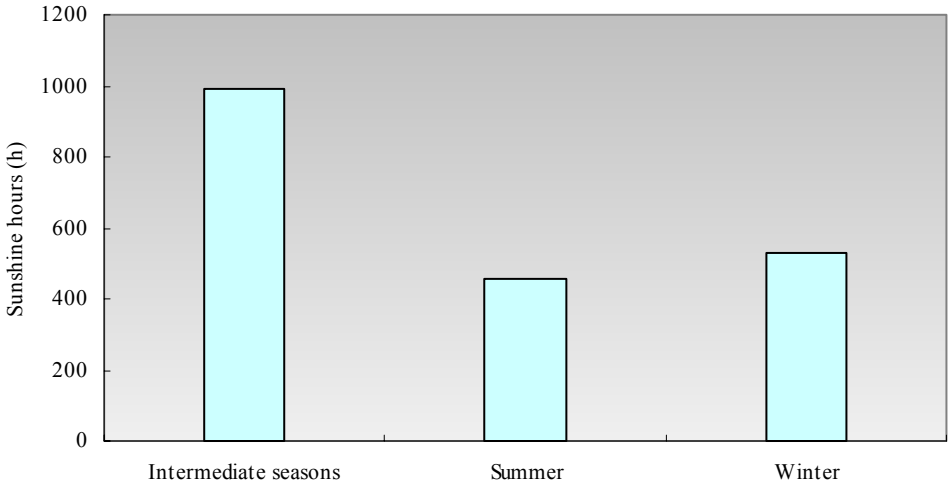

Fig. 5-2 Annual sunshine hours of Tokyo

Fig. 5-2 illustrates the summarized sunshine hours during the whole year. There are about 1000 hours sunshine in the intermediate season and around 500 hours sunshine respectively in summer and winter can be used. Totally there are approximately 2000 sunshine hours can be used, which accounts for nearly 23% of the whole year. The potentiality for the solar energy use is considerable.

5.3 VENTILATION RATE WITH AREA RATIO OF OPENINGS

As it is known, area ratio of openings influences natural ventilation rate greatly. Here to the prototype building, the influence of the area ratio upon natural ventilation rate will be discussed. The inlet area is set as 3 m^2, 6 m^2 and 12 m^2 respectively. Changing the outlet area to adjust the area ratio of outlet to inlet, ventilation rate with different area ratio is examined.

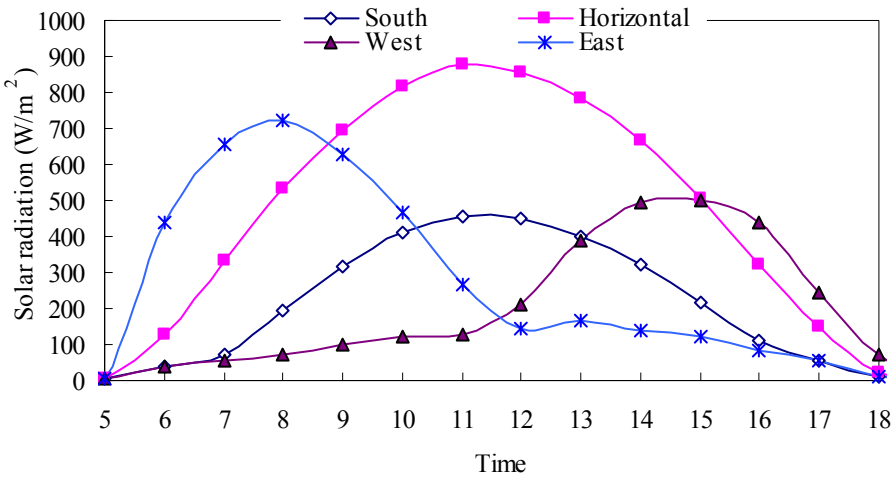

Fig. 5-3 Solar radiation of each direction in some sunny day

Fig. 5-3 shows the solar radiation data of some sunny day in the intermediate season of Tokyo. The data of 12 o'clock is used as the boundary conditions of each wall of the solar chimney. The area settings of outlets and inlets are shown in Table 5-1.

Table 5-1 Area settings of outlet and inlet

Area ratio (Outlet/Inlet)	Inlet	Outlet
0.5	3 m^2	1.5 m^2
	6 m^2	3 m^2
	12 m^2	6 m^2
1	3 m^2	3 m^2
	6 m^2	6 m^2
	12 m^2	12 m^2
1.5	3 m^2	4.5 m^2
	6 m^2	9 m^2
	12 m^2	18 m^2
2	3 m^2	6 m^2
	6 m^2	12 m^2
	12 m^2	24 m^2
2.5	3 m^2	7.5 m^2
	6 m^2	15 m^2
	12 m^2	30 m^2
3	3 m^2	9 m^2
	6 m^2	18 m^2
	12 m^2	36 m^2
3.5	3 m^2	10.5 m^2
	6 m^2	21 m^2
	12 m^2	42 m^2
4	3 m^2	12 m^2
	6 m^2	24 m^2
	12 m^2	48 m^2

Ventilation rate of the prototype building with different area ratio of outlet to inlet is shown in Fig. 5-4. It is obvious that the ventilation rate goes up with the increasing of the area ratio of outlet to inlet. Furthermore, to the same area ratio of outlet to inlet, ventilation rate rises with the increasing of the inlet area. For all the three curves, the variation gradient at first is quite sharp and when the outlet area becomes over 2 times of the inlet area, the increasing of the ventilation rate turns to be very slow. When the outlet area becomes over 3 times of the inlet area, there is almost no change with the ventilation rate. It means the area ratio of 2~3 is reasonable to obtain appropriate ventilation rate.

On the other hand, when the outlet area is set as 3 m^2, 6 m^2 and 12 m^2, and changing the inlet area to adjust the area ratio of inlet to outlet, the same results will be obtained. However the greatest flow per unit area of openings is obtained when the inlet and outlet areas are equal. Increasing the outlet area over inlet area, or vice versa, the ventilation rate is also increased but not in proportion to the added area. This is in accordance with the variation gradient of all these three curves. But considering the position of the neutral pressure plane, it is preferable to make the outlet area not less than the inlet area.

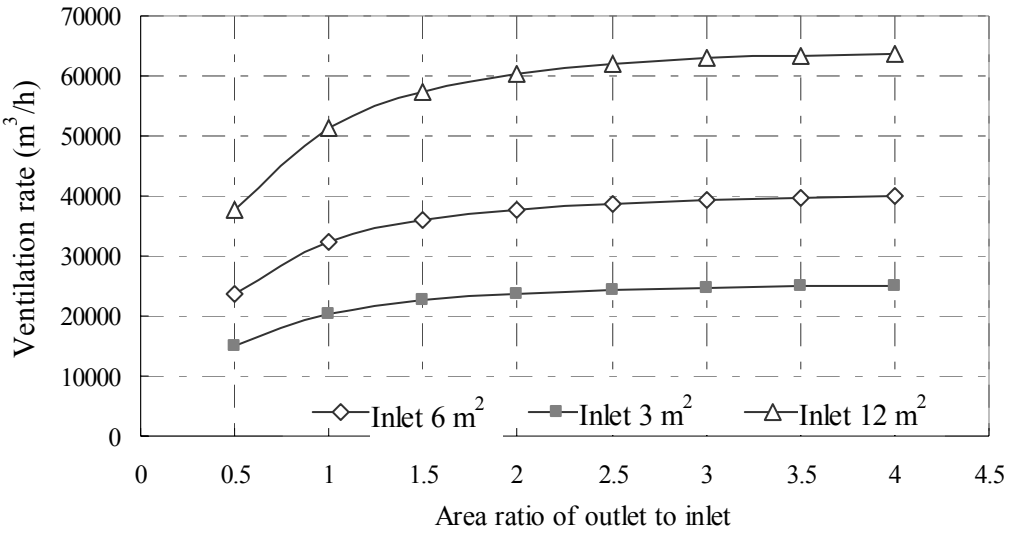

Fig. 5-4 Ventilation rate with area ratio of openings

Of course, the designer can decide the inlet area according to the practical requirements. Here considering only the atrium/utility space as the ventilated space, the inlet area of 6 m^2

(1/45 of the floor area of the atrium) is used to make further discussions. From the discussion in last chapter, to meet the requirements of smoke control, the area ratio of outlet to inlet is expected to be over 2. Here from the safety side, taking the area ratio of outlet to inlet as 3 (Outlet 18 m^2 / Inlet 6 m^2), the following discussion is carried out.

The solar radiation data shown in Fig. 5-3 is used to calculate the ventilation rate of the whole day. Just as shown in Fig. 5-5, the ventilation rate fluctuates with the variation of solar radiation of each direction. Considering the air change rate of the utility space, it is all over 2 times per hour for all hours. Since there is no long term staying occupant in the utility space, and almost no heat release equipment, it is predicted good indoor environment can be obtained only by natural ventilation.

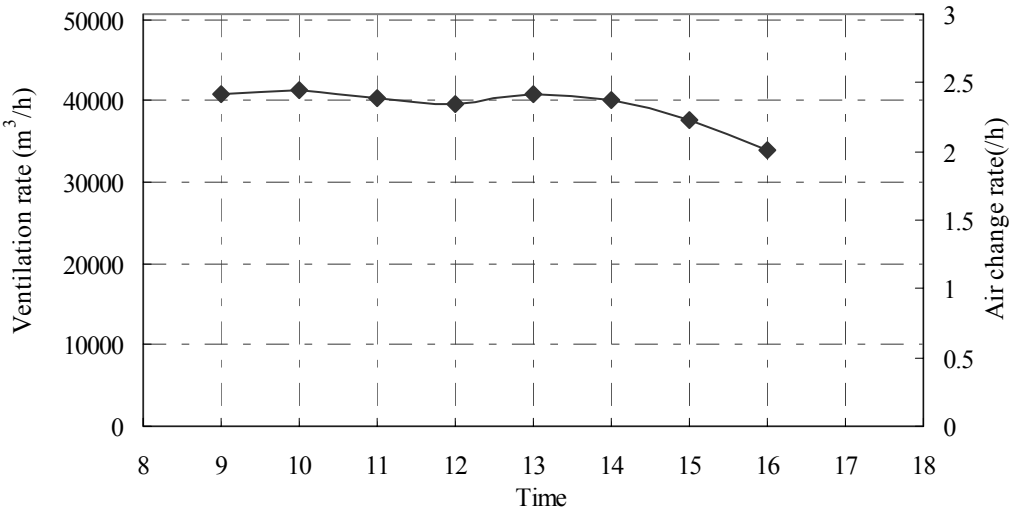

Fig. 5-5 Ventilation rate of some sunny day
(Outlet 18 m^2/Inlet 6 m^2)

5.4 VENTILATION RATE WITH DIMENSION OF THE CHIMNEY

5.4.1 Influence of height of the solar chimney

When considering the ventilation rate of the prototype building, both the area ratio of openings and the height of the solar chimney are important factors. They affect the ventilation rate simultaneously. The influence of the area ratio of openings has been

discussed and the area ratio of 3 (Outlet 18 m^2 / Inlet 6 m^2) is chosen to discuss detail performance of the prototype building. Here with the same area setting, ventilation rate with height of the chimney is examined. Just as shown in Fig. 5-6, with the increasing of the solar chimney height, the ventilation rate almost shows a linear growth. Considering the air change rate of the atrium/utility space, when the solar chimney is higher than 7.5 m, the air change rate becomes over 2 times per hour. At the design phase of such a building, the height of the solar chimney and the area ratio of openings can be decided according to the practical requirements. Of course, the height of the solar chimney should also meet the requirements of keeping the neutral pressure plane of the smoke layer staying inside the solar chimney.

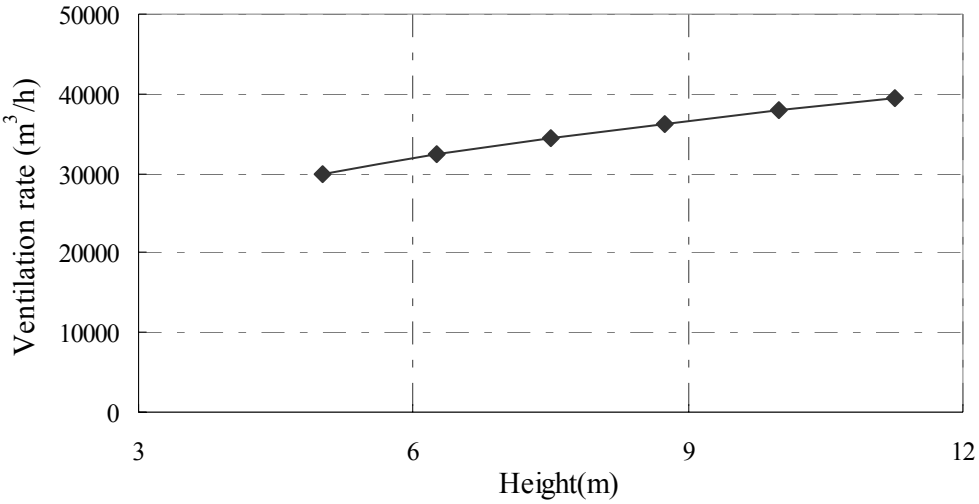

Fig. 5-6 Ventilation rate with the height of the chimney (Outlet 18 m^2/Inlet 6 m^2)

5.4.2 Influence of width of the solar chimney

Although for the prototype building, the width of the solar chimney has been considered as 12.5 m, it also can be adjusted according to practical requirement. Here ventilation rate with width of the solar chimney is also examined. Just as shown in Fig. 5-7, the ventilation rate increases almost linearly with increasing of the width of the chimney. Comparing with Fig. 5-6, they almost show the same variation tendency. However considering the growing ventilation rate per unit height or per unit width, it is found the influence of the height is greater than that of the width. Actually the variation of height or width of the chimney affects

the heat exchange area of the chimney with the airflow passing through the chimney. Of course it is predicted that increase or reduction of the area of the main thermal storage wall (the north-facing wall) will the most greatly influence the ventilation rate from the term of the whole year.

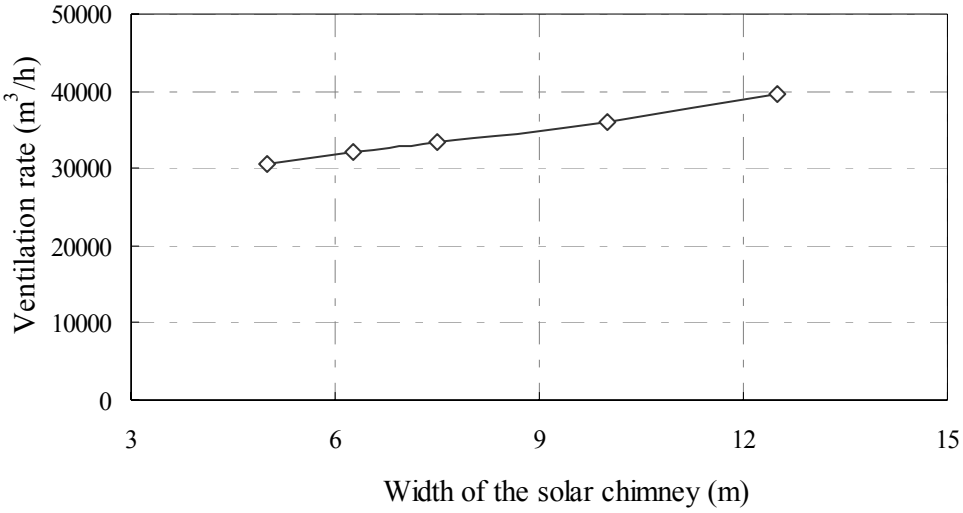

Fig. 5-7 Ventilation rate with the width of the chimney (Outlet 18 m^2/Inlet 6 m^2)

5.5 VENTILATION RATE THROUGHOUT THE YEAR

5.5.1 Defect of the prototype building

Assuming the appropriate climate conditions for natural ventilation as the dry bulb temperature not less than 17℃ and not greater than 28℃, and at the same time the relative humidity is in the range of 40~70%, there are about 1400 hours during which natural ventilation can be expected in Tokyo. Among the 1400 hours, most of them are concentrated in summer and intermediate seasons (Fig. 5-8).

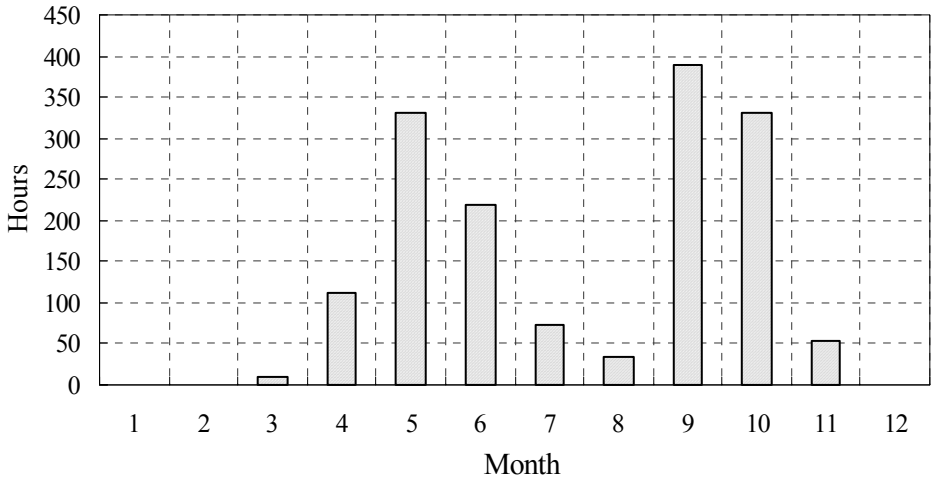

Fig. 5-8 Period appropriate for natural ventilation in Tokyo

However as it is known, the solar altitude angle is varying during the whole year. The quantity of the solar radiation, which can reach the surface of the thermal storage wall, is quite related with the solar altitude angle. In summer the solar altitude becomes low, the thermal storage wall absorbs little solar radiation and natural ventilation rate is low. Natural ventilation rate of the prototype building throughout the whole year changes as shown in Fig. 5-9 (The inlet area is set as 6 m^2 and the outlet area is 18 m^2, the monthly average solar radiation data of the typical meteorological year is used). Ventilation rate of the prototype building is high in winter and low in summer. Comparing with Fig. 5-8, during the period when natural ventilation is the most needed, ventilation rate is low due to the falling of the solar altitude. The ventilation rate in January is highest and in June it is just about 60% of that in January. It is difficult to say that the natural ventilation system is appropriate. Here to improve the performance of the natural ventilation system of the prototype building, the performance improved prototype building is proposed.

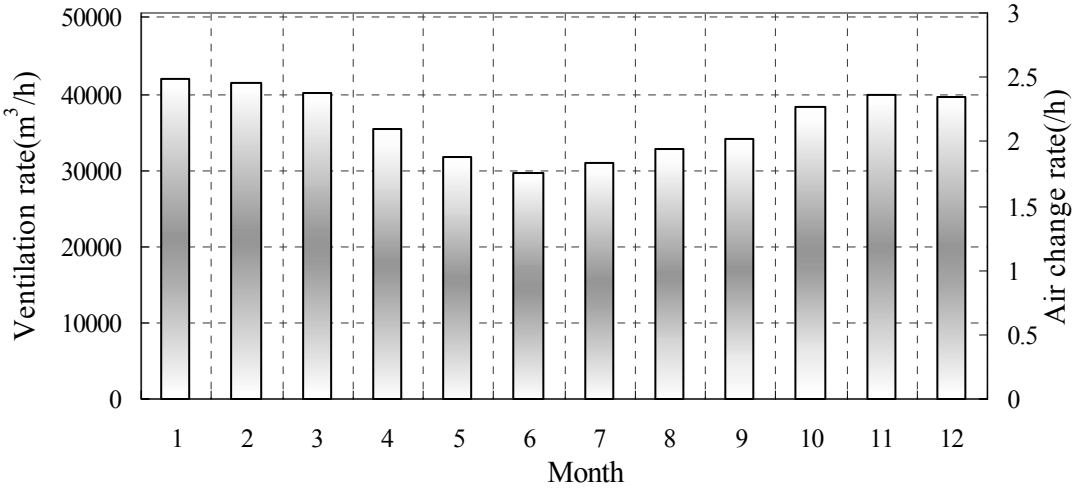

Fig. 5-9 Ventilation rate throughout the year in Tokyo

5.5.2 Proposition of the performance improved prototype building

Just as shown in Fig. 5-10, the height of the solar chimney is kept the same as before. To obtain more solar radiation, the main thermal storage wall is made inclined and its influence to the ventilation rate is examined. The low side of the thermal storage wall is made as axis, and the thermal storage wall is inclined toward the outside. Therefore even when the solar altitude is high, much solar radiation can reach the surface of the thermal storage wall and effective natural ventilation can be expected.

The solar radiation data of June (in which the solar altitude is the highest of the whole year) is used, and the ventilation rate of the performance improved prototype building (θ is set as 90°, 75°, 60° and 45° respectively) is calculated. As shown in Fig. 5-11, ventilation rate increases with the inclining of the thermal storage wall. The smaller the θ is, the more solar radiation will reach the thermal storage wall, and then more ventilation rate is obtained. Furthermore, temperature rise of the air flowing in and out of the building is increasing too with inclining of the thermal storage wall. The range of temperature rise is about 6~14°C.

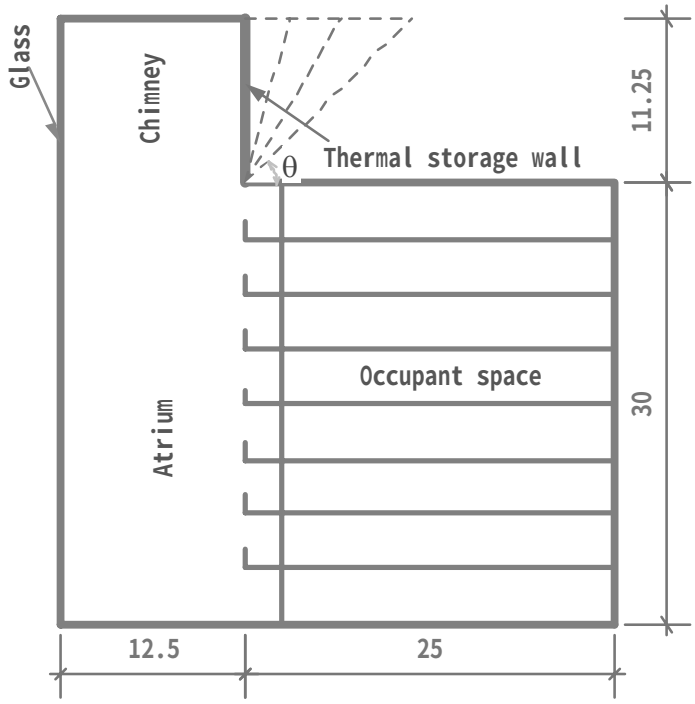

Fig. 5-10 Outline of the performance improved prototype building
(θ: angle between the thermal storage wall and the horizontal plane)

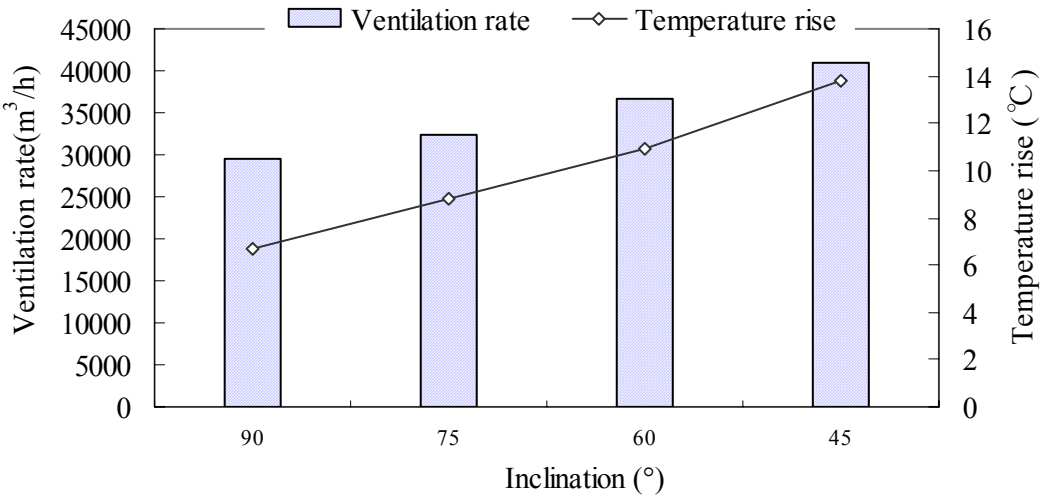

Fig. 5-11 Ventilation rate and temperature rise with different inclination
(Outlet 18 m^2/Inlet 6 m^2)

The inclination of 45° is adopted to calculate the monthly ventilation rate of the performance improved prototype building. Just as mentioned before, the inlet area is set as 6 m^2 and the outlet area is set as 18 m^2. The monthly average solar radiation data of the typical meteorological year is used. The results are shown in Fig. 5-12. As it is shown, comparing with the ventilation rate of January, the ventilation rate in June becomes 88% of that in January. Stable ventilation rate can be expected throughout the whole year.

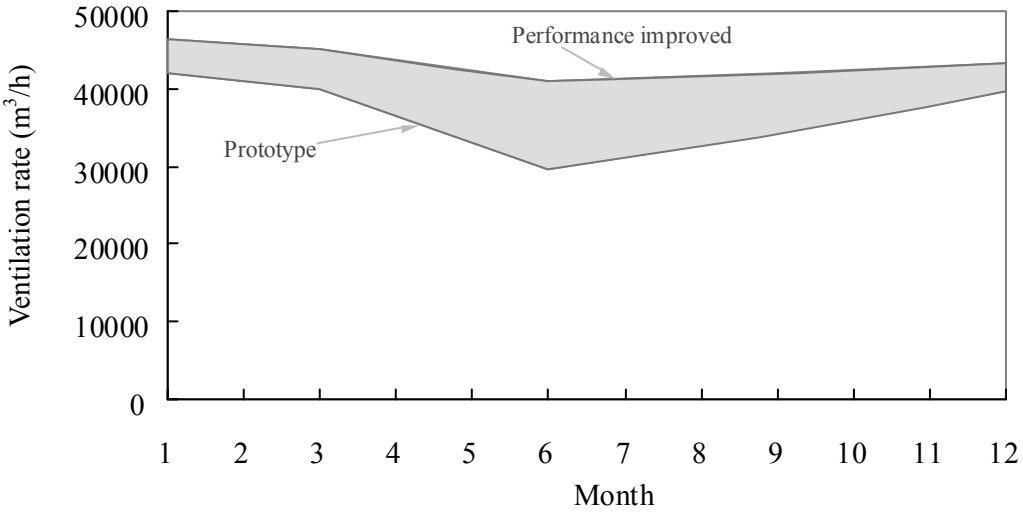

Fig. 5-12 Ventilation rate increase of the performance improved prototype building (θ = 45°) (Outlet 18 m^2/Inlet 6 m^2)

5.5.3 Examination of the smoke control performance of the performance improved prototype building

In above discussion, the inclination of the main thermal storage wall makes the smoke accumulation space larger and it is thought to be advantageous to smoke control. To confirm it, the smoke control performance of the performance improved prototype building, is examined. The setting of the numerical modeling for the smoke control is just as the same as that described in Chapter 4.

Just as shown in Fig. 5-13, the neutral pressure plane forms above the occupant space. The performance improved prototype building meets the requirement of the smoke control.

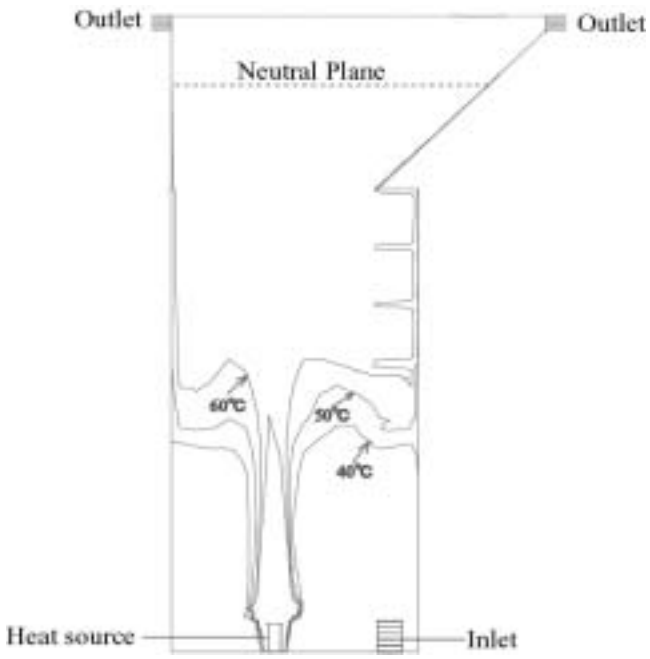

Fig. 5-13 Section of the temperature distribution and the neutral plane
(Outlet 18 m^2/Inlet 6 m^2; Outside temperature: 27 °C)

5.6 VENTILATION RATE IN DIFFERENT REGIONS

In previous discussion, the natural ventilation performance of the prototype building is examined based on the climate data of Tokyo. Actually the quantity of the solar radiation that reaches the region is quite concerned with the latitude of the region. The vertical direction in higher latitude will receive more solar radiation. Considering the regions in Japan and taking the Hokkaido for an example, the latitude of Wakkanai city (in Hokkaido) is around 45.41°, which is approximately 10° higher than that of Tokyo. Solar radiation in the south direction of Wakkanai (The monthly average solar radiation data of the typical meteorological year is used) is shown in Fig. 5-14. It is obvious that in summer and intermediate seasons, solar radiation of Wakkanai is quite more than that of Tokyo. Assuming the appropriate climate conditions for natural ventilation as the dry bulb temperature not less than 17 °C and not greater than 28 °C, and at the same time the relative humidity is in the range of 40~70%, the period for natural ventilation can be about 230 hours in Wakkanai during the whole year.

Of course the climate in Wakkanai is colder than that of Tokyo due to the higher latitude.

To improve the ventilation effectiveness in Wakkanai, the preheating of the outside air is recommended.

Besides Japan, natural ventilation is attracting more and more attention in all over the world. Especially in Northern Europe, even in summer the outside climate is mild and thermally comfortable, buildings with natural ventilation system are prosperous. For example, the latitude of London is 51.33° , solar radiation of the south direction throughout the year is shown in Fig. 5-14 (calculated according to SHARE 1997), which is quite more than that of Tokyo. The data shown in Fig. 5-14 is used as the boundary conditions and the ventilation rate of the prototype building is calculated. As shown in Fig. 5-15, ventilation rate in Tokyo varies quite obviously throughout the year; while in London, stable ventilation rate can be expected.

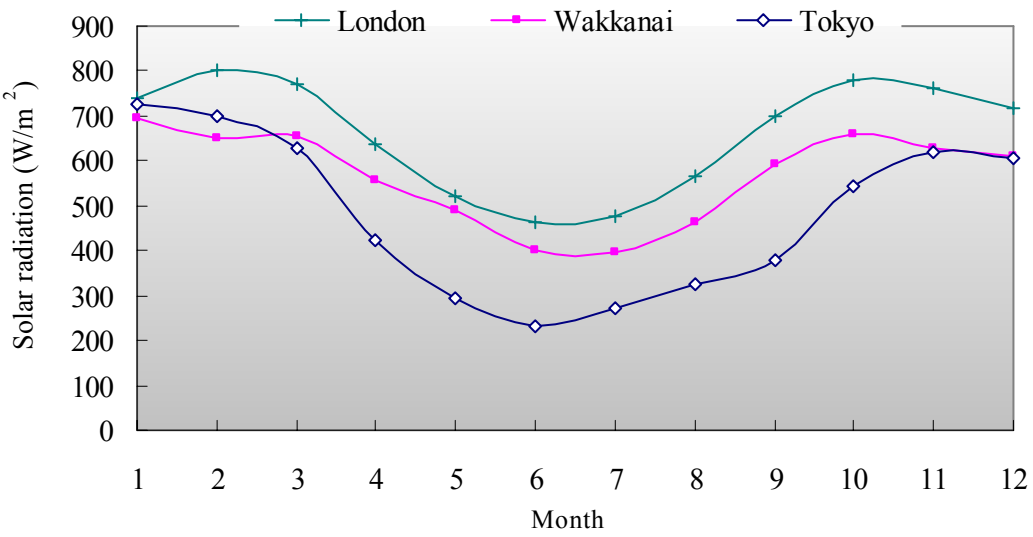

Fig. 5-14 Solar radiation of the south direction in different regions

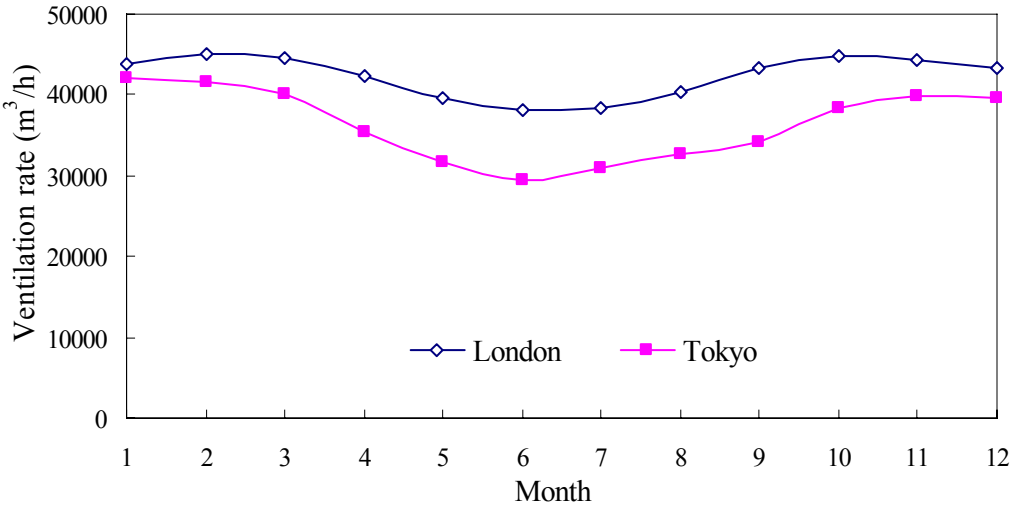

Fig. 5-15 Ventilation rate in different regions (Outlet 18 m^2/Inlet 6 m^2)

5.7 WIND EFFECT

5.7.1 Wind pressure exerted on building surface

There are two kinds of driving force for natural ventilation. One is buoyancy force caused by the temperature difference of outdoor and indoor environment, and the other one is pressure difference on the surface of the building caused by outdoor wind. The buoyancy ventilation effectiveness has been examined in previous discussion. Actually the wind force has quite influence on the practical ventilation effectiveness. Here considering both buoyancy force and wind force, the ventilation effectiveness of the prototype building is discussed.

Buildings are usually exposed to winds, causing each leakage path to experience either a pressure rise or fall at the exterior of the building. The pressure P_w that wind exerts on a surface can be expressed as

$$P_w = \frac{1}{2} C_w \rho_0 V^2 \qquad (5\text{-}1)$$

where

C_w is dimensionless pressure coefficient;

ρ_0 is outside air density, kg/m^3;

V is wind velocity, m/s.

Generally the pressure coefficient C_w is in the range of –0.8 to 0.8, with positive value for windward walls and negative value for leeward walls. The pressure coefficient depends on building geometry and local wind obstructions, and varies locally over the wall surface. Wind velocity V increases with elevation above the ground, and it is expressed by the power law equation:

$$V = V_0 (\frac{z}{z_0})^n \qquad (5\text{-}2)$$

where

V is wind velocity, m/s;

V_0 is velocity at reference elevation, m;

z is elevation of velocity V, m;

z_0 is reference elevation, m;

n is wind exponent, dimensionless.

In this research the place is thought as flat terrain and a value of 0.16 for the wind exponent is used. The reference elevation is considered as 7 m according to the AmeDAS Data.

5.7.2 Outlets distributed in windward and leeward respectively

For the simplification of the discussion, two cases are assumed. At first assuming the outlets are distributed symmetrically on both sides of the prototype building, one is in the windward direction and the other is in the leeward direction, the wind effect on the inlets is neglected. Considering the geometry of the prototype building, the pressure coefficient for windward direction is taken as 0.7 and for leeward is –0.4. The wind pressure calculated from Equation (5-1) and (5-2) is set as the pressure boundary conditions of the outlets (Table

5-2). And the climate data of 12 o'clock shown in Fig. 5-3 is used as the boundary conditions of the chimney walls. The inlet area is set as 6 m^2 and the outlet area is 18 m^2. The ventilation effectiveness of the prototype building with different outside wind velocity is examined.

Table 5-2 Wind pressure exerted on the outlet and inlet

Wind velocity (m/s)	Wind pressure at the outlets (Pa)		Wind pressure at the inlets (Pa)
	Windward (+)	Leeward (-)	
0	0	0	0
0.5	0.185	0.106	0
1	0.739	0.423	0
1.5	1.664	0.951	0
2	2.958	1.690	0
3	6.655	3.803	0
5	18.486	10.564	0

Note: C_w for windward is taken as 0.7 and for leeward is –0.4.

Fig. 5-16 shows the variation of the airflow rate of the outlets with the increasing of the outside wind velocity. The airflow rate of the outlet in the leeward rises continuously with the increasing of the outside wind velocity. On the other hand when the outside wind velocity is lower than 1 m/s, indoor air is extracted from both the outlets; when the wind velocity furthermore increases, the airflow from the outlet in the windward reduces to near zero and when the wind velocity is greater than 1.5 m/s, the airflow changes the direction. The outside air turns to flow into the building through the outlet in the windward.

As it is known, the main driving force of the natural ventilation for the prototype building is buoyancy force caused by the temperature difference between the outdoor and indoor environment. Of course the temperature difference is promoted by the solar chimney, which introduces solar radiation to warm the indoor environment. However when taking the wind effect into consideration, it is known from Fig. 5-17, the buoyancy ventilation rate decreases with the increasing of the wind velocity. When the wind velocity becomes greater than 2 m/s,

the airflow rate flowing in from the outlet in the windward is greater than the buoyancy ventilation rate. This means the outside wind effect becomes dominant over the buoyancy force.

Natural ventilation of the prototype building is promoted by stack effect occurring due to the temperature difference of the outdoor and indoor environment. The fresh air is drawn in from the inlets, passes throughout the building and then is extracted from the outlets. However when the outside wind effect becomes prevailing, airflow mainly flows in from the outlet in the windward and flows out from the outlet in the leeward. Ventilation of the indoor space cannot be expected.

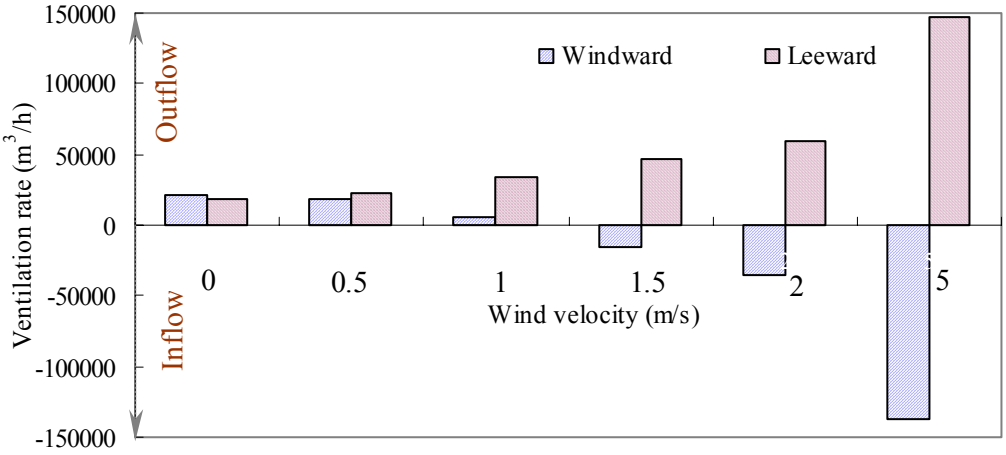

Fig. 5-16 Airflow rate of the outlets with different wind velocity (Outlet 18 m^2/Inlet 6 m^2)

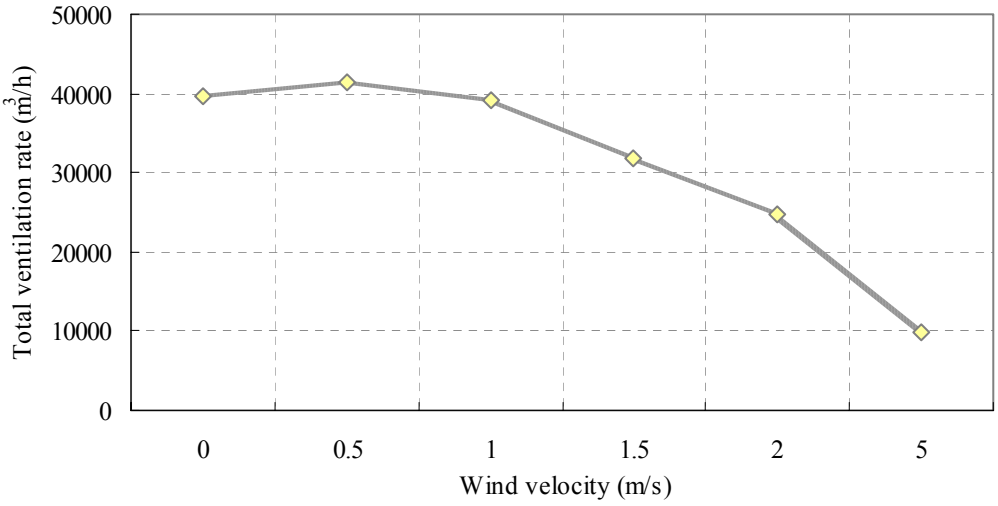

Fig. 5-17 Total ventilation rate with different wind velocity (Outlet 18 m^2/Inlet 6 m^2)

5.7.3 Outlets in leeward and inlets in windward

Considering the most reasonable arrangement of the openings, that means the inlets are all distributed in the windward direction and the outlets are all distributed in the leeward direction. The inlet area is set as 6 m^2 and the outlet area is set as 18 m^2. The pressure coefficient for windward direction is taken as 0.7 and for leeward is –0.4. The wind pressure calculated from Equation (5-1) and (5-2) is set as the pressure boundary conditions of the outlets and the inlets (Table 5-3). And the climate data of 12 o'clock shown in Fig. 5-3 is used as the boundary conditions of the chimney walls. Ventilation rate with different wind velocity is shown in Fig 5-18. Just as predicted, the ventilation rate rises with the increasing of the outside wind velocity. Considering the quantity of the fresh air introduced into the building, the greater wind velocity is preferable, while excessive velocity will influence the distribution of the indoor airflow and make it in disorder. In practice when considering the ventilation planning of a building, not only the ventilation effectiveness but also the indoor airflow property should be counted. Measures to prevent from the directive influence of excessive wind velocity need to be contrived.

Table 5-3 Wind pressure exerted on outlets and inlets

Wind velocity (m/s)	Wind pressure at the outlets (Pa) Leeward (-)	Wind pressure at the inlets (Pa) Windward (+)
0	0	0
1	0.42	0.42
2	1.69	1.68
5	10.56	10.50

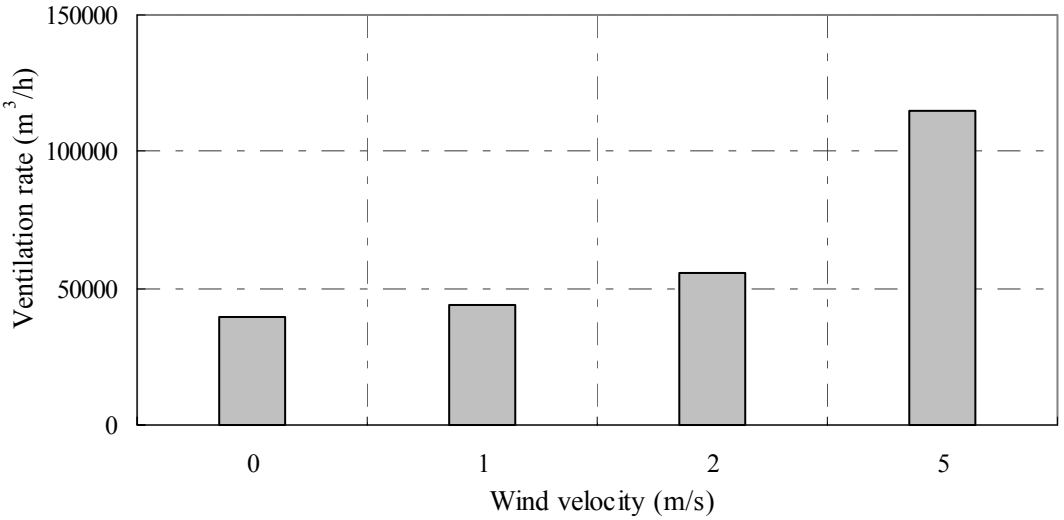

Fig. 5-18 Ventilation rate with different wind velocity (Outlet 18 m^2/Inlet 6 m^2)

5.7.4 Wind data of Tokyo

According to above discussions, since wind direction and wind velocity are quite important when deciding the arrangement of the ventilation openings, it is always necessary to grasp the wind data throughout the whole year of the local region. Here the wind data of Tokyo is presented. The average wind velocity during the intermediate seasons is about 2 m/s as shown in Fig. 5-19. The wind direction in the intermediate season (April, May and June) is illustrated in Fig. 5-20. It seems difficult to know the prevailing direction. To avoid the minus affection of the varying wind direction and obtain stable ventilation rate, measures to reduce the wind effect are recommended.

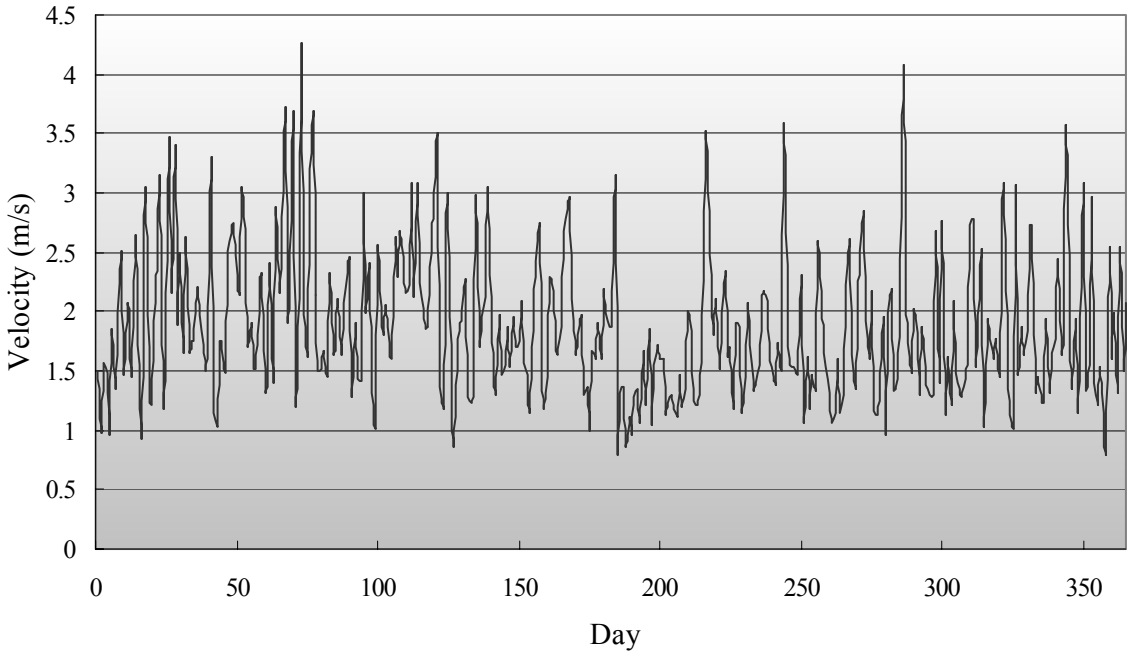

Fig. 5-19 Wind velocity of Tokyo throughout the year
(Daily average velocity of the Typical Meteorological year)

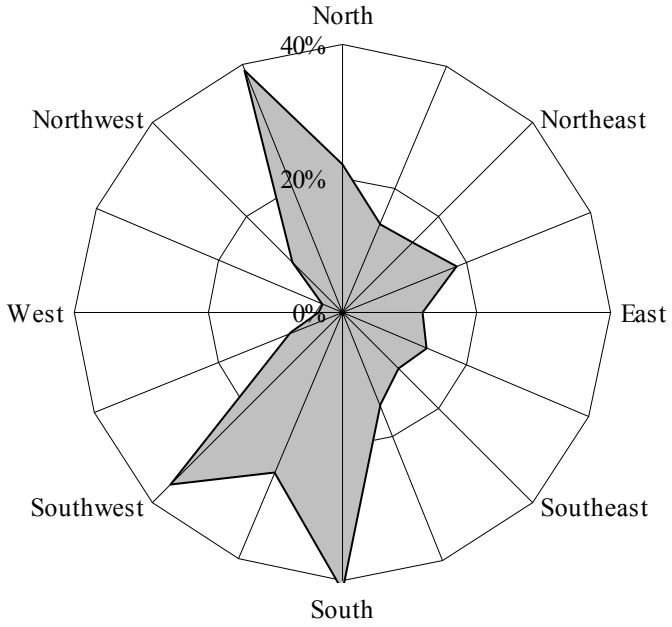

Fig. 5-20 Wind direction of Tokyo in intermediate season
(The Typical Meteorological year)

5.8 DISCUSSION

As the proposed prototype building, setting the inlet as 6 m^2 and outlet as 18 m^2, the ventilation rate throughout the whole year reaches 30,000~42,000 m^3/h. Considering the ventilation in the occupant space, the standard area floor is about 850 m^2 and the ceiling height is about 3 m, the total volume of the 8 floors space is about 20,000 m^3. The air change rate of the occupant space is about 1.5~2.1 times per hour.

Usually the necessary ventilation rate to remove the load in a space can be calculated as:

$$V = \frac{Q}{\rho C_p (t - t_0)} \tag{5-3}$$

where

V is necessary ventilation rate, m^3/h;

Q is total cooling load, W;

ρ is density of the air, $kg/m^{3;}$

C_p is specific heat of the air, 1.002 kcal/kg·K;

t is set indoor air temperature, here is taken as 28 ºC;

t_0 is outside air temperature, ºC.

Assuming the cooling load for the occupant space as 120 W/m^2, the necessary ventilation rate to remove the cooling load of the total occupant space can be expressed as shown in Fig. 5-21.

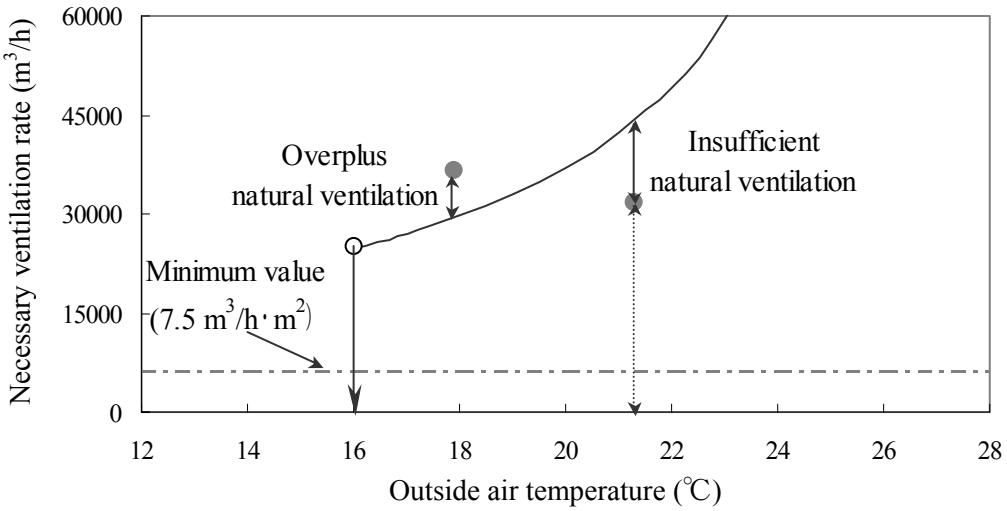

Fig. 5-21 Necessary ventilation rate with outside air temperature

Just as shown in Fig. 5-21, the necessary ventilation rate increases quickly with the temperature rise of the outside air. Because of the high cooling load and large space volume, the necessary ventilation rate for the occupant space is quite great. It is clear that the natural ventilation rate discussed in this research cannot meet the requirement. But as the supplement of the mechanical ventilation and from the point of indoor air quality, the effectiveness of the natural ventilation system can be quite expected with appropriate control.

In case of the utility space, there is no long term staying occupant. Therefore necessary ventilation rate is scarce and the requirement for thermal comfort control is not so sensitive; natural ventilation in such a space is relatively easy. Since the volume of the utility space is about 17,000 m^3/h, the air change rate obtained from natural ventilation reaches 1.8~2.5 times per hour. It is thought sufficient to such a space.

5.8 SUMMARY

In this chapter, the detail natural ventilation performance of the prototype building has been discussed. The results can be summed up as following:

(1) Natural ventilation rate of the prototype building increases with the ascending of the outlet area. However when the outlet area becomes over 2 times of the inlet area, the growth gradient slows down, which means setting the area ratio of outlet to inlet as 2~3 is preferable to obtain appropriate ventilation rate. At the same time, with the same area ratio of outlet to inlet, the greater inlet area makes more ventilation rate. Although the same area ratio of inlet to outlet can promote the same ventilation rate, to ensure the neutral pressure plane forming in the chimney, it is recommended to make the outlet area not less than the inlet area.

(2) The dimension of the chimney, including height, width and length, will affect the natural ventilation performance. Ventilation rate increases with the growth of any of the three factors. It is thought that rising of the height, width or the length of the chimney will all increase the thermal storage wall area that can absorb the solar radiation.

(3) Since the quantity of the solar radiation that can be absorbed by the thermal storage wall varies with seasons and regions, ventilation performance of the prototype building in regions like Tokyo is not stable throughout the year. The ventilation rate is highest in winter when the necessity for natural ventilation rate is very small and quite lower in the intermediate seasons when natural ventilation is mostly required. To obtain stable ventilation rate throughout the year, improve method is suggested and stable ventilation rate of the performance improved prototype building is confirmed. Furthermore, considering the high latitude regions such as London, since the quantity of the solar radiation that can reach the thermal storage wall is relatively stable throughout the year, preferable ventilation rate can be expected without any improvement.

(4) Wind pressure exerted on the surface of buildings will affect the effectiveness of the natural ventilation. The airflow rate of the outlet in the leeward rises continuously with the increasing of the outside wind velocity. And at the same time the airflow rate of the outlet in

the windward decreases. Arrangement of the outlet and inlet according to the wind climate of the local place is quite important. Considering the quantity of the fresh air introduced into the building, the greater wind velocity is preferable, while excessive velocity will influence the distribution of the indoor airflow and make it in disorder. In practice when considering the ventilation planning of a building, measures to prevent from the directive influence of excessive wind velocity need to be contrived.

CHAPTER 6

DETAIL PERFORMANCE OF THE SMOKE CONTROL SYSTEM

CHAPTER 6
DETAIL PERFORMANCE OF THE SMOKE CONTROL SYSTEM

As reported in Chapter 4, the compatibility of natural ventilation and smoke control in the prototype building has been verified. And the validity of the CFD technique has also been confirmed. In this paper, the same CFD technique is used to predict the detail performance of the smoke control system. Parameters those will affect the smoke control performance of the prototype building are considered to include mainly height of the solar chimney, area ratio of outlet to inlet, and the outside climate conditions. In addition, the affection of the property of the fire source will be also examined.

6.1 NUMERICAL MODELING

Just as described in Chapter 4, the κ-ε model is used to predict the detail performance of the smoke control system. The computational domain is basically divided into a grid of 0.75m×0.75m×0.75m control volumes. Additional grid points are embedded near the walls, around the inlets and outlets, and around the heat source to enable better resolution in these areas. As to the boundary conditions, all walls are set as adiabatic. Outlets and inlets are set as pressure boundary conditions. The fire source is set as a cylinder thermal source with a heat release rate of 2187.5 kW.

6.2 SMOKE CONTROL PERFORMANCE WITH DIFFERENT AREA RATIO OF OPENINGS

As it is known, the area ratio of openings is a very important factor, which will influence the position of the neutral pressure plane. Here smoke control performance with different area ratio of outlet to inlet and different inlet area with keeping the area ratio constant is examined. At first the inlet area is set as 1/45 of the floor area of the atrium and the outlet area is changed to adjust the area ratio of outlet to inlet. The variation of the neutral pressure plane and the smoke extract rate are discussed. The area conditions of outlets and inlets are listed in Table 6-1.

Table 6-1 Area conditions of outlets and inlets

Area ratio (Outlet/Inlet)	Inlet	Outlet
1	6 m^2	6 m^2
2	6 m^2	12 m^2
3	6 m^2	18 m^2
4	6 m^2	24 m^2
5	6 m^2	30 m^2

Just as shown in Fig. 6-1, the position of the neutral pressure plane rises with the increasing of the outlet area. When the area ratio of outlet to inlet is 1, the neutral pressure plane is at about the half height of the atrium, when the area ratio of outlet to inlet increases to 2, the neutral pressure plane rises to around the border of the atrium and the chimney, and when the area ratio of outlet to inlet becomes over 2, the neutral pressure plane goes up to be inside the chimney. Furthermore, the variation gradient of the neutral pressure plane decreases with the increasing of the outlet area.

Fig. 6-2 shows the variation of the smoke extract rate with the increasing of the outlet area. The tendency is just as the variation of the neutral pressure plane. The smoke extract rate rises with the expanding of the outlet area. And the variation gradient decreases with the increasing of the area ratio of outlet to inlet.

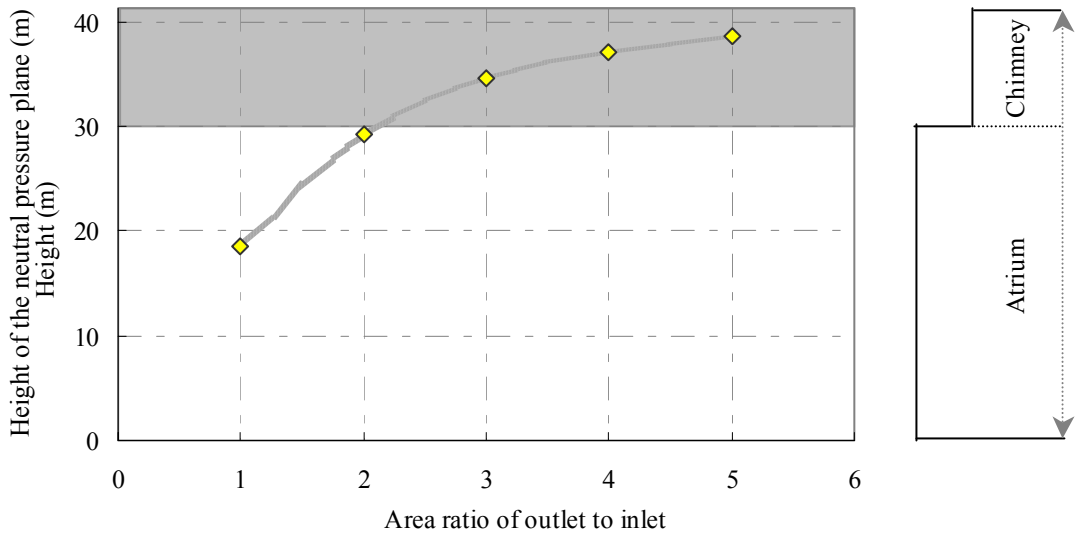

Fig. 6-1 Variation of the neutral pressure plane with different area ratio (Inlet = 6 m^2)

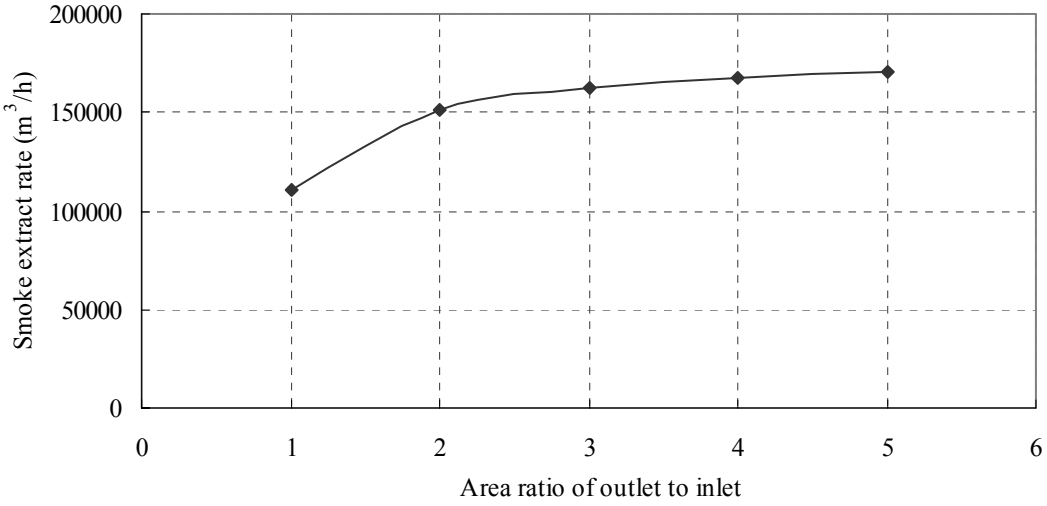

Fig. 6-2 Smoke extract rate with different area ratio (Inlet = 6 m^2)

At the same time keeping the area ratio of outlet to inlet as 2 and smoke control performance with different inlet area is examined. Smoke extract rate increases with the expanding of the inlet area and consequently the temperature of the smoke layer decreases. When the inlet area is set as 3 m^2, the smoke layer temperature reaches over 90 °C. Considering the fear of exposure to the smoke for a short duration, greater inlet area or lower smoke temperature is preferable.

As it can be predicted, with the same area ratio of outlet to inlet, the neutral pressure plane does not change so much. The temperature of the smoke just affects the neutral pressure plane slightly. Fig. 6-4 reflects the influence of the smoke temperature.

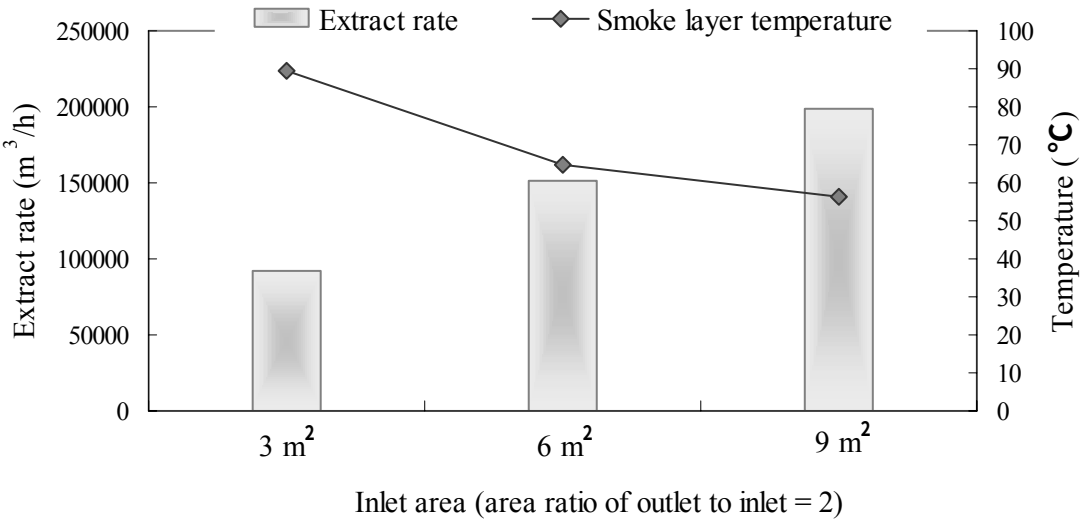

Fig. 6-3 Extract rate and smoke layer temperature with different inlet area

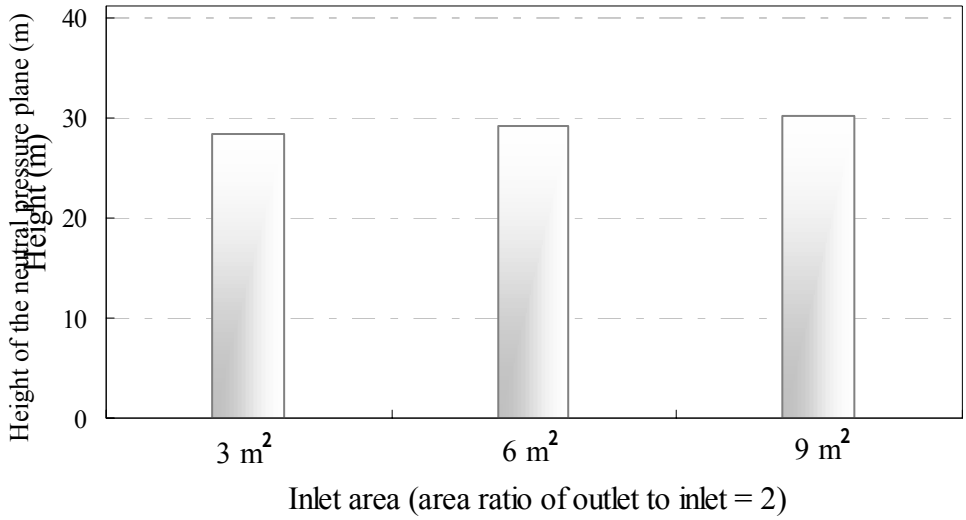

Fig. 6-4 Neutral pressure plane with different inlet area

6.3 INFLUENCE OF DIMENSION OF THE SOLAR CHIMNEY

6.3.1. Influence of height of the chimney

The height of the solar chimney not only affects the position of the neutral pressure plane. Since the smoke accumulation space also varies with the changing of the height of the solar chimney, it is thought the height of the solar chimney will influence the smoke control performance of the prototype building.

As discussed above, to make the neutral pressure stay inside the solar chimney, the area ratio of outlet to inlet need to be greater than 2. Here from the safety side, the area ratio is set as 3 and the influence of the height of the solar chimney upon the smoke control performance is examined. As shown in Fig. 6-5, the height of the neutral pressure plane almost increases linearly with the height of the solar chimney. Although as the prototype building, the solar chimney is set as about 3 storeys high, the results reveal that with the area ratio of outlet to inlet as 3, the height of the solar chimney is adjustable according to the requirements of the design.

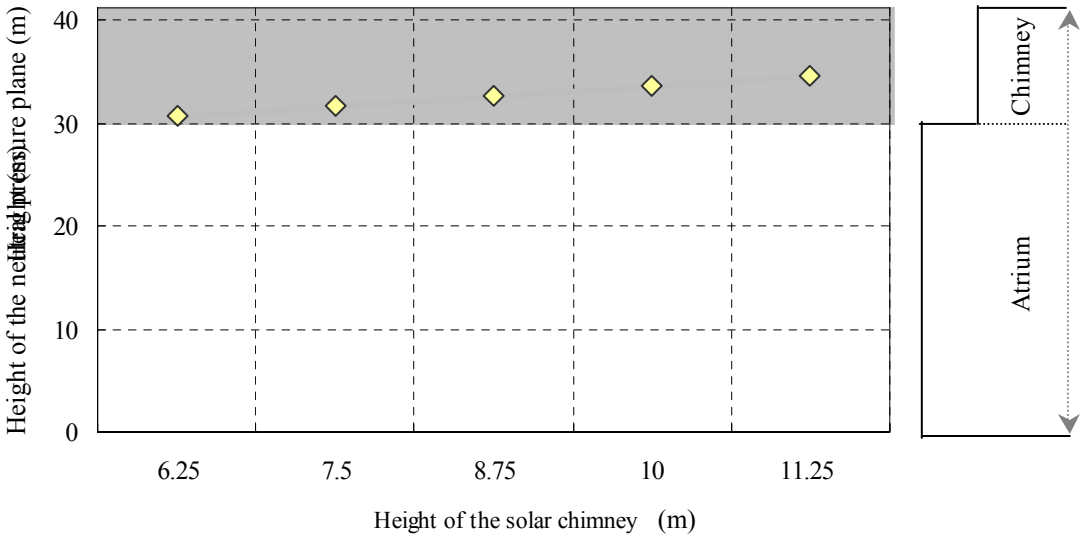

Fig. 6-5 Variation of the neutral pressure plane with the height of the solar chimney (Outlet 18 m^2/Inlet 6 m^2)

Fig. 6-6 shows the smoke extract rate with different height of the solar chimney. It shows that the smoke extract rate increases with the rising of the height of the solar chimney. The high smoke extract rate can lead to low smoke temperature and high smoke interface.

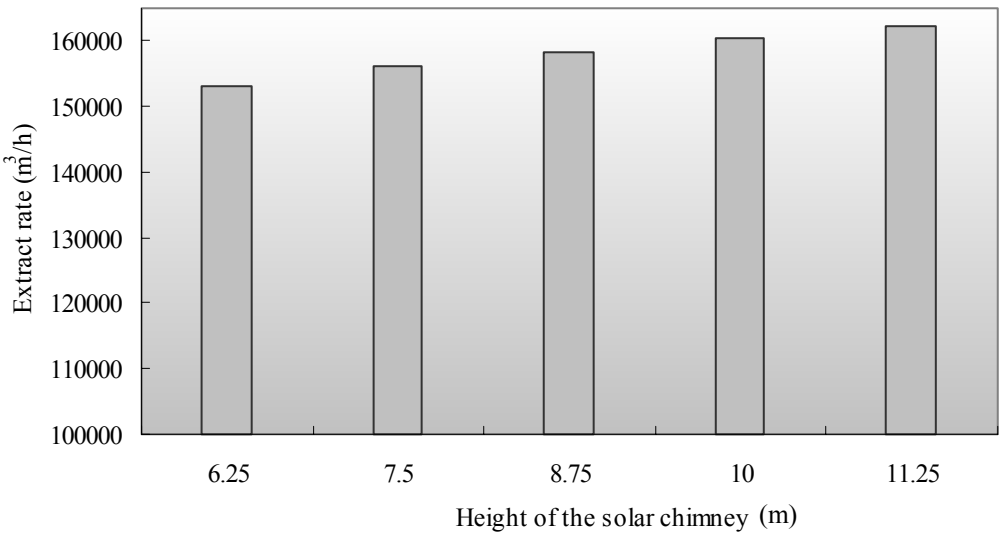

Fig. 6-6 Smoke extract rate with the height of the solar chimney (Outlet 18 m^2/Inlet 6 m^2)

6.3.2 Influence of width of the chimney

Here the influence of the width of the chimney on the smoke control performance will be discussed. Fig. 6-7 shows the variations of the height of the neutral pressure plane and the smoke extract rate with the width of the chimney. It reveals that both the height of the neutral pressure plane and the smoke extract rate are almost not affected by the width of the chimney.

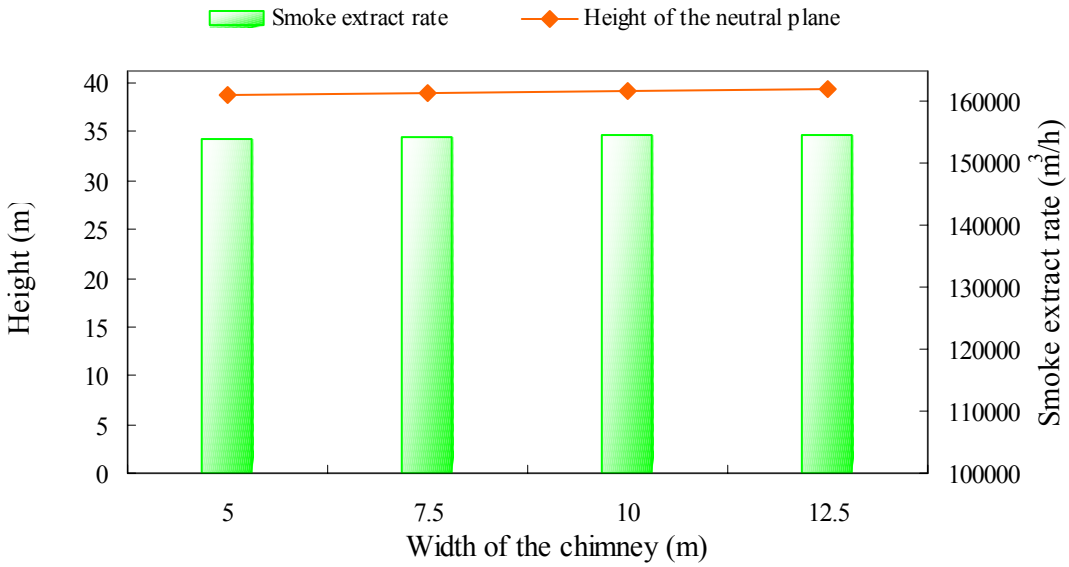

Fig. 6-7 Smoke extract rate and the neutral pressure plane of different width of the chimney (Outlet 18 m^2/Inlet 6 m^2)

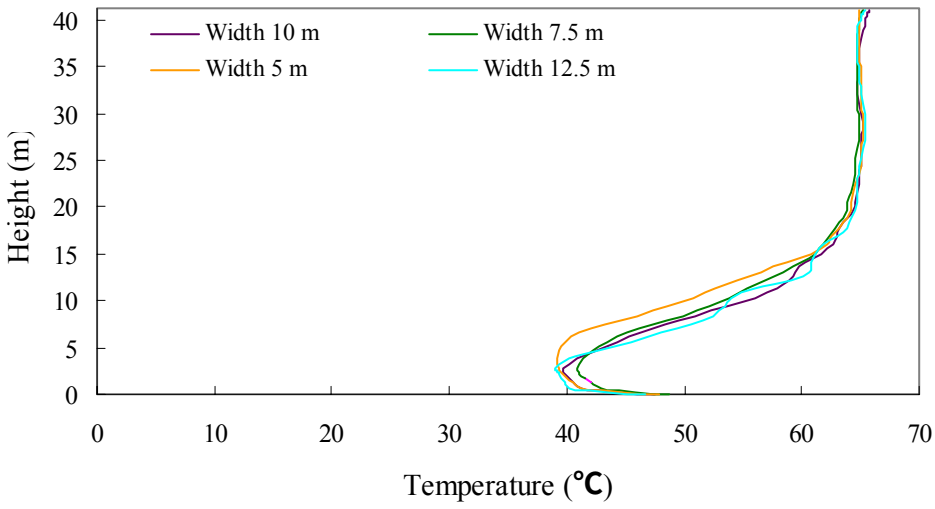

Fig. 6-8 Temperature distribution of different width of the chimney (Outlet 18 m^2/Inlet 6 m^2)

Furthermore, the temperature distribution of these four widths shows almost no difference (Fig. 6-8). Changing the length of the chimney and the same results are obtained. Therefore it can be concluded that when considering the finial status of the smoke property, the width or the length of the chimney just has very little effect.

6.4 COMPARISON OF DIFFERENT DESIGN FIRES

6.4.1 Steady fires

Till now, all discussions are based on a fire size of around 2,000 kW. Actually there are may be larger fires occurring in atria. Table 6-2 shows the usual steady design fire sizes for atria.

Table 6-2 Steady design fire sizes for atria

Type	Size (kW)
Minimum fire for fuel restricted atrium	2,000
Minimum fire for atrium with combustibles	5,000
Large fire	25,000

Here assuming the fire size as 5,000 kW, the smoke control performance of the prototype building is examined.

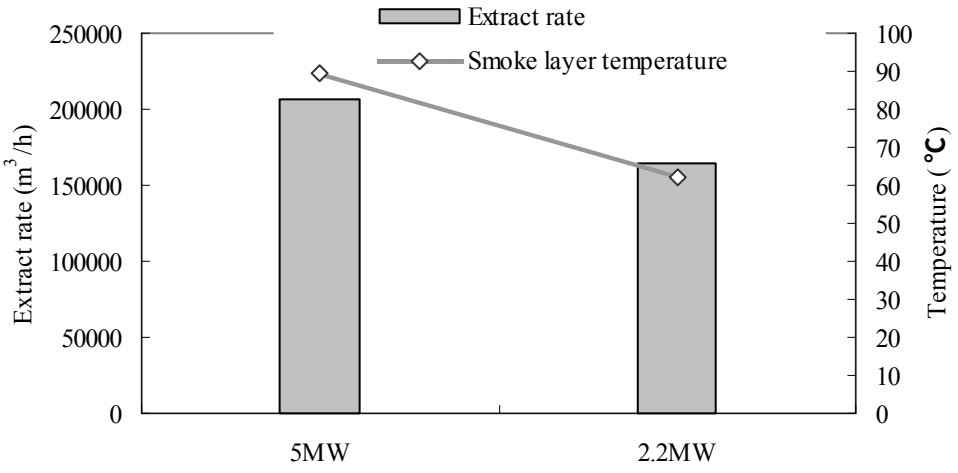

Fig. 6-9 Extract rate and smoke layer temperature with different fire size (Outlet 18 m^2/Inlet 6 m^2)

Fig. 6-9 shows the extract rate and smoke layer temperature of two different fire sizes respectively. Since the heat release rate of the 5,000 kW fire is over 2 times of that of the 2,200 kW fire, of course as it is expected the smoke layer temperature of the 5,000 kW fire is higher than that of the 2,200 kW fire. And smoke extract rate in case of the 5,000 kW fire is greater than that in case of the 2,200 kW.

Corresponding to the temperature rise inside the atrium, the smoke layer height of the 5,000 kW is lower than that of the 2,200 kW fire. However the position of the neutral pressure plane hardly changes. It stays at around half height of the solar chimney.

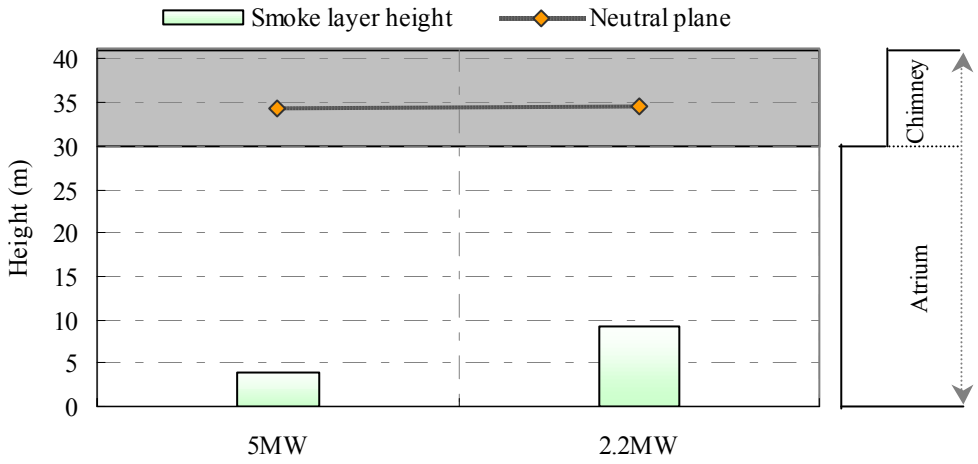

Fig. 6-10 Smoke layer height and neutral pressure plane with different fire sizes (Outlet 18 m^2/Inlet 6 m^2)

In this research, the position of the neutral pressure plane is the most important factor. It is clear that even with a larger fire such as 5,000 kW, the neutral pressure plane stays inside the solar chimney. Smoke spread to the safety zones can be prevented. But considering the fire-resisting performance of the partition materials and the risk of escape persons exposed to the smoke, it is recommended to control the smoke layer temperature lower than 120 ℃.

6.4.2 Unsteady fires

Fires frequently proceed through an incubation period of slow and uneven growth followed by a period of established growth, which is often represented by an idealized parabolic equation (Heskestad 1984):

$$Q = a(t - t_0)^2 \tag{6-1}$$

where

Q is heat release rate of fire, kW;

a is fire growth coefficient, kW/s^2;

t is time after ignition, s;

t_0 is effective ignition time, s.

It is generally recognized that consideration of the incubation period is not necessary for design of atrium smoke control systems, and Eq. (6-1) can be expressed as:

$$Q = at^2 \tag{6-2}$$

where t is the time after effective ignition, and fires following Eq. (6-2) are called t-squared fires. Table 6-3 lists values of a for some general fire types.

Table 6-3 Typical fire growth coefficients

Types of t-squared fires	Fire growth coefficient (kW/s^2)
Slow	0.002931
Medium	0.01127
Fast	0.04689
Ultra Fast	0.1878

Fire growth may be approximated by the t-squared curve for some time. Because of limitations of fuel or limitations of combustion air, t-squared fire growth eventually must stop. Generally limitations of fuel and of combustion air can result in a nearly constant rate of heat release following a t-squared fire growth. Because atria are large spaces, the growth of fires in atria is usually not restricted by lack of combustion air.

Here assuming a medium t-squared fire occurring in the atrium and it is grows up to 5 MW eventually, just shown in Fig. 6-11. Smoke control performance of the prototype building under the unsteady fire will be discussed.

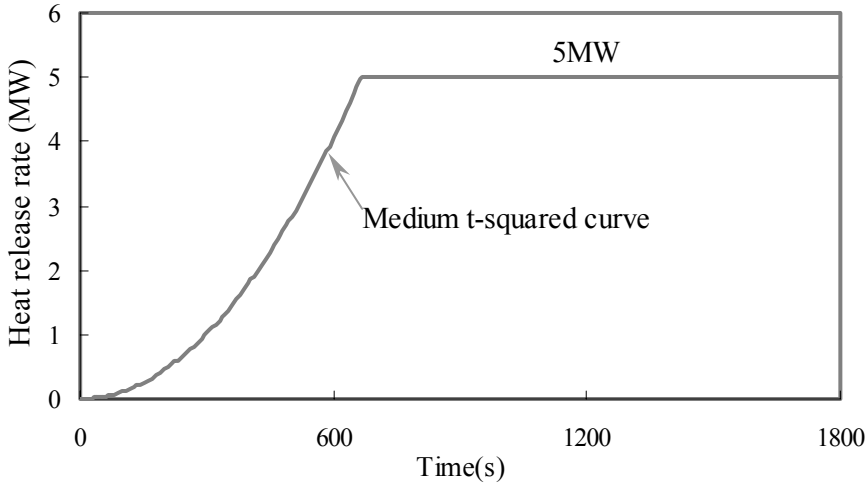

Fig. 6-11 Medium t-squared growth up to steady fire 5 MW

Fig. 6-12 shows the centerline temperature distribution of the fire plume. Since the heat release rate of the t-squared fire is very small in the initial phase, it takes about 105 seconds for the fire plume to reach the top of the chimney, while in case of the steady fire, it takes just about 25 seconds.

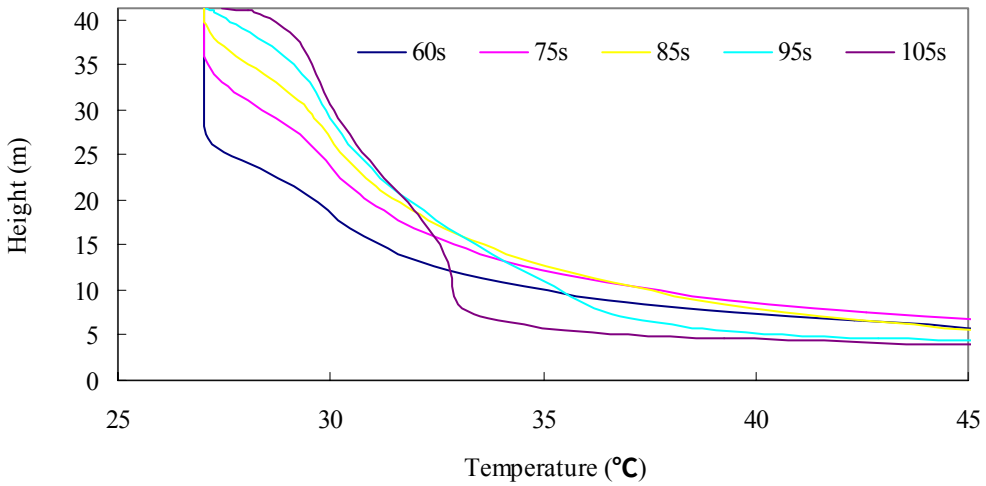

Fig. 6-12 Centreline temperature distribution of the fire plume

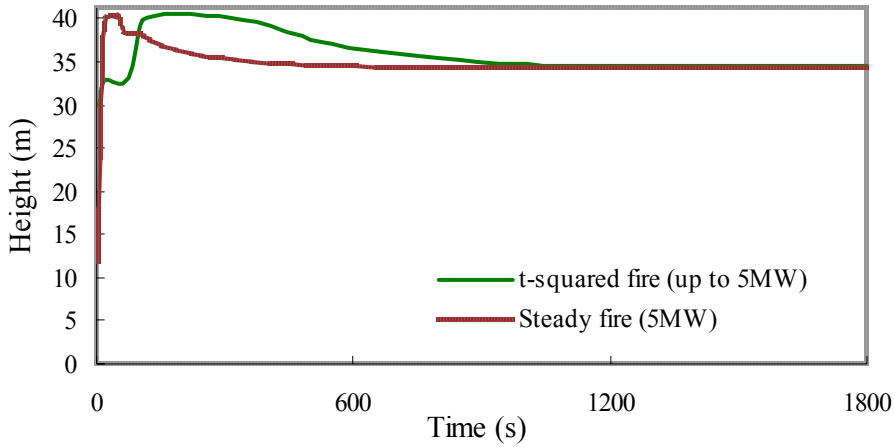

Fig. 6-13 Variation of the neutral pressure plane

Fig. 6-13 shows the variation of the neutral pressure plane. Comparing with the steady fire, the t-squared fire reveals a slow variation gradient. Since the t-squared fire finally stops at a value equal to the steady fire, the neutral pressure plane of the two different fires consequently forms at the same position. They both stay inside the chimney and smoke infiltration from the atrium to the adjacent space can be expected.

6.5 WIND EFFECT

Just as stated in Chapter 5, as long as wind exists, it will cause wind pressure on the building façade. The calculation method for wind pressure is listed in Chapter 5. Here the influence of the outside wind on the smoke extract is discussed.

6.5.1 Outlets distributed in windward and leeward respectively

For the simplification of the discussion, two cases are assumed. At first assuming the outlets are distributed symmetrically on both sides of the prototype building, one is in the windward direction and one is in the leeward direction, the wind effect on the inlets is neglected. Considering the geometry of the prototype building, the pressure coefficient for windward direction is taken as 0.7 and for leeward is –0.4. The wind pressure calculated according to Eq. (5-1) and Eq. (5-2) is set as the pressure boundary conditions of the outlets (Table 6-4). The inlet area is set as 6 m^2 and the outlet area is 18 m^2.

Table 6-4 Wind pressure exerted on the outlet and inlet

Wind velocity (m/s)	Wind pressure at the outlets (Pa)		Wind pressure at the inlets (Pa)
	Windward (+)	Leeward (-)	
0	0	0	0
0.5	0.185	0.106	0
1	0.739	0.423	0
1.5	1.664	0.951	0
2	2.958	1.690	0
5	18.486	10.564	0
10	73.945	42.254	0

Note: C_w for windward is taken as 0.7 and for leeward is –0.4.

Fig. 6-14 shows the variation of the smoke extract rate of the outlets with the increasing of the outside wind velocity. The extract rate of the outlet in the leeward rises continuously with the growth of the outside wind velocity. On the other hand when the outside wind velocity is lower than 2 m/s, smoke is extracted from both the outlets; when the wind velocity increases to 5 m/s, smoke extracted from the outlet in the windward reduces to near zero, and at the meantime, instead of extracting the smoke to outside, the outside air becomes to flow into the building through the outlet in the windward.

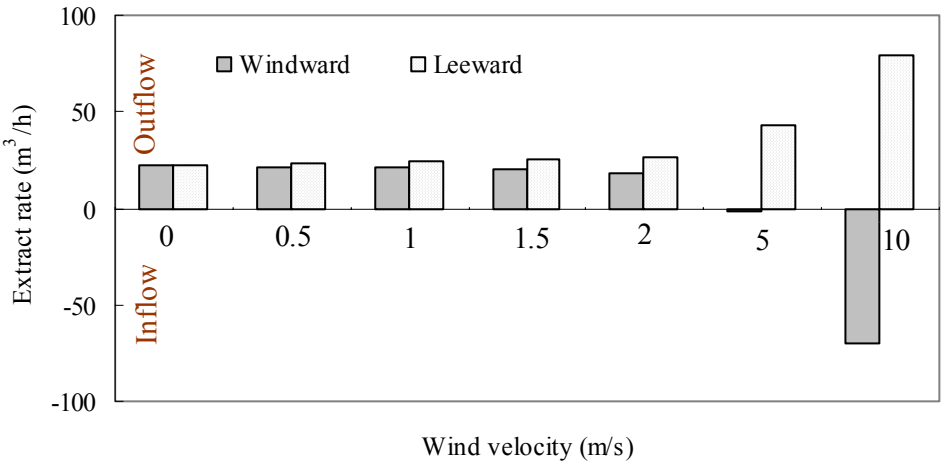

Fig. 6-14 Extract rates at the outlets with different wind velocity
(Outlet 18 m^2/Inlet 6 m^2)

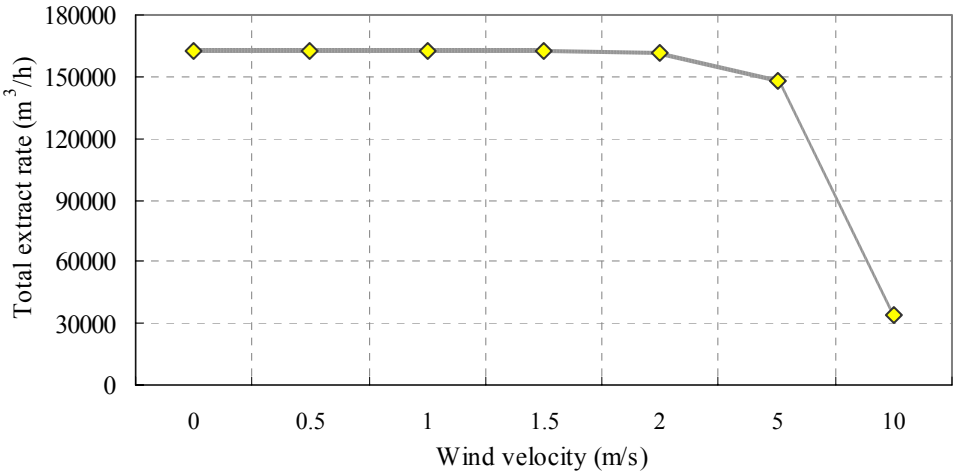

Fig. 6-15 Total extract rate of both the outlets

With respect to the total extract rate of both the outlets, as shown in Fig. 6-15, there is no obvious change when the wind velocity is less than 2 m/s. When the wind velocity becomes greater than 2 m/s, the total extract rate begins to fall down. The reduction of the total extract rate also means the decrease of the supply fresh air. Therefore the temperature distribution inside the atrium rises with the decline of the supply air.

Fig. 6-16 shows the variation of the neutral pressure plane with the increase of the outside wind velocity. When the wind velocity becomes greater than 2 m/s, the neutral pressure plane begins to fall down. When the wind velocity is over 5 m/s, the neutral pressure plane falls down to lower than the bottom of the solar chimney, which means smoke has the risk of spreading to the evacuation space under such conditions.

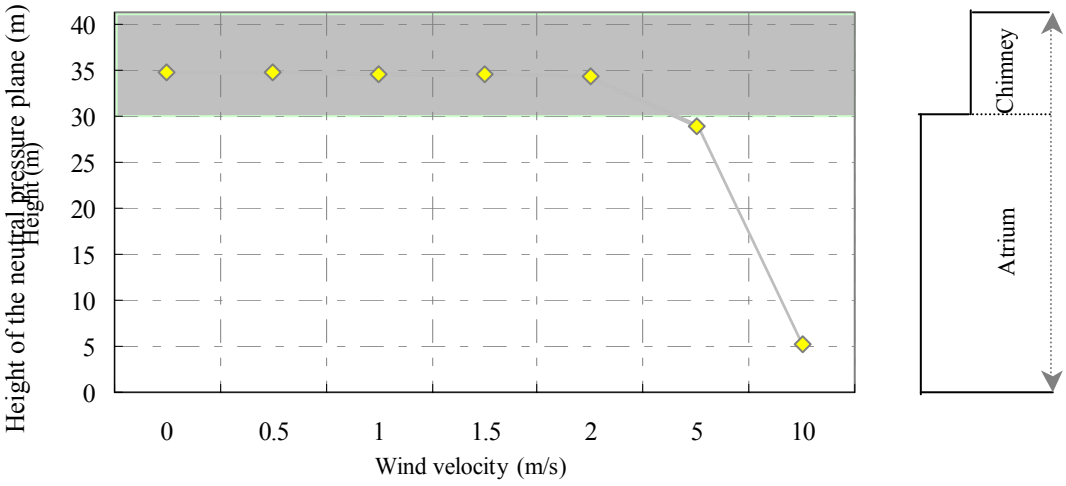

Fig. 6-16 Variation of the neutral pressure plane (Outlet 18 m^2/Inlet 6 m^2)

6.5.2 Outlets in leeward and inlets in windward

Considering the most reasonable arrangement of the openings, that means the inlets are all distributed in the windward direction and the outlets are all distributed in the leeward direction. The inlet area is set as 6 m^2 and the outlet area is set as 18 m^2. The pressure coefficient for windward direction is taken as 0.7 and for leeward is –0.4. The wind pressure calculated according to Eq. (5-1) and Eq. (5-2) is set as the pressure boundary conditions of the outlets and the inlet (Table 6-5).

Table 6-5 Wind pressure exerted on outlets and inlets

Wind velocity (m/s)	Wind pressure at the outlets (Pa) Leeward (-)	Wind pressure at the inlets (Pa) Windward (+)
0	0	0
1	0.42	0.42
2	1.69	1.68
5	10.56	10.50

Smoke extract rate with different wind velocity is shown in Fig. 6-17. Just as predicted, it rises with the increasing of the outside wind velocity. The neutral pressure plane also goes up to near the top of the chimney with the growing of the wind velocity (Fig. 6-18). In general view of fire safety, it is preferable to extract the smoke out of the building as quickly as possible. Therefore it is better to arrange the inlets in the windward and the outlets in the leeward. Just as problems in natural ventilation, the wind data of the local region is very important to the designer.

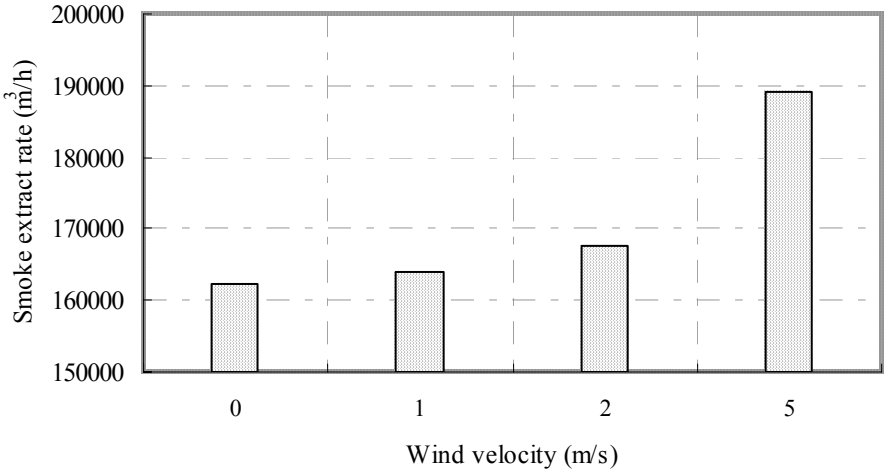

Fig. 6-17 Smoke extract rate with wind velocity (Outlet 18 m^2/Inlet 6 $m^{2)}$

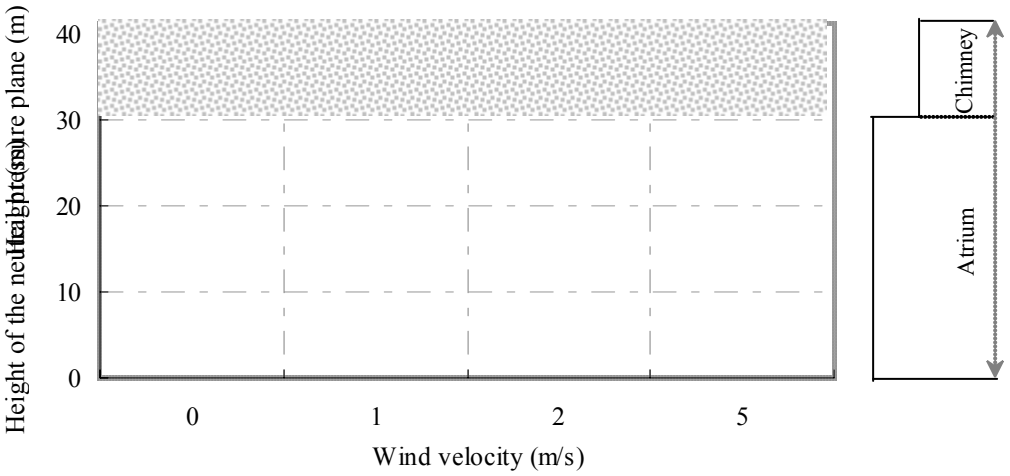

Fig. 6-18 The neutral pressure plane with wind velocity

6.6 DISCUSSION OF THE SPACE PARTITION PLANNING RESTED ON THE CONCEPT OF SMOKE PREVENTION BY PRESSURE DIFFERENCE

The prototype building is proposed as a natural ventilated building, and at the same time the natural ventilation system can also be used to carry out smoke control, which makes the smoke control/evacuation plan of the building very simple. The possibility of planning such

a building has been discussed and confirmed. As mentioned above, effective ventilation can be obtained and in case of a fire, with the neutral pressure plane forming inside the chimney, the pressure of the atrium is lower than ambient. The prospect that fire safety in the building can be secured is confirmed. Grounding on the concept of the prototype building, the space partition plan is discussed from the viewpoint of fire prevention.

6.6.1 Planning with the utility space completely open to the atrium

From the viewpoint of architecture design, the planning with the utility space completely open to the atrium is thought to be natural. Considering the plane planning as shown in Fig. 6-19, when a fire happens at the base of the atrium, since smoke prevention between the utility space and the staircase/safety zone is possible, if persons staying in the utility space and the occupant space can escape to the safety zone, their safeties are secured. As to those persons staying in the utility space, their safeties depend on whether they can escape to the safety zone before the smoke layer descends to the critical height. As to those persons staying in the occupant space, since fire detected time is later than the utility space, the planning of passing the utility space to reach the safety zone is thought to be difficult. Escape route from the occupant space directly to the safety zone is necessary to be secured.

6.6.2 Planning with the utility space separated from the atrium

Supposing the utility space is separated from the atrium by wire glass and openings (Fig. 6-20) for ventilation are located between the utility space and the atrium, if the pressure of the atrium can be kept lower than that of the utility space, even without closing the openings, smoke spread from the atrium to the utility space can be prevented. Then the whole utility space becomes safety zone, persons staying in the utility space and the occupant space can escape without a hitch. But considering the permissible temperature of the glass, the smoke layer temperature should be controlled to be not so high.

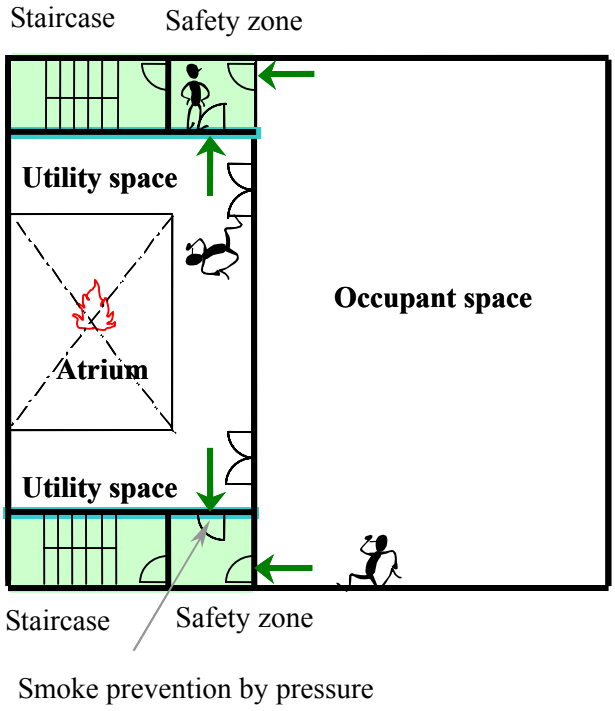

Fig. 6-19 Escape planning with the utility space completely open to the atrium

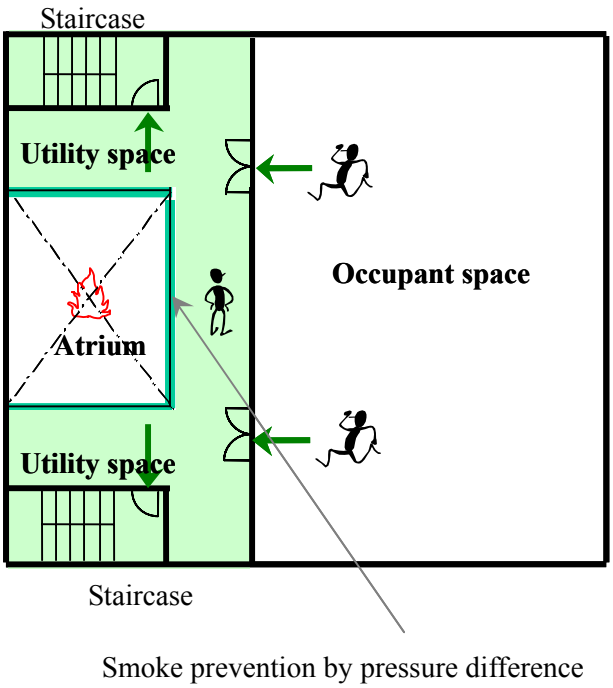

Fig. 6-20 Escape planning with the utility space separated from the atrium

6.7 SUMMARY

In this chapter, the detail smoke control performance of the prototype building has been discussed. The results can be summed up as following:

(1) The position of the neutral pressure plane rises with the increasing of the area ratio of outlet to inlet. When the area ratio of outlet to inlet becomes greater than 2, the neutral pressure plane stays in the chimney. Smoke extract rate also increases with expanding of the outlet area. However when the outlet area becomes over 2 times of the inlet area, the growth gradient slows down. At the same time, with the same area ratio of outlet to inlet, the greater inlet area leads to greater smoke extract rate and lower smoke layer temperature.

(2) The height of the chimney influences the neutral pressure plane significantly while the width or the length of the chimney just has a very little effect. The designers can decide the dimension of the chimney according to practical requirements. In fact there are always restrictions on the dimension of the chimney from the aspects of design or laws. From this point the opening area or the area ratio has wider adjustability.

(3) Different design fires are used to check the smoke control performance of the prototype building. Although the smoke extract rate or the smoke layer temperature varies with different design fires, for all cases, the neutral pressure plane keeps staying in the chimney. It sufficiently reflects the advantage of the passive smoke control method-self adjustable and therefore reliable.

(4) The wind effect to the smoke control performance is also discussed. Based on the assumptions in this research, the wind velocity lower than 2 m/s does not affect the smoke control performance so much. However when the wind velocity becomes greater than 5 m/s, smoke cannot be extracted from the outlet in the windward and the neutral pressure plane descends to the occupant space. Considering the height of the chimney, the velocity at such height is considered strong. Setting the outlet in the windward should be avoided.

CHAPTER 7

DESIGN OF NATURAL VENTILATION/SMOKE CONTROL SYSTEM BASED ON DISCUSSIONS OF THE PROTOTYPE BUILDING

CHAPTER 7
DESIGN OF NATURAL VENTILATION/SMOKE CONTROL SYSTEM BASED ON DISCUSSIONS OF THE PROTOTYPE BUILDING

In this chapter the natural ventilation and smoke control performance of the prototype building are synthetically evaluated. Furthermore, the procedure for designing a natural ventilated building with passive smoke control function is given. Finally as application of this research, one more type building is introduced.

7.1 ACCESS OF THE PROTOTYPE BUILDING

7.1.1 Natural ventilation performance

As the proposed prototype building, setting the inlet area as 6 m^2 and changing the outlet area, the ventilation rate throughout the whole year reaches 30,000~40,000 m^3/h. Considering the ventilation in the occupant space, the standard floor area is about 850 m^2 and the ceiling height is about 3 m, the total volume of the 8 floors space is about 20,000 m^3. The air change rate of the occupant space by natural ventilation is about 1.5~2 times per hour. Assuming the necessary air change rate for the office room as 6 times per hour, the natural ventilation rate still cannot completely meet the requirement. But as the supplement of the mechanical ventilation and from the point of indoor air quality, the effectiveness of the natural ventilation system can be quite expected with appropriate control. In case of the utility space, there is no long term staying occupant. Therefore necessary ventilation rate is scarce and the requirement for thermal comfort control is not so sensitive, natural ventilation in such a space is relatively easy. Since the volume of the utility space is about 17,000 m^3/h, the air change rate obtained from natural ventilation reaches 1.8~2.4 times per hour. It is thought sufficient to such a space.

Although the ventilation rate rises with the increasing of the outlet area, when the outlet area becomes over 3 times of the inlet area, the ventilation rate tends to be constant. Even with greater outlet area, ventilation rate increases no more. Therefore from the point of ventilation effectiveness, it is thought appropriate to take the area ratio of outlet to inlet as

2~3.

On the other hand, increasing the outlet area can make the neutral pressure plane form at high position. The pressure of the space below the neutral pressure plane is positive to the ambient. If openings are set between the space and the outside, the outside air will flow into the space. For the prototype building, as long as the neutral pressure plane forms inside the chimney, effective ventilation can be expected in the atrium space. In this research, the air temperature of the atrium is assumed to be as the same as the outside air and temperature rise occurs only in the chimney; therefore the neutral pressure plane forms almost automatically inside the chimney. In fact temperature rise in the atrium part also happens, although it is not so obvious as in the chimney, the neutral pressure plane is considered to fall a little than those situations discussed in this research. Thus it is recommended to make the upper openings a little greater than the lower openings.

The driving force of the natural ventilation, stack effect, becomes significant with increasing the height of the solar chimney, which leads to the growing of the natural ventilation rate. As the results, the ventilation rate rises almost linearly with the height of the solar chimney. Usually the height of the solar chimney can be set as 2 or 3 storeys high according to the practical needs of the building.

For the prototype building, all walls of the solar chimney are set as vertical. As it is discussed before, ventilation effectiveness is quite related with the quantity of the solar radiation absorbed by the thermal storage wall, in regions like Tokyo, the solar altitude becomes higher in summer and the vertical thermal storage wall cannot receive enough solar radiation, which makes the ventilation rate of the prototype building becomes insufficient in summer. Therefore when people design such a building in regions like Tokyo, other measures should be taken to enhance more absorption of solar radiation.

The climate condition is quite important for carrying out natural ventilation. The outside wind can improve the natural ventilation performance, and can also downgrade it. The setting of the openings according to the wind climate conditions is quite important.

7.1.2 Smoke control performance

According to the results of CFD and reduced scale model experiments, in an event of a fire occurring at the base of the atrium, the upper part of the atrium is filled with smoke. Even with greatly increasing the outlet area, the smoke layer inevitably descends to around

the 2nd floor, which means only the space lower than the 2nd floor is clear. Therefore, if the staircase is not separated from the atrium in the evacuation planning, before the smoke layer descends to the occupant space, evacuation of the whole building must be finished. The solar chimney can reserve some quantity of smoke, but there is only about 60s when the smoke layer descends to the bottom of the chimney. Therefore it is necessary to separate the evacuation staircase/safety zone from the atrium.

In case the staircase/safety zone is separated from the atrium, to prevent smoke propagating into the staircases/safety zones, all openings or leakages between the staircases/safety zones and the atrium should be closed. Since the prototype building is supposed to be natural ventilated building, essentially it is not easy to meet the requirement. In the mean time, even there are leakage paths existing between the atrium and the staircases/safety zones, if the pressure of the atrium can be kept as lower than that of the staircases/safety zones, smoke insulation from the atrium to the staircases/safety zones is possible. Here if the neutral pressure plane forms above the top of the staircase/safety zone, the pressure of the staircase/safety zone is higher than that of the atrium/chimney. Therefore smoke propagation from the atrium to the staircase/safety zone can be prevented.

The results of CFD and experiments show setting the outlet area as 2~3 times of the inlet area can make the neutral pressure plane form inside the solar chimney. At the same time, the setting of the openings is also favorable to natural ventilation. It is thought to be a reasonable planning.

7.2 DESIGN METHOD FOR A BUILDING WITH NATURAL VENTILATION AND SMOKE CONTROL PERFORMANCE

In this research, natural ventilation is planed for the prototype building, and at the same time smoke control method is discussed based on the natural ventilation system. Here the design method for a natural ventilated building with smoke control function is summarized.

7.2.1 Planning for natural ventilation

Ventilation rate and the position of the neutral pressure plane are used to evaluate the effectiveness of the natural ventilation system. The factors that will affect the ventilation rate mainly include the possibly absorbed solar radiation, the height of the solar chimney, the

opening area, and the area ratio of the outlet to inlet. The factors that will influence the position of the neutral pressure plane mainly include the height of the atrium/chimney and the area ratio of outlet to inlet. The possibly absorbed solar radiation is decided by the solar radiation, the performance of the glazing wall and the thermal storage walls. Of course the solar radiation varies with regions, seasons, days and hours. The performance of the glazing wall and the thermal storage wall can be selected to meet the requirements. There is no so much adjustability for the designers. Increasing the height of the solar chimney can not only increase the ventilation rate, but also can make the neutral pressure plane stay in high position. However from the aspects of design, structure, cost, laws and other factors, restrictions should appear. The greater opening area and greater area ratio of outlet to inlet are advantageous to ensure preferable ventilation rate, and are the most important factors that will affect the position of the neutral pressure plane. Furthermore, the opening area and the area ratio of outlet to inlet may cause problems, such as rain, noise, and the intrusion of insects. These are thought of as soluble from the equipment side.

According to above discussions, as the design direction, designers can determine the chimney height in permissible range firstly, and then adjust the opening area and the area ratio of outlet to inlet till preferable ventilation rate and neutral pressure plane can be obtained.

7.2.2 Planning for smoke control

Based on the concept of this research, the enough condition to realize the smoke control performance is to make the pressure of the atrium part lower than that of the safety zone/staircase, which in this research includes making the neutral pressure plane between the atrium/chimney and the outside stay inside the chimney. To make the neutral pressure plane stay above the occupant space is the same as that for natural ventilation. This can be realized by adjusting the area ratio of outlet to inlet against the permissible building shape. Furthermore, considering the pressure difference distribution, in case of a fire, since high temperature smoke descends to the atrium space, the neutral pressure plane is thought of as forming at lower position than in case of natural ventilation even with the same opening conditions. That means, if the neutral pressure plane in case of a fire can form in the chimney, it will certainly form in the chimney in case of natural ventilation.

Rested on above consideration, the design flow for a building with natural ventilation and

smoke control function can be summarized as following:

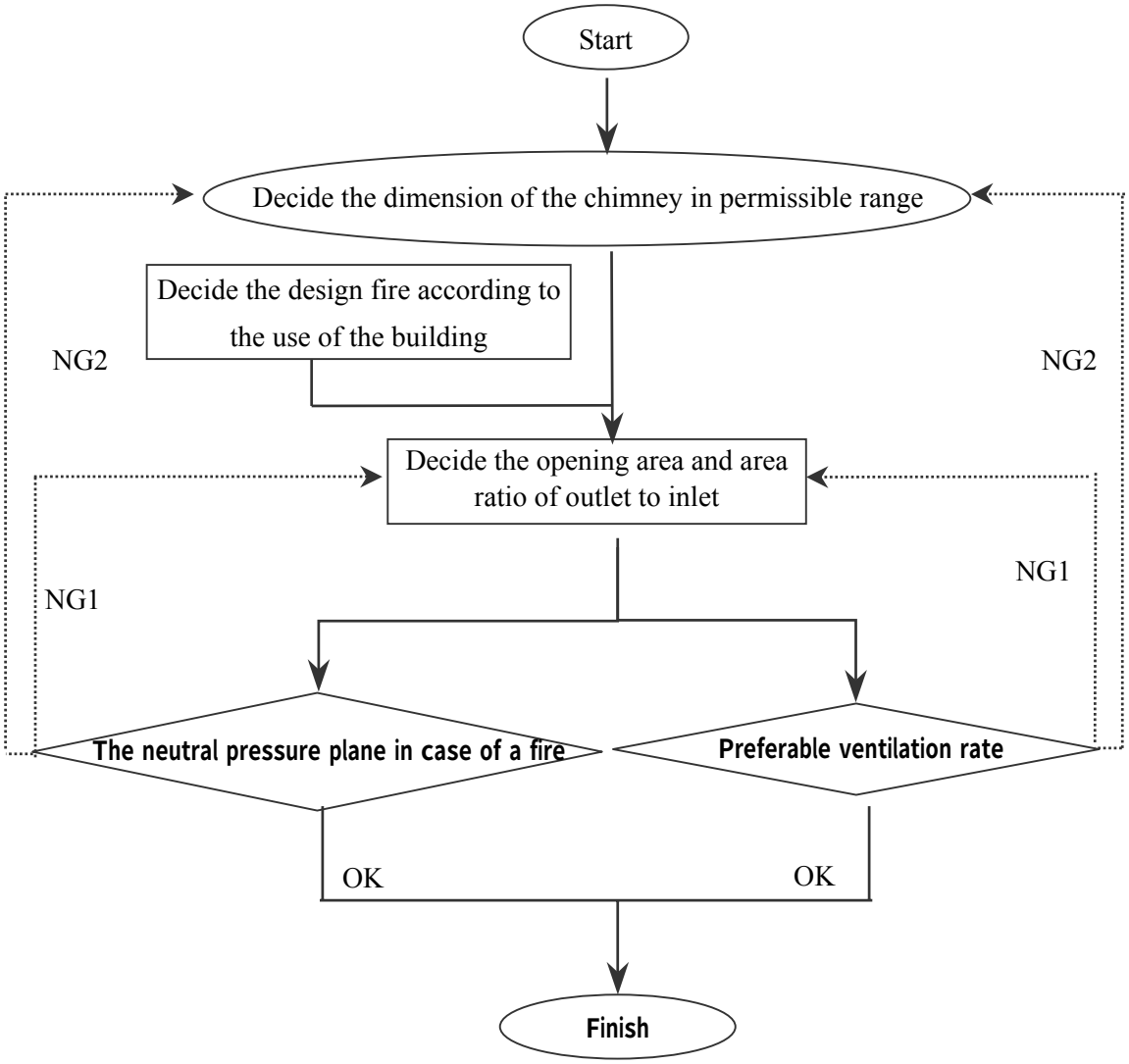

Fig. 7-1 Design procedure for a building with natural ventilation and smoke control performance

7.3 APPLICATION OF THE CONCEPT OF THE PROTOTYPE BUILDING

As the essence of the prototype building, stack effect is the driving force for both natural ventilation and smoke spread. The stack effect can be promoted by introducing the solar radiation. Preferable natural ventilation rate and the position of the neutral pressure plane can be obtained by adjusting the height of the solar chimney and the area ratio of the outlet to inlet. As the application of this concept, one more type building is introduced.

Fig. 7-2 shows the outline of the building with a ventilation shaft. The upper part of the shaft functions as a solar chimney, with thermal storage walls to promote stack effect in the shaft. The shaft goes through the occupant space of each floor. Exhausted air from each floor gathers in the shaft and then is extracted from the openings on top of the shaft. Fresh air is drawn into the occupant space through exterior windows.

Just as mentioned before, there are openings between the occupant space and the shaft at each floor. When a fire happens at any floor, smoke will flow into the shaft and then through the openings at each floor, it is predicted that smoke will spread to the space where in absence of the shaft, no smoke will invade (Fig. 7-3). Furthermore, since only openings for ventilation are set up between the occupant space and the shaft, smoke generated from the fire room cannot be extracted as soon as possible. Therefore smoke extract effectiveness for the fire room cannot be expected. Putting these concerns in mind, the smoke control possibility for the building with a ventilation shaft will be discussed.

(1) Influence on the fire safety of each floor

Just as the atrium building, the objective of the control is to make the neutral pressure plane stay in the chimney. It should be noted that for the atrium building, the volume of the smoke storage space is large, while for the building with a ventilation shaft, since the cross section of the ventilation shaft is very small, it has almost no smoke storage effect. However, actually the openings between the shaft and the occupant space can be controlled. If the neutral pressure plane of the smoke layer can stay above the occupant space, even if the smoke layer descends to below the occupant space, smoke will not infiltrate into the occupant space. Therefore the existing of the shaft will not influence the escape activity of the other floors. To achieve this objective, the height of the chimney and the opening area conditions should be discussed.

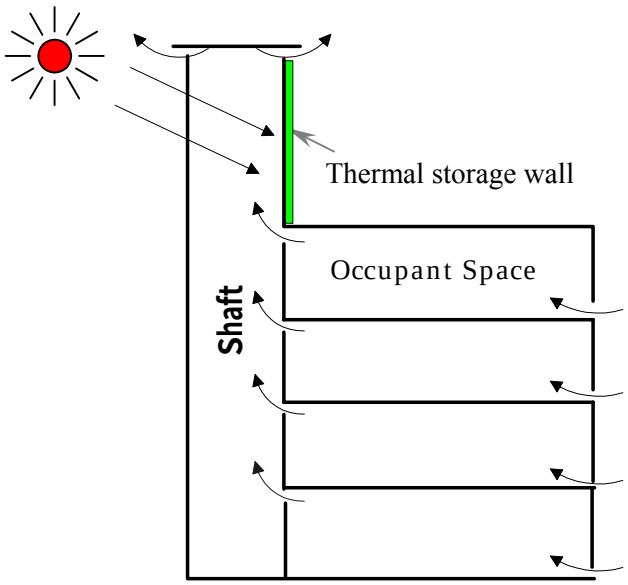

Fig. 7-2 Outline of the building with a ventilation shaft

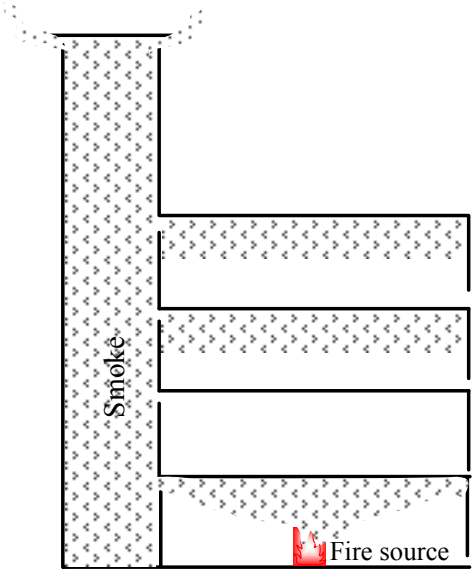

Fig. 7-3 Smoke spread through the shaft

It is probably possible to set smoke detector connected fire dampers at the openings between the shaft and the occupant space, and then the smoke descending to the occupant space can be prevented by the fire dampers. However since the shaft is used for daily natural

ventilation, the closing of the fire damper caused by non fire alarm may frequently happen. Furthermore, pressure loss becomes greater due to the setting of the fire damper. For above reasons, the setting of the fire dampers becomes discreet in planning.

(2) Escape from the fire room

The smoke extract effectiveness of the shaft cannot be very expected probably. However for the space where escape time can be shortened, such as the office building and so on, it is considered to be not so much inconvenient. For example, for an office room smaller than 500 m^2, even without smoke extraction, there is almost no problem to escape from the occupant space. That means, the necessity of smoke extract for a office room is very small. Therefore for the building with a ventilation shaft, although the smoke extract effectiveness of the shaft cannot be greatly expected, this will not specially influence the escape behavior. It is not necessary to introduce extra smoke control method except the shaft itself.

CHAPTER 8

CONCLUSIONS

CHAPTER 8
CONCLUSIONS

For the purpose of energy conservation and requirements for improving indoor air quality, buildings employing natural ventilation are increasing recently, among which the planning of utilizing atria or vertical shafts to promote stack ventilation is not scarce. In conventional researches, 'Sterile tube' solution has frequently been used, but due to the many restrictions on the atrium design and the use of the building/atrium, it is always not favored by designers. As for the other solutions, such as using a great number of shutters to separate adjacent spaces from the atrium, besides high initial cost, it is difficult to ensure that all shutters work properly, because they are only used in case of emergency and if only one of those shutters fails to close, evacuation behavior may be delayed or fail. Proper smoke control method is urgent to be found out. In fact natural ventilation and smoke movement own the same nature--both are driven by stack effect and have the same purpose of exhausting unnecessary gas (air or smoke) from buildings, which means it is possible to solve these two problems in the same way. Therefore in this thesis, the possibility of using the same system both for natural ventilation and smoke control is examined.

In chapter 1, Background of this research is introduced and objective of this research is established.

In chapter 2, to inspect the possibility of realizing smoke control based on a natural ventilation system, a prototype building is proposed. It is thought to be an 8-storey office building with a large atrium in the south direction. Above the atrium a space for promoting natural ventilation and reserving smoke is designed, which in this thesis is called solar chimney. The concept of natural ventilation and smoke control in the prototype building is explained and possible fire safety planning is discussed. It is difficult to secure the fire safety if the escape route/staircase is completely open to the atrium. However if the main escape route is separated from the atrium by walls, smoke prevention by pressure difference is feasible. The conventional researches about solar chimney and smoke control methods in atrium buildings are also introduced.

In chapter 3, to inspect natural ventilation and smoke control performance of the prototype building, reduced scale model experiments are carried out. Considering operability of the experimental model and the effectiveness of similarity laws, the criterion of the reduced scale model is decided as 1/25. As to the natural ventilation experiments, several series experiments with different opening area conditions and different wall temperature are conducted. Increasing the outlet area leads to lower temperature rise in the atrium/chimney space and higher neutral pressure plane. Since temperature rise normally happens inside the chimney, as long as area ratio of the outlet to inlet is greater than 1, the neutral pressure plane stays in the chimney. In addition, high wall temperature promotes more ventilation rate. Finally to confirm the natural airflow in the experimental model, visualization experiments are carried out. Smoke generation stick is used and since there is almost no heat released from the stick, the smoke movement is thought of as reflecting the natural air flow. Smoke stagnation at some height of the chimney is observed which is considered as reflecting the phenomenon of the low temperature air gradually fusing into the high temperature air. When the outlet area is half of the inlet area, smoke propagation in the partitioned space is observed. As to the smoke control experiments, experiments with two different kinds of fire sources are carried out. In the experiments with ethanol as the fire source, increasing the area ratio of outlet to inlet makes temperature rise in the atrium/chimney space smaller and the neutral pressure plane form in higher position. In the experiments with ethanol and smoke generation stick as the fire source, by observation of the smoke movement, when the area ratio of the outlet to inlet is greater than 2, the neutral plane forms above the occupant space. And although there are openings at the boundary of the atrium and the utility space, smoke does not spread into the partitioned space. Smoke prevention by pressure difference is confirmed. It is verified that natural ventilation can be realized in the prototype building and smoke control is possible based on the natural ventilation system through the reduced scale model experiments.

In chapter 4, the CFD method used in this research is introduced. In the simulation of natural ventilation, a indoor zero-equation model is used and in that of smoke control, standard κ-ε model is employed. The experimental results are used to prove the validity of the CFD method. Through the comparison of the results of CFD and experiments, the CFD method is thought of as effective in reproducing the airflow phenomena of natural ventilation

and the phenomena accompanying with a fire in the prototype building. Then the CFD method is used to predict the natural ventilation and smoke control performance of the full-scale prototype building. As the results, when the area ratio of the outlet to inlet is greater than 2, natural ventilation rate for the utility space reaches 2 times per hours. Since there is no long term staying person in the utility space, such ventilation rate is thought to be enough. And when a fire breaks out, the neutral pressure plane stays above the occupant space; smoke infiltration into the safety zone/staircase can be prevented. Compatibility of natural ventilation and smoke control in the prototype building is confirmed.

In chapter 5, the CFD method introduced in Chapter 4 is used to discuss the detail natural ventilation performance of the prototype building. Natural ventilation rate of the prototype building goes up with the increasing of the outlet area. However when the outlet area becomes over 2 times of the inlet area, the growth gradient of ventilation rate slows down, which means setting the area ratio of the outlet to inlet as 2~3 is preferable to obtain appropriate ventilation rate. The dimension of the chimney, including height, width and length, will affect the natural ventilation performance. Ventilation rate increases with the growth of any of these three factors. Since the quantity of the solar radiation that can be absorbed by the thermal storage wall varies with seasons and regions, ventilation performance of the prototype building in regions like Tokyo is not stable throughout the year. The ventilation rate is highest in winter when the necessity for natural ventilation rate is very small and quite lower in the intermediate seasons when natural ventilation is mostly required. To obtain stable ventilation rate throughout the year, improve method is suggested and stable ventilation rate of the performance improved prototype building is confirmed. Wind pressure exerted on the surface of buildings will affect the effectiveness of the natural ventilation. The airflow rate of the outlet in the leeward rises continuously with the increasing of the outside wind velocity. And at the same time the airflow rate of the outlet in the windward decreases. Arrangement of the outlet and inlet according to the wind climate of the local place is quite important.

In chapter 6, detail smoke control performance of the prototype building is discussed. The position of the neutral pressure plane rises with the increasing of the area ratio of the outlet to inlet. When the area ratio of the outlet to inlet becomes greater than 2, the neutral pressure

plane stays in the chimney. Smoke extract rate also increases with expanding of the outlet area. However when the outlet area becomes over 2 times of the inlet area, the growth gradient slows down. The height of the chimney influences the neutral pressure plane significantly while the width or the length of the chimney just has a very little effect. The designers can decide the dimension of the chimney according to practical requirements. In fact there are always restrictions on the dimension of the chimney from the aspects of design or laws. From this point the opening area or the area ratio has wider adjustability. Different design fires are used to check the smoke control performance of the prototype building. Although the smoke extract rate or the smoke layer temperature varies with different design fires, for all cases, the neutral pressure plane keeps staying in the chimney. It sufficiently reflects the advantage of the passive smoke control method-self adjustable and therefore high reliable. The wind effect on the smoke control performance is also discussed. Based on the assumptions in this research, the wind velocity lower than 2 m/s does not affect the smoke control performance so much. However when the wind velocity becomes greater than 5 m/s, smoke cannot be extracted from the outlet in the windward and the neutral pressure plane descends to below the occupant space. Considering the height of the chimney, the velocity at such height is considered strong. Setting the outlet in the windward should be avoided. Finally rested on the concept of smoke prevention by pressure difference, two different space partition planning are presented.

In chapter 7, natural ventilation and smoke control performance of the prototype building is synthetically evaluated. Furthermore, the procedure for designing a natural ventilated building with passive smoke control function is given. Finally as application of the concept of this research, one more type building is introduced.

To secure fire safety of a building with natural ventilation planning, a new smoke control method is proposed in this research. As the prototype building, the space of the solar chimney can be used to promote natural ventilation by absorbing solar radiation, and at the same time making the neutral plane stay in the chimney, smoke prevention can be realized by pressure difference. This concept is confirmed by reduced scale model experiments and CFD calculation.

REFERENCES

REFERENCES

Afonso C, Oliveira A. Solar chimneys: simulation and experiment. Energy and Buildings, 2003;Vol.32: 71-79.

ASHRAE 1997: ASHRAE Fundamentals, American Society of Heating, Refrigerating and Air-conditioning Engineers, Inc.

Bouchair. A. Solar chimney for promoting cooling ventilation in southern Algeria. Building Service Engineering, Research and Technology, 1994; 29(4): 495-500.

Bouchair A, Fitzgerald D, Tinker JA. Moving air using stored solar energy. Proceedings of the 13th National Passive Solar Conference. Cambridge, MA: ASES. pp. 33-38,1988.

Cooper, L.Y., M. Harkleroad, J. Quintiere, W. Rinkinen. An experimental study of upper hot layer stratification in full-scale multiroom fire scenarios. Journal of Heat Transfer, 1982; 104: 741-749.

Cristofalo SD, Orioli S, Silvestrini G, Alessandro S. Thermal behavior of "Scirocco rooms" in ancient Sicilian villas. Tunneling and Underground Space Technology 1989;4(4): 471-473.

Fang, J.B., J.N. Breese. Fire development in residential basement rooms. NBSIR 80-2120. Gaithersburg, MD: National Bureau of Standards (now NIST), 1980.

Garry D.L., George V.H. Large-scale physical model studies for an atrium smoke exhaust system. ASHRAE Transactions: Symposia, CH-99-8-2 (RP-899): 676-698,1999.

George V. H., Gary D. L., Shu Cao. Numerical study of the effectives of atrium smoke exhaust systems. ASHRAE Transactions: Symposia, CH-99-8-3 (RP-899): 699-715,1999.

Hansell G. O., Morgan H. P. Smoke control in atrium buildings using depressurization. Fire

Science & Technology, Vol.10 No.1 & No.2 (11-26), 1999.

Janssen JE. The history of ventilation and temperature control. ASHRAE Journal, 1999;41(10):48-70.

Kenichi Kimura. Fundamental theories of building services, revised edition. Gakkensha Publisher, 1997. (in Japanese)

Klote J. H., D.Sc., P. E. Prediction of smoke movement in atria. ASHRAE Transactions: Symposia. BN-97-5-2: 534-553,1997.

Klote J. H., D.Sc., P.E. New developments in atrium smoke management. ASHRAE Transactions: Symposia. DA-00-6-2: 620-626,2000.

Klote, J.H., J.A. Milke. Design of Smoke Management systems. Atlanta: American Society of Heating, Refrigerating and Air-Conditioning Engineers, Inc., 1992.

Kummar S, Sinha S, Kumar N. Experimental investigation of solar chimney assisted bioclimatic architecture. Energy Conversion and Management, 1998; 39(5/6): 441-444.

Law, M. Air-supported structures: Fire and smoke hazards. Fire prevention 148: 24-28,1982.

McCaffrey B.J. Purely Buoyant Diffusion Flames: Some Experimental Results. NBSIR 79-1910,1979.

Morgan, H.P. Smoke control methods in enclosed shopping complexes of one or more stories: A design summary. Borehamwood, Herts., U.K.: Fire Research Station, 1979.

Morgan, H.P., G.O. Hansell. Atrium buildings: Calculating smoke flows in atria for smoke control design. Fire Safety Journal 12: 9-12,1987.

Nielsen P.V. The selection of turbulence models for prediction of room airflow. ASHRAE Transactions: Symposia. SF-98-10-1: 1119-1127,1998.

Peacock, R.D., V. Babrauskas. Analyses of large-scale fire test data. Fire Safety Journal, 17: 387-414,1991.

Qingyan Chen, Weiran Xu. A zero-equation turbulence model for indoor airflow simulation. Energy and Buildings, 1998; 28 (2): 137-144.

Ray Sinclair. CFD simulation in atrium smoke management system design. ASHRAE Transactions: Symposia. AT-01-11-1: 711-719,2001.

Saxon R. Atrium buildings: Development and design. London, The Architectural Press, 1983.

Shuzo Murakami. Model experiments on the natural ventilation. Summaries of the Technical Papers of Annual Meeting, Architectural Institute of Japan, pp 5-6, 1980. (In Japanese)

Shuzo Murakami, Shinsuke Kato, Chol Nam Kong and Hiroyuki Nakagawa. Model experiment on indoor climate and space air distribution of large-scale room. Productive research, Vol.39 No.9: 35-42,1987.

SungWoo Cho, Ken-ichi Kimura. Study on the performance prediction of solar chimney in natural ventilation system for a school building. J. Archit. Plann. Environ. Eng., AIJ, No. 537, 37-42,2000. (In Japanese)

Takashi Shoda, Takao Tsuchiya. Modeling criteria for the room air Motion, Part 1 Practical Similarity Criteria for the Room Air Motion. Journal of SHASE, No.17: 1-11,1981. (In Japanese)

Toshio Yamanaka et al.. Ventilation performance of solar chimneys. Summaries of Technical

papers of Annual Meeting, The Society of Heating, Air-Conditioning and Sanitary Engineers of Japan, pp 55-58, 2002.

Uichi Inoue. Air-Conditioning Handbook, revised edition, Maruzen Corporation, 1996.

Uichi Inoue. Building services, revised edition, Ichigaya Publisher, 1996. (In Japanese)

Yasutaka Nakajima et al.. Building facility. Asagura Publisher, 1995. (In Japanese)

Z.D. Chen, P. Bandopadhayay. An experimental investigation of a solar chimney model with uniform wall heat flux. Building and Environment, 2003; 38: 893-906.

RELATED PAPERS

W. Ding, Y. Hasemi, Y. Ninegishi. The performance of the natural ventilation system with the function of smoke control. Transactions of the Society of Heating, Air-conditioning and Sanitary Engineers of Japan, No.93, 2004. (In press) (In Japanese)

W. Ding, Y. Hasemi, Y. Minegishi, T. Yamada. Smoke control based on a solar assisted natural ventilation system. Building and Environment. (In press)

W. Ding, Y. Hasemi, Y. Minegishi. Compatibility of natural ventilation and smoke control in an atrium building. Transactions of Architectural Institute of Japan, Vol.569, pp 1-6, 2003. (In Japanese)

W. Ding, Y. Minegishi, Y. Hasemi. Model experiment and simulation on a solar assisted ventilation system. Journal of Asian Architecture and Building Engineering, Vol.1 No.2, pp 73-78, November 2002.

S. Nishimoto, Y. Egawa, S. Tanaka, Y. Minegishi, W. Ding, Y. Hasemi. Possibility of a natural ventilation system with smoke control function in an atrium building: Part 1. Basic concept of passive smoke control in an atrium building. Summaries of Technical Papers of Annual Meeting, AIJ, pp 45-46, 2003. (In Japanese)

Y. Egawa, S. Nishimoto, S. Tanaka, Y. Minegishi, W. Ding, Y. Hasemi. Possibility of a natural ventilation system with smoke control function in an atrium building: Part 2. Assessment of natural ventilation performance by reduced scale model experiments. Summaries of Technical Papers of Annual Meeting, AIJ, pp 47-48, 2003. (In Japanese)

S. Tanaka, Y. Egawa, S. Nishimoto, Y. Minegishi, W. Ding, Y. Hasemi. Possibility of a natural ventilation system with smoke control function in an atrium building: Part 3. Assessment of smoke control performance by reduced scale model experiments. Summaries of Technical Papers of Annual Meeting, AIJ, pp 49-50, 2003. (In Japanese)

W. Ding, Y. Egawa, S. Nishimoto, S. Tanaka, Y. Minegishi, Y. Hasemi. Possibility of a

natural ventilation system with smoke control function in an atrium building: Part 4. Examination on the compatibility of natural ventilation and smoke control by CFD. Summaries of Technical Papers of Annual Meeting, AIJ, pp 51-52, 2003. (In Japanese)

Y. Minegishi, Y. Egawa, S. Nishimoto, S. Tanaka, W. Ding, Y. Hasemi. Possibility of a natural ventilation system with smoke control function in an atrium building: Part 5. Passive smoke control methods based on safety zone division. Summaries of Technical Papers of Annual Meeting, AIJ, pp 53-54, 2003. (In Japanese)